Spring 5-19-2017

Design, Synthesis and Glioblastoma Activity of 1,3-Diazinane Based Aryl Amides and Benzo Fused Heterocycles

Rebecca Hron
University of New Orleans, rhron@tulane.edu

Design, Synthesis and Glioblastoma Activity of 1,3-Diazinane Based Aryl Amides and Benzo Fused Heterocycles

A Dissertation

Submitted to the Graduate Faculty of the
University of New Orleans
in partial fulfillment of the
requirements for the degree of

Doctor of Philosophy
In
Chemistry

By

Rebecca J. Hron

B.S. Tulane University, 2011
M.S. University of New Orleans, 2014

May, 2017

Table of Contents

List of Figures

List of Tables

Abbreviations

DNA	Deoxyribonucleic acid
HDM2	Human double minute two homolog
HDMX	Human double minute two homolog x
ATM	Ataxia-telangiectasia mutated
ATR	Ataxia-telangiectasia and Rad3 related
DNA-PK	DNA dependent protein kinase
Chk1	Checkpoint kinase 1
Chk2	Checkpoint kinase 2
RING	Really interesting new gene
ARF	Alternate reading frame
YY1	Yin and yang 1 protein
HAUSP	Herpesvirus-associated ubiquitin specific protease
DAXX	Death-associated protein 6
RASSF1A	Ras associated domain family 1
c-Abl	Abelson murine leukemia
WIP1	Wild type p53 induced phosphatase 1
CBP	cAMP response element-binding protein
p300	Adenovirus early region 1A binding protein 300
Bcl-XL	B-cell lymphoma extra large
Bcl-2	B-cell lymphoma 2
Bak	Bcl-2 homologous antagonist killer
Bax	Bcl-2 associated x protein

TSP-1	Thrombospondin-1
BAI1	Brain specific angiogenesis inhibitor 1
VEGF	Vascular endothelial growth factor
bFGF	Basic fibroblast growth factor
HECT	Homologous to the E6-AP carboxyl terminus
FAD/$FADH_2$	Flavin adenine dinucleotide
ATP	Adenosine triphosphate
NMR	Nuclear magnetic resonance spectroscopy
PSA	Polar surface area
ClogP	Calculated logP
GA	Glioblastoma activity

Abstract

The development of novel targeted therapeutics for the treatment of cancer remains difficult due to the complex nature of the disease itself as well as the challenges associated with the synthesis of these therapeutics. Impediments to the discovery of novel drug candidates include lack of available starting materials and access to well-developed syntheses which are both convenient and economically feasible. Semicarbazides, for instance, are a critical synthon for the manufacture of numerous biologically important molecules. Historically, convenient methods for the synthesis of semicarbazides and their derivatives did not exist. Recently, a facile and efficient method for the preparation of semicarbazides via their corresponding phenyl carbamates was developed. These phenyl carbamate intermediates may also be used to prepare a wide variety of other derivatives such as substituted ureas as well as the aryl carbamoyl derivatives of 1,3-diazinane-5-carboxamide.

While exploring the preparation of the aryl carbamoyl derivatives of 1,3-diazinane-5-carboxamide, it was found that these compounds possess anti-cancer activity against the glioblastoma LN-229 cell line. Intrigued by these results, additional analogues were designed, leading to the development of a small library of chromenopyrimidinedione and pyrimidinequinolinedione compounds as potential anti-cancer agents. Indeed, these two classes of compounds, with many of the derivatives novel, produced a selection of interesting molecules with potent anti-cancer activity against the glioblastoma cell line LN-229 at biologically relevant concentrations. Taken together, these results provide a unique approach not only to the design but also towards the synthesis of novel therapeutics intended for use as anti-cancer agents.

Keywords: Chromenopyrimidinediones, Pyrimidinequinolinediones, Semicarbazides, 1,3-Diazinane Aryl Amides, Benzo fused heterocycles

Chapter 1: Design, Synthesis and Biological Evaluation of Chromenopyrimidinediones

1.1 Introduction

In the last few years, there has been a renaissance in the area of cancer research leading to the identification of a plethora of cellular pathways and mechanisms which have been suggested to regulate the progression of cancer. Although an overwhelming number of potential anti-cancer targets have been pinpointed, the basic approach to the development of novel anti-cancer therapeutics remains unchanged: Interruption of the activities which are required for cancer expansion such as increased ATP synthesis, rapid DNA replication and apoptotic inhibition. The disruption of these processes exerts a dual-pronged effect in that the malignant cells cannot acquire enough resources to support the accelerated cell division necessary for metastasis and in that programmed cell death, which is may be considered the opposite of metastasis, may take place. Since cancer is widely defined as uncontrolled cell growth, it is appropriate to investigate the key players involved in the regulation of the cell cycle. Although numerous regulators of the cell cycle have been identified, the p53 protein which is incidentally known as "guardian of the genome,"[1] is one of the most popular and well-studied. The p53 protein exists as a tetramer and has a well-established role in the regulation and maintenance of cellular activities including the cell cycle, apoptosis, DNA damage and repair, senescence and angiogenesis, a hallmark of tumorigenesis[2]. In fact, most types of cancer can be traced to the dysregulation of p53 expression including breast, lung, bladder, brain, pancreas, stomach, cervical and liver cancers in addition to sarcoma, lymphoma and neuroblastoma[3]. For these reason, p53 expression and its associated processes are popular targets for the design and discovery of novel anti-cancer therapeutics.

1.2 Modulation of p53 Expression

The manipulation of p53 expression is not a simple task since p53 expression is modulated by a sophisticated network of mechanistic interactions involving an array of proteins, enzymes and co-factors[4]. Additionally, it has been suggested that the p53 protein may have a dual functionality, acting as both a transcription factor and through alternative, transcriptionally independent processes[5]. When the p53 protein acts as a transcription factor, there are three key steps to the activation of the p53 gene: Stabilization of the p53 protein, anti-repression from HDM2 and HDMX and promoter activation[4]. Initially, stabilization was thought to occur via the phosphorylation of the p53 protein *N*-terminus by kinases such as ATM, ATR, DNA-PK and Chk1/Chk2[4]. While it is evident that these kinases phosphorylate the p53 protein *N*-terminus, it remains unknown as to which specific kinases phosphorylate the p53 *N*-terminus in response to different kinds of stress[4]. When the p53 protein is phosphorylated, HDM2 cannot bind to it and the phosphorylated p53 is free to bind to DNA at the p53 promoter region and initiate transcription of the p53 protein[4,6].

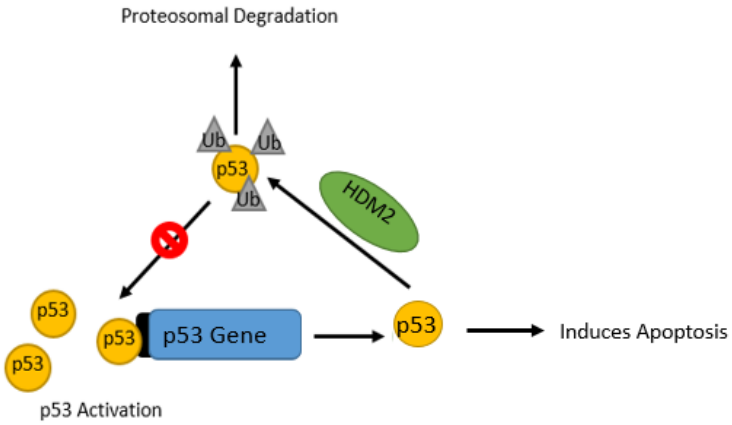

Figure 1.1: Simplified visual representation of the auto regulatory feedback loop between p53 and HDM2

HDM2 and its murine homolog MDM2, are RING finger domain E3 ligases specific to p53 and negatively modulate the expression of the p53 gene by controlling the degree of ubiquitination that occurs on the p53 protein, which ultimately determines the fate of p53 expression and downstream activities[4]. If the p53 protein undergoes monoubiquitination, it is exported from the nucleus to the cytoplasm where it may remain monoubiquitinated or undergo further ubiquitination. In the instance of polyubiquitination, the p53 protein is tagged for proteosomal degradation by the cell and can therefore not act as a transcription factor to influence p53 expression[7]. However, the regulation of HDM2 itself is multi-faceted, being mediated by the participation of several entities. Although there is still much to learn about the interaction of the p53 protein with HDM2, several research groups have shown that the tumor suppressor ARF inhibits the binding of the HDM2 enzyme to the p53 protein[4]. In normal, healthy cells the ARF tumor suppressor gene is active at low levels but rapidly increases expression when the cell experiences oncogenic stress[4]. The consequence of this increased ARF expression is that the increased ARF protein levels then initiate p53 degradation, which allows for the apoptotic inhibition associated with cancer[4]. HDM2 is also influenced by HDMX, which acts as a negative regulator of p53 expression by enhancing HDM2 activity. HDMX enhances the interaction between HDM2 and the p53 protein, leading to p53 protein degradation[4]. In this case, the *C*-terminus of the HDM2 enzyme binds to HDMX to form a heterodimer, which ubiquitinates p53 more effectively than HDM2 alone,[8] leading to increased polyubiquitination tagging the p53 protein for proteosomal degradation by the cell. The transcription factor YY1 also serves as a positive regulator of HDM2,[4] thereby making YYI a negative regulator of p53 expression. Conversely, it has been found that the ribosomal proteins L5, L11 and L23 exert inhibitory effects on HDM2[4]. An additional layer of complexity involves the deubiquitinating enzyme

HAUSP. Unlike HDM2, which promotes the ubiquitination of p53, HAUSP facilitates the deubiquitination and destabilization of the p53-HDM2 complex[4]. The activity of HAUSP in turn is controlled by the protein DAXX, and the assembly of the HAUSP-DAXX complex is negatively regulated by another protein known as RASSF1A[4].

The HDM2 protein itself may undergo modifications as well, including phosphorylation and acetylation. Interestingly, the phosphorylation of HDM2 can have either an activating or inhibitory effect, depending on the site of phosphorylation. Phosphorylation by the kinases ATM or c-Abl at Ser 395 and Tyr 394 in the murine model exert an inhibitory effect on HDM2 while phosphorylation at Ser 166 and 186 enhances HDM2 activity[4]. Dephosphorylation of HDM2 by the phosphatase WIP1 acts to stabilize HDM2, leading to diminished p53 expression. CBP/p300, a histone acetyltransferase, acts on both the HDM2 protein and p53 protein, acetylating lysine residues present on the *C*-terminus of p53 as well as acting as a negative modulator of HDM2[4]. Since these modifications are exclusive of one another, competition is thought to occur between them to control the status of p53 expression within the cell.

The second step of p53 activation, anti-repression, occurs via acetylation and phosphorylation of the p53 protein. These modifications disrupt the ubiquitin ligase activity of HDM2 and HDMX, allowing the p53 protein to bind to DNA and initiate transcription of the p53 gene[4]. Accordingly, it has been found that acetylated the p53 protein is protected from ubiquitination by HDM2 and thus eschews degradation[4].Once the p53 protein is free from the negative influence of HDM2 and HDMX, referred to as anti-repression, it can bind to the core DNA binding domain in a sequence specific manner. The binding of the p53 protein to DNA itself is controlled by modifications such as phosphorylation, ubiquitination, methylation, summoylation, neddylation and acetylation[4]. Interestingly, the p53 protein was discovered to be the first non-histone

substrate to be controlled by both acetylation and deacetylation[4]. The histone acetyltransferase CBP/p300 is responsible for the acetylation of p53 and has been found to be crucial for key elements of p53 gene activation including the recruitment of necessary cofactors and the formation of an easily accessible chromatin conformation[4].

Once the p53 gene has been translated into the functional p53 protein, in the case of apoptosis, it localizes in the cytoplasm before migrating to the mitochondria, which is mediated by an E3 ligase called HSL2, and occurs independently of HDM2[4]. Once on the mitochondria, the p53 protein interacts with anti-apoptotic factors belonging to the Bcl family, such as Bcl-XL and Bcl-2, which in turn promote the activity of pro-apoptotic factors such as Bak and Bax[4].These pro-apoptotic factors facilitate the release of apoptotic activators, including cytochrome c, from the mitochondria to initiate a chain reaction of cellular events resulting in apoptosis[4].

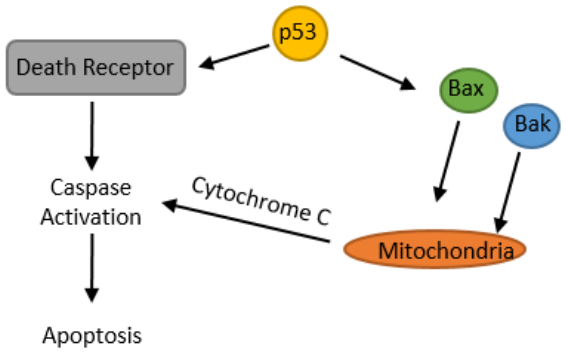

Figure 1.2: Mechanism of p53 activation on events leading to apoptosis

1.3 The p53 Protein as a Cancer Target

Considering these developments towards the understanding of the mechanism of p53 expression, certain segments of the p53 auto regulatory feedback loop have been pinpointed for the development of potential anti-cancer therapeutics. In keeping with its role as the "cellular gatekeeper[9]," p53 has been implicated in the control of angiogenesis, which is a rudimentary process in the development of malignant tumors. The activity of p53 can both activate anti-angiogenic factors such as TSP-1 and BAI1 and deactivate pro-angiogenic factors such as the vascular growth factor VEGF and bFGF[10] to suppress tumor formation. Most research directed towards the control of p53 expression has focused on HDM2 and the protein-protein interaction between HDM2 and p53. The importance of HDM2 was first discovered through the over-expression of the MDM2 protein in murine tumor cell lines[11]. Later, it was also found that increased levels of the HDM2 protein were present in liposarcoma, osteosarcoma, esophageal carcinoma and colon cancer at values ranging from nine to ninety percent[10]. Considering the critical role HDM2 plays in the expression of p53, the most reasonable approach to control cell cycle dysregulation via p53 expression is to manipulate the activity of HDM2. However, the regulation of HDM2 presents another degree of complexity since there are several approaches to achieve HDM2 inhibition. One such approach focuses on the disruption of the HDM2-p53 protein-protein interaction while another approach focuses on the enzymatic inhibition of HDM2's inherent E3 ligase activity[5]. Regardless of the exact mechanism, it has been widely proposed that the inhibition of HDM2 restores functionality to the p53 expression pathway by preventing HDM2 from acting as a negative regulator of p53. Under these circumstances unrestrained cell growth is halted and cell cycle regulation would be permitted.

1.4 HDM2 as a Target

The importance of HDM2 as a negative regulator of p53 expression necessitates a deeper understanding of the p53-HDM2 protein-protein interaction. Protein-protein interactions are generally more difficult to analyze than typical enzyme-substrate interactions because protein-protein interactions span over much larger surface areas and do not have the precise lock and key relationship that many enzymes and their substrates exhibit[12]. Indeed, crystal structures of the p53-HDM2 binding domain have revealed that a surface area of nearly 690$Å^2$ of the HDM2 protein is occupied by the p53 protein[12]. The same crystal structures of the p53-HDM2 protein complex also demonstrate that the binding of p53 to HDM2 is largely governed by the steric interference between the HDM2 cleft and the α helix of p53[12]. It has been suggested that during the course of this interaction, the Phe-19, Trp-23 and Leu-26 residues on the p53 protein effectively compact as to maximize Van der Waals interactions with the HDM2 binding surface[12]. Some researchers even believe that the Trp-23 is the most important residue involved in the p53-HDM2 protein-protein interaction,[10] since the addition of chlorine on the 6 position of the Trp-23 indole ring of p53 results in a drastic increase in the efficacy of HDM2. It has been postulated that this result is explained by the ability of this chlorine to interact with HDMX[12], which is a positive regulator of HDM2. Additionally, it has also been suggested that critical hydrogen bonding occurs between the Phe-19 amide portion of p53 and the Gln-72 of HDM2 as well as between the Trp-23 of p53 and the Leu-54 carbonyl of HDM2[12] to further enhance the protein-protein interaction of p53 with HDM2.

Additional modeling of the p53-HDM2 protein-protein interaction has pinpointed the critical binding residues down to a 15-residue sequence present on the p53 transactivation domain[12]. Further investigation of 15 and 12-mer phage libraries subsequently narrowed the critical residues down to 11, 10, 9 and 8-mer phage sequences[12]. The octapeptide H-Phe-Met-Asp-Tyr-Trp-Glu-Gly-Leu-NH_2 was ultimately determined to be the minimum sequence required for the inhibition of HDM2[12]. Considering the ability of these peptide sequences to effectively disrupt the p53-HDM2 protein-protein interaction leading to diminished HDM2 activity, the very first HDM2 inhibitors were initially designed using peptides with the intent to mimic the protein-protein interaction of HDM2 and p53[12]. Unfortunately, there are practical disadvantages to this approach, which are largely attributed to the inability of the peptides to effectively cross the cell membrane as well as their questionable stability under cellular conditions[12].

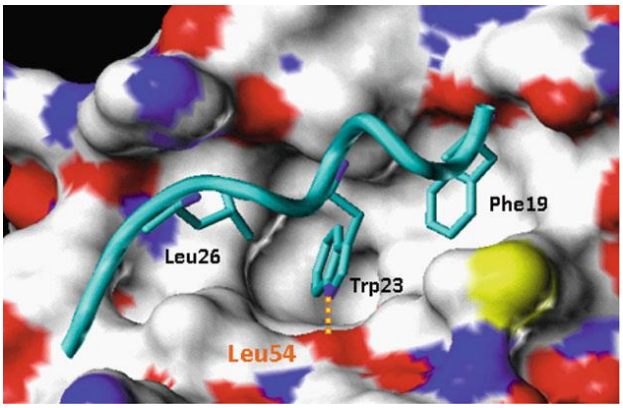

Figure 1.3: Crystal structure of p53 residues 13-29 in complex with HDM2[10]

However, the discovery of this critical octapeptide sequence enabled the development of a non-peptide pharmacophore based on the results of high-throughput screening[12]. The initial identification of these proposed non-peptide pharmacophores ignited interest in the development of HDM2 inhibitors based on these structures. In 2005, Yang et al. presented a series a series of

10-phenyl substituted 7-nitro-pyrimido[4,5-b]quinoline-2,4-diones, known as HL198 and shown in Figure 1.4, which were found to significantly inhibit HDM2 induced ubiquitination of p53[5]. Structural features of these analogues include a tricyclic heteroaromatic ring system with nitro substitution in the 7 position in addition to *N*-phenyl substitution on the central ring which bears additional substituents such as chloro and methyl groups. While the HL198 analogues were found to be highly effective in the inhibition of HDM2's E3 ligase activity, they were perhaps too effective, having undesired effects on other E3 ligases including RING and HECT domain E3 ligases[5]. Although the overzealous E3 ligase activity of the HL198 series of compounds may seem disappointing, it is actually a very promising result because it demonstrates the potential for the development of small molecules as potent inhibitors of HDM2.

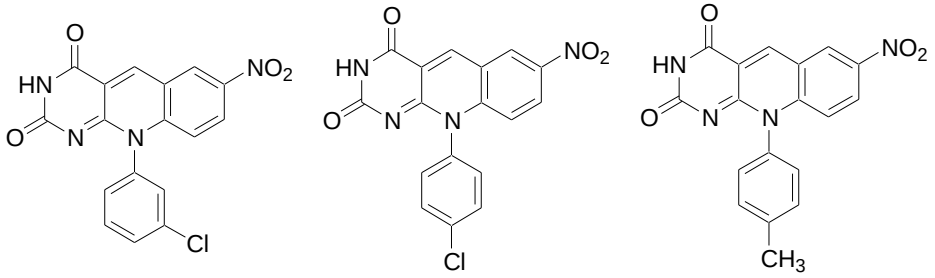

HLI98C HLI98D HLI98E

Figure 1.4: Structures of a few HLI98 compounds[5] designed as HDM2 inhibitors

1.5 Known HDM2 Inhibitors

Considering the profound implications of successful HDM2 inhibition, several compounds have recently been identified as potent HDM2 inhibitors. The largest group of these compounds, referred to as the Nutlins, is also one of the most-studied. Derivatives belonging to his class include RG7112/RO5045337[13] and RG7388/RO550378[14]. Other non-Nutlin compounds exhibiting successful HDM2 inhibition include the piperidinone AMG232[15] and the spirooxindole SAR405838/MI-77301[10].

Table 1.1:Comparison of small molecule inhibitors of HDM2 under clinical investigation

Small Molecule HDM2 Antagonists in Clinical Development					
Compound	**Class**	**K_D***	**IC_{50}****	**Status**	**Company**
RG7112/RO5045337[13]	*Cis*-imidazoline	2.9	581	Did not pass Phase 1	Roche
RG7388/RO550378[14]	*Cis*-imidazoline	0.15	45	Phase 3(Acute Myeloid Leukemia)	Roche
AMG232[15]	Piperidinone	0.045	9.1	Phase I (Acute Myeloid Leukemia) Phase I/II (Malignant Melanoma)	Amgen
SAR405838/MI-77301[10]	Spirooxindole	0.88	100	Completed Phase I	Sanofi

*K_D values are in nM and were calculated via surface plasmon resonance spectroscopy binding assay; ** IC_{50} values are in nM and for SJSA-1 cell line[16]

1.5.1 Nutlins

The Nutlin family of compounds was one of the very first successful classes of HDM2 inhibitors. The Nutlins are characterized by their trademark the *cis*-imidazoline core which serves as an excellent scaffold for extensive modifications leading to promising molecules for further clinical development[10]. RG7112/RO5045337 and RG7388/RO550378 are two examples of the first Nutlins synthesized as inhibitors of the HDM2-p53 protein-protein interaction.

1.5.1.1RG7112/RO5045337

RG7112/RO5045337, one of the most thoroughly researched HDM2 inhibitors, was developed by Hoffman-La Roche and has the distinction of being the first HDM2 inhibitor to enter Phase I clinical trials[10]. Extensive research suggests that RG7112/RO5045337 has the ability to promote apoptosis in cells exhibiting wild type p53 via p53 protein stabilization by the inhibition of HDM2. This p53 stabilization promotes transcription of the p53 gene and translation into the functional p53 protein, leading to subsequent accumulation of the p53 protein within the cell[13]. Crystal structures of RG7112/RO5045337 bound to HDM2 show that the haloaryl moieties of

RG7112/RO5045337interact with the Leu 26 and critical Trp 23 residues of HDM2 while the ethoxy group of the molecule contacts the Phe 19 residue HDM2. The *cis*-imidazoline core enables these dendritic substituents to assume a flexible 3-dimensional conformation that optimizes binding of the molecule to the HDM2 protein. In fact, it has also been noted that RG7112/RO5045337 possesses a higher binding affinity for HDM2 than the wild-type p53, with a K_D value of 9.67 nM compared to the K_D value for wild type p53, which is on the order of 1.00 μM[13]. The increased binding affinity of RG7112/RO5045337 for HDM2 over the wild-type p53 means that RG7112/RO5045337 will bind to HDM2 preferentially, inhibiting HDM2 as opposed to the wild-type p53.

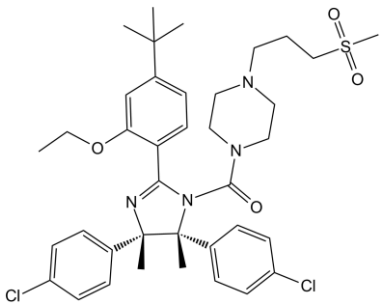

Figure 1.5: Structure of RG7112

Unfortunately, the biological testing results of RG7112/RO5045337 were not without any drawbacks. One of the biggest disadvantages of RG7112/RO5045337 was the high concentration necessary to achieve inhibition in 50% of the cells *in vitro*. In this case, a concentration of 581 nM was required to elicit the desired results in the osteosarcoma SJSA-1 cell line[16]. This high concentration has serious practical implications because in humans, multi-gram dosing is required for efficacy, which is highly undesirable for a drug candidate. Another serious drawback to RG7112/RO5045337 was discovered during Phase I clinical trials. During Phase I clinical trials of RG7112/RO5045337 it was shown that while it exhibits marked inhibition

against several types of leukemia, it also shows very high gastrointestinal toxicity, with "serious adverse side effects" present in nearly 82 out of the 116 patients[13]. Intense adverse side effects are highly undesirable, especially when they afflict the majority of patients treated with a potential drug candidate. For these reasons, the development of RG7112/RO5045337 was halted.

1.5.1.2 RG7388/RO550378

The second Nutlin to enter Phase I clinical trials was a derivative of the *cis*-imidazoline compound RG7112/RO5045337 known as RG7388/RO550378[14]. This new compound was intended to act as a fine-tuned version of the original RG7112/RO5045337 in terms of both potency and specificity, leading to an effective HDM2 antagonist with less toxicity. From a structural standpoint, RG7388/RO550378 retains several structural features of the original RG7112/RO5045337, such as the inclusion of haloaryl substituents that bind to the Leu 26 and Trp 23 residues in HDM2 as well as the inclusion of alkoxy moieties in close proximity to the tert-butyl group, which interact with the Phe 19 residue of HDM2 and the classic Nutlin *cis*-imidazoline core. However, instead of a single chlorine, RG7388/RO550378 has both chlorine and fluorine on the corresponding phenyl rings. Another modification is the replacement of an ethoxy group with a methoxy group. Although the alkoxy groups in both compounds are near the tert-butyl moiety, in RG7388/RO550378, the tert-butyl group is not present on the same aromatic ring as the alkoxy group.

On a cellular level, RG7388/RO550378 functions by the same mechanism as its predecessor, by preventing the protein-protein interaction of HDM2 and p53[14]. Like RG7112/RO5045337, RG7388/RO550378 has a higher binding affinity than the wild type p53 for HDM2 with a K_D value of 9.79 nM[14]. RG7388/RO550378 exhibits improved potency against osteosarcoma cell line SJSA-1, with an IC_{50} value of 45nM compared to the 581nM value for

RG7112/RO5045337. In this aspect RG7388/RO550378 is more successful than its predecessor, making RG7388/RO550378 a suitable candidate for further development. In fact, RG7388/RO550378 is now under Phase III clinical trials for acute myeloid leukemia, with a filing date expected in 2019 or later.

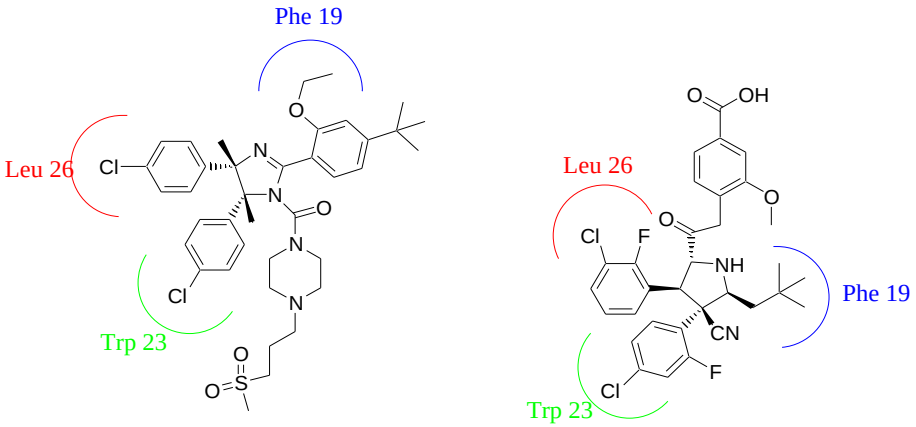

RG7112/RO5045337 RG7388/RO550378

Figure 1.6: Comparison of proposed HDM2 antagonist interaction with HDM2[14](modified from Reference 14)

1.5.2 Other classes of HDM2 Inhibitors

1.5.2.1 AMG232

AMG232 is a non-Nutlin compound belonging to a class of piperidinones currently under investigation as potent p53-HDM2 inhibitors. AMG232 is somewhat similar to the Nutlin derived compounds in that they both contain nitrogenous heterocycles with specified stereochemistry and haloaryl substituents. AMG232 is also similar RG7112/RO5045337 in that they both contain sulfonyl groups. With a K_D of 0.045 nM,[15]AMG232 has an even higher affinity for HDM2 than RG7112/RO5045337 and RG7388/RO550378, which have K_D values of 2.9nM[13] and 0.015nM[14], respectively. AMG 232 also has a lower IC_{50} value than RG7112/RO5045337 and RG7388/RO550378, with requiring only a 9.1 nM concentration to achieve 50% inhibition in vitro[15]. Initially AMG232 was found to be active against the

osteosarcoma cell line SJSA-1 and is now in clinical trials both alone and in combination with other drugs[15]. Phase I clinical trials for the treatment of acute myeloid leukemia using AMG232 as the sole therapeutic agent are currently in progress. However, the application of AMG232 in combination with other drugs such as Trametinib and Dabrafenib is expected to enter Phase II clinical trials soon.

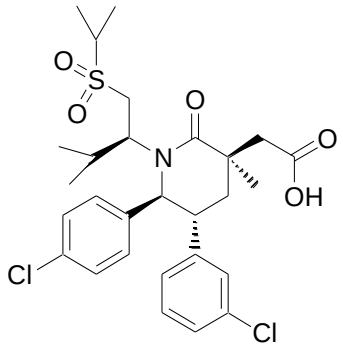

Figure 1.7: Structure of AMG 232

1.5.2.2 SAR405838/MI-77301

Another example of a powerful small molecule inhibitor of HDM2 is the spirooxindole compound SAR405838/MI-77301. This molecule has the unique distinction of being the only HDM2 inhibitor to achieve full tumorigenic suppression in the SJSA-1 cell line[10]. SAR405838/MI-77301 is structurally similar to other active HDM2 inhibitors in that it has haloaryl substitution, with one ring containing chlorine only and the other containing both chlorine and fluorine ortho to one another. This compound is also a heterocycle with stereochemistry. Features present in the other HDM2 inhibitors, such as amide linkers and tert-butyl groups, may be found in SAR405838/MI-77301 also. Biological testing results show that SAR405838/MI-77301 has an IC_{50} value of 100nM, which may be considered to be on the high end of acceptable IC_{50} values for suitable drug candidates[10]. It was also shown that

SAR405838/MI-77301has a reasonable binding affinity to HDM2, with a K_D value of 0.88nM[17]. Disappointingly, SAR405838/MI-77301 is also one of the first HDM2 inhibitors to exhibit inhibitor resistance[18]. To overcome this challenge, the efficacy of SAR405838/MI-77301 in combination with other drugs such as Pimasertib[10] was investigated and recently completed Phase I clinical trials.

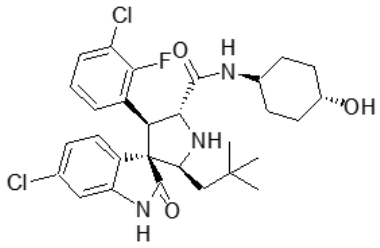

Figure 1.7: Structure of SAR405838/MI-77301

1.6 Implications of Known HDM2 Inhibitors to Our Research

Several classes of compounds possessing a wide variety of structural features have been proposed as small molecule inhibitors of HDM2. We have identified prevailing motifs among these candidates which we believe contribute to HDM2 inhibition. In all cases, there are diverse combinations of substituents to comprise a molecule with either a five or six membered heterocyclic core connected to haloaryl moieties, especially chlorinated compounds, in conjunction with a carbonyl moiety. During the course of our investigation of HDM2 inhibitors, we came across the 5-deazaflavins, which at first seem unrelated to some of the other known HDM2 inhibitors, but upon closer examination share many of the same core structural features. Characterized by a planar, tricyclic heteroaromatic ring system, the deazaflavins are naturally occurring redox cofactors with high reduction potentials[19]. The enhanced reduction potential of

the deazaflavins is critical to their function and in our case, may allude to their ability to bind to HDM2. Considering the information we have regarding the crystal structure of p53-HDM2 protein-protein interaction, it is possible that hydrogen bonding may occur between the N-H of the 5-deazaflavin and the Gln-72 of HDM2, mimicking the interaction of the hydrogen bonding which occurs between the Gln-72 of HDM2 and the Phe-19 amide of the p53 protein. The two carbonyl groups present in 5-deazflavin also provide the opportunity for additional hydrogen bonding to HDM2. Based on these findings, we believe that a molecule which incorporates a polycyclic heteroaromatic core as a scaffold for a variety of functionalized derivatives as well as an innate capacity to act as a strong reducing agent, has the possibility to undergo a redox reaction with residues on HDM2, mimicking the binding of p53 and thus acting as a HDM2 inhibitor. Two such classes of compounds which fit these criteria and have the possibility to incorporate a range of structural modifications are the chromenopyrimidinediones and the pyrimidinequinolinediones. Towards this end, our goal was to design and develop a library of substituted chromenopyrimidinedione and pyrimidinequinolinedione derivatives as potential anti-cancer agents via HDM2 inhibition.

1.7 Structural Relationship to FAD/$FADH_2$

During our investigation, we discovered that our chromenopyrimidinedione and pyrimidinequinolinedione target compounds are considerably similar in terms of structural features to the enzymatic cofactor flavin adenine dinucleotide (FAD) as well as its reduced form, $FADH_2$. This finding caused us to realize that our target compounds have the ability to function by an alternate pathway other than our originally intended route of HDM2 inhibition. Given the structural similarity of our compounds to both FAD and $FADH_2$, we believe that it is a strong possibility that our compounds may function through the FAD/$FADH_2$ redox pathway. FAD and

$FADH_2$ are prosthetic groups which are covalently bound to a dehydrogenase and are therefore referred to as cofactors or coenzymes[20]. During cellular respiration, the oxidation of $FADH_2$ to FAD generates two electrons, which then enter the electron transport chain[20]. The electron transport chain is an intricate series of redox reactions which ultimately generates an electrochemical gradient which initiates ATP synthase activation and consequently generates ATP to be used as energy currency by the cell[20]. Incidentally, ATP synthesis is a popular target for cancer research because cancer cells have been shown to have increased energy needs which necessitate the rapid generation of ATP[21]. By designing a series of analogues which are structurally similar enough to FAD and $FADH_2$ to enter the electron transport chain but also dissimilar enough to prevent the efficient generation of ATP, cancer cells will not be able to generate enough energy to support the cellular activities necessary for their survival.

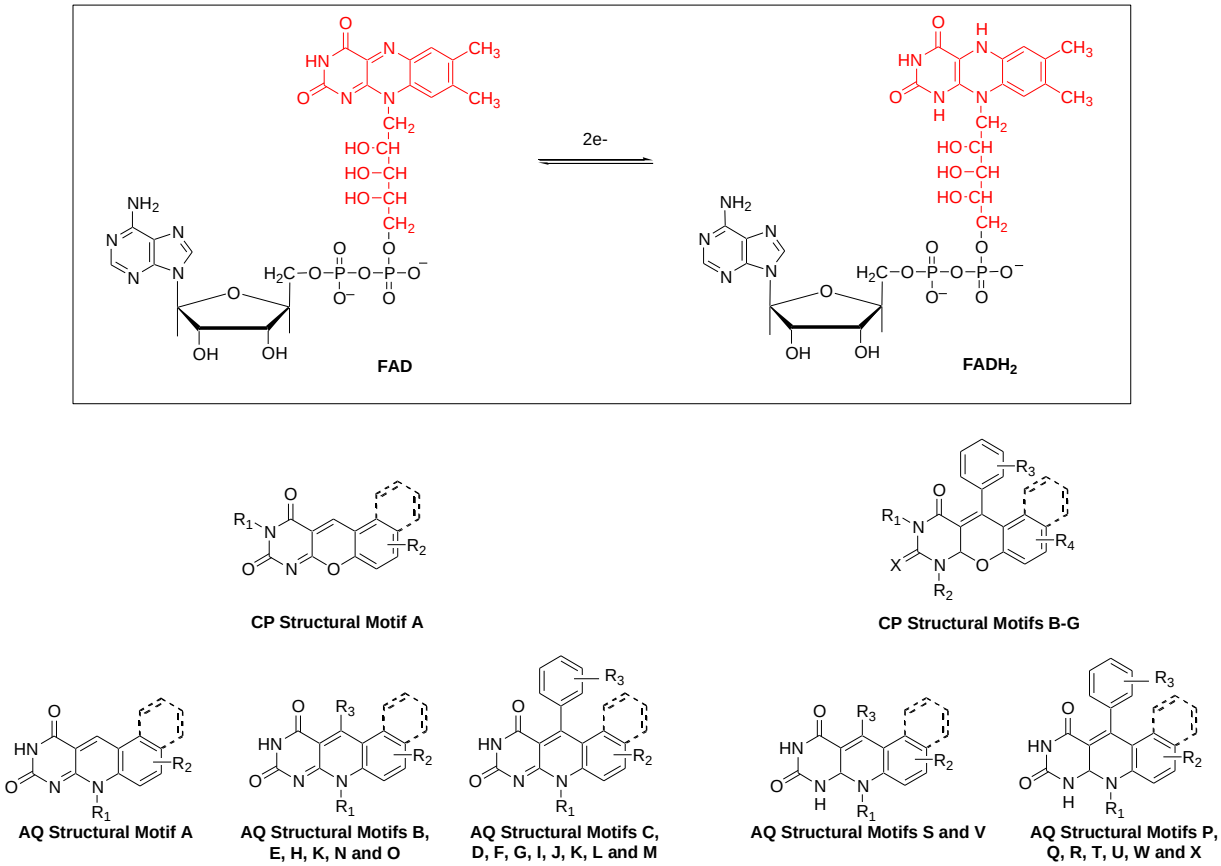

Figure 1.8: Comparison of our CP and AQ compounds to FAD and $FADH_2$, which are rotated to provide clarity

In terms of structural characteristics, our intended chromenopyrimidinedione and pyrimidinequinolinedione target compounds share several similarities with FAD and $FADH_2$ in that they are both tricyclic, heteroaromatic and contain a pyrimidinedione moiety. When designing our chromenopyrimidinedione (CP) compounds, we chose to add a phenyl ring to the 5 position of the core structure to mimic the size of the ribose moiety present in FAD and $FADH_2$. We selected a phenyl ring because although the phenyl ring and the ribose chain are similar in size, they differ in their physical properties such as lipophilicity, which is often a key aspect contributing a molecule's biological activity. Another significant feature of our CP

compounds is that the lipophilicity of the molecule may be tailored by the addition of functional groups such as polar hydroxy, nitro or methoxy groups. We were also interested to explore the synthesis and biological activity of alkylated pyrimidinequinolinedione (AQ) compounds. In the design of the AQ compounds, we chose to introduce *N*-alkyl substitution on the central ring to mimic the ribose chain of FAD and $FADH_2$. More specifically, we decided to focus on *N*-methyl and *N*-butyl substitution since they are comprised of three and four carbon chains, respectively, which is close to the five-carbon chain of ribose. Like FAD and its reduced form $FADH_2$, CP and AQ compounds may be either reduced or oxidized, simulating the same redox properties as FAD/$FADH_2$. The ability of our target compounds to potentially inhibit accelerated ATP synthesis and prevent apoptotic inhibition by HDM2 makes them a promising and exciting class of compounds for the development of novel anti-cancer therapeutics.

1.8 Synthetic Approach

Our initial approach was to design a synthesis that would be applicable to the preparation of biologically relevant chromenopyrimidinediones as well as their *N*- alkylated analogues, the *N*-alkyl pyrimidinequinolinediones. The decision to include both *O*- an *N*- heterocyclic analogs was a logical progression since *O*- and *N*- heterocyclic rings represent a strong motif among successful therapeutic agents[22]. In fact, the pyranopyrimidines, which are very similar in structure to our target compounds, have been shown to possess a wide variety of biological applicability, ranging from anti-bacterial and anti-fungal[23] properties to anti-convulsant[24] and even anti-cancer[25] activities.

Previously, only a handful of aryl substituted *N, N*-dimethyl chromenopyrimidinediones have been synthesized. Unfortunately, the synthetic procedures used to obtain them are less than ideal. Drawbacks to these methods include the use of exotic catalysts such as $InCl_3$[26] and silotungstic

acid[27], in addition to the preparation of catalysts including $ZrOCl_2$/nano TiO_2[28] and H_3PO_4/Al_2O_3[29] and the use of specialized microwave reactors[30]. These methods focus on the optimization of experimental conditions using the model reaction of an aromatic aldehyde, 2-naphthol and *N*, *N*-dimethyl barbituric acid. Although these methods are somewhat viable for the model reaction, it is largely unknown as to how well these methods will translate into the preparation of derivatives including different aromatic phenols, substituted barbituric acids and a larger variety of substituted aromatic aldehydes.

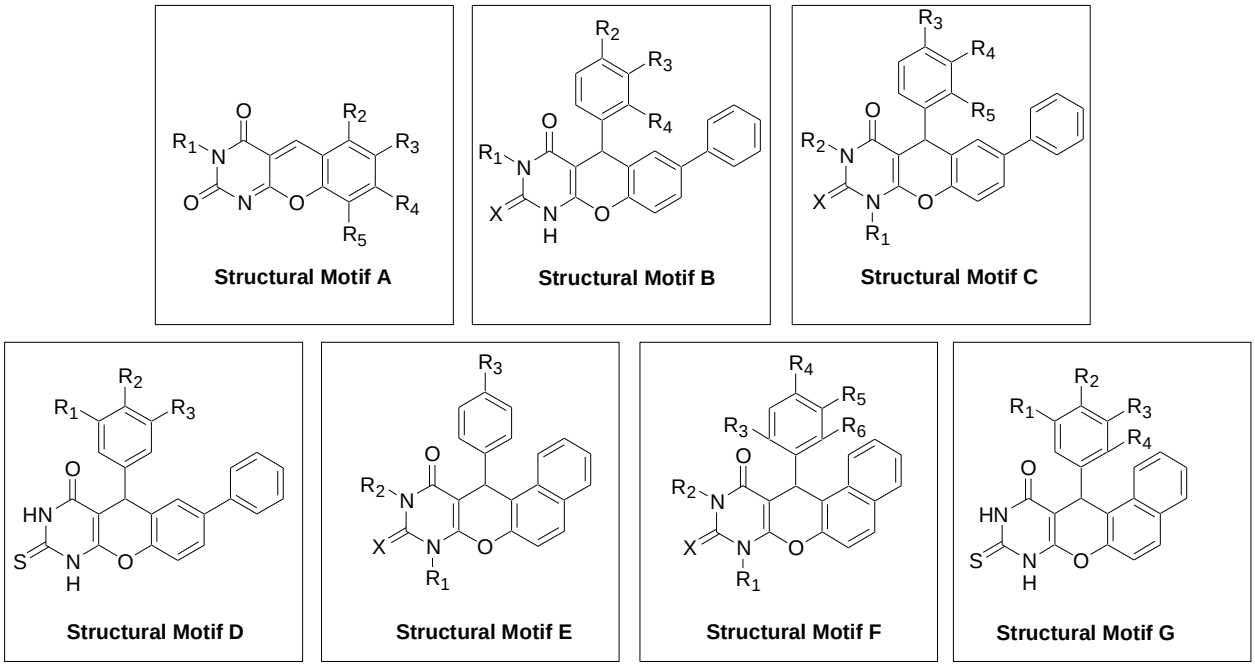

Figure 1.9: Structural Motifs A-G of substituted chromenopyrimidine-2, 4-diones

Considering the lack of convenient preparation methods for a wide variety of derivatives, we wished to develop an extensive library of chromenopyrimidinediones with variabilities in three different areas. In our case, the barbituric acid moiety may be unsubstituted, *N*-methyl or *N*, *N*- dimethyl. Additionally, the aromatic phenol may be 2-naphthol, 4-phenyl phenol,

3-methylphenol, 2-methoxyphenol, 4-methoxyphenol or 4-bromophenol. Substituents on the aromatic portion may either electron withdrawing or electron donating. Reactions involving *N*-monosubstituted barbituric acid have additional flexibility in that they may be either oxidized or reduced, unlike *N*, *N*- dimethyl barbituric acid, which does not have the possibility for oxidation. Using these parameters, it is possible to synthesize an expansive library of chromenopyrimidinediones as potential anti-cancer compounds.

1.9 Experimental

1.9.1. Synthesis of Starting Materials

1.9.1.1 Preparation of Ortho Hydroxyl Substituted Aryl Aldehydes

In order to explore the synthesis of the chromenopyrimidinediones, we first began with the synthesis of a simplified version of our target structure, without any phenyl substitution in the 5 position. The synthesis of this class of compounds begins with the condensation of the *N*-substituted barbituric acid with the ortho hydroxyl substituted aryl aldehyde. The activated methylene group of the barbituric acid forms an enol, which then reacts with the carbonyl of the ortho hydroxyl substituted aryl aldehyde to form an aldol intermediate which then undergoes elimination and subsequent dehydration to furnish the coupled product. This condensation is accomplished by refluxing in acetic acid to yield the open ring which upon continued refluxing in acetic acid, is dehydrated to yield the closed ring chromenopyrimidinedione.

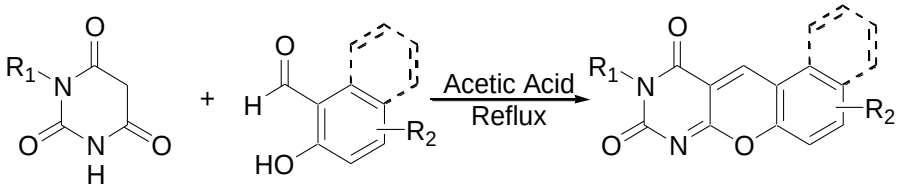

Figure 1.10: Synthesis of substituted chromenopyrimidine-2, 4- diones via *N*-substituted barbituric acid and ortho hydroxy aryl aldehydes

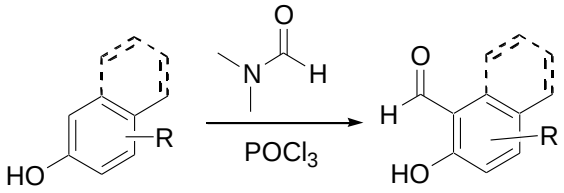

Figure 1.11: Vilsmeier Formylation of phenols to furnish ortho hydroxyl substituted aryl aldehydes

In several cases, the desired substituted ortho hydroxyl substituted aryl aldehydes are not commercially available. However, we found that the desired ortho hydroxyl substituted aryl aldehyde may be prepared via the Vilsmeier Formylation of the corresponding phenol using phosphorus oxychloride and *N*, *N*-dimethylformamide[31]. The Vilsmeier Formylation occurs via electrophilic substitution by a halomethyliminium salt which is formed *in situ* by *N*, *N*-dimethylformamide and phosphorous oxychloride. The only hindrance to this method is that the aromatic compound must be electron rich. However, in our experience, we have not found this to impede the synthesis of our desired ortho hydroxyl substituted aryl aldehydes, regardless of the substituents on the aromatic moiety.

1.9.1.2 Preparation of Substituted Barbituric Acids via Substituted Ureas

For the preparation of a diverse library of substituted chromenopyrimidine-2, 4- diones, a variety of *N*-substituted and *N*, *N*-disubstituted barbituric acids are required. Unfortunately, not only are the barbituric acids themselves unavailable but in some cases the starting materials needed to synthesize them are also not commercially available, economically feasible to purchase or inconvenient to produce in the quantities needed to prepare a library of derivatives. Thus, one of our goals was to develop a convenient and economical method for the preparation of *N*-substituted and *N*, *N*-disubstituted barbituric acids.

Traditionally, barbituric acids are prepared by the classic malonic ester synthesis combining diethyl malonate and urea with sodium ethoxide as a base[32]. Although this is a reliable method for the synthesis of some barbituric acids, it can be inconvenient in that sodium ethoxide is most effective when prepared fresh, since it decomposes over time, which requires the handling of solid sodium. Additionally, it is possible that undesired polyalkylation of the enolate may occur. Not only does polyalkylation lead to low yields due to the formation of multiple products, but it also contributes to difficult isolation of the desired barbituric acid. An alternative method for the synthesis of barbituric acids is the reaction of malonic acid, the corresponding urea and acetic anhydride under microwave irradiation at 60°C[33]. While this is a clever and innovative method, it has only shown to be applicable for a handful of *N*-alkyl substituted barbituric acids. Although this is an improvement in some regards and provides an alternative to the classical malonic ester synthesis, a more generalized method for a variety of substituents is required.

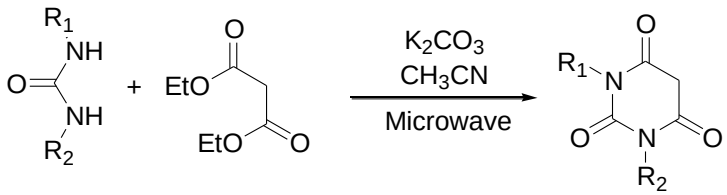

Figure 1.12: Base condensation of substituted urea and diethyl malonate to form *N*-substituted and *N*, *N*- disubstituted barbituric acids

Considering the shortcomings of the available methods for the preparation of a variety of *N*- and *N*, *N*- disubstituted barbituric acids, we developed a method which may be considered in some aspects as a hybrid of the previous two methods in that it uses the same starting materials of diethyl malonate and urea as the classic malonic ester synthesis but replaces sodium ethoxide

with potassium carbonate as the base and utilizes acetonitrile as the solvent with microwave heating. Not only is this route safer than the traditional method, it allows for a wide variety of *N*-substitution including *N*-methyl, *N*, *N*- dimethyl, *N*-phenyl and *N*-(4-nitro) phenyl groups. Using this procedure, it is possible to prepare a variety of *N*-substituted and *N*, *N*-disubstituted barbituric acids in acceptable yields for subsequent reaction with ortho hydroxyl substituted aryl aldehydes to furnish a diverse library of chromenopyrimidine-2, 4- diones.

However, in order for this method to be feasible, the corresponding substituted ureas must also be readily available. Urea is industrially prepared by combining liquid ammonia and liquid carbon dioxide at temperatures ranging from 150°C to 200°C and pressures up to 300 atmospheres[34]. While this is an acceptable method for the preparation of unsubstituted urea, its high temperatures and pressures are not amenable to a variety of functional groups. Thus, it was also necessary to locate a method for the synthesis of substituted ureas in the case that the desired substituted ureas are not commercially available. Here, we employed our previously developed synthesis for the preparation of semicarbazides[35], which proceeds through a phenyl carbamate intermediate. In this example, instead of reacting the phenyl carbamate intermediate with hydrazine hydrate to form a semicarbazide, the phenyl carbamate can be reacted with ammonia instead to produce the substituted urea product.

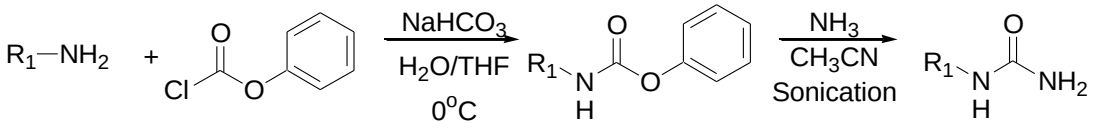

Figure 1.13: Synthesis of substituted ureas via phenyl carbamates

1.9.2 Synthesis of Chromenopyrimidinediones

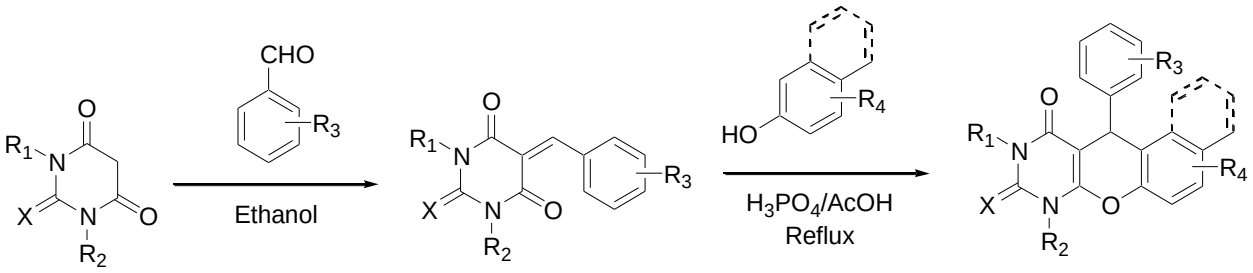

Figure 1.14: Synthesis of chromenopyrimidinediones via *N*-substituted or *N*, *N*-disubstituted barbituric acid, the corresponding aryl aldehyde and the corresponding aromatic phenol

Initially, the preparation of the chromenopyrimidinediones was carried out as a two-step synthesis, with the first step being the condensation of the barbituric acid and aryl aldehyde to form the condensation product and the second step being the reaction of this intermediate with the corresponding phenol. The first step was carried out in an ethanolic solution at room temperature overnight to yield the pure crystalline condensation product. This intermediate was then combined with the appropriate phenol and refluxed in a phosphoric acid-acetic acid solution to furnish the appropriate product.

In order to decrease the reaction time, we used refluxing acetic acid instead of room temperature ethanol as the solvent to provide the same barbituric acid-aldehyde condensation product. This alteration resulted in a dramatic reduction in the reaction time. Considering the success of utilizing refluxing acetic acid as the reaction media, we wondered if we could conduct this synthesis as a one-pot experiment, combining the barbituric acid, aromatic aldehyde, phenol in a refluxing solution of phosphoric acid and acetic acid. In this instance, the condensation product is formed *in situ* before immediately undergoing a reaction with the phenol. This intermediate then undergoes dehydration to yield the closed ring chromenopyrimidinedione. If the reaction is

allowed to continue refluxing for a longer period of time, the compound undergoes slow oxidation by elemental oxygen present in the atmosphere to yield the oxidized form of the compound. An interesting variation of this synthesis is the replacement of substituted barbituric acids with thiobarbituric acid derivatives such as *N*-methyl thiobarbituric acid. We chose to incorporate sulfur in the structure of our target compounds because since sulfur and oxygen have the same number of valence electrons, they share similar electronic properties. Sulfur, however, has a larger atomic radius than that of oxygen and also tends to exhibit increased lipophilicity. Fortunately, the majority of the methods available for the preparation of barbituric acids and their derivatives are also applicable to the preparation of thiobarbituric acids and their derivatives as well. In this way thiobarbituric acid and its derivatives react similarly to barbituric acid under identical reaction conditions to create an entirely new set of analogues with distinct physical properties.

1.9.3 Proposed Mechanism of Chromenopyrimidinedione formation

The first step in the preparation of chromenopyrimidinediones is the formation of a carbon-carbon bond between the methylene group of the barbituric acid (starting material 1) and the carbonyl carbon of the aldehyde (starting material 2). This carbon-carbon bond formation occurs by the nucleophilic attack of the aldehyde carbonyl by the electrons of the activated methylene group of the barbituric acid. This nucleophilic attack is accomplished by the protonation of the aldehyde oxygen, in our case using the acidic media, which makes the aldehyde more susceptible to nucleophilic attack. Since barbituric acid, with its activated methylene group, can exist in either its enol or keto form, under these conditions, it adopts the enol conformation. The enol form of the barbituric acid thereby effectively functions as a nucleophile. The electrons from the double bond of the enol attack the carbonyl carbon of the aldehyde, resulting in the formation of

intermediate 1. Intermediate 1 exists in equilibrium with Intermediate 2, which undergoes prompt dehydration to form carbocation Intermediate 3. This transient carbocation species then loses a proton to form a double bond and yield Intermediate 4. Intermediate 4 is the first of the intermediate species formed during the course of the reaction which is stable enough to be identified by NMR.

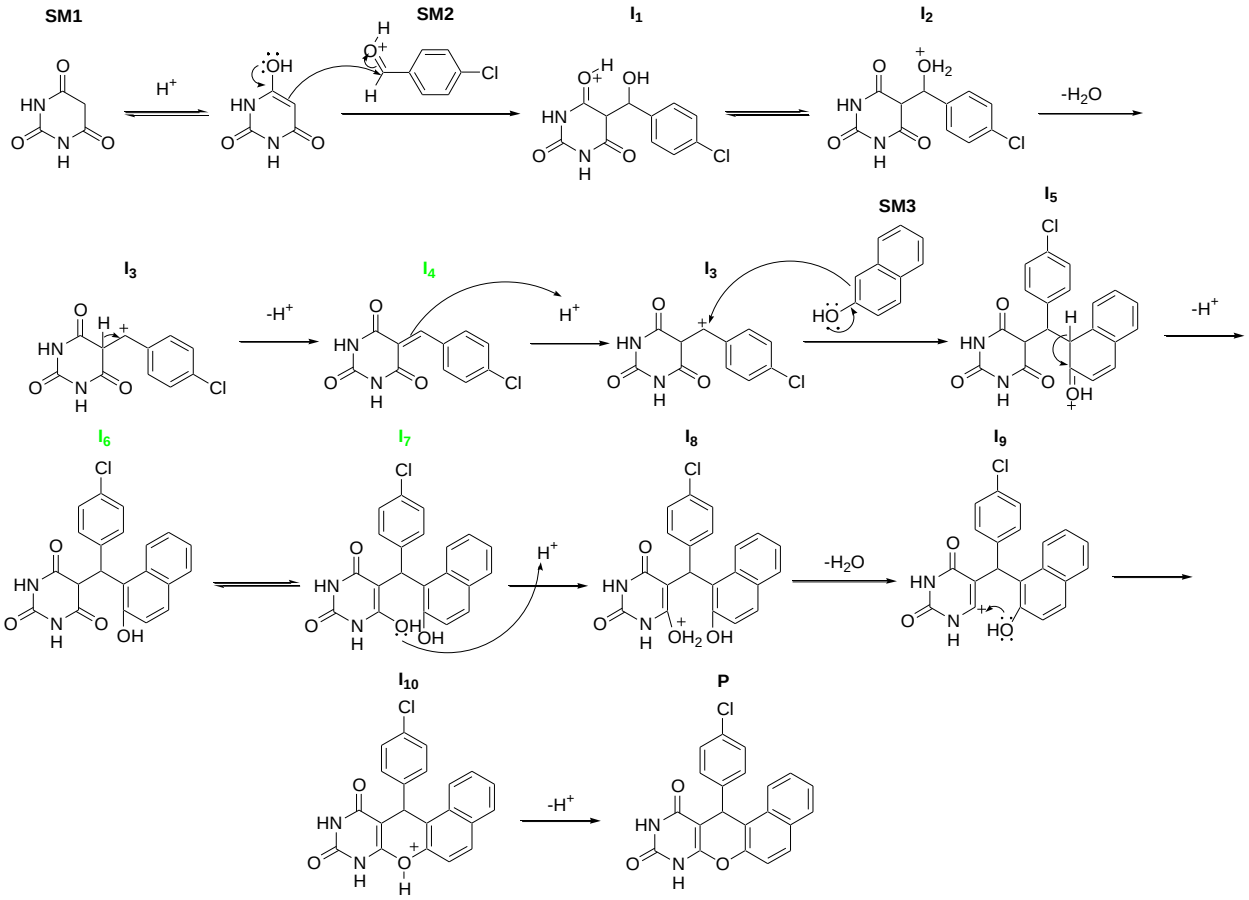

Figure 1.15: Mechanism of chromenopyrimidinedione formation

Due to the acidic reaction conditions, the double bond electrons of Intermediate 4 interact with the protons present in the reaction media to revert to Intermediate 3. However, when Intermediate 3 is in the presence of the substituted phenol (starting material 3) which has ortho directing properties, the lone pair electrons on the oxygen of the phenol move to the ortho position and attack the carbocation of Intermediate 3 to form Intermediate 5. Intermediate 5 then undergoes aromatization via the loss of a proton to form Intermediate 6, the second intermediate which is stable enough to be detected by NMR. Intermediate 6, which is in equilibrium with Intermediate 7, which may also be identified by NMR. Intermediate 7 is the enol tautomer of Intermediate 6, which has the keto form of the barbituric acid and the enol form of the phenol. Since this reaction is carried out under acidic conditions, the barbituric acid enol is protonated and subsequently experiences the loss of one water molecule to form Intermediate 9, with its vinylic carbocation. The lone pair electrons on the oxygen of the remaining enol of the substituted phenol moiety attack the vinylic carbocation to close the ring and yield Intermediate 10. Under the acidic reaction conditions, Intermediate 10, with its protonated oxygen immediately loses its proton to give the product.

In order to support our proposed mechanism, we carried out an NMR experiment to follow the progress and identify key intermediates. In this example, samples were taken from a reaction mixture of barbituric acid with 4-chlorobenzaldehyde and 2-naphthol in a refluxing mixture of 1:2 phosphoric acid: acetic acid at 0 minutes before heating and then with heating at10 minutes, 30 minutes and finally 2 hours. At 0 minutes, majority of the reaction mixture is composed of starting material (SM), with small signals indicating the formation of the intermediate and to a less extent, the product. The easiest starting material signals to follow are the barbituric acid N-H at ~11 ppm and the CH_2 hydrogens of the methylene group at ~3.4 ppm. At ~5.8 ppm the signal

corresponding to the open ring intermediate (I) is present along with a signal at ~5.6 ppm which corresponds to the same signal in the closed ring system of the product (P). After 10 minutes the signals for the starting material as well as the intermediate begin to decrease while the product signals increase. After 30 minutes, the peaks corresponding to the product predominate with small signals still present indicating the presence of residual starting material and intermediate. After 2 hours, the reaction mixture shows signals for the product almost exclusively, with no signals for the intermediate and very small signals for the starting material due to the presence of excess starting material.

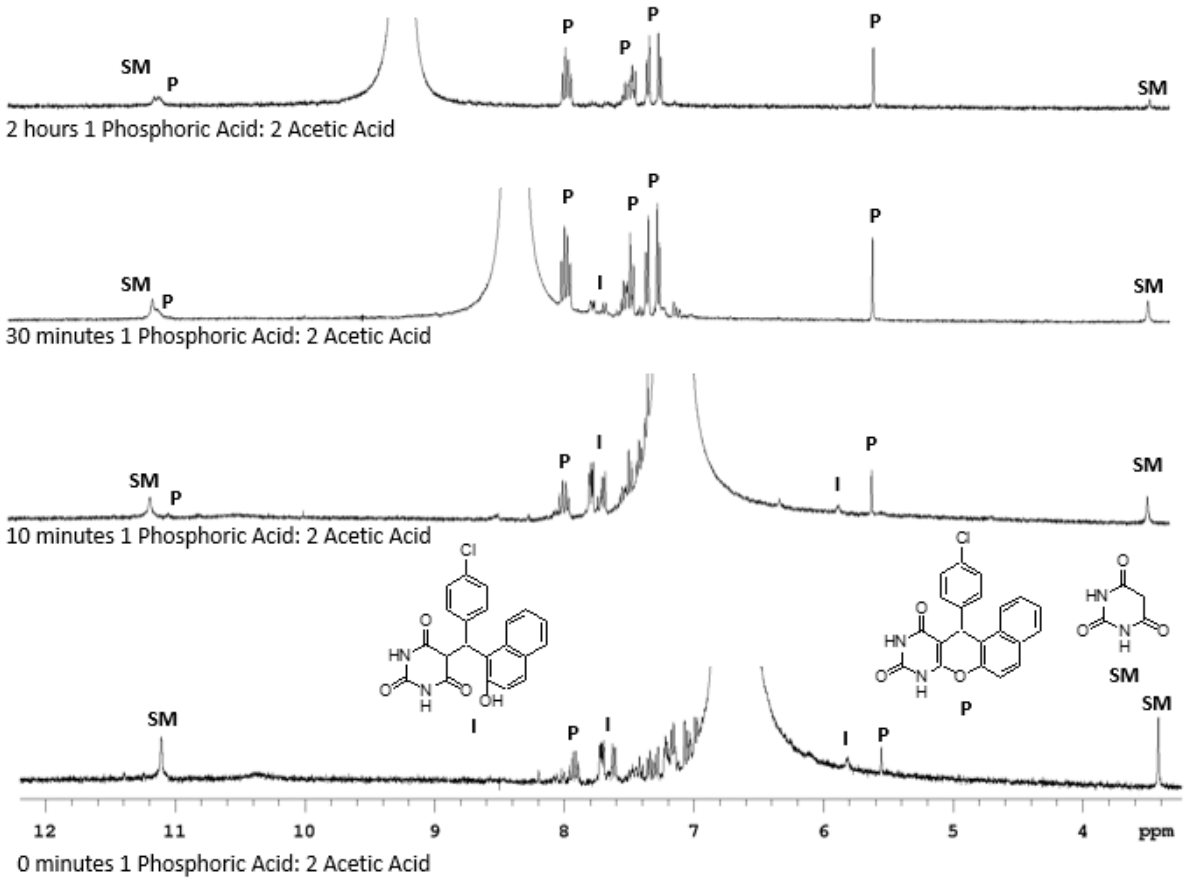

Figure 1.16: NMR experiment monitoring the progress of the reaction between barbituric acid, 2-naphthol and 4-chlorobenzaldehyde in a 1:2 solution of phosphoric acid: acetic acid

While at least one intermediate can be identified from the reaction carried out in a 1:2 mixture of phosphoric acid to acetic acid, as shown in Figure 1.17, we wished to further slow the reaction rate in order to identify additional intermediates. In the next experiment, we carried out the same reaction but instead decreased the volume of phosphoric acid, using only 5 drops of phosphoric acid in 25 ml of acetic acid. After 10 minutes with heating, the reaction mixture NMR shows signals for the starting material barbituric acid N-H at ~11ppm as well as the barbituric acid-aldehyde condensation product (I_1). Signals corresponding to the intermediate I_1 include the N-H peaks, which are slightly downfield from the starting material N-H which are located at ~11ppm and the proton corresponding to the double bond hydrogen, which is present at ~8.3 ppm. After 30 minutes, the starting material signals continue to further decrease while the intermediate I_1 signals continue to emerge.

Due to the slow progress of the reaction under these conditions, the next sample was taken after 20 hours. At this time point, the starting material has been totally consumed and the signals for the intermediate I_1 have decreased. There is also evidence of the formation of another intermediate (I_2) which corresponds to the open ring product as well as the closed ring product (P). The signal at ~5.8 ppm corresponds to the open chain intermediate I_2 while the signal at ~5.6 ppm corresponds to the same signal in the closed system of the product. After 48 hours, the intermediates I_1 and I_2 have decreased and the signals for the product continue to increase, which is visible by the change in the ratio of the signal at ~5.6ppm of the product to the rest of the peaks. Under these conditions, this reaction requires an extended period of time to go to completion. However, in this instance we have included the NMR of the final product, which was obtained by heating the reactants in 5 ml of pure phosphoric acid for 20 minutes, for comparison. While heating in pure phosphoric acid is the fastest method for the formation of the

desired product, the vigorous reaction conditions and high temperature can lead to the decomposition of certain functional groups and for this reason, is not applicable to the preparation of a wide variety of derivatives.

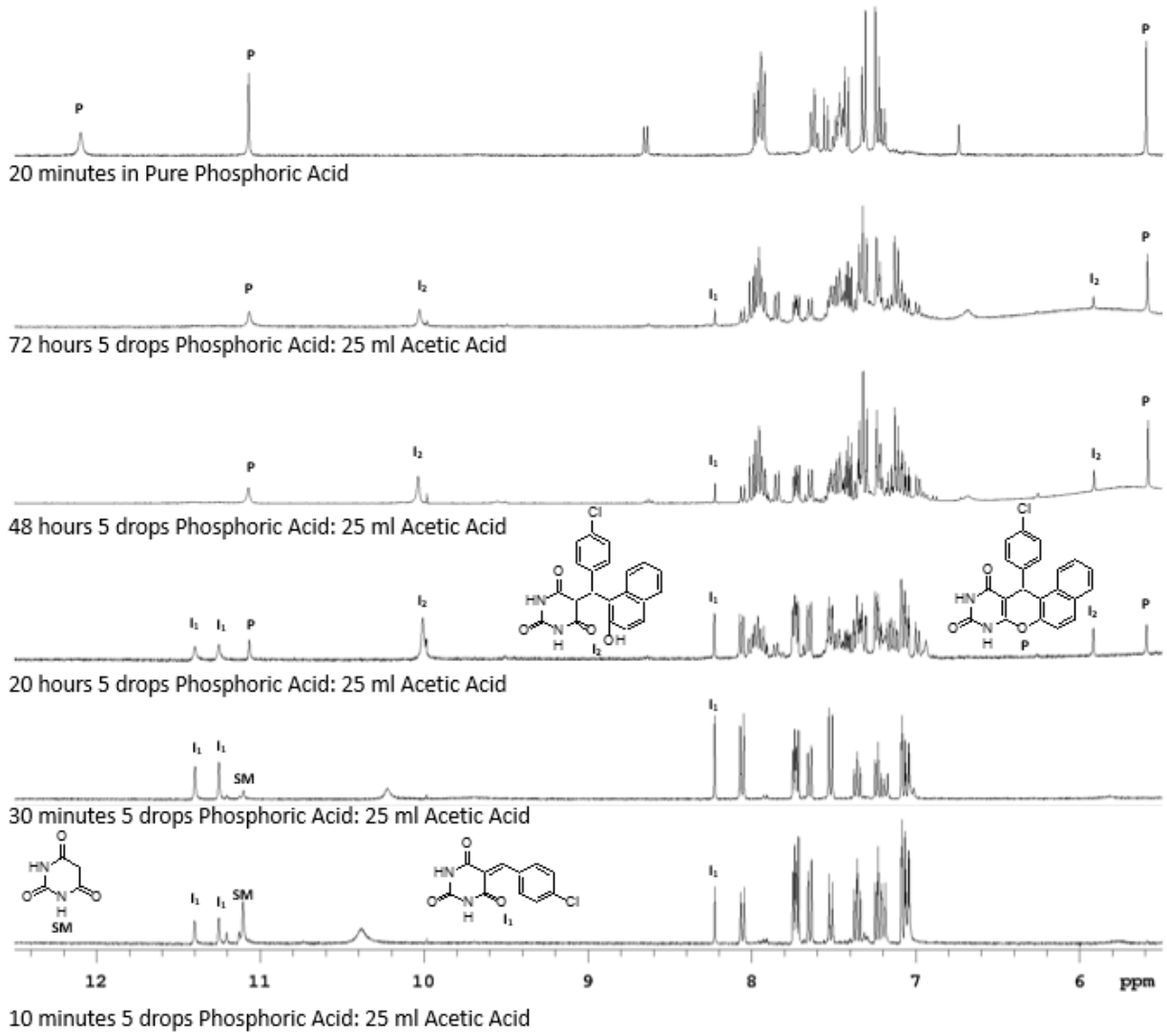

Figure 1.17: NMR experiment monitoring the progress of the reaction between barbituric acid, 2-naphthol and 4-chlorobenzaldehyde in 25ml of acetic acid with 5 drops of phosphoric acid

1.10 Biological Testing Results

1.10.1 Preliminary Biological Testing Results

Initially, biological testing was conducted on a small selection of compounds to determine their efficacy against the B16 melanoma cell and CL lymphoma cell lines (Biological testing courtesy of Lee Roy Morgan). The most promising compounds, **CP1** and **CP10**, both exhibited excellent activity against both B16 melanoma and CL lymphoma cell lines at concentrations of 0.5 μg/ml. Interestingly, both **CP1** and **CP10** have no *N*-substitution or additional substitution on the associated aromatic rings. Considering the promising results of these compounds, we decided to expand upon this structure by incorporating additional aryl substituted moieties in addition to the inclusion of sulfur via thiobarbituric acid.

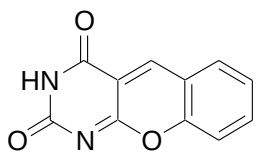

CP1

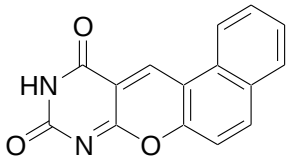

CP10

Figure 1.18: Structures the most active compounds from preliminary biological screening

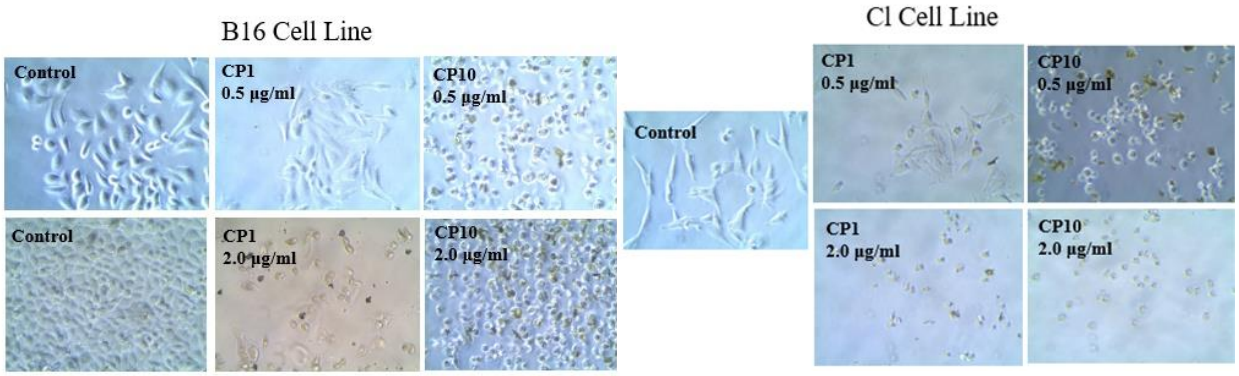

Figure 1.19: Cell testing results of CP1 and CP10 compounds in B16 and CL cell lines at concentrations of 0.5 μg/ml and 2.0 μg/ml

1.10.2 Biological Testing Against Glioblastoma

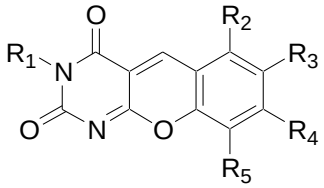

Structural Motif A

Table 1.2: Calculated molecular descriptors and biological activity of Structural Motif A (Method A) compounds against the LN-229 cell line

Compound	R_1	R_2	R_3	R_4	R_5	ClogP	pKa	PSA*	GA**
CP1	H	H	H	H	H	0.80	6.22	67.76	10
CP2	C_6H_5	H	H	H	H	2.68	-1.39	58.97	100
CP3	H	H	OCH_3	H	H	0.64	6.22	76.99	10
CP4	CH_3	H	OCH_3	H	H	0.86	N/A	68.20	1
CP5	H	H	H	H	OCH_3	0.64	6.22	76.99	10
CP6	CH_3	H	H	H	OCH_3	0.86	N/A	68.20	1
CP7	H	H	H	CH_3	H	1.31	6.22	67.76	1
CP8	CH_3	H	H	CH_3	H	1.54	N/A	58.97	10
CP9	H	H	Br	H	H	1.57	6.37	67.76	10
CP10	H	$-(CH_2)_4-$		H	H	1.79	6.22	67.76	1

*PSA= Polar Surface Area in $Å^2$; **GA= Glioblastoma cell line LN-229 activity in µg/ml; Calculated molecular descriptors obtained from Chem Axon's Marvin Sketch Software

Further biological testing of our compounds in 100µg/ml and 10µg/ml concentrations was carried out against the glioblastoma cell line LN-229 (courtesy of Donna Neumann). We selected the LN-229 cell line because not only is it an aggressive form of cancer, but it also contains mutant p53[36]. Since we propose that our compounds prevent the dysregulation of the p53 pathway, this is also one way in which we can evaluate the suggested mechanism of our molecules. Our initial studies began by exploring the activity based on simple variations of the core chromenopyrimidine-2,4-dione structure, Motif A. Unsubstituted **CP1**, showed good activity at 10 µg/ml. This result is not surprising since the predicted molecular descriptors of

logP and pKa for **CP1** are close to the ideal values. The calculated logP value of 0.80 and the pKa of 6.22 are close to the ideal values of 1.00 and 6.00, respectively. Although the polar surface area of 67.76 $Å^2$ is not near the ideal value of 100 $Å^2$, this does not impact its activity. Thus, we were interested to see what effect various substitutions would have on the activity of these analogues against the glioblastoma LN-229 cell line.

One of the first variations we explored was *N*- phenyl substitution on the barbituric acid portion of the molecule, resulting in **CP2**. Although **CP2** is active at 100 μg/ml concentrations, it is inactive at lower concentrations such as 10 μg/ml. Thus, for this group of compounds this modification was not investigated further. However, we found that the *N*-methyl (**CP4**, **CP6** and **CP8**) and *N*-unsubstituted (**CP3**, **CP5**, **CP7**, **CP9** and **CP10**) analogues were active at both 100 μg/ml concentrations as well as 10 μg/ml concentrations. Substituents present on active compounds include methoxy groups in either the 3 (**CP3** and **CP4**) or 4 (**CP5** and **CP6**) position, methyl (**CP7**), bromo (**CP9**) and naphthyl (**CP10**) groups. The efficacy of these compounds is further supported by their calculated molecular descriptors, with calculated logP values ranging from 0.80 to 2.00, pKa values ranging from 6.22 to 6.37 and polar surface areas ranging from 68.2 $Å^2$to 76.99 $Å^2$.

Considering the number of compounds which showed activity at 10 μg/ml, we wished to test these compounds at an even lower concentration of 1 μg/ml. Compounds showing activity at this lower concentration include **CP4**, **CP6**, **CP7** and **CP10**. **CP4** and **CP6**, which are both *N*-methyl substituted compounds, also have methoxy substitution in the 7 and 9 positions, respectively, which means that they have identical values for their calculated molecular descriptors. **CP4** and **CP6** have calculated logP values of 0.86, which is well within range of the optimal value of 1.0. These two compounds also have polar surface areas of 68.20$Å^2$, which is a little on the low side.

The other compounds which are active at 1 μg/ml, **CP7** and **CP10**, are both *N*- unsubstituted, with **CP7** bearing methyl substitution at position 8 and **CP10** having a phenyl group fused at positions 2 and 3. **CP7** and **CP10** have reasonable calculated logP values of 1.31 and 1.79, respectively, as well as identical pKa values of 6.22. The pKa value of 6.22 is very close to the desired value of 6.00. Similarly to **CP4** and **CP6**, **CP7** and **CP10** also have lower polar surface areas of 67.76 $Å^2$.

Overall, given the selection of compounds active at the low concentration of 1 μg/ml, a few trends are noticeable in regards to their logP, pKa and polar surface area values. The calculated logP values of these compounds with excellent activity are fairly close to the ideal value of 1.00, having a minimum of 0.86 and a maximum of 1.79. For the compounds which have pKa values, namely **CP7** and **CP10**, their pKa values of 6.22 are very close to the desired value of 6.00. However, the polar surface areas of these compounds are lower than the ideal polar surface area of 100 $Å^2$. This may be explained by the reality that smaller compounds closer to 90$Å^2$ are in some instances more successful in crossing the cellular membrane.

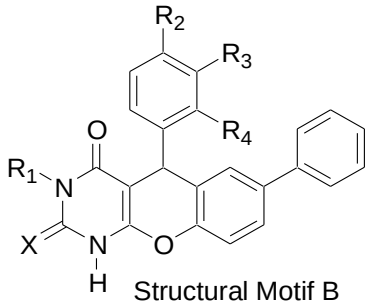

Structural Motif B

Table 1.3: Calculated molecular descriptors and biological activity of Structural Motif B (Method B) compounds against the LN-229 cell line

Compound	R_1	R_2	R_3	R_4	X	ClogP	pKa	PSA*	GA**
CP11	H	H	H	H	O	4.15	8.77	67.43	10
CP12	H	H	H	H	S	5.04	7.80	50.36	10
CP13	H	C_6H_5	H	H	O	5.80	8.77	67.43	100
CP14	H	F	H	H	O	4.30	8.89	67.43	100
CP15	H	F	H	H	S	5.19	7.80	50.36	10
CP16	H	H	H	Cl	O	5.65	7.80	50.36	10
CP17	H	Cl	H	H	O	4.76	8.89	67.43	100
CP18	CH_3	H	H	Br	O	5.81	7.80	50.36	10
CP19	H	H	Br	H	S	5.81	7.80	50.36	10

*PSA= Polar Surface Area in $Å^2$; **GA= Glioblastoma cell line LN-229 activity in µg/ml; Calculated molecular descriptors obtained from Chem Axon's Marvin Sketch Software

Considering these results, we wished to explore further variations, such as the inclusion of an additional phenyl group which is not in conjugation with the core structure, giving rise to compounds **CP11-19** in Table 1.2, which fit into Structural Motif B. Here we started with the unsubstituted **CP11**, which had reasonably good activity at 10 µg/ml before exploring additional substitutions. Here, we introduce the replacement of one of the carbonyl oxygens with a sulfur, which will result in an increase in the overall lipophilicity of the molecule. **CP12**, the sulfur analog of **CP11**, exhibits good activity at 10 µg/ml concentrations as well. Similar to Structural Motif A, these compounds may be either *N*-methyl substituted (**CP18**) or *N*- unsubstituted (**CP11**, **CP12**, **CP15**, **CP16** and **CP19**). In this case, we explored the effect of halogen

substituents such as fluoro (**CP15**), chloro (**CP16** and **CP17**) and bromo (**CP18** and **CP19**). Interestingly, all of the halogenated compounds except for **CP17** were active at concentrations of 10 μg/ml. Perhaps what is even more interesting is that chloro compound **CP16**, where chlorine is in the 4 position, is active at lower concentrations, whereas chloro compound **CP17**, where chlorine is in the 2 position is not. **CP13** and **CP14**, which have phenyl and fluoro substitution also at the 2 position, respectively, are also inactive at lower concentrations. In this example it appears that substitution at the 2 position results in a decrease in activity. Another interesting observation is that although **CP14** is not active at lower concentrations, its sulfur analogue, **CP15** does show activity at lower concentrations. The replacement of oxygen by sulfur in this instance leads to a compound with increased lipophilicity, a lower pKa and a smaller polar surface area. Ironically, the calculated molecular descriptors of logP and polar surface area are closer to the ideal values for **CP14** than they are for **CP15**. However, **CP15**, the sulfur analogue, shows a pKa value which is closer to the ideal value than that of **CP14**, suggesting that pKa plays an important role in the activity of these compounds. Considering these results, we wanted to further investigate the role that *N*-substitution plays in the activity of these compounds.

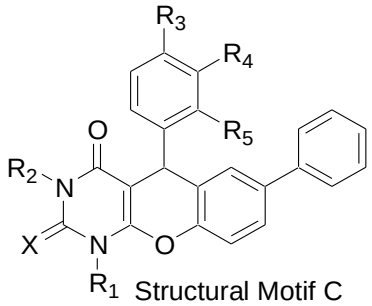

Structural Motif C

Table 1.4: Calculated molecular descriptors and biological activity of Structural Motif C (Method B) compounds against the LN-229 cell line

Compound	R_1	R_2	R_3	R_4	R_5	X	ClogP	pKa	PSA*	GA**
CP20	H	H	H	Cl	Cl	O	5.36	8.58	67.43	100
CP21	CH_3	CH_3	H	Cl	Cl	O	5.81	N/A	49.85	100
CP22	CH_3	CH_3	H	Cl	Cl	S	6.70	N/A	32.78	10
CP23	H	H	Cl	H	Cl	O	5.36	8.58	67.43	100
CP24	CH_3	CH_3	Cl	H	Cl	O	5.81	N/A	49.05	100
CP25	H	H	Cl	Cl	H	O	5.36	8.58	67.43	10
CP26	CH_3	CH_3	Cl	Cl	H	O	5.81	N/A	49.85	100
CP27	H	H	Cl	Cl	H	S	6.25	7.80	50.36	10

*PSA= Polar Surface Area in $Å^2$; **GA= Glioblastoma cell line LN-229 activity in µg/ml; Calculated molecular descriptors obtained from Chem Axon's Marvin Sketch Software

Introducing *N*, *N* substitution into Structural Motif B, leads to Structural Motif C. Structural Motif C compounds may be either *N*, *N*- dimethyl or unsubstituted, with both examples yielding biological activity at 10 µg/ml concentrations (**CP22**, **CP25** and **CP27**). This variation also explores the effect of dichloro substitution on the aryl moiety. Here we see that although all compounds of this category are active at 100 µg/ml, only a handful are active at lower concentrations. Similar to the example in Table 1.3, **CP21** is inactive at lower concentrations while its sulfur analogue, **CP22**, is active at lower concentrations. This outcome was somewhat unexpected since the calculated physical descriptors for **CP21** are closer to the targeted values than those for **CP22**. These results suggest that smaller, more lipophilic compounds such as **CP21** are more efficient in modulating apoptosis in the presence of mutant p53.

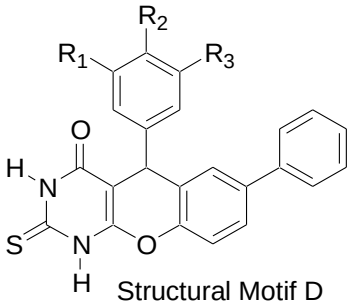

Structural Motif D

Table 1.5: Calculated molecular descriptors and biological activity of Structural Motif D (Method B) compounds against the LN-229 cell line

Compound	R_1	R_2	R_3	ClogP	pKa	PSA*	GA**
CP28	H	H	NO_2	4.98	7.80	96.18	10
CP29	H	NO_2	H	4.98	7.80	96.18	10
CP30	H	OH	OCH_3	4.58	7.80	79.22	10
CP31	OCH_3	OCH_3	OCH_3	4.57	8.80	78.05	10

*PSA= Polar Surface Area in $Å^2$; **GA= Glioblastoma cell line LN-229 activity in µg/ml; Calculated molecular descriptors obtained from Chem Axon's Marvin Sketch Software

We also wished to explore the structural modifications necessary to impart enhanced biological activity exclusively for sulfur analogues of Structural Motifs B and C, leading to the formation of Structural Motif D, shown in Table 1.5. Although in this case, only *N*-unsubstituted derivatives are explored, both electron donating substituents such as trimethoxy substituted **CP 31** and **CP30** as well as electron withdrawing groups such as nitro compounds **CP28** and **CP29** are included. Interestingly, all compounds belonging to Structural Motif D, **CP28**-**CP30**, are active at both 100 µg/ml as well as 10 µg/ml concentrations. In terms of the calculated physical properties, these compounds have calculated logP values ranging from 4.57 to 4.98, which is higher than the ideal value, but apparently still low enough to impart favorable activity. The pKa values range from 7.80 to 8.80, which is near the targeted value of 6.00. These derivatives also have higher polar surface areas ranging from 78.05 $Å^2$ to 96.18 $Å^2$, which are closer to the ideal value of 100 $Å^2$ than previously synthesized compounds.

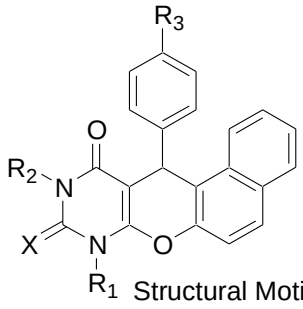

Structural Motif E

Table 1.6: Calculated molecular descriptors and biological activity of Structural Motif E (Method B) monofluoro and monochloro substituted compounds against the LN-229 cell line

Compound	R_1	R_2	R_3	X	ClogP	pKa	PSA*	GA**
CP32	H	H	H	O	3.50	8.77	67.43	100
CP33	H	H	F	O	3.64	8.89	67.43	10
CP34	H	H	F	S	4.53	7.80	50.36	10
CP35	H	H	Cl	O	4.10	8.55	67.43	10
CP36	H	CH_3	Cl	O	4.32	9.07	58.64	10
CP37	CH_3	CH_3	Cl	O	4.55	N/A	49.85	100
CP38	H	H	Cl	S	4.99	7.80	50.36	10

*PSA= Polar Surface Area in $Å^2$; **GA= Glioblastoma cell line LN-229 activity in µg/ml; Calculated molecular descriptors obtained from Chem Axon's Marvin Sketch Software

Considering the promising results of Structural Motifs B-D, we were interested to investigate the implications of adding an aromatic group to the core moiety that is in conjugation with the rest of the system to form tetracyclic Structural Motif E, unlike the previous structures, which were tricyclic. Structural Motif E includes *N*- unsubstituted derivatives as well as *N*, *N*-dimethyl and *N*- methyl substituents. Although all compounds were active at 100 µg/ml, only the *N*-unsubstituted derivatives (**CP33**, **CP34**, **CP35** and **CP38**) and *N*-methyl substituted **CP36** are active at the lower concentration of 10 µg/ml. This class of compounds focuses primarily on derivatives with halogen substitution, such as fluorine and chlorine at position 3 while including their sulfur and oxygen analogs for comparison. All of the halogenated compounds either lacking *N*-substitution or having *N*-methyl monosubstitution were active at lower concentrations. Since

CP32, which lacks both *N*-substitution as well as halogen substitution, is inactive, in this case, the inclusion of a halogen appears to be important for optimal biological activity. One would assume this is due to an increase in lipophilicity, however, the calculated logP values only differ between **CP32** and **CP33** by an increase of 0.14. The pKa values are also fairly close, with an increase of 0.12 by the inclusion of fluorine in position 3 in **CP33**. The polar surface areas, however, are the same for both **CP32** and **CP33**. This example illustrates how a minimal increase in lipophilicity and pKa can mean the difference between good and marginal activity.

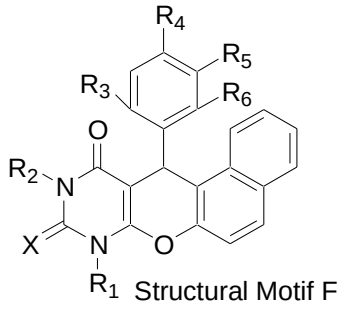

Structural Motif F

Table 1.7: Calculated molecular descriptors and biological activity of Structural Motif F (Method B) di and tri chloro substituted compounds against the LN-229 cell line

Compound	R_1	R_2	R_3	R_4	R_5	R_6	X	ClogP	PKa	PSA*	GA**
CP39	H	H	H	H	Cl	Cl	O	4.70	8.58	67.43	10
CP40	H	CH_3	H	H	Cl	Cl	O	4.93	9.06	58.64	100
CP41	CH_3	CH_3	H	H	Cl	Cl	O	5.15	N/A	49.85	100
CP42	H	H	H	H	Cl	Cl	S	5.59	7.80	50.36	10
CP43	H	H	H	Cl	H	Cl	O	4.70	8.58	67.43	10
CP44	H	CH_3	H	Cl	H	Cl	O	4.93	9.06	58.64	10
CP45	H	H	H	Cl	H	Cl	S	5.59	7.80	50.36	10
CP46	H	H	H	Cl	Cl	H	O	4.70	8.58	67.43	10
CP47	H	CH_3	H	Cl	Cl	H	O	4.93	9.07	58.64	10
CP48	CH_3	CH_3	H	Cl	Cl	H	O	5.15	N/A	49.85	10
CP49	H	H	H	Cl	Cl	H	S	5.59	7.80	50.36	10
CP50	H	H	Cl	Cl	H	Cl	S	6.20	7.80	50.36	10

*PSA= Polar Surface Area in $Å^2$; **GA= Glioblastoma cell line LN-229 activity in µg/ml; Calculated molecular descriptors obtained from Chem Axon's Marvin Sketch Software

In Structural Motif F, we wished to further explore the effect of multiple chlorine substituents in various positions on the aromatic ring in combination with the tetracyclic core structure in both oxygen and sulfur analogues. Derivatives of this class may have dichloro or trichloro substitution in positions 3, 4, 5 or 6 of the aromatic ring. These compounds may be *N*-unsubstituted, *N*-methyl substituted or *N*, *N*- dimethyl substituted. All compounds belonging to Structural Motif F exhibited biological activity at a concentration of 100 μg/ml, with ten of the twelve analogues (**CP39** and **CP42- CP50**) having activity at lower concentrations of 10 μg/ml. **CP40** and **CP41**, the two compounds which did not have activity at lower concentrations did not have values for the calculated molecular descriptors which were vastly different from the rest of the active compounds. In fact, the average calculated logP values for all compounds active at 100 μg/ml was 5.18, the average pKa was 7.00 and the average polar surface area was 56.61 $Å^2$. However, the average values for derivatives which were active at lower concentrations were slightly higher than the average calculated physical descriptors at higher concentrations, with an average calculated logP of 5.21, average pKa of 7.50 and average polar surface area of 57.09 $Å^2$. Although these changes between the predicted molecular descriptors of compounds active at higher versus lower concentrations are subtle, they provide valuable insight into the ideal profile of derivatives functioning as apoptotic regulators.

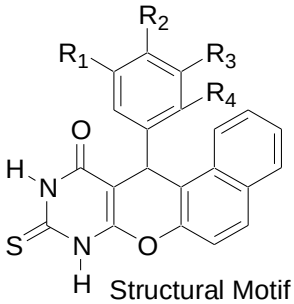

Structural Motif G

Table 1.8: Calculated molecular descriptors and biological activity of Structural Motif G (Method B) substituted 2-sulfanylidene compounds against the LN-229 cell line

Compound	R_1	R_2	R_3	R_4	ClogP	pKa	PSA*	GA**
CP51	H	H	H	Br	5.15	7.80	50.36	10
CP52	H	H	Br	H	5.15	7.80	50.36	10
CP53	H	H	OH	H	4.08	7.79	70.59	100
CP54	H	H	NO_2	H	4.33	7.80	96.18	10
CP55	H	NO_2	H	H	4.33	7.80	96.18	10
CP56	4-pyridinyl				3.17	5.03	63.25	100
CP57	Br	H	OCH_3	H	5.00	7.80	59.59	10
CP58	OCH_3	OCH_3	OCH_3	H	3.91	7.80	78.05	10

*PSA= Polar Surface Area in $Å^2$; **GA= Glioblastoma cell line LN-229 activity in µg/ml; Calculated molecular descriptors obtained from Chem Axon's Marvin Sketch Software

Considering the success of the sulfur analogues across all structural motifs, we designed Structural Motif G to further investigate which structural characteristics confer fine-tuned biological activity among tetracyclic sulfur compounds. Substituents on the aromatic ring may be halogens, as with the case of **CP51** and **CP52** which are bromo substituted, electron donating trimethoxy and hydroxy (**CP53** and **CP58**) as well as electron withdrawing nitro substituents (**CP54** and **CP55**). Other derivatives include the replacement of the substituted aryl moiety with the nitrogen heterocycle pyridine (**CP56**) as well as the inclusion of both bromo and methoxy groups (**CP57**). At 100µg/ml concentrations, all Structural Motif G analogues were active. However, at lower concentrations, the hydroxy **CP53** and pyridinyl **CP56** derivatives were not active. Comparing the calculated molecular descriptors of **CP56** to the rest of the compounds

active at lower concentrations, the calculated logP, pKa and polar surface area are all slightly lower than that or more potent compounds. Interestingly, for **CP53**, the predicted physical properties are similar to those of compounds active at lower concentrations. One suggestion for the diminished activity of **CP53** at lower concentrations is that the close proximity of the hydroxy group to the tetracyclic core prevents the necessary interaction needed to facilitate binding of **CP53** to the HDM2 protein, our proposed target.

1.11 Discussion

We were able to successfully design and develop a small library of chromenopyrimidinediones as potential HDM2 inhibitors. Utilizing either method A or B, described here, a variety of derivatives were synthesized. Areas of variation throughout this small library include *N*-substitution on the barbituric acid moiety, which can be either *N*-phenyl, *N*- methyl, *N*, *N*- dimethyl or *N*-unsubstituted. Another alteration that can be made on the barbituric acid portion is the replacement of the carbonyl oxygen with a sulfur, since sulfur lends itself to an increase in the lipophilicity of the molecule to which it is attached. In addition to these options, the core structure may be either tricyclic or tricyclic with an attached phenyl group that is not in conjugation with the rest of the molecule or tetracyclic. Additionally, a host of substituents may also be present to create unique electronic profiles. Substituents may be electron donating groups such as hydroxy, methyl or methoxy, electronically neutral hydrogen or phenyl or electron withdrawing such as the nitrogen heterocycle pyridine, halogens including fluorine, bromine and chlorine or nitro groups.

Nearly all synthesized compounds show biological activity against the glioblastoma cell line LN-229 at 100 μg/ml concentrations, with 80% of these compounds also have activity at lower concentrations of 10 μg/ml. Of these compounds active at 10μg/ml, four (**CP4**, **CP6**, **CP7** and

CP10) were found to be active at even lower concentrations of 1μg/ml. Tetracyclic compounds showed enhanced activity over the tricyclic derivatives. Oxygen and sulfur compounds were found to be equally potent. However, we found that the *N*-unsubstituted compounds represent the majority of biologically active compounds active at lower concentrations. Another interesting observation was that the substituents on more active compounds were electronically diverse, including methoxy groups, halogens such as fluorine, bromine and chlorine as well as nitro substituents.

Along with biological testing results, we also used the parameters of calculated logP, pKa and polar surface area as described in the "sweet spot" approach for drug discovery and design[37] as a guide. Calculated logP, pKa and polar surface area values provide insight into how easily a molecule may cross membranes, which is a major drawback to many drugs, especially those intended to cross the blood-brain barrier such as for the treatment of glioblastoma. Ideal values for the calculated logP, pKa and polar surface area are defined as approximately 1.00, 6.00 and 100 $Å^2$, respectively. Our compounds which are active at 10 μg/ml concentrations show an average calculated logP of 4.26 with values ranging from 0.64 to 6.70. These compounds also exhibited an average pKa value of 7.09, with individual values ranging from 6.22 to 9.07. The average polar surface area of 63.73 $Å^2$ with a maximum of 96.18 $Å^2$ and a minimum of 32.78 $Å^2$ is much lower than the targeted value of 100 $Å^2$. It is interesting to note that although the average calculated logP and polar surface area values for the compounds with enhanced activity are notably lower than the ideal values, they still possess potent activity. Taken together, the biological testing results as well as the calculated physical descriptors provide a dual-pronged approach to successfully identifying novel chromenopyrimidinediones with excellent activity (**CP4**, **CP6**, **CP7** and **CP10**) as potential HDM2 inhibitors.

Chapter 2: Design, Synthesis and Biological Evaluation of *N*-Alkylated Pyrimidinequinolinedione Derivatives

2.1 Introduction

The nitrogenous analogues of the chromenopyrimidinediones, the pyrimidinequinolinediones, provide another source of variation since the central nitrogen atom can bear additional substituents such as methyl or butyl moieties, mimicking the five-carbon ribose chain of FAD and $FADH_2$. The synthesis of the pyrimidinequinolinediones is similar to that of the chromenopyrimidinediones, except in this case, a substituted aniline is used instead of a substituted phenol and phosphoric acid is not necessary. Like the preparation of the chromenopyrimidinediones, the synthesis of the pyrimidinequinolinediones can be carried out as either a two-step synthesis or a one-pot reaction, both in refluxing acetic acid. Upon continued refluxing in acetic acid, the reduced compound is slowly converted into its oxidized form. Using this methodology, a wide variety of analogues may be prepared to form a small library.

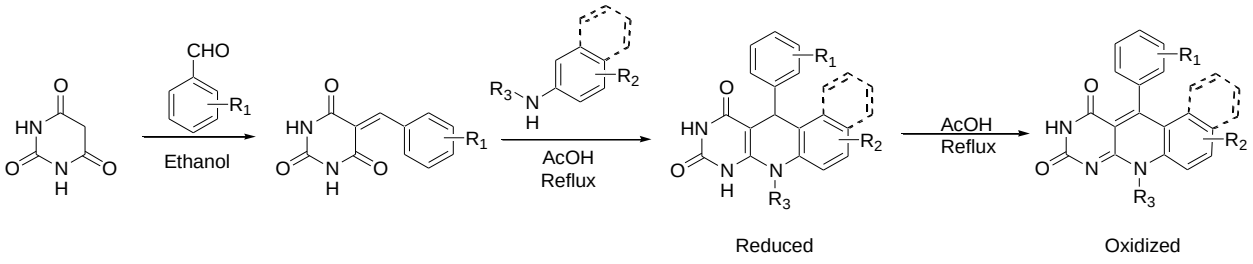

Figure 20: Synthesis of pyrimidinequinolinediones via *N*-substituted or *N*, *N*-disubstituted barbituric acid, an aryl aldehyde and the corresponding aniline

2.2 Preparation of *N*-Alkylated Anilines

2.1.1 *N*-Alkylated Anilines from Primary Anilines

While many of the substituted anilines are readily available, *N*-substituted anilines, especially *N*-alkylated anilines, have extremely limited availability. If the substituted primary aniline is readily available, *N*-methylation of this substituted primary aniline may be accomplished using the previously described method[38] of *N*-methylation of primary amines via benzotriazole. In this reaction, the first step involves the coupling of the primary aniline nitrogen to the benzotriazole nitrogen by a formaldehyde linker. This intermediate then undergoes reduction with sodium borohydride, reducing the CH_2 linkage between the benzotriazole and the aniline to yield the *N*-methylated aniline. For the synthesis of other *N*-substituted anilines, appropriate aldehydes may be substituted for formaldehyde to yield the corresponding *N*-substituted aniline.

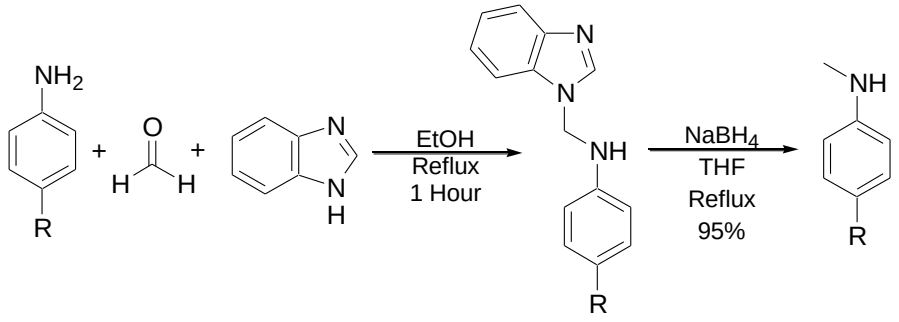

Figure 21: Synthesis of substituted *N*-methyl anilines from readily available substituted primary aromatic amines

2.2.2 *N*-Alkylated Anilines from Phenols

In some cases, the substituted primary anilines are not readily available, but their substituted phenol analogues are available and often times more economical to purchase. Fortunately, *N*-substituted anilines may be prepared from substituted phenols[39]. In the first step, the phenol is

converted to an ester via the Williamson Ester Synthesis. In the second step, this ester is readily converted to an amide by nucleophilic acyl substitution with methyl amine. In the third and final step, this amide undergoes a rearrangement and elimination to give the desired secondary amine. This rearrangement begins with the deprotonation of the amide hydrogen leading to an anion which then carries out a nucleophilic attack on the same carbon to which the ester oxygen is attached. At this time, a five-membered transition state in which the C-O bond of the ester and the C-N bond of the amide to the same carbon exist simultaneously. However, the weaker C-O bond breaks first to furnish the oxygen anion, which carries out a nucleophilic attack on the carbonyl carbon, breaking the C-N amide bond. The broken C-N bond results in the deprotonated *N*-substituted aniline, which extracts a proton from water to form the neutral product.

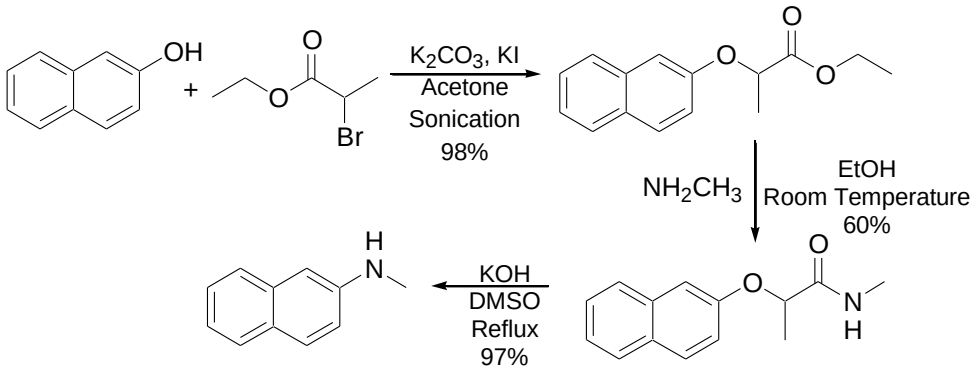

Figure 22: Synthesis of *N*-alkylated anilines from phenols

Using this methodology, we successfully prepared several of our starting materials, including *N*-methyl 2-naphthylamine, *N*-butyl 2-naphthylamine and *N*-methyl aniline. An example of this method as it applies to our synthetic goal is shown below. In this instance 2-naphthol is converted into the corresponding ester via a base catalyzed reaction with

ethyl-2-bromopropanoate. This ester is then combined with *N*-methylamine, which carries out a nucleophilic attack on the carbonyl carbon of the ester. The attack of the *N*-methyl amine leads to the aforementioned five-membered transition state, in which the C-O bond cleaves to form the *N*-methylanilium anion which then extracts a proton from water to yield the uncharged *N*-methyl aniline.

2.3 Biological Testing Results

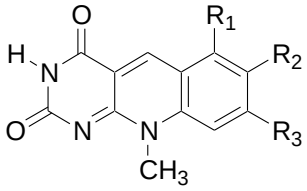

Structural Motif A

Table 2.1: Calculated molecular descriptors and biological activity of Structural Motif A (Method A) compounds against the LN-229 cell line

Compound	R_1	R_2	R_3	ClogP	pKa	PSA*	GA**
AQ1	H	CH_3	H	1.15	1.13	61.77	NA
AQ2	H	CH_3	CH_3	1.66	1.31	61.77	NA
AQ3	H	Cl	H	1.24	0.08	61.77	NA
AQ4	H	Br	H	1.40	0.29	61.77	NA
AQ5	-$(CH)_4$-		H	1.62	0.86	61.77	NA
AQ6	Same as **AQ5** with C_4H_9			2.95	1.54	61.77	NA

*PSA= Polar Surface Area in $Å^2$; **GA= Glioblastoma cell line LN-229 activity in µg/ml; NA= No Activity at the maximum 100 µg/ml concentration; Calculated molecular descriptors obtained from Chem Axon's Marvin Sketch Software

We began our investigation with the synthesis of the 10-*N*-methylpyrimidinequinolinedione core structure as well as its derivatives, forming Structural Motif A. Compounds belonging to this class may be substituted on three different positions on the phenyl ring and may include substituents such as methyl groups (**AQ1** and **AQ2**) and halogens such as chlorine and bromine (**AQ3** and **AQ4**). Additionally, a naphthyl group may replace the terminal phenyl portion of Structural Motif A, as in the cases of **AQ5** and **AQ6**. **AQ6** also incorporates another variation

with the replacement of the *N*-methyl group of the central ring with an *N*-butyl group instead. We chose to investigate primarily *N*-alkyl substituted compounds for two reasons. One of those reasons is because we believe these derivatives will exhibit enhanced activity due to their increased lipophilicity, which is important for drugs intended to cross the blood-brain barrier. Introducing *N*-alkyl substitution, especially single carbon methyl and four carbon butyl, mirrors the five-carbon ribose chain of FAD and $FADH_2$. Whereas our previously synthesized chromenopyrimidinediones, which may be considered oxygen analogues to the pyrimidinequinolinediones, explored the idea of *N*- substitution on the barbituric acid moiety, we chose to focus on simple *N*- unsubstituted compounds due to the lack of activity shown by the *N*- substituted chromenopyrimidinediones. Unfortunately, this set of derivatives did not exhibit the significant biological activity we had hoped for at concentrations of 10 µg/ml. Upon further analysis of the calculated molecular descriptors of these analogues, this result makes sense because the pKa values for these compounds are too far away from the desired value of approximately 6.00, ranging from a minimum of 0.08 to a maximum of 1.54. The calculated logP values are reasonably within range of the desired value of 1.00. However, the polar surface areas of these compounds are low, which could explain the lack of activity. Considering these results, we chose to synthesize a series of target structures to bring the calculated physical descriptors closer to the desired values.

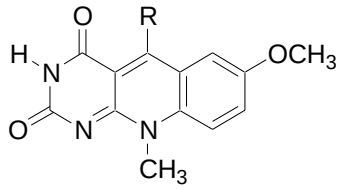

Structural Motif B

Table 2.2: Calculated molecular descriptors and biological activity of Structural Motif B (Method A) compounds against the LN-229 cell line

Compound	R	ClogP	pKa	PSA*	GA**
AQ14	phenyl	1.91	0.53	71.00	NA
AQ15	2-pyridinyl	1.08	-0.11	83.89	NA
AQ16	3-pyridinyl	0.69	0.36	83.89	NA
AQ17	4-pyridnyl	0.69	0.22	83.89	NA

*PSA= Polar Surface Area in $Å^2$; **GA= Glioblastoma cell line LN-229 activity in µg/ml; NA= No Activity at the maximum 100 µg/ml concentration; Calculated molecular descriptors obtained from Chem Axon's Marvin Sketch Software

In order to increase the polar surface area, an aromatic moiety was added to the 5 position of Structural Motif A to form Structural Motif B. Aromatic groups included simple phenyl (**AQ14**) as well as the heterocyclic 2-pyridinyl (**AQ15**), 3- pyridinyl (**AQ16**) and 4-pyridinyl (**AQ17**) entities. As predicted, this modification led to a marginal increase in the polar surface area of these derivatives, although it is still slightly lower than the desired value. Calculated logP values remained favorable while the pKa values are still far too low. The lack of activity exhibited by all analogues in this class suggests that the calculated molecular descriptors for these compounds must be closer to the desired values to elicit the desired biological activity.

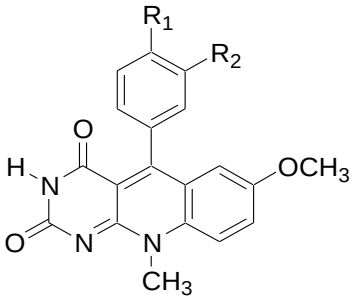

Structural Motif C

Table 2.3: Calculated molecular descriptors and biological activity of Structural Motif C (Method A) compounds against the LN-229 cell line

Compound	R_1	R_2	ClogP	pKa	PSA*	GA**
AQ7	H	OH	1.61	0.51	91.23	NA
AQ10	OCH_3	H	1.75	0.56	80.23	NA
AQ11	CH_3	H	2.42	0.55	71.00	NA
AQ13	C_6H_5	H	3.56	0.53	71.00	NA
AQ18	Br	H	2.68	0.53	71.00	NA
AQ21	Cl	H	2.51	0.53	71.00	NA
AQ22	SCH_3	H	2.54	0.53	71.00	NA
AQ23	CF_3	H	2.79	0.53	71.00	NA
AQ24	H	NO_2	1.85	0.47	116.82	NA
AQ25	NO_2	H	1.85	0.46	116.82	NA

*PSA= Polar Surface Area in $Å^2$; **GA= Glioblastoma cell line LN-229 activity in µg/ml; NA= No Activity at the maximum 100 µg/ml concentration; Calculated molecular descriptors obtained from Chem Axon's Marvin Sketch Software

The next modification we wished to explore was the addition of substituents in two possible positions on the phenyl ring. This set of compounds, belonging to Structural Motif C, exhibits a variety of electronically diverse substituents, including electron donating, electron neutral and electron withdrawing moieties. Our goal in adding these substituents was to bring the calculated physical descriptors closer to the target values, which we hoped would improve their activity. This strategy was successful in bringing the calculated polar surface area closer to the desired values in the case of hydroxyl substituted **AQ7**. However, although more favorable polar surface area values were achieved, the calculated logP values increased while the pKa values are still too low. Given this data, it is not a surprise that these derivatives lack activity. However, the

substitution on these derivatives is quite simple, leading to the idea that perhaps a more sophisticated approach involving combinations of multiple functional groups in different positions to achieve a unique electronic profile is necessary.

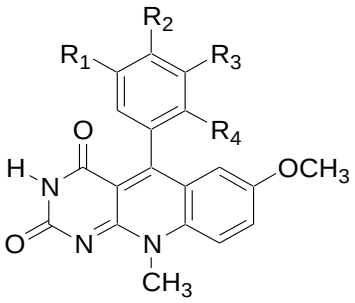

Structural Motif D

Table 2.4: Calculated molecular descriptors and biological activity of Structural Motif D (Method A) compounds against the LN-229 cell line

Compound	R_1	R_2	R_3	R_4	ClogP	pKa	PSA*	GA**
AQ8	H	OH	OCH_3	H	1.45	0.54	100.46	NA
AQ9	H	OCH_3	OCH_3	H	1.59	0.54	89.46	NA
AQ12	H	H	$-(CH)_4-$		2.90	0.49	71.00	NA
AQ19	H	H	Cl	Cl	3.12	0.42	71.00	NA
AQ20	H	Cl	Cl	H	3.12	0.51	71.00	NA
AQ26	NO_2	OH	OCH_3	H	1.39	0.48	146.28	NA
AQ27	NO_2	H	H	OH	1.55	0.37	137.05	NA

*PSA= Polar Surface Area in $Å^2$; **GA= Glioblastoma cell line LN-229 activity in µg/ml; NA= No Activity at the maximum 100 µg/ml concentration; Calculated molecular descriptors obtained from Chem Axon's Marvin Sketch Software

In an attempt to tailor the activity of these derivatives, we explored the effects of incorporating multiple substituents in four different positions on the aromatic ring, leading to Structural Motif D. Substituents on the phenyl ring include various combinations of hydroxyl, methoxy, dichloro and nitro groups. Additionally, the phenyl ring may be replaced with a 1-naphthyl group as in the example of **AQ12**, leading to a tetracyclic structure. It was our hope that the combination of these substituents would lead to favorable activity. Unfortunately, that was not

necessarily the case. The calculated logP values are somewhat within the range of the targeted value of 1.00, but the pKa values are still too low to favor diffusion across membranes, as is often the case for drugs targeting the central nervous system. The polar surface area values vary greatly, ranging from 71.00 Å² to 146.28 Å². Molecules with slightly lower polar surface areas such as 71.00 Å², however, has a better chance of entering the cell than molecules with a larger polar surface areas such as 146.28 Å². Nevertheless, this structural motif did not produce any biologically active analogues.

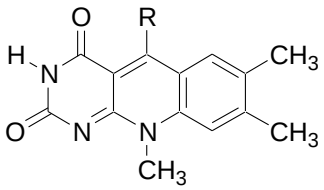

Structural Motif E

Table 2.5: Calculated molecular descriptors and biological activity of Structural Motif E (Method A) compounds against the LN-229 cell line

Compound	R	ClogP	pKa	PSA*	GA**
AQ33	Phenyl	3.09	0.93	61.77	NA
AQ34	2-pyridinyl	2.26	0.30	74.66	NA
AQ35	3-pyridinyl	1.88	0.76	74.66	NA
AQ36	4-pyridinyl	1.88	0.62	74.66	NA

*PSA= Polar Surface Area in $Å^2$; **GA= Glioblastoma cell line LN-229 activity in µg/ml; NA= No Activity at the maximum 100 µg/ml concentration; Calculated molecular descriptors obtained from Chem Axon's Marvin Sketch Software

Considering these results, we decided to revisit another variation of the core structure, resulting in the formation of Structural Motif E. Structural Motif E is similar to Structural Motif B, except that the methoxy group in the position 7 is replaced by two methyl groups in positions 7 and 8, respectively. Similarly to Structural Motif B, Structural Motif E also has identical aromatic substituents at position 5. The aromatic substituents may be phenyl as in the case of **AQ33** or

heterocyclic 2-pyridinyl, 3-pyridinyl or 4-pyridinyl as in the cases of **AQ 34**, **AQ35** and **AQ36**, respectively. It was predicted that this modification would lead to an increase in the lipophilicity of the derivatives and in this way perhaps effectively compensate for the low pKa values. While this alteration does produce more lipophilic molecules with higher calculated log P values ranging from 1.88 to 3.09, it is not enough to offset the less than desirable pKa and polar surface area values. Therefore, although this alteration does change the calculated molecular descriptors slightly, it is not enough to substantially affect the biological activity of compounds **AQ33-AQ36**, which show no biological activity.

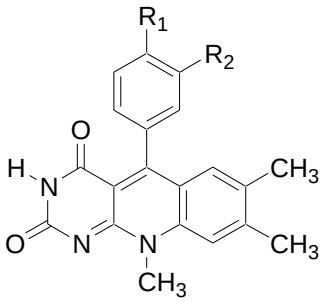

Structural Motif F

Table 2.6: Calculated molecular descriptors and biological activity of Structural Motif F (Method A) compounds against the LN-229 cell line

Compound	R_1	R_2	ClogP	pKa	PSA*	GA**
AQ30	OCH_3	H	2.94	0.96	71.00	NA
AQ31	CH_3	H	3.61	0.95	61.77	NA
AQ32	C_6H_5	H	4.74	0.93	61.77	NA
AQ37	Br	H	3.86	0.92	61.77	NA
AQ38	Cl	H	3.70	0.92	61.77	NA
AQ41	SCH_3	H	3.72	0.93	61.77	NA
AQ42	CF_3	H	3.97	0.92	61.77	NA
AQ43	H	NO_2	3.03	0.87	107.59	NA
AQ44	NO_2	H	3.03	0.86	107.59	NA

*PSA= Polar Surface Area in $Å^2$; **GA= Glioblastoma cell line LN-229 activity in µg/ml; NA= No Activity at the maximum 100 µg/ml concentration; Calculated molecular descriptors obtained from Chem Axon's Marvin Sketch Software

Despite these results, we continued to pursue our investigation by further modification of Structural Motif E, leading to Structural Motif F. Structural Motif F includes two possible areas of monosubstitution on the phenyl ring. Substituents may be electron donating, electronically neutral or electron withdrawing, creating a unique electronic profile. The consequence of this modification echoes that of previous structural motifs, with an increase in the calculated logP values while the pKa values remain low and the polar surface area values range from a minimum value of 61.77Å² to a maximum value of 107.59Å². Not surprisingly, this combination of physical descriptors did not produce any biologically active analogues from Structural Motif F, leading us to explore additional modifications.

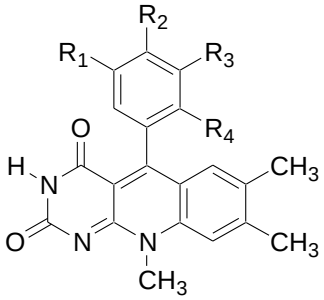

Structural Motif G

Table 2.7: Calculated molecular descriptors and biological activity of Structural Motif G (Method A) compounds against the LN-229 cell line

Compound	R_1	R_2	R_3	R_4	ClogP	pKa	PSA*	GA**
AQ28	H	OH	OCH_3	H	2.63	0.93	91.23	NA
AQ29	H	OCH_3	OCH_3	H	2.78	0.93	80.23	NA
AQ39	H	H	Cl	Cl	4.30	0.81	61.77	10
AQ40	H	Cl	Cl	H	4.30	0.90	61.77	NA
AQ45	NO_2	OH	OCH_3	H	2.57	0.88	137.05	NA
AQ46	Br	H	H	OH	3.56	0.80	82.00	NA
AQ47	Cl	H	H	OH	3.39	0.80	82.00	10
AQ48	NO_2	H	H	OH	2.73	0.76	127.82	NA

*PSA= Polar Surface Area in $Å^2$; **GA= Glioblastoma cell line LN-229 activity in µg/ml; NA= No Activity at the maximum 100 µg/ml concentration; Calculated molecular descriptors obtained from Chem Axon's Marvin Sketch Software

In Structural Motif G, the variety of substituents is increased by adding two more positons where substitution may occur. Unlike the previous sets of derivatives, this structural motif produced two compounds, **AQ39** and **AQ47**, which were biologically active against the LN-229 cell line at 10 µg/ml concentrations. While the pKa and polar surface area values of these two active derivatives are still low at 0.81 and 0.80 and 61.77Å² and 82.00 Å², respectively, they show increased lipophilicity, with calculated logP values of 4.30 and 3.39. Interestingly, both **AQ39** and **AQ40**, which are both dichloro substituted, have nearly identical values for their calculated physical descriptors, yet **AQ39** is active while **AQ40** is inactive. The only difference between these two compounds is the position of their dichloro substituents, with **AQ39** having chlorine as R_3 and R_4, and **AQ40** having chlorine as R_2 and R_3. Another interesting observation is that while active compound **AQ47** has a hydroxyl group as R_4 and chlorine as R_3, other derivatives where the chlorine is replaced by groups such as bromo (**AQ46**) and nitro (**AQ48**), activity is abolished. While the biological activity of **AQ47** may be partially attributed to the ability of the hydroxyl group to hydrogen bond to HDM2, mimicking the bonding of p53 to HDM2. The difference in activity between similar derivatives such as **AQ46** and **AQ47** which differ only in their halogen substituents of bromine and chlorine, is that the smaller, more compact chlorine is preferred over the larger, bromine, which creates a more sterically favorable binding environment for HDM2.

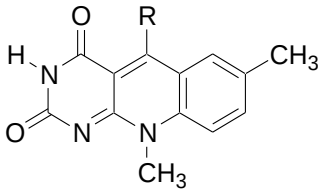

Structural Motif H

Table 9: Calculated molecular descriptors and biological activity of Structural Motif H (Method A) compounds against the LN-229 cell line

Compound	R	ClogP	pKa	PSA*	GA**
AQ55	C_6H_6	2.58	0.74	61.77	NA
AQ56	2-pyridinyl	1.75	0.11	74.66	NA
AQ57	3-pyridinyl	1.36	0.57	74.66	NA
AQ58	4-pyridinyl	1.36	0.43	74.66	NA

*PSA= Polar Surface Area in $Å^2$; **GA= Glioblastoma cell line LN-229 activity in µg/ml; NA= No Activity at the maximum 100 µg/ml concentration; Calculated molecular descriptors obtained from Chem Axon's Marvin Sketch Software

Considering the success of replacing the 7-methoxy of our original Structural Motif B with two methyl groups at positions 7 and 8, we were interested to explore the effects of introducing one methyl group in the 7 position. In Structural Motif H, we studied the effect of this modification with phenyl (**AQ55**), 2-pyridinyl (**AQ56**), 3-pyridinyl (**AQ57**) and 4-pyridinyl (**AQ58**) groups in the 5 position. This alteration led to reasonable calculated logP values ranging from 1.36 to 2.58, but unsatisfactory pKa values and polar surface area values. The pKa values remain below 1.0, as opposed to the targeted value of 6.0. The polar surface areas also remain on the low side, with a minimum polar surface area of 61.77Å² as seen in **AQ55** and a maximum polar surface area of 74.66Å² as seen in the analogues **AQ56**, **AQ57** and **AQ58**. Considering these observations, it was expected that analogues **AQ55-AQ58** would not show any considerable biological activity.

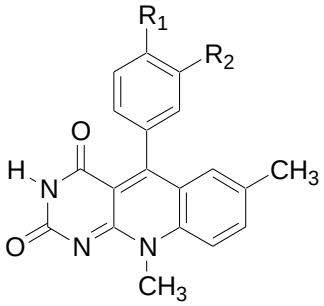

Structural Motif I

Table 2.9: Calculated molecular descriptors and biological activity of Structural Motif I (Method A) compounds against the LN-229 cell line

Compound	R_1	R_2	ClogP	pKa	PSA*	GA**
AQ49	H	OH	2.28	0.72	82.00	NA
AQ52	OCH_3	H	2.42	0.77	71.00	NA
AQ54	C_6H_5	H	4.23	0.74	61.77	10
AQ59	Br	H	3.35	0.74	61.77	NA
AQ60	Cl	H	3.18	0.74	61.77	NA
AQ63	SCH_3	H	3.21	0.74	61.77	NA
AQ64	H	NO_2	2.52	0.68	107.59	NA
AQ65	NO_2	H	2.52	0.67	107.59	NA

*PSA= Polar Surface Area in $Å^2$; **GA= Glioblastoma cell line LN-229 activity in µg/ml; NA= No Activity at the maximum 100 µg/ml concentration; Calculated molecular descriptors obtained from Chem Axon's Marvin Sketch Software

Nevertheless, we were still interested to see what effect R_1 and R_2 monosubstitution on the phenyl ring would have on the biological activity of these derivatives, leading to the formation of Structural Motif I. The only analogue of this class showing biological activity at 10µg/ml concentrations is the phenyl substituted derivative **AQ54**. Perhaps not incidentally, **AQ54** with a value of 4.23 has the highest calculated logP of this class of compounds as well. The combination of this increase in lipophilic character with a low pKa value of 0.74 and a low polar surface area value of 61.77 $Å^2$ is sufficient for **AQ54** to exhibit biological activity. Other derivatives belonging to Structural Motif I also have low pKa values, but also have either insufficient lipophilicity or are too high in their polar surface area.

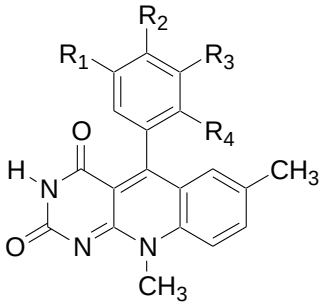

Structural Motif J

Table 2.10: Calculated molecular descriptors and biological activity of Structural Motif J (Method A) compounds against the LN-229 cell line

Compound	R_1	R_2	R_3	R_4	ClogP	pKa	PSA*	GA**
AQ50	H	OH	OCH_3	H	2.12	0.75	91.23	NA
AQ51	H	OCH_3	OCH_3	H	2.26	0.75	80.23	NA
AQ53	H	H	$-(CH)_4-$		3.57	0.70	61.77	NA
AQ61	H	H	Cl	Cl	3.79	0.63	61.77	NA
AQ62	H	Cl	Cl	H	3.79	0.72	61.77	NA
AQ66	NO_2	OH	OCH_3	H	2.06	0.69	137.05	10
AQ67	Br	H	H	OH	3.05	0.62	82.00	NA
AQ68	Cl	H	H	OH	2.88	0.61	82.00	NA
AQ69	NO_2	H	H	OH	2.22	0.58	127.82	NA

*PSA= Polar Surface Area in $Å^2$; **GA= Glioblastoma cell line LN-229 activity in µg/ml; NA= No Activity at the maximum 100 µg/ml concentration; Calculated molecular descriptors obtained from Chem Axon's Marvin Sketch Software

The next modification we wished to investigate was the effect of additional substitution in two other possible positions on the phenyl ring, leading to Structural Motif J. Like Structural Motif I, Structural Motif J produced one biologically active compound, **AQ66**. **AQ66** has a moderate calculated logP value of 2.06, a low pKa of 0.69 and a high polar surface area of 137.05 $Å^2$, which is the highest of the group. Considering the activity of **AQ54** from Structural Motif I and **AQ66** from Structural Motif J, it is possible that perhaps low pKa values may be compensated for by higher calculated logP values or in the case of **AQ 66**, higher than desired polar surface area values. This suggestion is logical because pKa values outside of the range of 4.00-6.00 have difficulty crossing cellular membranes, while highly lipophilic analogues freely cross cellular

membranes. One criticism of molecules with increased lipophilicity is that they will be cleared out of the system too quickly. However, when combined with another physical descriptor which limits the ability of a molecule to cross membranes, such as a low pKa or a high polar surface area, these analogues are not able to be cleared from the body as quickly as they would be with pKa values between 4.00 and 6.00 and polar surface area values closer to 100Å^2.

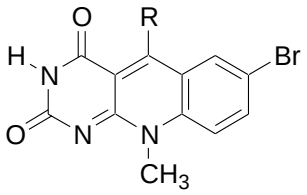

Structural Motif K

Table 2.11: Calculated molecular descriptors and biological activity of Structural Motif K (Method A) compounds against the LN-229 cell line

Compound	R	ClogP	pKa	PSA*	GA**
AQ77	phenyl	2.84	-0.10	61.77	NA
AQ78	2-pyridinyl	2.00	-0.73	74.66	NA
AQ79	3-pyridinyl	1.62	-0.27	74.66	NA
AQ80	4-pyridinyl	1.62	-0.41	74.66	NA

*PSA= Polar Surface Area in Å^2; **GA= Glioblastoma cell line LN-229 activity in µg/ml; NA= No Activity at the maximum 100 µg/ml concentration; Calculated molecular descriptors obtained from Chem Axon's Marvin Sketch Software

Another variation we wished to explore was the effect of the replacement of the 7-methyl group with a larger halogen, such as bromine, forming an entirely new Structural Motif K. Unlike the previous methyl and methoxy groups which are electron donating, in this case, bromine is slightly electron withdrawing. The inclusion of bromine in the 7 position in combination with aromatic substituents in the 5 position such as phenyl (**AQ77**), 2-pyridinyl (**AQ78**), 3-pyridinyl (**AQ79**) and 4-pyridinyl (**AQ80**) did not yield any compounds with biological activity. This lack

of activity may be explained by the low calculated logP values in conjunction with even lower pKa values. The modest lipophilicity of these analogues might be sufficient to cross into the cell if the pKa values were closer to the optimal values. However, the combination of low lipophilicity coupled with negative pKa values does not make it probable that such molecules will be able to reach their target cells and are thus, inactive.

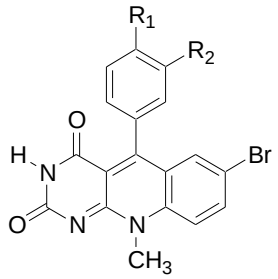

Structural Motif L

Table 2.12: Calculated molecular descriptors and biological activity of Structural Motif L (Method A) compounds against the LN-229 cell line

Compound	R_1	R_2	ClogP	pKa	PSA*	GA**
AQ70	H	OH	2.53	-0.12	82.00	NA
AQ73	OCH_3	H	2.68	-0.07	71.00	NA
AQ74	CH_3	H	3.35	-0.08	61.77	NA
AQ76	C_6H_5	H	4.48	-0.10	61.77	10
AQ81	Cl	H	3.44	-0.10	61.77	NA
AQ83	CF_3	H	3.71	-0.10	61.77	10
AQ84	NO_2	H	2.78	-0.17	107.59	NA

*PSA= Polar Surface Area in $Å^2$; **GA= Glioblastoma cell line LN-229 activity in µg/ml; NA= No Activity at the maximum 100 µg/ml concentration; Calculated molecular descriptors obtained from Chem Axon's Marvin Sketch Software

Considering the results of Structural Motif K, we designed Structural Motif L, which incorporates two substituents with a variety of electronic characteristics, providing another source of derivatives. In the case of all of these derivatives, this modification leads to an increased lipophilicity and an even lower pKa. The polar surface areas range from a minimum of

61.77 Å² to a maximum of 107.59 Å². However, despite the divergence of these values from the targeted values, both **AQ76** and **AQ83** both possess strong biological activity. **AQ76** has R_1 substitution with an additional phenyl group, which increases the lipophilicity of the molecule. **AQ83** also has enhanced lipophilicity due to a trifluoromethyl substituent at R_1 as well. Both **AQ76** and **AQ83** follow the trend previously seen in other active derivatives where an elevation in the calculated logP value in combination with a low pKa and a low polar surface area can lead to biological activity.

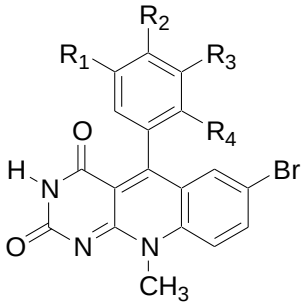

Structural Motif M

Table 103: Calculated molecular descriptors and biological activity of Structural Motif M (Method A) compounds against the LN-229 cell line

Compound	R_1	R_2	R_3	R_4	ClogP	pKa	PSA*	GA**
AQ71	H	OH	OCH_3	H	2.37	-0.09	91.23	NA
AQ73	H	OCH_3	OCH_3	H	2.68	-0.07	71.00	NA
AQ75	H	-$(CH)_4$-		H	3.82	-0.11	61.77	NA
AQ82	H	Cl	Cl	H	4.04	-0.12	61.77	NA
AQ85	NO_2	OH	OCH_3	H	2.31	-0.15	137.05	NA
AQ86	Cl	H	H	OH	3.14	-0.23	82.00	NA
AQ87	NO_2	H	H	OH	2.47	-0.26	127.82	NA

*PSA= Polar Surface Area in $Å^2$; **GA= Glioblastoma cell line LN-229 activity in µg/ml; NA= No Activity at the maximum 100 µg/ml concentration; Calculated molecular descriptors obtained from Chem Axon's Marvin Sketch Software

Encouraged by these results, we were next interested to see what effect the introduction of further substituents would have on the biological activity of these analogues, resulting in the

formation of Structural Motif M. Structural Motif M is characterized by the inclusion of two additional substituents, R_3 and R_4. Unfortunately, this set of analogues did not produce any biologically active compounds, despite having similar values for the calculated molecular descriptors to active compounds. Comparing the results of Structural Motif M to Structural Motif J, which produced one active compound and differs only in the replacement of the methyl in the 7 position with a bromine, perhaps the larger size of the bromine atom in combination with its slight electron withdrawing character and additional substitution on the 5-position phenyl makes it sterically and electronically unsuitable for binding to HDM2.

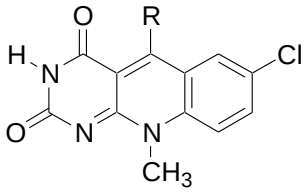

Structural Motif N

Table 2.14: Calculated molecular descriptors and biological activity of Structural Motif N (Method A) compounds against the LN-229 cell line

Compound	R	ClogP	pKa	PSA*	GA**
AQ91	1-naphthyl	3.66	-0.34	61.77	NA
AQ92	2-naphthyl	3.66	-0.31	61.77	NA
AQ93	4-biphenyl	4.32	-0.31	61.77	NA
AQ94	2-pyridinyl	1.84	-0.94	74.66	NA
AQ95	3-pyridinyl	1.45	-0.47	74.66	NA
AQ96	4-pyridinyl	1.45	-0.61	74.66	NA

*PSA= Polar Surface Area in $Å^2$; **GA= Glioblastoma cell line LN-229 activity in µg/ml; NA= No Activity at the maximum 100 µg/ml concentration; Calculated molecular descriptors obtained from Chem Axon's Marvin Sketch Software

The next modification we wished to explore was Structural Motif N, which replaces the bromine in the 7 position with chlorine instead. Although chlorine and bromine are both halogens, the bromine atom is larger than chlorine and in some cases, this size difference is often enough to

change the activity of the entire molecule. In this structural motif, substitution in the 5 position includes bicyclic groups such as 1-naphthyl (**AQ91**), 2-naphthyl (**AQ92**) and biphenyl (**AQ93**) as well as heterocyclic groups such as 2-pyridinyl (**AQ94**), 3-pyridinyl (**AQ95**) and 4-pyridinyl (**AQ96**). However, these modifications along with the replacement of the previous motif's bromine atom with a chlorine atom do not have significant effects on the predicted physical properties of these analogues or their biological activity.

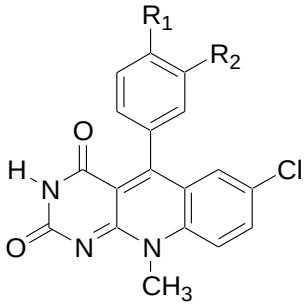

Structural Motif M

Table 2.15: Calculated molecular descriptors and biological activity of Structural Motif M (Method A) compounds against the LN-229 cell line

Compound	R_1	R_2	ClogP	pKa	PSA*	GA**
AQ88	H	OH	2.37	-0.33	82.00	NA
AQ90	CH_3	H	3.18	-0.28	61.77	NA
AQ97	Br	H	3.44	-0.31	61.77	NA
AQ98	Cl	H	3.27	-0.31	61.77	NA
AQ100	SCH_3	H	3.30	-0.30	61.77	NA
AQ101	NO_2	H	2.61	-0.37	107.59	NA

*PSA= Polar Surface Area in $Å^2$; **GA= Glioblastoma cell line LN-229 activity in µg/ml; NA= No Activity at the maximum 100 µg/ml concentration; Calculated molecular descriptors obtained from Chem Axon's Marvin Sketch Software

Despite the lack of biological activity of Structural Motif N, we were still interested to explore the effect of introducing additional substituents on the phenyl ring, forming new Structural Motif M. In this case, the calculated logP values increase slightly, while the pKa values are still too

low. The polar surface areas for these derivatives vary from 61.77Å² to 107.59Å², although these changes are not significant enough to encourage biological activity.

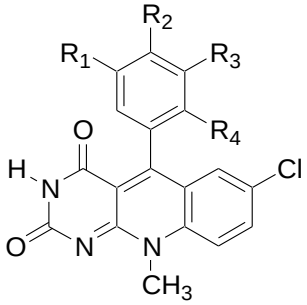

Structural Motif N

Table 11: Calculated molecular descriptors and biological activity of Structural Motif N (Method A) compounds against the LN-229 cell line

Compound	R_1	R_2	R_3	R_4	ClogP	pKa	PSA*	GA**
AQ89	H	OH	OCH_3	H	2.21	-0.30	91.23	NA
AQ99	H	Cl	Cl	H	3.88	-0.33	61.77	NA
AQ102	NO_2	OH	OCH_3	H	2.15	-0.35	137.05	NA
AQ103	NO_2	H	H	OH	2.31	-0.47	127.82	NA

*PSA= Polar Surface Area in $Å^2$; **GA= Glioblastoma cell line LN-229 activity in µg/ml; NA= No Activity at the maximum 100 µg/ml concentration; Calculated molecular descriptors obtained from Chem Axon's Marvin Sketch Software

The next modification we wished to explore was the introduction of additional substituents resulting in Structural Motif N. Similarly to previous structural motifs, this chlorine analogue is characterized by a variety of substituents on four possible positions on the phenyl ring in the 5 position. This modification leads to reasonable calculated logP values, ranging from 2.15 to 3.88, very low pKa values, all below 1.0 and increased polar surface areas ranging from a minimum of 61.77Å² to a maximum of 137.05Å², which is strongly disfavored to cross cellular membranes. Unfortunately, these alterations are not sufficient enough to produce any candidates with potent biological activity.

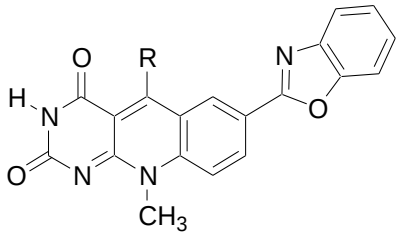

Structural Motif O

Table 2.17: Calculated molecular descriptors and biological activity of Structural Motif O (Method A) compounds against the LN-229 cell line

Compound	R	ClogP	pKa	PSA*	GA**
AQ104	4-hydroxy-3- methoxyphenyl	2.98	-1.19	117.26	NA
AQ105	2-pyridinyl	2.61	-1.81	100.69	NA
AQ106	4-pyridinyl	2.22	-1.50	100.69	NA

*PSA= Polar Surface Area in $Å^2$; **GA= Glioblastoma cell line LN-229 activity in µg/ml; NA= No Activity at the maximum 100 µg/ml concentration; Calculated molecular descriptors obtained from Chem Axon's Marvin Sketch Software

Considering the modest results of the previous structural motifs including 7-methoxy, 7-methyl, 7,8-dimethyl, 7-bromo and 7-chloro analogues, we wanted to approach the modification of our target compound from a different perspective, by including a heterocyclic benzoxazole group in the 7 position. This modification results in Structural Motif O, which like previous structural motifs, may also have an aromatic substituent on the 5 position. Substituents include 4-hydroxy-3-methoxyphenyl (**AQ104**) as well as the heterocyclic 2-pyridinyl (**AQ105**) and 3-pyridinyl (**AQ106**). This set of analogues exhibits the lowest pKa values yet, ranging from a minimum value of -1.81 to a maximum value of -1.19. The calculated lipophilicities of these compounds are higher than the defined ideal value stated in literature, but not high enough to compensate for the low pKa values. The polar surface area for **AQ104** is higher than desired at 117.26 $Å^2$, while the replacement of the 4-hydroxy-3-methoxyphenyl group of **AQ104** with either 2-pyridinyl (**AQ105**) or 3-pyridinyl (**AQ106**) functionalities results in a more favorable polar surface area of 100.69 $Å^2$. However, these values for the polar surface area in **AQ105** and **AQ106** are not

influential enough to confer biological activity to these derivatives. Until this point, all pyrimidinequinolinedione compounds have been oxidized in regards to the barbituric acid portion of the molecule. Considering the possibility of these molecules to either undergo redox reactions with key components of the targeted HDM2 pathway or inhibit the accelerated ATP synthesis required by rapidly dividing cancer cells by mimicking FAD/$FADH_2$, we believe it is necessary to investigate the reduced analogues of these target compounds as well.

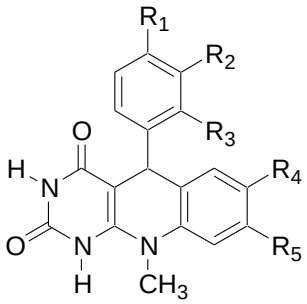

Structural Motif P

Table 2.18: Calculated molecular descriptors and biological activity of Structural Motif P (Method B) compounds against the LN-229 cell line

Compound	R_1	R_2	R_3	R_4	R_5	ClogP	pKa	PSA*	GA**
AQ107	H	OH	H	CH_3	CH_3	3.50	0.59	81.67	NA
AQ108	H	-$(CH)_4$-		CH_3	CH_3	4.79	0.58	61.44	10
AQ109	Br	H	H	Br	H	4.31	-0.48	61.44	NA
AQ110	H	Cl	Cl	Br	H	4.75	-0.56	61.44	NA

*PSA= Polar Surface Area in $Å^2$; **GA= Glioblastoma cell line LN-229 activity in µg/ml; NA= No Activity at the maximum 100 µg/ml concentration; Calculated molecular descriptors obtained from Chem Axon's Marvin Sketch Software

The first reduced structural motif we began with was Structural Motif P, which includes up to three substituents on the phenyl ring in position 5 and up to two substituents on the terminal tricyclic ring in positions 7 and 8 and provides a good starting point for the investigation of these reduced compounds. Substituents on the phenyl ring in the 5 position may be hydroxyl (**AQ107**),

bromo (**AQ109**) or dichloro (**AQ110**). Additionally, the entire phenyl group may be replaced with a 1- naphthyl group, as in the case of **AQ108**. Substitution in positions 7 and 8 may be dimethyl (**AQ107** and **AQ108**) or bromo (**AQ109** and **AQ110**). Overall, this set of compounds shows increased lipophilicity ranging from a minimum of 3.50 to a maximum of 4.75 and pKa values which are still low, but not as low as other derivatives. **AQ108**, however, is the lone compound of this group to exhibit biological activity at concentrations of 10 µg/ml. With a calculated logP of 4.79, **AQ108** has the highest logP value of this class of compounds. **AQ108** also has a slightly increased pKa value of 0.58, relative to the previous compounds synthesized, and a smaller polar surface area at 61.44 $Å^2$.

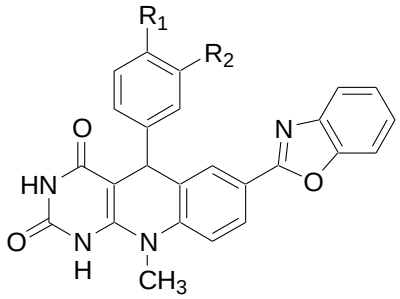

Structural Motif Q

Table 2.19: Calculated molecular descriptors and biological activity of Structural Motif Q (Method B) compounds against the LN-229 cell line

Compound	R_1	R_2	ClogP	pKa	PSA*	GA**
AQ111	H	OH	3.84	-1.65	107.70	NA
AQ113	OCH_3	H	3.99	-1.61	96.70	NA
AQ115	C_6H_5	H	5.79	-1.64	84.47	10
AQ116	H	H	4.14	-1.63	84.47	NA
AQ117	phenyl = 2-pyridinyl		2.93	-1.70	100.36	NA
AQ118	Br	H	4.91	-1.44	84.47	10
AQ119	Cl	H	4.75	-1.64	84.47	10
AQ122	SCH_3	H	4.77	-1.63	84.47	NA
AQ123	H	NO_2	4.08	-1.69	133.27	NA
AQ124	NO_2	H	4.08	-1.70	133.27	NA

*PSA= Polar Surface Area in $Å^2$; **GA= Glioblastoma cell line LN-229 activity in µg/ml; NA= No Activity at the maximum 100 µg/ml concentration; Calculated molecular descriptors obtained from Chem Axon's Marvin Sketch Software

Continuing with our investigation of reduced compounds, the next set of structures we wished to explore was Structural Motif Q, which includes a benzoxazole in the 7 position as well as a phenyl ring in the 5 position which may bear substituents in two possible positions on the ring. Substituents on the phenyl ring range from electron donating hydroxyl groups (**AQ111**) to electron donating nitro groups (**AQ123** and **AQ124**) in addition to the replacement of the phenyl group with a heterocyclic, 2-pyridinyl group (**AQ117**). Of this class of derivatives, **AQ115**, **AQ118** and **AQ119** show biological activity. This case follows the trend of active compounds possessing higher than desired logP values perhaps in compensation for much lower pKa values.

The average calculated logP of these active analogues at 5.15 is much higher than the desired value of 1.00 and the average pKa is -1.57, which is much lower than the targeted 6.00. The polar surface areas of these compounds, however, are closer to the desired value, with all of these active derivatives having polar surface areas of 84.47 Å^2.

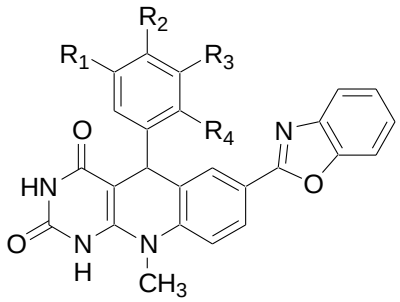

Structural Motif R

Table 12: Calculated molecular descriptors and biological activity of Structural Motif R (Method B) compounds against the LN-229 cell line

Compound	R_1	R_2	R_3	R_4	ClogP	pKa	PSA*	GA**
AQ112	H	OCH_3	OCH_3	H	3.83	-1.63	105.93	1
AQ114	H	H	-$(CH)_4$-		5.13	-1.66	84.47	10
AQ120	H	H	Cl	Cl	5.35	-1.71	84.47	NA
AQ121	H	Cl	Cl	H	5.35	-1.65	84.47	10
AQ125	NO_2	OH	OCH_3	H	3.62	-1.67	162.75	NA

*PSA= Polar Surface Area in Å^2; **GA= Glioblastoma cell line LN-229 activity in µg/ml; NA= No Activity at the maximum 100 µg/ml concentration; Calculated molecular descriptors obtained from Chem Axon's Marvin Sketch Software

Structural Motif R introduces additional substitution into Structural Motif Q including dimethoxy substitution (**AQ112**), dichloro substitution (**AQ120** and **AQ121**) and even the combination of 4-hydroxy-3-methoxy-5-nitro substitution (**AQ125**). As in the case of other derivatives, the phenyl group in the 5 position may also be replaced with a 1-naphthyl group (**AQ114**). Active compounds of this class include **AQ112**, **AQ114** and **AQ121**. All three active

analogues still exhibit low pKa values with an average pKa of -1.67. However, derivatives **AQ114** and **AQ121** have increased lipophilicity, with calculated logP values of 5.15 and 5.35, respectively, as well as lower polar surface areas of 84.47 Å^2. However, **AQ112** exhibits the best activity of all derivatives synthesized to this point, with biological activity at the low concentration of 1µg/ml. Interestingly, **AQ112** also exhibits increased lipophilicity although not as high as **AQ114** and **AQ121** in addition to a slightly higher polar surface area of 105.93 Å^2.

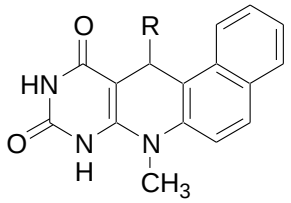

Structural Motif S

Table 13: Calculated molecular descriptors and biological activity of Structural Motif S (Method B) compounds against the LN-229 cell line

Compound	R	ClogP	pKa	PSA*	GA**
AQ134	Phenyl	3.76	0.03	61.44	NA
AQ131	1-naphthyl	4.75	0.00	61.44	10
AQ132	2-naphthyl	4.75	0.02	61.44	10
AQ135	3-pyridinyl	2.54	-0.04	74.33	NA
AQ136	4-pyridinyl	2.54	-0.01	74.33	NA

*PSA= Polar Surface Area in Å^2; **GA= Glioblastoma cell line LN-229 activity in µg/ml; NA= No Activity at the maximum 100 µg/ml concentration; Calculated molecular descriptors obtained from Chem Axon's Marvin Sketch Software

The next modification we wished to explore was the creation of a tetracyclic system, as opposed to the previously described systems which are primarily tricyclic. The inclusion of an additional aromatic system not only increases the delocalization of pi-electrons in the molecule but also increases the size of the molecule so that it can adopt a unique shape that may have enhanced binding ability to our target HDM2. Structural Motif S incorporates a fused phenyl ring at the

6 and 7 positions with a variety of aromatic substituents in the 5-position including phenyl (**AQ134**), 1-naphthyl (**AQ131**), 2-naphthyl (**AQ132**) and 3-pyridinyl (**AQ132**) moieties. **AQ131** and **AQ132**, which are 1-naphthyl and 2-napthyl substituted, respectively, are the two active compounds of this class with biological activity against the LN-229 cell line at concentrations as low as 10 µg/ml. It is not surprising that these active compounds show increased lipophilicity, with calculated logP values of 4.75 for both analogues. **AQ131** and **AQ132** still exhibit low pKa values of 0.00 and 0.002, respectively, but these values are a step in the right direction and more favorable than the very low pKa values found in other structural motifs. These compounds also exhibit modest polar surface areas of 61.44 Å^2. These observations further support the idea that the detrimental effects of low pKa values on the membrane permeability of drugs may be overcome with by an increase in lipophilicity.

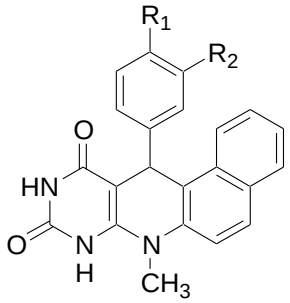

Structural Motif T

Table 2.22: Calculated molecular descriptors and biological activity of Structural Motif T (Method B) compounds against the LN-229 cell line

Compound	R_1	R_2	ClogP	pKa	PSA*	GA**
AQ126	H	OH	3.46	0.01	81.67	NA
AQ129	OCH_3	H	3.60	0.05	70.67	NA
AQ130	CH_3	H	4.27	0.05	61.44	NA
AQ133	C_6H_5	H	5.41	0.03	61.44	10
AQ137	Br	H	4.53	0.03	61.44	NA
AQ138	Cl	H	4.37	0.02	61.44	10
AQ141	H	NO_2	3.70	-0.02	107.26	NA
AQ142	NO_2	H	3.70	-0.04	107.26	NA
AQ143	SCH_3	H	4.39	0.03	61.44	NA
AQ144	CF_3	H	4.64	0.03	61.44	10

*PSA= Polar Surface Area in $Å^2$; **GA= Glioblastoma cell line LN-229 activity in µg/ml; NA= No Activity at the maximum 100 µg/ml concentration; Calculated molecular descriptors obtained from Chem Axon's Marvin Sketch Software

Introducing further substitution on the phenyl ring furnishes Structural Motif T. Structural Motif T incorporates a variety of electronically diverse substituents ranging from electron donating groups such as hydroxyl moieties (**AQ126**) to electron withdrawing groups such as nitro substituents (**AQ 141** and **AQ142**) with other substituents falling somewhere in between the two in terms of electronic effects. When R_1 is phenyl substituted, which effectively turns the phenyl substitution at position 5 into biphenyl substitution, compound **AQ133** is obtained. **AQ133**, which is biologically active, has the highest lipophilicity of this set of analogues with a calculated logP value of 5.10 and modest pKa and polar surface area values of 0.03 and

61.44 Å^2, respectively. If R_1 is a halogen, such as chlorine or bromine, derivatives **AQ137** and **AQ138** are produced. Interestingly, **AQ137**, the bromine analogue, and **AQ138**, the chlorine analogue, have nearly identical values for the calculated molecular descriptors, yet **AQ138** is active while **AQ137** is inactive. As possible explanation for this observation is that the increase in size associated with bromine is not compatible with the desired cellular target, HDM2. Similar to previous compounds of other structural motifs, active derivative **AQ138** has an elevated calculated logP value of 4.37 accompanied by modest values for both pKa and polar surface area. The addition of a trifluoromethyl group to the para position of the phenyl ring forms **AQ144**, the third compound of this class to exhibit biological activity. **AQ144** is similar to the two other active derivatives of this group, **AQ133** and **AQ138**, in terms of the calculated molecular descriptors, having an intermediate lipophilicity and nearly identical pKa and polar surface area values.

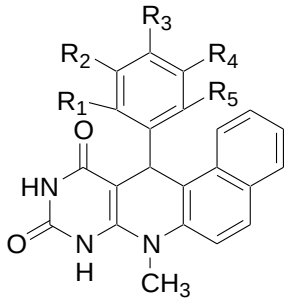

Structural Motif U

Table 2.23: Calculated molecular descriptors and biological activity of Structural Motif U (Method B) compounds against the LN-229 cell line

Compound	R_1	R_2	R_3	R_4	R_5	ClogP	pKa	PSA*	GA**
AQ127	H	H	OH	OCH_3	H	3.30	0.04	90.90	NA
AQ128	H	H	OCH_3	OCH_3	H	3.45	0.04	79.90	NA
AQ139	H	H	H	Cl	Cl	4.97	-0.05	61.44	10
AQ140	H	H	Cl	Cl	H	4.97	0.01	61.44	10
AQ145	H	Br	H	H	OH	4.23	-0.04	81.67	10
AQ146	Br	H	H	H	OH	4.23	-0.08	81.67	10
AQ147	H	Cl	H	H	OH	4.06	-0.05	81.67	NA
AQ148	H	NO_2	OH	OCH_3	H	3.24	-0.01	136.72	NA
AQ149	H	H	OH	NO_2	H	3.40	0.00	127.49	10
AQ150	H	NO_2	H	H	OH	3.40	-0.08	127.49	10

*PSA= Polar Surface Area in $Å^2$; **GA= Glioblastoma cell line LN-229 activity in µg/ml; NA= No Activity at the maximum 100 µg/ml concentration; Calculated molecular descriptors obtained from Chem Axon's Marvin Sketch Software

Increasing the substitution on the phenyl portion of Structural Motif T results in the formation of Structural Motif U. In this case, halogenated analogues such as the dichloro compounds **AQ139** and **AQ140** as well as the combination of hydroxyl and bromo substituents present in compounds **AQ145** and **AQ146** produced biologically active compounds. As expected, the halogenated active compounds have increased lipophilicity, with calculated logP values ranging from 4.23 to 4.97. In keeping with the previously described trend, these active halogenated derivatives have low pKa values and low to modest polar surface areas. If both nitro and hydroxyl groups are introduced, compounds **AQ149** and **AQ150** are formed. Interestingly,

although the hydroxyl group is electron donating and the nitro group is electron withdrawing, these two analogues show excellent biological activity. Similar to other active compounds with both lower calculated logP values and pKa values, **AQ149** and **AQ150** also show higher polar surface areas of 127.49 Å^2.

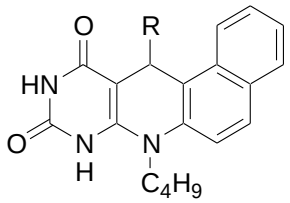

Structural Motif V

Table 2.24: Calculated molecular descriptors and biological activity of Structural Motif V (Method B) compounds against the LN-229 cell line

Compound	R	ClogP	pKa	PSA*	GA**
AQ156	Phenyl	5.09	0.74	61.44	10
AQ154	1-naphthyl	6.07	0.71	61.44	10
AQ157	2-pyridinyl	4.00	0.57	74.33	NA
AQ158	3-pyridinyl	3.87	0.66	74.33	NA
AQ159	4-pyridinyl	3.87	0.70	74.33	NA

*PSA= Polar Surface Area in Å^2; **GA= Glioblastoma cell line LN-229 activity in µg/ml; NA= No Activity at the maximum 100 µg/ml concentration; Calculated molecular descriptors obtained from Chem Axon's Marvin Sketch Software

Given the exciting results of compounds belonging to Structural Motifs S, T and U, the next modification we wished to explore was the replacement of *N*-methyl group of the central ring with an *N*-butyl group to create Structural Motif V. In this class of analogues, aromatic substitution may occur in the 5 position with moieties such as phenyl (**AQ156**), 1-naphthyl (**AQ154**), 2-pyridinyl (**AQ157**), 3-pyridinyl (**AQ158**) or 4-pyridinyl (**AQ159**) groups. In the case of **AQ156**, which has a simple phenyl substitution, the relative increase in lipophilicity to a calculated logP value of 5.09 in conjunction with a very slightly higher pKa value of 0.74 and

modest polar surface area of 61.44 Å² lead to biological activity. If R is 1-naphthyl, biologically active derivative **AQ154** is formed. **AQ154** has even further increased lipophilicity with a calculated logP value of 6.09. **AQ154** also has a similar pKa value to that of **AQ156**, with **AQ154** having a pKa of 0.71 and **AQ156** having a pKa of 0.74, both of which are considered low pKa values.

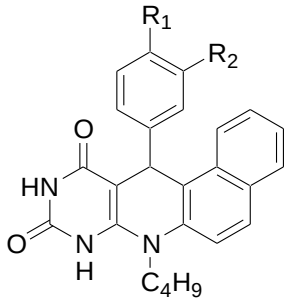

Structural Motif W

Table 2.25: Calculated molecular descriptors and biological activity of Structural Motif W (Method B) compounds against the LN-229 cell line

Compound	R_1	R_2	ClogP	pKa	PSA*	GA**
AQ151	H	OH	4.78	0.72	81.67	NA
AQ153	OCH_3	H	4.93	0.76	70.67	10
AQ155	C_6H_5	H	6.73	0.73	61.44	10
AQ160	Br	H	5.85	0.73	61.44	10
AQ161	Cl	H	5.69	0.73	61.44	10
AQ164	H	NO_2	5.03	0.68	107.26	10
AQ165	NO_2	H	5.03	0.67	107.26	10

*PSA= Polar Surface Area in $Å^2$; **GA= Glioblastoma cell line LN-229 activity in µg/ml; NA= No Activity at the maximum 100 µg/ml concentration; Calculated molecular descriptors obtained from Chem Axon's Marvin Sketch Software

If additional substituents are introduced to the phenyl ring, Structural Motif W is formed. Structural Motif W is perhaps one of the most promising structural motifs of all, with six of the seven compounds of this group having biological activity at concentrations of 10 µg/ml in the LN-229 cell line. These active analogues have a variety of substituents, from the electron donating methoxy group in **AQ153** to the electron withdrawing nitro group in **AQ165**. The only

compound of this class which did not show biological activity was hydroxyl substituted analogue **AQ 151**, which incidentally, has the lowest logP value of this group. As alluded to in previous instances, these active derivatives possess elevated lipophilicity, with an average calculated logP value of 5.43 in combination with modest pKa values. The polar surface areas of active compounds vary, with a minimum of 61.44 Å² and maximum of 107.26 Å², which is slightly higher than the desired value.

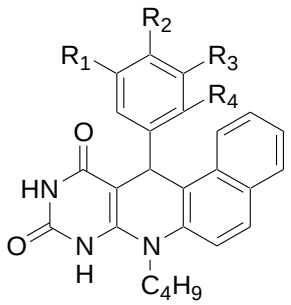

Structural Motif X

Table 2.26: Calculated molecular descriptors and biological activity of Structural Motif X (Method B) compounds against the LN-229 cell line

Compound	R_1	R_2	R_3	R_4	ClogP	pKa	PSA*	GA**
AQ152	H	OCH_3	OCH_3	H	4.77	0.74	79.90	10
AQ162	H	H	Cl	Cl	6.29	0.65	61.44	10
AQ163	H	Cl	Cl	H	6.29	0.71	61.44	1
AQ166	Br	H	H	OH	5.55	0.66	81.67	10
AQ167	NO_2	OH	OCH_3	H	4.56	0.69	136.72	NA

*PSA= Polar Surface Area in $Å^2$; **GA= Glioblastoma cell line LN-229 activity in µg/ml; NA= No Activity at the maximum 100 µg/ml concentration; Calculated molecular descriptors obtained from Chem Axon's Marvin Sketch Software

Structural Motif X is a modification of Structural Motif W which incorporates additional positions for multiple substitutions on the phenyl ring. Derivatives may be dimethoxy (**AQ152**), dichloro (**AQ162** and **AQ163**), 2-hydroxy-5-bromo (**AQ166**) or 4-hydroxy-3-methoxy-5-nitro (**AQ167**) substituted. Like Structural Motif W, Structural Motif X is one of the most exciting groups of compounds of this entire library, with four of the five compounds having potent

biological activity at concentrations of 10 µg/ml and one, **AQ163**, having excellent biological activity at an even lower concentration of 1µg/ml. Not surprisingly, with a calculated logP of 6.29, **AQ163** has the highest lipophilicity of any compound in this entire library. **AQ163** also has a low pKa of 0.71 and a modest polar surface area of 61.44Å². The only compound which is not biologically active, **AQ167**, has decreased lipophilicity in comparison to the active analogues but also has a higher polar surface area of 136.72 Å², both of which are not conducive to biological activity. The active compounds of this class have the highest lipophilicity of all compounds across all structural motifs, with an average calculated logP value of 5.73. However, the pKa value and polar surface areas remain low.

2.4 Conclusion

Using the simple and convenient method described here, we prepared a library of 168 pyrimidinequinolinedione derivatives as potential anti-cancer agents. The synthesis of these compounds involves a facile, one pot reaction of the appropriate barbituric acid, substituted aniline and aromatic aldehyde in refluxing acetic acid. One of the challenges we encountered was the availability of specific building blocks, such as alkylated anilines. However, we were able to circumvent this obstacle by employing methods previously described[38,39] for the synthesis of alkylated anilines from the corresponding phenol or primary aniline. In the case where the substituted phenol is readily available, the phenol may be converted into an ester followed by subsequent conversion into an amide which then undergoes rearrangement and elimination to furnish the alkylated amine. When the primary aniline is available, the aromatic amine may be coupled to formaldehyde and benzotriazole before undergoing a reduction by sodium borohydride to yield the *N*-alkylated aniline. Utilizing these methodologies, we synthesized a

diverse selection of substituted pyrimidinequinolinediones for evaluation as potential anti-cancer agents via HDM2 inhibition.

Considering the previous biological results of the chromenopyrimidinediones, we chose to focus on the refinement of *N*-unsubstituted barbituric acid derivatives. Other features of our target structures include either tricyclic or tetracyclic core structures as well as a variety of substituents with electron donating, electron neutral and electron withdrawing properties. Unlike the chromenopyrimidinediones, the pyrimidinequinolinediones did not show widespread activity, with only 36 of the 168 compounds having activity against the glioblastoma cell line LN-229 at 10 µg/ml and two compounds (**AQ112** and **AQ163**) having excellent activity at the low concentration of 1µg/ml. Ironically, these results are more helpful because they show which specific structural features contribute to enhanced activity. Overall, the most successful structural motifs of this library were Structural Motifs W and X, which are *N*-butyl alkylated tetracycles. Substituents prevalent on active compounds range from electron donating methoxy groups to halogens such as bromine and chlorine as well as combinations of substituents such as hydroxyl and halogen groups or nitro, hydroxyl and methoxy groups on the phenyl ring.

Another important observation regarding these derivatives involves their values for the calculated molecular descriptors in relation to the targeted ideal values. The ideal values for calculated molecular descriptors which allude to optimal biological activity have been previously defined[40] as ~1.0 for logP, ~6.00 for pKa and ~100 $Å^2$. However, previous research[41] has suggested that the ideal values for drugs intended to act on the central nervous system are closer to ~2 for logP, between 4-10 for pKa and 60-70$Å^2$ for polar surface area, with the upper threshold being 90$Å^2$. Nearly all of the synthesized derivatives showed very low pKa values, with **AQ6** having the highest pKa value at 1.54. However, active compounds not only had low

pKa values, with an average pKa of 0.06 but also exhibited higher calculated logP values, with the average calculated logP value of 4.06 for all active compounds. In this case, it appears that the increase in lipophilicity compensates for the low pKa value. When the pKa value of a molecule lies outside of the optimal range, the molecule will have difficulty crossing the cellular membranes. Thus, increasing the lipophilicity of the molecule increases the possibility that the molecule will be able to cross membranes. In fact, a higher lipophilicity is a desired for compounds designed to cross the blood-brain barrier, since it has been estimated that nearly 56% of drugs acting on the central nervous system enter via passive lipoidal permeability[42]. The derivatives which we identified as biologically active also showed polar surface both higher and lower than the ideal values, ranging 61.44Å^2 to 137.05Å^2. However, the average polar surface area of 77.25Å^2, fits well within the range of optimal for central nervous system acting drugs. This observation is explained by the inverse relation of lipoidal diffusion to polar surface area[42]. Using the calculated molecular descriptors in combination with biological testing results, we were able to identify 36 biologically active compounds against the LN-229 glioblastoma cell line in 10 µg/ml concentrations, with analogues **AQ112** and **AQ163** having the best activity across all of the synthesized derivatives.

Chapter 3: Preparation of Substituted Semicarbazides from Corresponding Amines and Hydrazines via Phenyl Carbamates

3.1 Introduction

The class of compounds known as semicarbazides are unique in that they have widespread influence in the areas of chemical syntheses as well as therapeutic and industrial purposes. In industry, the corrosion of steel equipment such as boilers, feed lines and other steam powered machinery by the oxygen present in water poses great safety and economic concerns[43]. Usually dissolved oxygen is first removed with a deaerating heater and the final trace amounts of oxygen are removed with a chemical scavenger[43]. Although hydrazine has been found to be an excellent oxygen scavenger, it has associated toxicity risks, making it a non-viable option. 4-phenyl, 4-isopropyl and 4,4-diethyl semicarbazides offer a safe and effective alternative for the removal of oxygen from feed water to prevent corrosion and damage to industrial infrastructures[43].

In biological systems, free radicals are well-known for their destructive effects. Routine cellular processes produce low levels of reactive oxygen species, which are scavenged by either endogenous antioxidants or antioxidants derived from supplementation[44]. However, in some instances these pathways which inactivate reactive oxygen species are dysfunctional. In this case, reactive oxygen species accumulate within the cell, causing oxidative stress[44]. Oxidative stress has been implicated in the physical destruction of cells as well as in diseases such as cancer, autoimmune and neurodegenerative disorders[44]. Analogous to the idea of oxygen scavengers to prevent corrosion in steel structures, semicarbazides can also scavenge reactive oxygen species in cells to ameliorate the detrimental effects of reactive oxygen species[45].

3.2 Importance of Semicarbazides in Medicinal Chemistry

Semicarbazides have also been used in catalytic applications to fine-tune the action of chiral aziridines by creating a semicarbazide-chiral aziridine hybrid as a ligand for asymmetric syntheses[46]. Asymmetric syntheses are vitally important due to their ability to produce chiral, enantiomerically pure compounds. This is of particular consequence in pharmaceuticals, where different enantiomers of the same compounds can have vastly different effects. One of the most popular examples of this dual nature is ketamine. While S (+) ketamine is known for its anesthetic value, R (-) ketamine is known to induce violent hallucinations[47]. Another example is the Parkinson's medication dihydroxy-3,4 phenylalanine (Dopa). Initially, dopa was marketed as a racemic mixture, which is easier to manufacture since the two isomers do not have to be separated[47]. However, the d-isomer was found to promote agranulocytosis, a serious condition which leads to a decrease in white blood cell counts and affects the ability of the immune system to function properly[47].

Semicarbazides can also serve as important building blocks for scaffolds of larger molecules. In solid state combinatorial chemistry, semicarbazide based polystyrene resins have been used as solid supports to provide the appropriate aldehyde and ketone building blocks required for the discovery of novel caspase inhibitors[48]. Caspases are a well-known for their apoptotic activity. However, in some cases apoptosis is abnormally accelerated, leading to neurodegenerative diseases such as Parkinson's, Alzheimer's and Huntington's diseases in addition to Amyotrophic Lateral Sclerosis (ALS)[49]. Thus, the inhibition of caspase activity to prevent aberrant programmed cell death has become the focus of several research groups. Caspase inhibitors are often bound to either aldehydes or ketone groups, which covalently bond to the cysteine residue near the enzymatic active site, delivering the inhibitor to its target[50]. Unfortunately, during the

synthesis of these inhibitors the aldehyde and ketone carbonyls are vulnerable to inadvertent degradation. Thus, various resins using semicarbazides have been designed to protect these valuable carbonyl moieties and maintain the integrity of the molecule[48].

Considering the limitless applications for semicarbazides and their derivatives, an efficient, convenient and economical method of preparation is imperative. Surprisingly, there is a vacuum in terms of available methods that are simple, cost-efficient and applicable to a wide variety of substituents. Most synthetic procedures for the preparation of semicarbazides utilize undesirable methods such as harsh reaction conditions, long reaction times or high temperatures and suffer from limitations in scope. Our goal was to devise a simple and efficient method using readily available starting materials and mild reaction conditions to produce a diverse library of semicarbazides.

3.3 Synthetic Approach to the Preparation of Semicarbazides

Semicarbazides can be deconstructed into three primary components: The amine moiety, the carbonyl source and the hydrazine moiety. Our strategy was to employ various chloroformates as the carbonyl source in combination with a variety of substituted amines to furnish the corresponding carbamate, which can then be transferred into the desired semicarbazide upon reaction with hydrazine.

3.3.1 Carbamate Synthesis

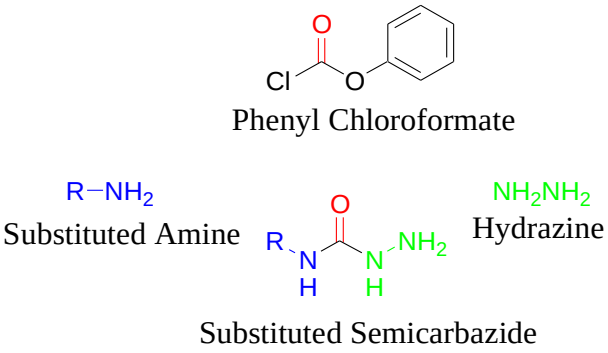

Figure 3.1: Building blocks of substituted semicarbazides

Chloroformates were selected as a carbonyl source because of the possibility to carry out a nucleophilic attack on the carbonyl to form the carbamate intermediate. This carbamate intermediate may undergo an additional nucleophilic attack on its carbonyl by hydrazine to yield a semicarbazide. To determine the best chloroformate for our intended purposes, we experimented with the reaction of methyl, ethyl and phenyl chloroformates to produce 4-pyridinyl, hydroxyphenyl and alkyl semicarbazides. The reaction of methyl chloroformate with the amine while successful in theory, were unsuccessful in practice due to their extremely low boiling points. We were, however, able to react ethyl and phenyl chloroformates to produce the corresponding ethyl and phenyl carbamates.

3.3.1.1 Ethyl Carbamates

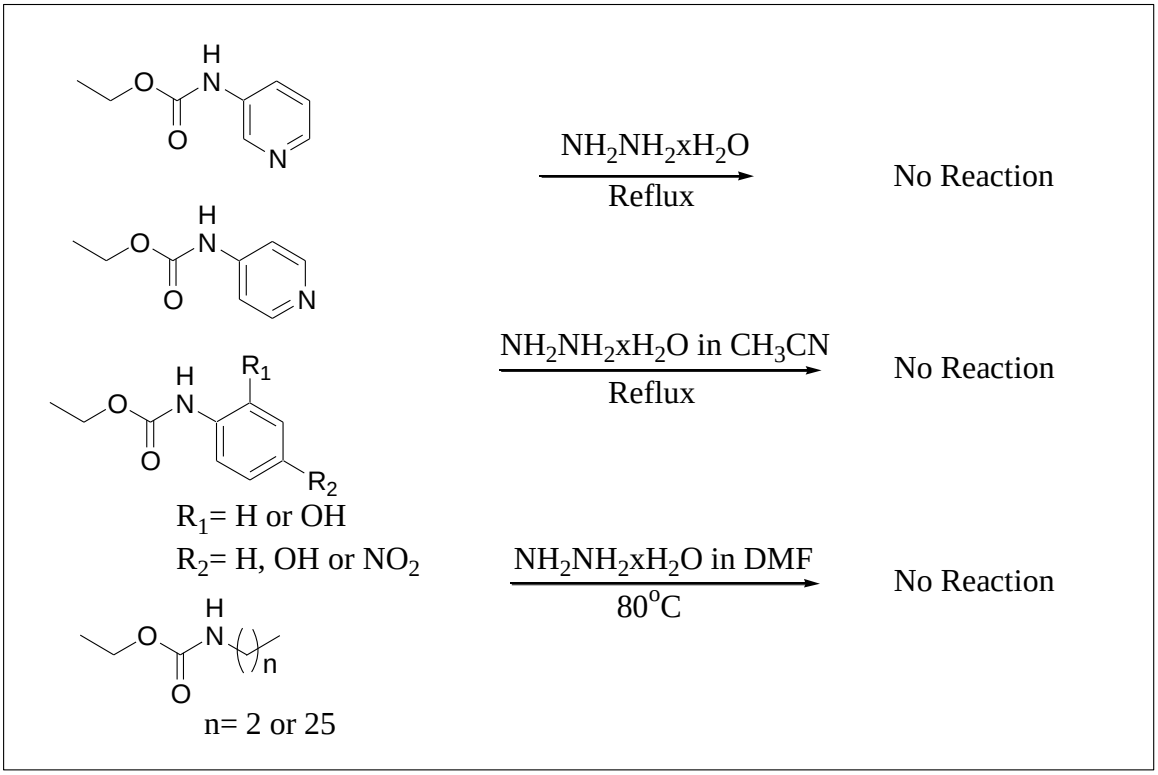

Figure 3.2: Reaction of ethyl carbamates under different conditions

The reaction of ethyl carbamates produced mixed results. Reaction conditions tested included refluxing neat hydrazine hydrate, hydrazine hydrate in refluxing acetonitrile and hydrazine hydrate in *N*, *N*-dimethyl formamide at 80°C. For hexyl semicarbazide, no product formation was detected even at elevated temperatures or alternative microwave heating. The lone success in this series of reactions was that of 4 (2-pyridinyl) semicarbazide, which we attributed to the autocatalytic character of the 2-pyridinyl substituent. There is a strong possibility that the 2-pyridyl moiety produces an autocatalytic effect due to the hydrogen bonding that can occur between the pyridine nitrogen and hydrazine. The consequence of this hydrogen bonding is that the hydrazine is then brought closer to the reaction center of the carbonyl carbon. In this scenario, there are two outcomes that can occur. One possibility is that this combination can

react sequentially as a nucleophile. The other option is that it can react as a base, which would result in the formation of the isocyanate, in this case, 2-pyridinylisocyanate. Here, we believe the latter to be the case since we isolated the isocyanate, which was verified via NMR. The resulting isocyanate can then react with hydrazine to give the intended 4-(2-pyridinyl)semicarbazide. The results of our studies with ethyl chloroformate lead us to the fortuitous realization that since the 2-pyridinyl moiety effectively functions as a base, the production of semicarbazides from ethyl carbamates requires elevated temperatures and a strong base. While the reaction of ethyl chloroformate under high temperatures in the presence of a strong base may be applicable to the preparation of some semicarbazides, it is certainly not a possibility in the case of base sensitive substituents, making it a non-viable option.

3.3.1.2 Phenyl Carbamate

Phenyl chloroformate was the next choice for the synthesis of our carbamate intermediate. In fact, the use of phenyl carbamates was originally cited as an alternative to the use of toxic phosgene; specifically, in the production of carbamate-urea molecules[51]. However, there are no viable methods available for the preparation of a phenyl carbamates bearing a variety of substituents. Due to the ability of the phenoxy group to leave readily as phenol during a nucleophilic attack on the carbonyl, phenyl carbamates are very reactive. However, this increased reactivity has dual consequences. While in one regard, this means that phenyl carbamates will readily react with hydrazines to easily provide semicarbazides, it also means that they will be more difficult to handle[52]. Nevertheless, we have found that phenyl carbamates may synthesized via the reaction of phenyl chloroformate and the amine of interest in an aqueous tetrahydrofuran solution with sodium bicarbonate as a base. While this reaction must be carried out on ice to prevent the decomposition of phenyl chloroformate, it is finished after all reagents

are present in the solution. Simple extraction following the completion of the reaction produces high yields (>90%) of the pure (>96%) substituted phenyl carbamate. Considering their high reactivity, one might presume that these phenyl carbamates would not be shelf-stable. Interestingly, our experience is that the synthesized phenyl carbamates are not only shelf-stable, but remain stable for extended periods of time. The intriguing combination of reactivity, scope of application and stability make phenyl carbamate the most appropriate choice for our intermediate en route to semicarbazides.

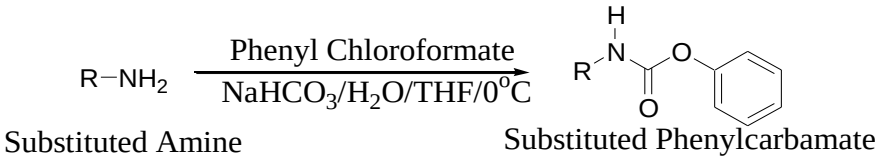

Figure 3.3: Reaction scheme for the formation of phenyl carbamates from the corresponding amine and phenyl chloroformate

Table 14: Phenyl carbamate derivatives and their associated yields

R	Carbamate	Yield
Ph	**2a**	98
4-MeOPh	**2b**	97
4-$EtCO_2$Ph	**2c**	97
2-HOPh	**2d**	91
3-HOPh	**2e**	91
4-HOPh	**2f**	93
4-PhOPh	**2g**	98
4-PhPh	**2h**	98
3,4,5-$(MeO)_3$Ph	**2i**	95
2,5-$(MeO)_2$Ph	**2j**	94
3,5-Me_2Ph	**2k**	91
2,4-Cl_2Ph	**2l**	96
3-BrPh	**2m**	92
2-pyridinyl	**2n**	91
4-pyridinyl	**2o**	93
1-naphthalenyl	**2p**	92
2-naphthalenyl	**2q**	97
n-propyl	**2r**	92
n-hexyl	**2s**	96

3.3.2 Conversion of Arylcarbamates to Semicarbazides

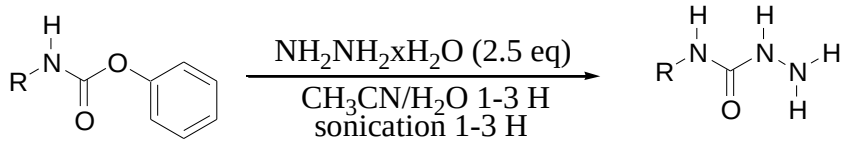

Substituted Phenylcarbamate

Substituted Semicarbazide

Figure 3.4: Scheme for the reaction of phenyl carbamates with hydrazine to form semicarbazides

Table 15: Semicarbazide derivatives and their associated yields

R	Semicarbazide	Yield
Ph	**3a**	93
4-MeOPh	**3b**	91
4-$EtCO_2$Ph	**3c**	94
2-HOPh	**3d**	96
3-HOPh	**3e**	95
4-HOPh	**3f**	97
4-PhOPh	**3g**	98
4-PhPh	**3h**	98
3,4,5-$(MeO)_3$Ph	**3i**	91
2,5-$(MeO)_2$Ph	**3j**	93
3,5-Me_2Ph	**3k**	91
2,4-Cl_2Ph	**3l**	95
3-BrPh	**3m**	94
2-pyridinyl	**3n**	93
4-pyridinyl	**3o**	91
1-naphthalenyl	**3p**	95
2-naphthalenyl	**3q**	97
n-propyl	**3r**	91
n-hexyl	**3s**	92

The second step in the synthesis of substituted semicarbazides, conversion of the substituted arylcarbamate intermediate to the substituted semicarbazide, is slightly more complex than the first step, depending on the chemical character of the substituents. Optimal reaction conditions for the synthesis of 5-arylsemicarbazides from phenyl carbamates were elucidated by altering the solvent, base, temperature and time while monitoring the reaction progress by NMR. An acetonitrile solution of the phenyl carbamate and 2.5 equivalents of hydrazine hydrate were

stirred at room temperature for 1 hour with sonication. It is necessary to use an excess of hydrazine hydrate because one equivalent is used as a base and an additional equivalent serves as the nucleophile. It is also necessary to add water dropwise to the reaction mixture to bring all reactants into the solution. Alternatively, solvents such as *N*, *N* dimethylformamide and tetrahydrofuran may be used; however, acetonitrile is the preferred solvent because it allows to ease of isolation and purification.

To enable us to visualize the progress of the reaction, NMR spectra of the reaction mixture were recorded at 10 minute intervals. At 0 minutes, the NMR shows the presence of both starting materials. There are many signals in the aromatic region, corresponding to the phenoxy moiety of the phenyl carbamate as well as the aryl carbethoxy portion of the molecule contributed by the substituted amine. After 10 minutes, both starting materials are still present, but another set of signals begins to emerge which corresponds to the product. At 60 minutes, the phenoxy signals of have disappeared, signaling that the phenol group has been removed. Additionally, we see the appearance of an N-H signal downfield, which relates to the N-H directly adjacent to the carbonyl.

Additional experimentation with a variety of functional groups including hydroxy, carbethoxy, carboxy, nitro or halogen moieties suggested that these reaction conditions are not only mild and convenient, but also applicable to the preparation of a variety of semicarbazide derivatives. An exception to the proposed general reaction conditions is the case of phenyl 4-alkylcarbamates. Here, heating in *N*, *N* dimethylformamide, tetrahydrofuran or acetonitrile is necessary to complete the reaction. However, the reaction of phenyl 4-alkylcarbamates in acetonitrile at 60°C with sonication for 12 hours gave the best yields.

In the case of mono-substituted hydrazines, similar reaction conditions may be used with a simple modification. Here, only one equivalent of hydrazine is used as a nucleophile, which means that a base is required. One equivalent of either *N*-methylmorpholine or anhydrous potassium carbonate may be used as a base, with each giving quantitative yields of the pure product. However, we prefer to use anhydrous potassium carbonate because as a solid it is easier to handle than liquid *N*-methylmorpholine. If larger substituents are desired, the ability of these substituents to sequester water must be considered. Here, the use of *N*-methylmorpholine is preferred as a base to prevent partial hydrolysis from taking place.

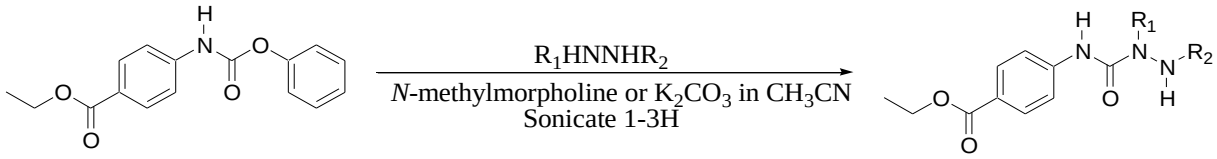

Carbamate Precursor Semicarbazide

Figure 3.5: Scheme for the reaction of multi-substituted hydrazines with phenyl carbamate to yield multi-substituted semicarbazides[35]

Table 16: Multi-substituted semicarbazides and their associated yields[35]

R_1	**R_2**	**Semicarbazide**	**Yield**
CH_3	H	**4a**	91
H	C_6H_5	**4b**	98
H	2,4-$(NO_2)_2$Ph	**4c**	92
H	CHOPh	**4d**	97
H	4-NO_2CHOPh	**4e**	91
H	4-$MeSO_2$Ph	**4f**	93
H	CO_2-cholesteryl	**4g**	90

3.4 Discussion

Some may note that theoretically, in the reaction of monosubstituted hydrazines it is possible to obtain two products. However, under the reaction conditions described above, exclusively one product is formed. This observation is most likely attributed to the mild reaction conditions, which favor the formation of the product as a function of electron density distribution. This finding further reinforces the importance of mild reaction conditions in the synthesis of semicarbazides. The novel method which we have developed presents a convenient and efficient method for the preparation of semicarbazides through the formation of the appropriate phenylcarbamate followed by the conversion of this phenylcarbamate into the desired semicarbazide using hydrazine. Our synthesis is not only convenient, but also efficient, with quantitative reaction yields. This method is applicable to both monosubstituted and polysubstituted semicarbazides, including a variety of substituents ranging from alkyl and alkoxy groups to heterocycles such as pyridine and halogens such as bromine and chlorine.

Chapter 4: Synthesis of *N*-aryl and *N*-arylcarbamoylamino Derivatives of 1, 3-diazinane-5-carboxamide

4.1 Introduction

In addition to their role as intermediates in semicarbazide synthesis, phenyl carbamates also serve an integral role as key intermediates in the synthesis of *N*-aryl and *N*-arylcarbamoylamino derivatives of 1, 3-diazinane-5-carboxamide. Analogues of this class of compounds have marked activity against a range of cancer types including melanoma, leukemia and sarcoma, presumably through the inhibition of topoisomerase II[53]. One of the hallmarks of cancer development is the precipitous cell growth without regulation. For this unrestrained cell growth to occur, cancer cells must follow the same process of DNA replication and cell division as healthy cells except at an accelerated rate. Due to this hyperactive replication and division, these cells often express higher levels of enzymes and proteins associated with these processes of the cell cycle. Therefore, a popular therapeutic strategy for targeting cancer is to hone in on the cellular activities that are required for the unrestrained division of cancer cells.

DNA replication is one of the most critical steps of the cell cycle and is modulated by a cascade of signaling events. Deweese et al. use the analogy of DNA as a long, coiled double stranded rope which is prone to knots and tangles during the processes of DNA recombination and replication[54]. For these events to take place, DNA must be separated into its individual strands, which is not possible when knots or tangles are present[54]. In this case, the knots are removed by a class of enzymes referred to as topoisomerases. Topoisomerases modulate DNA topology by generating either double (Type II topoisomerases) or single (Type I topoisomerases) stranded breaks within the molecule to relieve tangles[54]. Since cancer cells replicate at a rapid rate, they express increased levels of topoisomerases I and II, which makes the targeting of cancer cells via

topoisomerases more selective over healthy cells. To target cancer via topoisomerase activity, the topoisomerase of interest must be pinpointed. Although both topoisomerases have been the focus in the development of potential anti-cancer therapeutics, topoisomerase II is more popular, presumably because it generates a double stranded break as opposed to topoisomerase I's single stranded break, and is therefore more potent. Topoisomerase II agents are classified by their mechanisms, with the largest and most studied categories being the catalytic inhibitors and poisons.

4.2 Topoisomerase II

The topoisomerase II catalytic cycle begins with the binding of two strands of entangled DNA, referred to as the G (gate) and T (transported) segments, to the open N-terminal or "upper clamp" portion of the enzyme of the topoisomerase II enzyme[55]. After the initial binding of the G and T segments, two ATP molecules bind to the enzyme and dimerize the ATPase domain, which closes the N-terminal portion of the enzyme[55]. The G segment of DNA is cleaved via a double stranded break, and the T segment passes through it, resulting in the hydrolysis of one ATP molecule to ADP and phosphate[55]. At this point in the catalytic cycle, the DNA knot is relieved, the G segment is religated and the remaining ATP molecule is hydrolyzed[55]. Once the second ATP is hydrolyzed, the C-terminal portion or "lower clamp" of the topoisomerase II enzyme opens and the untangled G and T DNA strands are released[55].

4.3 Topoisomerase II Targeting Strategies

4.3.1 Topoisomerase II Poisons

Topoisomerase poisons, as their namesake implies, poison the cell. Poisoning can occur by different pathways, but two of the most understood mechanisms are through the accumulation of covalently bound DNA-topoisomerase II complexes and damaged DNA[56]. The accumulation of

DNA-topoisomerase II complexes occurs when topoisomerase II is upregulated, creating a subsequent spike in the steady-state levels of DNA-topoisomerase complexes[54]. When these steady-state levels of DNA-topoisomerase complexes accumulate in the cell, they become toxic and ultimately lead to cell death. Topoisomerase II poisons also introduce breaks into DNA but then prevent their religation, leading to the accumulation of fragmented DNA within the cell[56]. Examples of topoisomerase II poisons acting through this mechanism include the compounds referred to as etoposide and teniposide. Although topoisomerase poisons such as these are highly efficacious against leukemia, lung cancer and Kaposi's sarcoma, they are unfortunately associated with undesirable side effects such as myelosuppression, mucositis, nausea and alopecia[57].

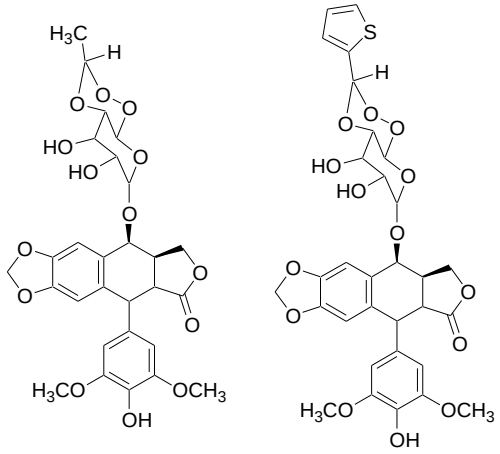

Figure 23: Structures of topoisomerase II poisons

4.3.2 Catalytic Inhibitors of Topoisomerase II

Catalytic inhibitors of topoisomerase II, as their namesake implies, interfere with critical stages of the topoisomerase II catalytic cycle. Examples of these inhibitors include aclarubicin and suramin[55]. Aclarubicin alters the catalytic cycle of topoisomerase II by intercalating into DNA[58], so that the topoisomerase II enzyme cannot access DNA and relieve knots or tangles ahead of the

replication fork, halting replication. It has been proposed that suramin, another catalytic inhibitor, prevents DNA-topoisomerase activity by binding to topoisomerase II instead of DNA, since topoisomerase II is basic and suramin is hexasulfated[59]. Although experimentally, suramin is a potent topoisomerase II inhibitor, it may be too potent, contributing to severe side effects including neuropathy and lymphopenia[57].

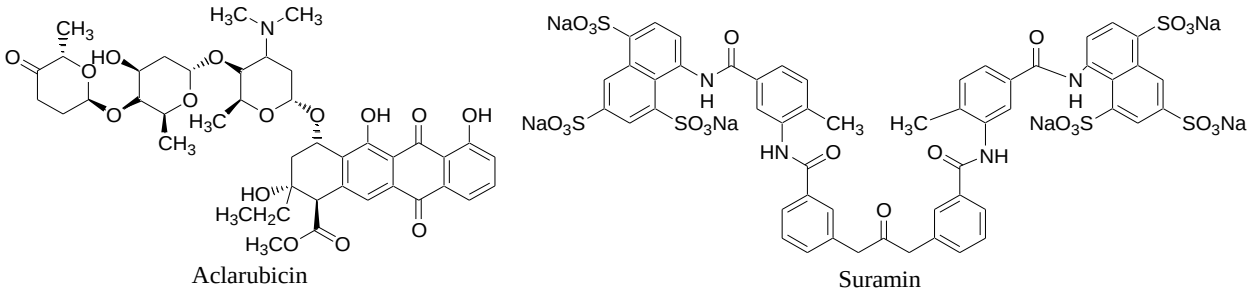

Figure 4.2: Structures of topoisomerase II catalytic inhibitors

4.4 Design of Target Compounds

Another inhibitor which has a slightly different mechanism of action than that of the topoisomerase II catalytic inhibitors and poisons is merbarone. Although merbarone is a topoisomerase II inhibitor, it is unique in that it is not a DNA intercalator, has no effect on DNA binding to topoisomerase II and has no effect on ATP hydrolysis[60]. Merbarone is one of the most thoroughly studied molecules designed as a topoisomerase II inhibitors to have previously demonstrated potent anti-cancer activity. Nevertheless, it has also been found that merbarone causes deleterious effects including genotoxicity, cytotoxicity and nephrotoxicity[57,61]. Ironically, merbarone also leads to endoreduplication, a harmful phenomenon in which cells continuously experience replication without the requisite cell division, leading to polyploidy and inducing a host of downstream genetic effects[61].

Although it has been shown experimentally that merbarone promotes a range of negative side effects and is therefore unsuitable for further development as a potential anti-cancer agent, it does provide a valuable starting point for the synthesis of a library of compounds combining potent anti-cancer activity without the harmful effects. We chose merbarone derivatives as a starting point for the synthesis of our library of potential anti-cancer agents because while it is a known topoisomerase II inhibitor, it does not completely abolish all protein-DNA interactions[60,62]. To construct our target compound, we first identified what we believe are key structural characteristics that are crucial to pharmacophore activity[53]. We proposed six core structural motifs sharing a barbituric acid moiety where oxygen replaces the sulfur of merbarone in the 2 position of the 1, 3-diazinane ring. Unlike merbarone, Structural Motif A includes up to three substituents on the phenyl group in addition to various *N*-substitutions on the barbituric acid portion of the molecule. Replacing the phenyl moiety is with a naphthalenyl ring gives Structural Motif B. Similarly, replacing the phenyl moiety with an anthracenyl ring leads to Structural Motif C. Structural Motif D provides another layer of variation by exchanging the phenyl group for benzothaizolyl, which differs from the other variations among the proposed structural motifs in that it is a larger heterocycle. Another set of analogues is created when the phenyl portion is replaced with a benzamido group, which yields Structural Motif E. The final structural motif we included, Structural Motif F, has a phenylcarbamoylamino entity in place of the original phenyl ring. The benzamido and phenylcarbamoylamino moieties in Structural Motifs E and F are particularly interesting because of their potential to increase hydrogen bonding. To evaluate the ability of these target compounds to achieve optimal biological activity, we used the combination of calculated partition coefficients (ClogP), pKa and polar surface area (PSA) known as the "sweet spot" approach for drug discovery[37].

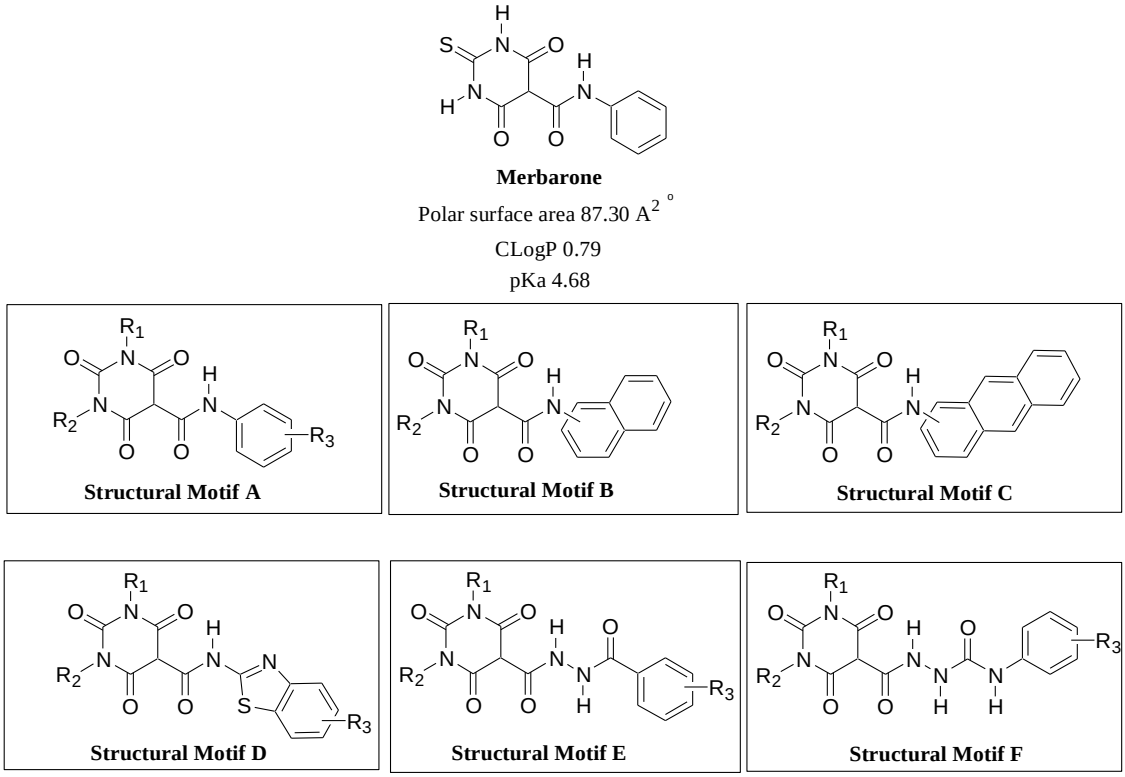

Figure 4.3: Structural motifs A-F based on the pharmacophore of merbarone

4.5 Preparation *N*-arylcarbamates

The first step in the preparation of substituted *N*-Aryl-2, 4, 6-trioxo-1, 3-diazinane-5-carboxamides[72] begins with the preparation of the *N*-arylcarbamate intermediate. Although *N*-arylcarbamates may be produced by other methods which involve the reaction of a substituted amine with the desired dicarbonate or chloroformate, these methods are not only inconvenient, but also require careful handling and storage. These aforementioned methods are also dangerous due to the inherent temperature sensitivity and rapid hydrolysis of chloroformates. Other methods utilizing di-tert-butyldicarbonate[63] and 1-alkoxycarbonyl-3-nitro-1,2,4-triazoles[64] have been developed as safe and convenient alternatives. Considering our previous work on the preparation of phenyl carbamates from phenyl chloroformate, we believe this method to be superior to the other existing methods for the formation of *N*-arylcarbamates[35].

4.5.1 Evaluation of *N*-arylcarbamates

Previously[35], we focused exclusively on the preparation of simple phenylcarbamates as opposed to *N*-aryl substituted carbamates as in this case. In order to determine which carbamate would be the most appropriate for the synthesis of our *N*-aryl substituted compounds, we evaluated ethyl, 4-nitrophenyl and phenyl chloroformate as reagents to produce the corresponding *N*-aryl substituted carbamates.

4.5.1.1 Ethyl carbamate

The preparation of ethyl carbamate is the most convenient and straightforward. This reaction can be done as an aqueous ethyl acetate bilayer containing sodium carbonate as the base. This reaction is finished after only a few minutes at room temperature, and the product may be isolated by collecting the organic layer, drying it over anhydrous sodium sulfate and the ethyl acetate solvent evaporated to furnish the stable ethyl *N*-arylcarbamate derivative. Although it would seem that the stability of the ethyl carbamate formed would be an advantage, we were concerned that the resulting ethyl *N*-arylcarbamates might in fact be too stable and uninclined to react with barbituric acid in the manner which we intended. In this way, we realized that a more reactive *N*-arylcarbamate would be necessary.

4.5.1.2 4-Nitrophenyl carbamate

At the opposite end of the spectrum, the preparation of 4-nitrophenyl *N*-arylcarbamate, while possible, requires special precautions due to the increased reactivity of the reagents. This reaction must be kept cold at all times, using an ice-cold water ethyl acetate solution of the aromatic amine to which 4-nitrophenyl chloroformate in ethyl acetate is added dropwise. Purification and isolation of 4-nitrophenylcarbamates must also be done at 0°C to avoid forming the symmetric diaryl urea byproduct, which lowers the yield and complicates isolation. In the

instance that the reaction is kept sufficiently cold enough such that the 4-nitrophenyl chloroformate does not decompose or form the diaryl urea, we found that 4-nitrophenylcarbamates make excellent intermediates for *C*-carboxamidation of barbituric acid.

4.5.1.3 Phenyl Carbamate

In order to find an *N*-arylcarbamate species which might have an intermediate reactivity falling between that of ethyl *N*-arylcarbamate and 4-nitrophenyl *N*-arylcarbamate, we revisited phenyl chloroformate as a reagent. The preparation of phenyl *N*-arylcarbamate is rapid and straightforward. The reaction of phenyl chloroformate with the aromatic amine of choice is carried out in an ice bath until all of the materials have been added to prevent decomposition of the phenyl chloroformate reagent. Once all of the starting materials have been added to the reaction mixture, the ice bath may be removed and the reaction mixture allowed to warm to room temperature. In the time it takes for the reaction to warm to room temperature, the reaction is complete. This method produces nearly quantitative yields and does not require additional purification.

4.5.1.4 *N*-Aryl Carbamate Selection

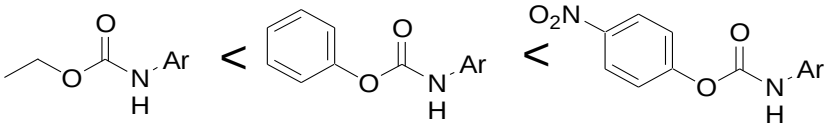

Figure 4.4: Relative reactivities of *N*-arylcarbamates

Considering the reactivity of each of the chloroformates used in the syntheses of their corresponding carbamates, we eliminated 4-nitrophenyl *N*-arylcarbamate, due to its high reactivity, which we did not think would be favorable for a variety of substituents. We also ruled out ethyl *N*-arylcarbamate, concerned that it might not be reactive enough. Phenyl *N*-arylcarbamate, with its moderate reactivity and tolerance of a wide variety of functional groups

such as aromatic halogens, carboxylic acids, esters, amides, nitrile, nitro, alkyl, and alkoxy groups, was the best choice for the *C*-carboxamidation of barbituric and thiobarbituric acids via the formation of the corresponding phenyl *N*-arylcarbamates[35].

4.5.2 Preparation of phenyl *N*-arylcarbamates

Although it was clear that the phenyl N-arylcarbamates were the best option for our synthetic plan, their synthesis was not as straightforward as the simple phenylcarbamates. While our previously described method utilizing sodium bicarbonate, tetrahydrofuran and water was successful for a handful of derivatives, it became evident that alternative reaction conditions with variations in the base and solvent of choice would be needed to accomplish the formation of substituted phenyl *N*-arylcarbamates. One of the main challenges we faced was the solubility of some of these materials. We explored reaction conditions including solvents such as ethyl acetate, tetrahydrofuran and pyridine and in the case of Method IV, a combination of ethyl acetate, tetrahydrofuran and pyridine. Base choices we used included sodium carbonate, pyridine, triethylamine and *N*-methylmorpholine. In investigating various combinations of these solvent and base options, we formulated Methods I-V according the solubility and reactivity of the original aniline.

Method I is the ideal choice for the preparation of phenyl *N*-arylcarbamates. Method I uses a solution of the desired aromatic amine in ethyl acetate/tetrahydrofuran, with sodium carbonate as a base dissolved in a minimal amount of water and phenyl chloroformate in tetrahydrofuran. The ratio of these solvents must be carefully adjusted so that all of the reagents are present in the solution. The reaction is done on ice and allowed to warm the room temperature before extraction and recrystallization from a mixture of ethyl acetate and hexane, if needed. However, some of the aromatic amines have unique solubilities, which required us to devise alternative

methods (Methods II-V) for the synthesis of their corresponding phenyl *N*-arylcarbamates. In Method II, ethyl acetate is the lone solvent and triethylamine is used as a base. Method III, designed for anilines that have a high solubility in tetrahydrofuran, uses tetrahydrofuran as the solvent and pyridine as the base. For less reactive anilines and anilines poorly soluble in tetrahydrofuran, Method IV is the method of choice. Method IV uses a solvent combination of ethyl acetate, tetrahydrofuran and pyridine, which acts as both a solvent and a base. Since this method is used for poorly soluble anilines, it is carried out in the presence of sonication at room temperature. Method V was developed for the case of reactive aryl amines and is carried out in ethyl acetate with *N*-methylmorpholine as the base. Using Methods I-V, we were easily able furnish a wide variety of substituted phenyl *N*-arylcarbamates for the next step of our synthesis.

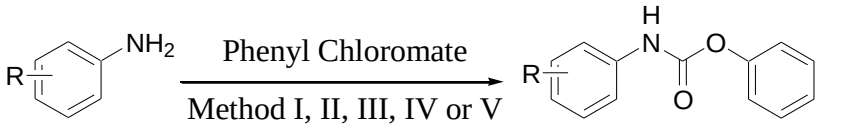

Aryl Amine Phenyl *N*-arylcarbamate

Table 4.1: Summary of preparation methods for *N*-arylcarbamates

Method	**Aniline Characteristics**	**Solvent**	**Base**
I	-	Ethyl acetate/ Tetrahydrofuran	Sodium Carbonate
II	-	Ethyl acetate	Triethylamine
III	High THF solubility	Tetrahydrofuran	Pyridine
IV	Less reactive; low solubility	Ethyl acetate/ Tetrahydrofuran/ Pyridine	Pyridine
V	Reactive	Ethyl acetate	*N*-methylmorpholine

4.6 *C*-Carboxamidation via Aryl Isocyanate

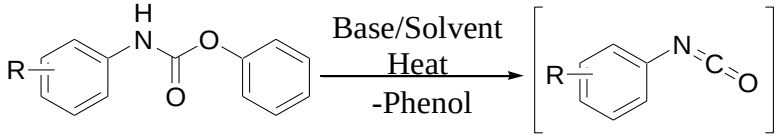

Phenyl *N*-arylcarbamate Aromatic Isocyanate

Figure 24: Formation of the aryl isocyanate intermediate *in situ*

The next step in the synthesis of the *N*-aryl and *N*-arylcarbamoylamine derivatives of 1,3-diazinane-5-carboxamide is the formation of the aryl isocyanate intermediate[65]. This transformation occurs *in situ* upon heating the phenyl *N*-arylcarbamate in the presence of a base, which eliminates easily detectable phenol from the phenyl *N*-arylcarbamate. The generation of aryl isocyanates *in situ* is an added advantage due to the toxicity associated with handling isocyanates. In the course of the reaction, the generated aryl isocyanate immediately reacts with the barbituric acid enolate anion, forming the product.

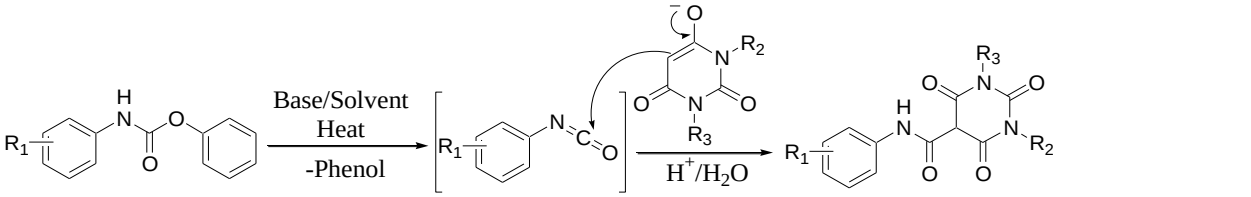

Phenyl *N*-arylcarbamate Aromatic Isocyanate N-Aryl-2,4,6-trioxo-1,3-diazinane-5-carboxamide

Figure 4.6: Formation of *N*-Aryl-2, 4, 6-trioxo-1, 3-diazinane-5-carboxamides from phenyl *N*-arylcarbamates via an aromatic isocyanate intermediate

Although we found several useful solvent and base combinations for the formation of the aryl isocyanate, our search began with pyridine (Method A), since it can act as both the solvent and the base. After refluxing in pyridine for 12 hours, the reaction is completed and the product may be isolated from the reaction mixture using simple acid precipitation. For further purification, the solid crude product may be refluxed in ethanol and filtered to give the pure product. Method A gives high yields of the pure product, with little if any formation of the symmetric diaryl urea side product. In this way, compounds **1**-**54** were prepared.

Table 4.2: Summary of methods available for *C*-carboxamidation

Method	Solvent	Base
A	Pyridine	Pyridine
B	DMSO	Triethylamine
C	DMSO	*N*-methylmorpholine
D	DMF	Sodium carbonate

Our goal was to decrease the reaction time required by Method A by solubilizing the reagents using a solvent with increased polarity. *N*, *N*-dimethylformamide and dimethyl sulfoxide were chosen as possible solvents with pyridine, trimethylamine, *N*-methylmorpholine and sodium carbonate selected as possible bases. Experimentation with different combinations of these solvents and bases showed that the optimal reaction conditions for the *C*-carboxamidation of barbituric and thiobarbituric acids involve refluxing dimethyl sulfoxide as the solvent with trimethylamine as the base, Method B. The reaction time for Method B is less than half of Method A, taking only 5 hours to complete. To remove any undesirable side products or impurities, the solid crude material can be refluxed in either ethanol or isopropanol and filtered to afford compounds **1**-**22**. Due to the moderate reaction time and ease of isolation, Method B became our preferential method for compounds without substitution on the nitrogen of the 1,3-

diazinane-2, 4, 6-trione portion of the target compound. For *N*-substituted and *N*, *N*- disubstituted barbituric acids, trimethylamine/dimethyl sulfoxide, *N*-methylmorpholine/dimethyl sulfoxide, pyridine or sodium carbonate/ *N*, *N*-dimethylformamide can be used to achieve *C*-carboxamidation. However, the most convenient of these options is sodium carbonate/*N*, *N*-dimethylformamide (Method D). In Method D, the sodium salt of barbituric acid is formed via sonication at a temperature of 100°C. To this sodium salt, the phenyl *N*-arylcarbamate is added and the reaction continued with sonication and heating. After 4 hours, the reaction is complete, furnishing compounds **23**-**80**. If further purification is desired, the isolated crude material may be refluxed in either isopropanol or ethanol. Compounds **81**-**100** were also prepared in nearly quantitative yields using Method D.

The synthesis of the unsubstituted carbamoylamino derivatives, which have low solubility in organic solvents, was challenging to not only prepare but also to analyze. Method B, using trimethylamine as the base and dimethyl sulfoxide as the solvent was found to be the most successful. For the isolation and purification of compounds **101**-**109**, their poor solubility is an advantage in this case because the product can be refluxed in in ethanol and simply filtered off to collect the solid product, which is insoluble. Since these compounds have low solubility in organic solvents, including dimethyl sulfoxide, recording an accurate NMR spectrum was a concern. Predictably, these unsubstituted carbamoyl derivatives are insoluble in deuterated chloroform ($CDCl_3$) and deuterated dimethyl sulfoxide (D_6). However, these analogues were found to be soluble in trifluoroacetic acid and in deuterated chloroform and deuterated dimethyl sulfoxide when trifluoroacetic acid is an additive. Considering this development, it was found that these compounds may be purified by recrystallization from a solution of tetrachloroethylene and trifluoroacetic acid. Since these compounds may be present as rotomers under the conditions

needed to solubilize them for NMR analysis, the proton NMR spectrum can appear complex[66]. The ratio of rotomers to one another also varies with the concentration of trifluoroacetic acid present in the sample. The approximate concentration of trifluoroacetic acid in the NMR solvent can be estimated using a comparison to either tetrachloroethylene, chloroform or dimethyl sulfoxide. Electrospray mass spectroscopy, however, produces a clearer picture of these compounds to verify their identity. After a few simple modifications, these seemingly difficult to prepare compounds were able to be produced in good to excellent yields.

C-carboxamidation to prepare mono and disubstituted carboxamides can be accomplished with Methods A, B and D. However, Method C, which utilizes *N*-methylmorpholine as a base and dimethyl sulfoxide as the solvent, produced the best results for yield and purity for compounds **110-136**. Like their analogues, these compounds also have limited solubility in organic solvents, which is challenging in some aspects but convenient in other aspects such as purification. In this case, removing impurities (if present) can be done by refluxing the crude material in ethanol or isopropanol before filtering off the insoluble material to obtain the pure product.

4.7 Biological Evaluation

We selected the glioblastoma cell line LN-229 for our anti-cancer screening because it is one of the most aggressive and difficult forms of cancer to treat, with no true curative treatment available to date[67]. The best treatment option available for glioblastoma consists of several steps beginning with surgery, followed by radiation and then chemotherapy, usually with temozolomide[68]. The 1, 3 and 5-year survival rates for those affected by glioblastoma after the aforementioned treatment are 46%, 18% and 18%. One of the major reasons behind the lack of effective anti-cancer treatments available for glioblastoma is that chemotherapeutic agents are

either too potent, causing side effects that are often worse than cancer itself or not potent enough because they cannot cross the blood-brain barrier to reach the source. The simplest approach to this problem is to transfer potential anti-cancer molecules into prodrugs that can cross the blood-brain barrier[69].

4.7.1 ClogP, pKa and PSA in Drug Discovery

The first step in the development of a potential therapeutic agent is to evaluate its absorption, distribution, metabolism, excretion and toxicity (ADMET)[40]. To estimate a therapeutic candidate's ADMET, parameters such as molecular logP, pKa and polar surface area can be evaluated[70]. The partition coefficient, logP is a measure of a compound's lipophilicity and can be either calculated or experimentally determined by the distribution of a given compound in a water-octanol system. The lipophilicity of a potential drug candidate is important because it is a good predictor of the ability of a molecule to cross cell membranes. Ideal compounds should be neither too lipophilic, not too hydrophilic, with a logP or calculated logP value greater than approximately 1.0. Another tool to measure membrane permeability including the ability to cross the blood-brain barrier, which is of paramount importance for potential glioblastoma treatments, is pKa. It has been estimated that the ideal value for pKa is approximately 6.0. The polar surface area, which is also determines the ability of a molecule to cross membranes, should be near the suggested value[40] of approximately 100 $Å^2$. Compounds with a polar surface area in excess of 140 $Å^2$ are too polar to cross the cell membrane while compounds designed to cross the blood-brain barrier[41] must have a polar surface area[71] of approximately 90 $Å^2$. Using these values as a guide, it is possible to obtain a clearer picture of which compounds may have the greatest value as potential treatments for glioblastoma.

4.7.2 Evaluation of ClogP, pKa and PSA

4.7.2.1 Structural Motif A

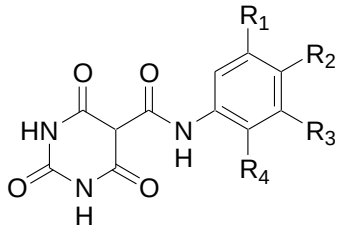

Phenyl substituted 2,4,6-trioxo-*N*-phenyl-1,3-diazinane-5-carboxamides

Table 17: Calculated molecular descriptors and biological activity of phenyl substituted 1, 3-dimethyl-2, 4, 6-trioxo-*N*-phenyl-1, 3-diazinane-5-carboxamidesagainst the LN-229 cell line

Compound	R_1	R_2	R_3	R_4	ClogP	pKa	PSA*	GA**
1	H	H	H	H	-0.10	4.20	104.37	NA
2	OH	H	H	H	-0.41	4.00	124.60	NA
3	H	OH	H	H	-041	3.99	124.60	100
4	CH_3	CH_3	H	H	0.99	4.37	104.37	100
5	H	OCH_3	H	H	-0.26	3.92	113.60	NA
6	OCH_3	OCH_3	H	H	-0.42	3.85	122.83	NA
7	OCH_3	OCH_3	OCH_3	H	-0.58	3.79	132.06	100
8	H	F	H	H	0.07	3.71	104.37	NA
9	H	Cl	H	H	0.50	3.71	104.37	NA
10	H	H	Cl	Cl	1.11	3.34	104.37	NA
11	H	Cl	H	Cl	1.11	3.34	104.37	NA
12	Cl	H	H	Cl	1.11	3.34	104.37	NA
13	H	Cl	Cl	H	1.11	3.34	104.37	NA
14	Cl	H	Cl	H	1.11	3.34	104.37	NA
15	H	Br	H	H	0.67	3.69	104.37	NA
16	H	H	Br	H	0.67	3.69	104.37	100
17	H	I	H	H	0.83	3.68	104.37	NA
18	H	CO_2H	H	H	-0.44	3.64	141.67	NA
19	H	CO_2Et	H	H	0.26	3.79	130.67	100
20	H	$CONH_2$	H	H	-1.25	3.89	147.46	NA
21	H	NO_2	H	H	-0.16	3.08	147.51	100
22	H	H	NO_2	H	-0.16	2.95	147.51	NA

*PSA= Polar Surface Area in $Å^2$; **GA= Glioblastoma cell line LN-229 activity in µg/ml; NA= No Activity at the maximum 100 µg/ml concentration; Calculated molecular descriptors obtained from Chem Axon's Marvin Sketch Software

Structural Motif A, composed of structures **1**-**22**, where R_1=R_2=H, has minor structural modifications from merbarone that result in substantial changes in the calculated logP, pKa and polar surface area. The calculated values suggest that compound **1** is unlikely to cross cell membranes, including the blood-brain barrier, and should have little or no activity. When hydroxyl moieties are incorporated, this adds to the polarity of the molecule overall, making it even less likely to be a successful therapeutic option. Nevertheless, these compounds should not be ruled out because their low solubility. These compounds are not highly soluble in either aqueous or organic media and so there is no way to verify the actual concentrations of these compounds that are coming into contact with the cell cultures.

Experimentally, compound **3** shows moderate anti-cancer activity, even though the calculated molecular descriptors predicted otherwise. In the case of compound **4**, incorporating two methyl groups increases the non-polar character of the compound, which would suggest more favorable values for the calculated physical descriptors. Indeed, the calculated logP is 0.99 and the polar surface area is closer to 100Å^2, with a value of 104.37Å^2. However, for trimethoxy compound **7**, the molecular descriptors are not as favorable. According to these values, compound **7** should be inactive. Again, experimentally, compound **7** exhibits moderate activity, most likely due to the contribution of the methoxy groups to the overall solubility of the molecule. For halogenated compounds **8**-**17**, the molecular descriptors predict improved physical properties from unsubstituted 1. However, the only compound which shows activity is compound **16**, a bromo substituted analogue, with activity of 100µg/ml.

A possible explanation for the disparity between calculated predictors and experimental results is the inherent limitations of computational methods, which give identical calculations for analogues bearing the same substituents even though they may be present on different positions

on the phenyl ring. An example of this is the set of calculated physical descriptors for compounds **10**-**14**, which are all dichloro compounds and have the same calculated physical descriptors. The other compounds falling into to category of Structural Motif A, such as 4-nitrophenyl derivatives, show reasonable activity.

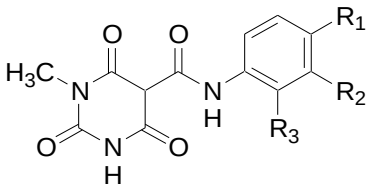

Phenyl substituted 1-methyl-2,4,6-trioxo-*N*-phenyl-1,3-diazinane-5-carboxamides

Table 18: Calculated molecular descriptors and biological activity of substituted 1-methyl-2, 4, 6-trioxo-*N*-phenyl-1, 3-diazinane-5-carboxamidesagainst the LN-229 cell line

Compound	R_1	R_2	R_3	ClogP	pKa	PSA*	GA**
23	H	H	H	0.12	4.22	95.58	NA
24	H	OH	H	-0.18	4.02	115.81	100
25	OH	H	H	-0.18	4.02	115.81	NA
26	OCH_3	H	H	-0.04	3.94	104.81	100
27	Cl	H	H	0.73	3.74	95.58	100
28	H	Cl	Cl	1.33	3.38	95.58	NA
29	Cl	H	Cl	1.33	3.38	95.58	NA
30	CO_2H	H	H	-0.22	3.65	132.88	NA

*PSA= Polar Surface Area in $Å^2$; **GA= Glioblastoma cell line LN-229 activity in µg/ml; NA= No Activity at the maximum 100 µg/ml concentration; Calculated molecular descriptors obtained from Chem Axon's Marvin Sketch Software

When methyl substitution occurs on one of the nitrogens of the 1, 3-diazinane portion of our lead compound, the expected result is higher lipophilicity. In fact, all of the molecular predictors validate this expectation, indicating increased lipophilicity, lower acidity and a smaller polar surface area. An illustration of this example is the comparison of compound **1** with compound **23**. In this instance, the calculated logP increases by 0.22 and the pKa also increases slightly by 0.02. The polar surface area however, decreases by 8.49 $Å^2$. These changes suggest that

compound **23** should have higher activity than compound **1** due to its ability to cross the blood-brain barrier. Nevertheless, again it is evident that this is not the case experimentally. In fact, neither compound **1** nor compound **23** have any detectable activity at concentrations of 100 μg/ml. Of the compounds with *N*-methyl substitution or belonging to Structural Motif A, the only compounds with activity at 100μg/ml are **24**, **26** and **27**, which bear hydroxy, methoxy and chloro moieties.

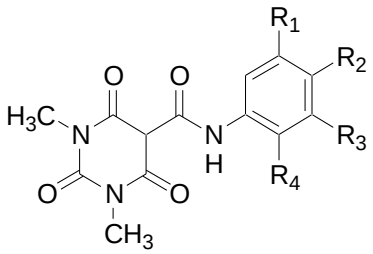

Phenyl substituted 1,3-dimethyl-2,4,6-trioxo-*N*-phenyl-1,3-diazinane-5-carboxamides

Table 19: Calculated molecular descriptors and biological activity of substituted 1, 3-dimethyl-2, 4, 6-trioxo-*N*-phenyl-1, 3-diazinane-5-carboxamidesagainst the LN-229 cell line

Compound	R_1	R_2	R_3	R_4	ClogP	pKa	PSA*	GA**
31	H	H	H	H	0.35	5.52	86.79	100
32	H	H	H	OH	0.04	5.34	107.02	100
33	H	H	OH	H	0.04	5.33	107.02	100
34	H	OH	H	H	0.04	5.32	107.02	100
35	H	CH_3	CH_3	H	1.37	5.67	86.79	NA
36	H	OCH_3	H	H	0.19	5.25	96.02	NA
37	H	OCH_3	OCH_3	H	0.03	5.17	105.25	NA
38	OCH_3	OCH_3	OCH_3	H	-0.13	5.10	114.48	NA
39	H	Cl	H	H	0.95	5.06	86.79	10
40	H	H	Cl	Cl	1.55	4.70	86.79	100
41	H	Cl	H	Cl	1.55	4.70	86.79	100
42	Cl	H	H	Cl	1.55	4.70	86.79	100
43	H	Cl	Cl	H	1.55	4.70	86.79	100
44	Cl	H	Cl	H	1.55	4.70	86.79	NA
45	H	Br	H	H	1.11	5.03	86.79	100
46	H	H	Br	H	1.11	5.03	86.79	100
47	H	I	H	H	1.27	5.01	86.79	100
48	H	CO_2H	H	H	0.00	4.11	124.09	100
49	H	CO_2Et	H	H	0.71	5.13	113.09	100
50	H	$CONH_2$	H	H	-0.80	5.22	129.88	NA
51	H	NO_2	H	H	0.29	5.00	129.93	100
52	H	H	NO_2	H	0.29	5.01	129.93	NA
53	H	H	H	C_6H_5	1.99	5.71	86.79	100
54	H	C_6H_5	H	H	1.99	5.71	86.79	100

*PSA= Polar Surface Area in $Å^2$; **GA= Glioblastoma cell line LN-229 activity in µg/ml; NA= No Activity at the maximum 100 µg/ml concentration; Calculated molecular descriptors obtained from Chem Axon's Marvin Sketch Software

Considering the results of the *N*-methyl substituted 1,3-diazinane compounds, we predict that analogues with *N*, *N*- dimethyl substitution on the 1,3-diazinane moiety will have increased lipophilicity compared to the previous derivatives. Interestingly, the calculated predictors for the *N*, *N*- dimethyl derivative compound **31**, which bears an unsubstituted phenyl group, are near the calculated physical descriptors for merbarone. In comparison to the unsubstituted compound **1**, the calculated logP for *N*-methyl substituted compound **23** increases by 0.22 and by 0.23 for

compound. Interestingly, this class of molecules has much better anti-cancer activity than their *N, N*- dimethyl derivatives. Perhaps due to the increased water solubility of the hydroxy substituted derivative, compounds **32**, **33** and **34** show reasonable activity at 100µg/ml concentrations. 4- chlorophenyl compound **39** is the most active of the monohalogenated phenyl compounds with activity at concentrations of 10 µg/ml. Compounds including dichloro analogues **40**, **41**, **42** and **43** also have activity at concentrations of 100 µg/ml. Additional compounds which are active in concentrations of are those with carboxylic acid, ester, 4-nitro and phenyl substituents such as compounds **48**, **49**, **52** and **53**, respectively. The most promising compound from this category is the monochlorinated compound **39** which, with biological activity at concentrations of 10µg/ml, has activity better than that of merbarone.

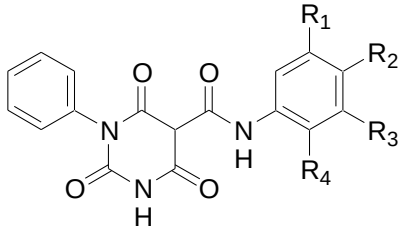

1-phenyl-2,4,6-trioxo-*N*-phenyl-1,3-diazinane-5-carboxamides

Table 4.6: Calculated molecular descriptors and biological activity of substituted 1-phenyl-2, 4, 6-trioxo-*N*-phenyl-1, 3-diazinane-5-carboxamidesagainst the LN-229 cell line

Compound	R_1	R_2	R_3	R_4	ClogP	pKa	PSA*	GA**
55	H	H	H	H	1.78	3.75	95.58	100
56	H	OH	H	H	1.48	3.58	115.81	NA
57	H	CH_3	CH_3	H	2.81	3.88	95.58	NA

58	H	OCH_3	H	H	1.62	3.53	104.81	100
59	H	OCH_3	OCH_3	H	1.46	3.48	114.04	NA
60	OCH_3	OCH_3	OCH_3	H	1.31	3.40	123.27	100
61	H	F	H	H	1.92	3.37	95.58	NA
62	H	Cl	H	H	2.38	3.36	95.58	NA
63	H	H	Cl	Cl	2.99	3.05	95.58	NA
64	H	Cl	H	Cl	2.99	3.05	95.58	100
65	Cl	H	H	Cl	2.99	3.05	95.58	NA
66	H	Cl	Cl	H	2.99	3.05	95.58	NA
67	Cl	H	Cl	H	2.99	3.05	95.58	NA
68	H	Br	H	H	1.11	3.33	95.58	100
69	H	I	H	H	2.71	3.31	95.58	100
70	H	CO_2H	H	H	1.44	3.35	132.88	100
71	H	$CONH_2$	H	H	0.63	3.50	138.67	NA
72	H	NO_2	H	H	1.72	3.82	138.72	NA
73	H	H	NO_2	H	1.72	3.79	138.72	NA
74	H	C_6H_5	H	H	3.43	3.79	95.58	NA

*PSA= Polar Surface Area in $Å^2$; **GA= Glioblastoma cell line LN-229 activity in µg/ml; NA= No Activity at the maximum 100 µg/ml concentration; Calculated molecular descriptors obtained from Chem Axon's Marvin Sketch Software

In the case of *N*-phenyl substituted derivatives of Structural Motif A, the addition of the phenyl group would be expected to produce compounds enhanced lipophilicity as well as increased acidity. The phenyl group would also be expected to contribute to an overall decrease in the available polar surface area of the molecule. As in the case with the synthesis and NMR analysis of some of these analogues, their solubility can pose unique challenges in their biological evaluation. According the calculated physical descriptors, calculated logP and polar surface area, it is predicted that compounds **55-74** should exhibit excellent biological activity against glioblastoma. However, this is not necessarily the case, with only compounds **55**, **58**, **60**, **64**, **68**, **69** and **70** having modest activity at 100 µg/ml and virtually no activity at even lower concentrations such as 10 µg/ml. Substituents contributing to the activity of these compounds are varied. Compound **55** is a simple phenyl group, while compounds **58** and **60** are methoxy and trimethoxy, respectively. Compounds **64**, **68** and **69** are mono and polyhalogenated, with

dichloro, bromo and iodo substituents. Compound **70** is dissimilar from all of these derivatives, with a carboxyl substituent. Given these results and considering the solubility challenges, it is difficult to accurately draw any conclusions about the contributions of these substituents to the biological activity of these derivatives.

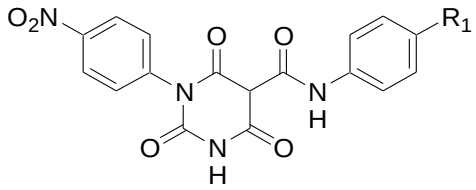

Phenyl substituted 1-(4-nitrophenyl)-2,4,6-trioxo-*N*-phenyl-1,3-diazinane-5-carboxamides

Table 4.7: Calculated molecular descriptors and biological activity of phenyl substituted 1-(4-nitrophenyl)-2, 4, 6-trioxo-*N*-phenyl-1, 3-diazinane-5-carboxamidesagainst the LN-229 cell line

Compound	**R_1**	**ClogP**	**pKa**	**PSA***	**GA****
75	H	1.72	3.32	138.72	NA
76	OCH_3	1.56	3.17	147.95	NA
77	F	1.86	3.02	138.72	NA
78	Cl	2.32	3.02	138.72	NA
79	$CONH_2$	0.57	3.15	181.81	NA
80	NO_2	1.66	3.48	181.86	NA

*PSA= Polar Surface Area in $Å^2$; **GA= Glioblastoma cell line LN-229 activity in µg/ml; NA= No Activity at the maximum 100 µg/ml concentration; Calculated molecular descriptors obtained from Chem Axon's Marvin Sketch Software

When substitution occurs on the phenyl portion of the *N*-phenyl substituent, the nitro group contributes to an increase in the polar surface area. This increase in polar surface area is higher than the targeted value of approximately $100Å^2$, with values ranging from $138.72Å^2$ to $181.86Å^2$. Considering this change, it is not likely that these analogues will have the desired activity. Indeed, this prediction is validated by the observation of a lack of activity at concentrations of 100 µg/ml. Due to the absence of activity at these concentrations, lower concentrations were not explored. Thus, we conclude that compound **39**, with its dimethyl diazinane substitution, chlorine present on the 4 position of the phenyl moiety and activity against glioblastoma cell line LN-229 in concentrations of 10 µg/ml, is the most likely candidate for further development of potential anti-cancer therapeutics of the analogues belonging to Structural Motif A.

4.7.2.2 Structural Motifs B and C

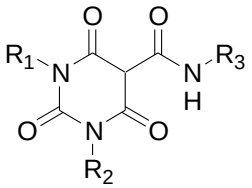

Substituted 2,4,6-trioxo-1,3-diazinane-5-carboxamide

Table 4.8: Calculated molecular descriptors and biological activity of substituted 2, 4, 6-trioxo-*N*-phenyl-1, 3-diazinane-5-carboxamidesagainst the LN-229 cell line

Compound	R_1	R_2	R_3	ClogP	pKa	PSA*	GA**
81	H	H	1-napththyl	0.89	4.41	104.37	100
82	H	H	2-napththyl	0.89	4.35	104.37	100
83	H	H	2-anthracenyl	1.88	4.43	104.37	100
84	CH_3	H	2-anthracenyl	2.10	4.42	95.58	100

85	CH_3	CH_3	1-napththyl	1.33	5.69	86.79	100
86	CH_3	CH_3	2-napththyl	1.33	5.64	86.79	100
87	CH_3	CH_3	2-anthracenyl	2.32	5.70	86.79	100
88	C_6H_5	H	1-napththyl	2.77	3.90	95.58	100
89	C_6H_5	H	2-napththyl	2.77	3.86	95.58	NA
90	C_6H_5	H	2-anthracenyl	3.76	3.92	95.58	100

*PSA= Polar Surface Area in $Å^2$; **GA= Glioblastoma cell line LN-229 activity in µg/ml; NA= No Activity at the maximum 100 µg/ml concentration; Calculated molecular descriptors obtained from Chem Axon's Marvin Sketch Software

We were also interested to see the effect of replacing the phenyl group of merbarone with larger aromatics such as anthracene and naphthalene, giving rise to Structural Modifications B and C. The calculated physical descriptors for compounds **81**-**90** are close to those of merbarone, with calculated logP values ranging from 0.89 to 3.76, pKa values from 3.86 to 5.69 and polar surface areas between 86.79$Å^2$ and 104.47$Å^2$, thus indicating the potential for reasonably potent activity. Although most of these analogues exhibited activity experimentally, it was lower than we had hoped, with activity at 100 µg/ml concentrations as opposed to lower concentrations.

4.7.2.3 Structural Motif D

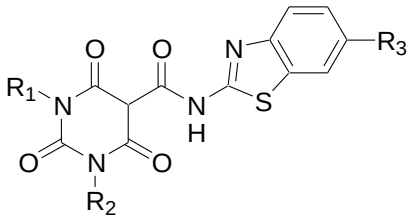

Substituted *N*-(1,3-benzothiazol-2-yl)-2,4,6-trioxo-1,3-diazinane-5-carboxamide

Table 20: Calculated molecular descriptors and biological activity of substituted N-(1, 3-benzothiazol-2-yl) -2, 4, 6-trioxo -1, 3-diazinane-5-carboxamidesagainst the LN-229 cell line

Compound	**R_1**	**R_2**	**R_3**	**ClogP**	**pKa**	**PSA***	**GA****
91	H	H	OCH_3	0.56	3.73	126.49	NA
92	H	H	NO_2	0.66	2.89	160.40	NA

93	CH_3	CH_3	OCH_3	1.01	5.08	108.91	NA
94	CH_3	CH_3	NO_2	1.11	4.82	142.82	NA
95	C_6H_5	H	OCH_3	2.45	3.38	117.70	100
96	C_6H_5	H	NO_2	2.54	3.65	151.61	100

*PSA= Polar Surface Area in $Å^2$; **GA= Glioblastoma cell line LN-229 activity in µg/ml; NA= No Activity at the maximum 100 µg/ml concentration; Calculated molecular descriptors obtained from Chem Axon's Marvin Sketch Software

Considering the results of Structural Motifs B and C, we decided to go in another direction with the replacement of the original phenyl group of merbarone. Here, we decided to incorporate the heteroaromatic 1, 3-benzothiazol-2-yl moiety to create analogues with Structural Motif D. However, the result of this substitution was that while acceptable calculated logP and pKa values were obtained, the polar surface area values were too high. Considering these calculated molecular descriptors, it is not surprising that only two compounds of this group, compounds **95** and **96**, show activity at concentrations of 100 µg/ml.

4.7.2.4 Structural Motif E

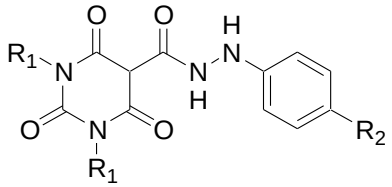

Substituted 2,4,6-trioxo-*N*-phenyl-1,3-diazinane-5-carbohydrazide

Table 4.10: Calculated molecular descriptors and biological activity of substituted 2, 4, 6-trioxo-*N*-phenyl-1, 3-diazinane-5-carbohydrazidesagainst the LN-229 cell line

Compound	**R_1**	**R_2**	**ClogP**	**pKa**	**PSA***	**GA****
97	H	H	-0.24	5.52	116.40	NA
98	H	NO_2	-0.30	3.17	159.54	NA

99	CH_3	H	0.21	7.22	98.82	NA
100	CH_3	NO_2	0.15	6.72	141.96	100

*PSA= Polar Surface Area in $Å^2$; **GA= Glioblastoma cell line LN-229 activity in µg/ml; NA= No Activity at the maximum 100 µg/ml concentration; Calculated molecular descriptors obtained from Chem Axon's Marvin Sketch Software

Having explored various combinations of structural modifications to the phenyl group of the original merbarone as well as different *N* and *N*, *N*- 1,3 diazinane substitution, our next approach was to alter the relationship of the diazinane group to the aromatic portion by increasing the distance between them. N-H linkers were employed as the means to this end, creating an exciting new class of compounds with Structural Motif E. However, our excitement was tempered by the observation that of the analogues prepared, only compound **100** with its nitrophenyl substitution on 1,3 diazinane has mediocre activity at concentrations of 100 µg/ml.

4.7.2.5 Structural Motif F

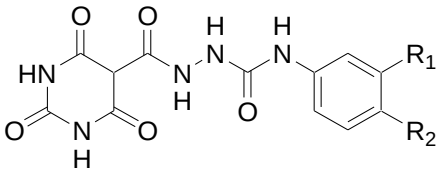

Substituted 2,4,6-trioxo-*N*-[(phenylcarbamoyl)amino]-1,3-diazinane-5-carboxamide

Table 4.11: Calculated molecular descriptors and biological activity of substituted 2, 4, 6-trioxo-*N*-[(phenylcarbamoyl)amino]-1, 3-diazinane-5-carboxamidesagainst the LN-229 cell line

Compound	R_1	R_2	ClogP	pKa	PSA*	GA**
101	H	H	-1.03	5.22	145.50	100
102	OH	H	-1.33	5.13	165.73	NA
103	H	OH	-1.33	5.16	165.73	NA
104	H	F	-0.88	5.09	145.50	NA
105	H	Cl	-0.42	5.13	145.50	100
106	Cl	Cl	0.18	5.05	145.50	NA
107	H	CN	-1.17	5.10	169.29	NA
108	H	NO_2	-1.09	3.25	188.64	NA
109	NO_2	OH	-1.39	3.28	208.87	NA

*PSA= Polar Surface Area in $Å^2$; **GA= Glioblastoma cell line LN-229 activity in µg/ml; NA= No Activity at the maximum 100 µg/ml concentration; Calculated molecular descriptors obtained from Chem Axon's Marvin Sketch Software

Intrigued by the idea of modifying the linker between the diazinane group to the aromatic moiety, we developed a derivative of the unsuccessful Structural Motif E, created by the incorporation of a urea as opposed to a simple N-H, to form Structural Motif F. In addition to the inclusion of a urea-type linker, as well as the substitutions on the phenyl moiety, there is the possibility of further modification by adding methyl, dimethyl and phenyl groups to the nitrogen of the 1,3-diazinane. The initial study of compounds belonging to Structural Motif F began with compounds lacking substation on the 1,3-diazinane group. In the case of these analogues, the urea unit leads to an undesirable migration from the ideal calculated physical descriptors, with decreased solubility, increase polarity as well as increased polar surface area. Based on these results it is expected that these derivatives would have little to no biological activity. However, compounds **101** and **105**, with no substituted and chlorophenyl substitution, respectively, show surprisingly moderate activity.

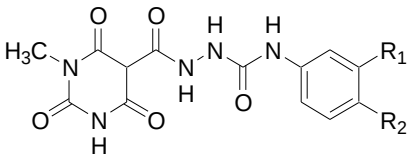

Phenyl substituted 1-methyl-2,4,6-trioxo-*N*-[(phenylcarbamoyl)amino]-1,3-diazinane-5-carboxamide

Table 4.12: Calculated molecular descriptors and biological activity of phenyl substituted 1-methyl-2, 4, 6-trioxo-*N*-[(phenylcarbamoyl) amino]-1, 3-diazinane-5-carboxamidesagainst the LN-229 cell line

Compound	**R_1**	**R_2**	**ClogP**	**pKa**	**PSA***	**GA****
110	H	H	-0.80	5.25	136.71	NA
111	OH	H	-1.10	5.17	156.94	NA
112	H	OH	-1.10	5.19	156.94	NA
113	H	F	-0.66	5.13	136.71	NA
114	H	Cl	-0.20	5.17	136.71	100
115	Cl	Cl	-0.41	5.09	136.71	NA
116	H	CN	-0.95	5.14	160.50	NA
117	H	NO_2	-0.86	3.30	179.85	100
118	NO_2	OH	-1.16	3.31	200.08	NA

*PSA= Polar Surface Area in $Å^2$; **GA= Glioblastoma cell line LN-229 activity in µg/ml; NA= No Activity at the maximum 100 µg/ml concentration; Calculated molecular descriptors obtained from Chem Axon's Marvin Sketch Software

Although this first set of compounds did not have the activity we had hoped for, the modest activity of compounds**101** and **105** encouraged the development of additional less polar derivatives. As with the other analogues, we began by introducing *N*-methyl substitution on the 1,3-diazinane. As anticipated, the calculated logP increases and the polar surface area decreases, putting the calculated physical descriptors closer to the ideal values. Thus, compounds **114** and **117**, chloro and nitro substituted analogues, respectively, exhibit activity at concentrations of 100 µg/ml.

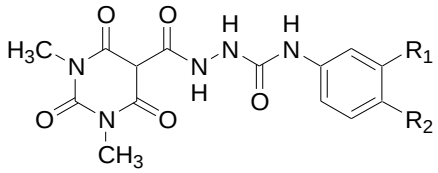

Phenyl substituted 1,3-dimethyl-2,4,6-trioxo-*N*-[(phenylcarbamoyl)amino]-1,3-diazinane-5-carboxamide

Table 4.13: Calculated molecular descriptors and biological activity of phenyl substituted 1, 3-dimethyl-2, 4, 6-trioxo-*N*-[(phenylcarbamoyl)amino]-1, 3-diazinane-5-carboxamidesagainst the LN-229 cell line

Compound	R_1	R_2	ClogP	pKa	PSA*	GA**
119	H	H	-0.58	6.93	127.92	NA
120	OH	H	-0.88	6.85	148.15	NA
121	H	OH	-0.88	6.87	148.15	10
122	H	F	-0.44	6.81	127.92	100
123	H	Cl	0.03	6.85	127.92	10
124	Cl	Cl	0.63	6.77	127.92	1
125	H	CN	-0.73	6.82	151.71	100
126	H	NO_2	-0.64	6.69	171.06	10
127	NO_2	OH	-0.94	6.89	191.29	10

*PSA= Polar Surface Area in $Å^2$; **GA= Glioblastoma cell line LN-229 activity in µg/ml; NA= No Activity at the maximum 100 µg/ml concentration; Calculated molecular descriptors obtained from Chem Axon's Marvin Sketch Software

To move our compounds even closer to the ideal calculated molecular descriptors, a second methyl group was added to give *N*, *N*-dimethyl substitution on the 1,3-diazinane. Although this modification did yield calculated physical descriptors closer to the desired values, the calculated logP was still lower than we had expected. Nevertheless, this group of derivatives produced some of the most interesting candidates out of the entire set of proposed molecules presented here. Two derivatives, fluoro substituted **122** and cyano substituted **125** have activity at 100 µg/ml. Even better results are obtained for compounds **121**, **123**, **126** and **127**, which bear hydroxy, chloro, nitro and 2-nitro 5-hydroxy substitution, respectively in concentrations of 10

µg/ml. The best activity against glioblastoma was compound **124**, 3,4 dichloro, with excellent activity at the low concentration of 1 µg/ml.

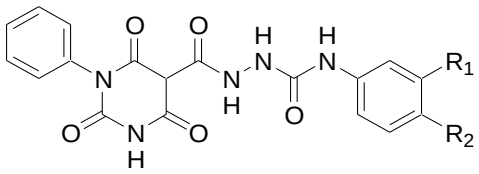

Phenyl substituted 1-phenyl-2,4,6-trioxo-*N*-[(phenylcarbamoyl)amino]-1,3-diazinane-5-carboxamide

Table 4.14: Calculated molecular descriptors and biological activity of substituted 1-phenyl-2, 4, 6-trioxo-*N*-[(phenylcarbamoyl)amino]-1, 3-diazinane-5-carboxamidesagainst the LN-229 cell line

Compound	R_1	R_2	ClogP	pKa	PSA*	GA**
128	H	H	0.86	3.80	136.71	NA
129	OH	H	0.55	3.74	156.94	NA
130	H	OH	0.55	3.76	156.94	NA
131	H	F	1.00	3.71	136.71	NA
132	H	Cl	1.46	3.74	136.71	100

133	Cl	Cl	2.06	3.76	136.71	100
134	H	CN	0.71	3.71	160.50	100
135	H	NO_2	0.80	4.48	179.85	100
136	NO_2	OH	0.49	4.48	200.08	100

*PSA= Polar Surface Area in $Å^2$; **GA= Glioblastoma cell line LN-229 activity in µg/ml; NA= No Activity at the maximum 100 µg/ml concentration; Calculated molecular descriptors obtained from Chem Axon's Marvin Sketch Software

Theoretically, replacing the dimethyl substitution on the 1,3-diazinane with a phenyl instead results in more favorable values for the calculated molecular descriptors. However, this is only true for the calculated logP values. The pKa values are lower than the ideal value of 6.00, ranging from 3.71-4.48. Not surprisingly, the polar surface area is higher than the optimal 100 $Å^2$ as well, ranging from 136.71$Å^2$ to 200.08$Å^2$, nearly twice that of the desired value. Despite these detriments, compounds **131-136**, with chloro, nitro, cyano and 2-nitro 5-hydroxy substitution, still exhibit modest activity at 100 µg/ml concentrations.

4.8 Discussion

Using previously described methods for the formation of *N*-arylcarbamates[35] followed by our procedures described here (Methods A-D), we successfully produced a wide variety of *N*-aryl and *N*-arylcarbamoylamino derivatives of 1, 3-diazinane-5-carboxamide through *C*-carboxamidation as potential anti-cancer agents. We developed our target compounds based on what we identified as key structural features present across several topoisomerase II inhibitors, such as merbarone. Calculated molecular descriptors were used in conjunction with biological evaluation against the glioblastoma LN-229 cell line to identify the most promising derivatives as potential anti-cancer therapeutics. Since most chemotherapeutic agents are ineffective against glioblastoma due to their inability to cross the blood-brain barrier, we examined physical

descriptors such as calculated logP, pKa and polar surface area to evaluate the potential of these derivatives to permeate the blood-brain barrier. Several extensive studies[40,41,70,71] have shown that the ideal values for these descriptors are approximately 1.0 for the partition coefficient, 6.0 for the pKa and 100 $Å^2$ for polar surface area with a value of 90 $Å^2$ being most favorable for crossing the blood-brain barrier.

Based on our analysis and biological evaluation of our library of 136 compounds, we have developed a handful of derivatives with similar or better activity than merbarone. Compound **121**, 1, 3-dimethyl-2, 4, 6-trioxo-N-[(phenylcarbamoyl)amino]-1,3-diazinane-5-carboxamide, in addition to its hydroxy, chloro and nitro analogues exhibited excellent action against the glioblastoma LN-229 cell line. However, the most potent derivative, with activity at 1 μg/ml, was dichloro compound **124**.

Chapter 5: Conclusions

We developed several classes of biologically interesting compounds designed as potent anti-cancer therapeutics. One challenge we faced was the preparation of our targeted compounds, since many starting materials were either not commercially available or far too expensive to be economically feasible. Thus, we developed a novel synthesis for the preparation of semicarbazides through their corresponding phenyl carbamate intermediates. This method is both convenient and applicable to synthesis of a variety of compounds such as ureas which can then be used to make substituted barbituric acids as well as aryl carbamoyl derivatives of 1,3-diazinane-5-carboxamides, which we have shown to possess anti-cancer activity.

We designed a series of aryl carbamoyl derivatives of 1,3-diazinane-5-carboxamides by incorporating what we believe to be key structural features of merbarone, a potent topoisomerase II inhibitor. Synthesized analogues were analyzed per the drug design and discovery approach which defines optimal computed physical parameters such as logP, pKa and polar surface area. Biological testing of these compounds against the glioblastoma cell line LN-229 identified several derivatives with moderate, good and excellent activity at concentrations of 100 µg/ml, 10 µg/ml and 1 µg/ml, respectively, with compound **124** having the best activity at 1 µg/ml. Considering the success of these derivatives, we were interested to explore more complex, polycyclic structures. The chromenopyrimidinediones as well as their nitrogenous analogues the pyrimidinequinolinediones, were designed to inhibit cancer growth by acting as either HDM2 inhibitors of the p53 pathway or by mimicking FAD/$FADH_2$ in the electron transport chain to influence the rapid ATP generation associated with the growing metabolic needs of cancer cells. Nearly all synthesized chromenopyrimidinediones exhibited activity at 100 µg/ml and 80% of these compounds were also active at lower concentrations of 10 µg/ml. Out of these compounds showing activity at 10 µg/ml, four of them, **CP4**, **CP6**, **CP7** and **CP10**, also showed activity at the lower concentration of 1 µg/ml. The pyrimidinequinolinediones, however, did not have as many biologically active compounds as the chromenopyrimidinediones at 10 µg/ml, but still produced valuable results providing insight into the structural features to which biological activity may be linked. Of the pyrimidinequinolinediones which were active at 10 µg/ml, two of these derivatives, **AQ112** and **AQ163**, were also active at 1 µg/ml. Using these results, more potent analogues of these compounds may be synthesized via additional refinements to the target structures. These refined target structures may be further investigated using multiple cancer cell lines to identify suitable candidates for development as possible anti-cancer agents.

References

1. Lane, D.P. Cancer: p53, Guardian of the Genome. *Nature* **1992**, 358, 15-16.

2. (a) Teodoro, J.G.; Evans, S.L.; Green, M.R. Inhibition of Tumor Angiogenesis by p53: A New Role for the Guardian of the Genome. *J Mol. Med*. **2007**, 85(11)1175-1186.; (b) Fridman, J.S.; Lowe, S.W. Control of Apoptosis by p53. *Oncogene* **2003**, 22, 9030-9040.; (c) Vousden, K.H.; Lu, X. Live or Let Die: The Cell's Response to p53. *Nat. Rev. Cancer* **2002**, 2(8)594-604.ol

3. Vogelstein, B.; Lane, D.; Levine, A.J. Surfing the p53 Network. *Nature* **2000**, 408 (6810) 307-310.

4. Kruse, J.P. and Gu, W. Modes of p53 Regulation. *Cell* **2009**, 134(4) 609-622.

5. Yang, Y.; Ludwig, R.L.; Jensen, J.P.; Pierre, S.A.; Medaglia, M.V.; Davydov, I.V.; Safiran, Y.J.; Oberoi, P.; Kenten, J.H.; Phillips, A.C.; Weissman, A.M.; Vousden, K.H.

Small Molecule Inhibitors of HDM2 Ubiquitin Ligase Activity Stabilize and Activate p53 in Cells. *Cancer Cell* **2005**, 7, 547-559.

6. Fang,S.; Weismann, A.M. Ubiquitin-Proteasome System. *Cell Mol Life Sci* **2004**, 61, 1546-1561.

7. Li, M.; Brooks, C.L.; Wu-Baer, F.; Chen, D.; Baer, R.; Gu, W. Mono Versus Polyubiquitination: Differential Control of p53 Fate by MDM2. *Science* **2003**, 302, 1972-1975.

8. Burgess, A.; Chia, K.M.; Haupt, S.; Thomas, D.; Haupt, Y.; Lim, E. Clinical Overview of MDM2/X Targeted Therapies. *Front. Oncol*. **2016**, 6 (7) 1-7.

9. Levine, A.J. p53, the Cellular Gatekeeper for Growth and Division. *Cell* **1997**, 88(3), 323-331.

10. Wang, S.; Zhao, Y.; Bernard, D.; Aguilar, A.; Kumar, S. Targeting the MDM2-p53 Protein-Protein Interaction for New Cancer Therapeutics. *Top. Med. Chem*. **2012**, 8, 57-80.

11. Farhazadeh, S.S.; Trusko, S.P.; George, D.L. Tumorigenic Potential Associated with Enhanced Expression of a Gene that is Amplified in a Mouse Tumor Cell Line. *EMBO J* **1991**, 10: 1565-1569.

12. Carry, J.C.; Garcia-Echeverria, C. Inhibitors of the p53/HDM2 Protein-Protein Interaction: Path to the Clinic. *Bioorg. Med. Chem. Lett*. **2013**, 23, 2480-2485.

13. Andreeff, M.; Kelly, K.R.; Yee, K.; Assouline, S.; Strair, R.; Popplewell, L.; Bowen, D.; Martinelli, G.; Drummond, M.W.; Vyas, P.; Kirschbaum, M.; Iyer, S.P.; Ruvolo, V.; Gonzalez,G.M.; Huang, X.; Chen, G.; Graves, B.; Blotner, S.; Bridge, P.; Jukofsky, L.; Middleton, S.; Reckner, M.; Rueger, R.; Zhi, J.; Nichols, G.; Kojima, K. Results of the Phase I Trial of RG7112, a Small Molecule MDM2 Antagonist in Leukemia. *Clin. Cancer Res*. **2016**, 22(4) 868-876.

14. Ding, Q.; Zhang, Z.; Liu, J.; Jiang, N.; Zhang, J.; Ross, T.M.; Chu, X.; Bartkovitz, D.; Podlaski, F.; Janson, C.; Tovar, C.; Filipovic, Z.M.; Higgins, B.; Glenn, K.; Packman, K.; Vassilev, L.T.; Graves, B. Discovery of RG7388, a Potent and Selective p53-MDM2 Inhibitor in Clinical Development. *J. Med. Chem.* **2013**, 56, 5979-5983.

15. Canon, J.; Osgood, T.; Olson, S.H.; Saiki, A.Y.; Robertson, R.; Yu, D.; Eksterowicz, J.; Ye, Q.; Jin, L.; Chen, A.; Zhou, J.; Cordover, D.; Kaufman, S.; Kendall, R.; Oliner, J.D.; Coxon, A.; Radinsky, R. The MDM2 Inhibitor AMG232 Demonstrates Robust Antitumor Efficacy and Potentiates the Activity of p53-Inducing Cytotoxic Agents. *Mol. Cancer Ther*. **2015**, 14, 649-658.

16. Sun, D.; Li, Z.; Rew, Y.; Gribble, M.; Bartberger, M.D.; Beck, H.P.; Canon, J.; Chen, A.; Chen, X.; Chow, D.; Deignan, J.; Duquette, J.; Eskterowicz, J.; Fisher, B.; Fox, B.M.; Fu, J.; Gonzalez, A.Z.; Gonzalez-Lopez De Turiso, F.; Houze, J.B.; Huang, X.; Jiang, M.; Jin, L.; Kayser, F.; Liu, J.; Lo, M.; Long, A.M.; Lucas, B.; McGee, L.R.; McIntosh, J.; Mihalic, J.; Oliner, J.D.; Osgood, T.; Peterson, M.L.; Roveto, P.; Saiki, A.Y.; Shaffer, P.; Toteva, M.; Wang, Y.; Wang, Y.C.; Wortman, S.; Yakowec, P.; Yan, X.; Ye, Q.; Yu, D.; Yu, M.; Zhao, X.; Zhao, J.; Zhu, J.; Olson, S.H.; Medina, J.C. Discovery of AMG 232, a Potent, Selective and Orally Bioavailable MDM2-p53 Inhibitor in Clinical Development. *J. Med. Chem*. **2014**, 57, 1454-1472.

17. Zhao, Y.; Yu, S.; Sun, W.; Liu, L.; Lu, J.; McEachern, D.; Shargary, S.; Bernard, D.; Li, X.; Zhao, T.; Zou, P.; Sun, D.; Wang, S. A Potent Small Molecule Inhibitor of the MDM2-p53 Interaction (MI-888) Achieved Complete and Durable Tumor Regression in Mice. *J. Med. Chem*. **2015**, 58, 1038-1052.

18. Jung, J.; Lee, J.S.; Dickson, M.A.; Schwartz, G.K.; Le Cesne, A.; Varga, A.; Bahleda, R.; Wagner, A.J.; Choy, E.; de Jonge, M.J.; Light, M.; Rowley, S.; Mace, S.; Watters, J. *TP53* Mutations Emerge with HDM2 Inhibitor SAR405838 Treatment in Dedifferentiated Liposarcoma. *Nature Commun*. **2016**, 1-7.

19. Dickens, M.P.; Roxburgh, P.; Hock, A.; Mezna, M.; Kellam, B.; Vousden, K.H.; Fisher, P.M. 5-Deazaflavin Derivatives as Inhibitors of p53 Ubiquitination by HDM2. *Bioorg. Med. Chem.* **2013**, 21 (22) 6868-77.

20. Salway, J.G.; *Metabolism at a Glance*, 3rd ed.; Wiley-Blackwell: **2004**.

21. Cairns, R.A.; Harris, I.S.; Mak, T.W. Regulation of Cancer Cell Metabolism. *Nat. Rev. Cancer* **2011**, 11, 85-95.

22. Khurana, J.M.; Lumb, A.; Chaudhary, A.; Nand, B. Synthesis and *In Vitro* Evaluation of Antioxidant Activity of Diverse Naphthopyranopyrimidines, Diazaanthra[2,3-*d*][1,3]dioxole-7,9-dione and Tetrahydrobenzo[a]xanthen-11-ones. *RSC Adv*. **2013**, 3, 1844-1854.

23. Bedair, A.H.; El-Hady, N.A.; El-Latif, M.S.; Fakery, A.H.; El-Agrody, A.M. 4-Hydroxycoumarin in Heterocyclic Synthesis Part III: Synthesis of Some New Pyrano [2,3-*d*] pyrimidine, 2-substituted[1,2,4]triazolo[1,5-*c*]pyrimidine and pyrimido [1,6-*b*][1,2,4]triazine Derivatives. *Farmaco* **2000**, 55, 708-714.

24. Joshi, K.C.; Jain, R.; Sharma, K.; Bhattacharya, S.K.; Goel, R.K. Spiro Heterocyclic Compounds III: Synthesis of Some Fluorine Containing Spiro[3H-indole-3,4(4H)-pyrano[2,3-*d*]pyrimidine]-2,5,7(1H)-triones as CNS Agents .*Indian Chem. Soc*. **1988**, 115, 202-204.

25. Jian, X.; Sun, Y.; Yao, J.; Cao, Y.; Kai, M.; He, N.; Zhang, X.; Wang, Y.; Wang, R. Core Scaffold-Inspired Concise Synthesis of Chiral Spirooxindole-Pyranopyrimidines with Broad Spectrum Anticancer Potency. *Adv. Synth. Catal*. **2012**, 354(5) 917-925.

26. Nandi, G.C.; Samai, S.; Kumar, R.; Singh, M.S. An Efficient One-Pot Synthesis of Tetrahydrobenzo[*a*]xanthene-11-one and diazabenzo[*a*]anthracene-9,11-dione Derivatives Under Solvent Free Conditions. *Tetrahedron* **2009**, 65, 7129-7134.

27. Jalde, S.S.; Chavan, H.V.; Adsul, L.K.; Dhakane, V.D.; Bandgar, B.P.; An Efficient Solvent-Free Synthesis of Naphthopyranopyrimidines Using Heteropolyacid as an Ecofriendly Catalyst. *Synth. React. Inorg. Met. Org. Chem.* **2014**, 44, 623-626.

28. Mohaqeq, M.; Safaei-Ghomi, J.; Shahbazi-Alavi, H. $ZrOCl_2$/nano TiO_2 as an Efficient Catalyst for the One-Pot Synthesis of Naphthopyranopyrimidines Under Solvent Free Conditions. *Acta Chim. Slov*. **2015**, 62, 967-972.

29. Shaterian, H.R.; Azizi, K.; Fahimi, N. Phosphoric Acid Supported on Alumina (H_3PO_4/Al_2O_3) as an Efficient and Reusable Catalyst for the One-Pot Synthesis of Benzoxanthene Pigments. *Res. Chem. Intermed*. **2014**, 40, 1403-1414.

30. Sun, X.J.; Zhou, J.F.; Zhao, P.S. Molecular Iodine-Catalyzed One-Pot Synthesis of Tetrahydrobenzo[*a*]xanthene-11-one and Diazabenzo[*a*]anthracene-9,11-dione Derivatives Under Microwave Irradiation. *J. Heterocyclic Chem.* **2011**, 48, 1347-1350.

31. Vilsmeier, A.; Haack, A. On the Action of Halophosphorous on Alkylformanilides: A New Method of Preparation of Secondary and Tertiary Para Alkylamino Benzaldehydes. *Che. Ber*. **1927**, 60, 199.

32. Dickey, J.B.; Gray, A.R. Barbituric Acid. *Org. Synth*. **1938**, 18, 8-9.

33. Devi, I.; Bhuyan, P.J. An Expedient Method for the Synthesis of 6-Substituted Uracils Under Microwave Irradiation in a Solvent-Free Medium. *Tetrahedron Lett*. **2005**, 46 (34) 5727-5729.

34. Beekhuis, H.A.; Lawrence, C.K. Process for the Production of Urea and an Ammonium Salt. US Patent 2056283 A, 1936.

35. Hron, R.; Jursic, B.S. Preparation of Substituted Semicarbazides from Corresponding Amines and Hydrazines via Phenyl Carbamates. *Tetrahedron Lett*. **2014** (55) 1540-1543.

36. Ishii, N.; Maier, D.; Merlo, A.; Tada, M.; Sawamura, Y.; Diserens, A.; Van Meir, E.G. Frequent Co-Alterations of *TP53*, *p16*/*CDKN2A*, $p14^{ARF}$, *PTEN* Tumor Suppressor Genes in Human Glioma Cell Lines. *Brain Pathol*. **1999**, 9 (3) 469-479.

37. Hann, M; Keserü, G. M. Finding the Sweet Spot: The Role of Nature and Nurture in Medicinal Chemistry. *Nat. Rev. Drug Discovery*, **2012**, 11, 355-365.

38. Katritzky, A.R.; Manju, K.; Singh, S.K.; Meher, N.K. Benzotriazole Mediated Amino-, Alkoxy-, and Alkylthio- Alkylation. *Teterahedron Lett*. **2005**, 61(10) 2555-2581.

39. Yu, J.; Zhang, P.; Shang, Z. Metal-Free C-N Bond-Forming Reaction: Straightforward Synthesis of Anilines Through the Cleavage of Aryl C-O Bonds and Amide C-N Bonds. *Tetrahedron Lett*. **2013**, 54, 3167-3170.

40. Keserü, G.M.; Makara, G.M. The Influence of Lead Discovery Strategies on the Properties of Drug Candidates. *Nat. Rev. Drug Discovery*, **2009**, 8, 203-212.

41. Pajouhesh, H.; Lenz, G.R. Medicinal Chemical Properties of Successful Central Nervous System Drugs. *Neuro Rx*. **2005**, 2 (4), 541-553.

42. Smith, D.; Artursson, P.; Avdee, A.; Di, L.; Ecker, G.F.; Faller, B.; Houston, J.B.; Kansy, M.; Kerns, E.H.; Kramer, S.D.; Lennernas, H.; van de Waterbeemd, H.; Sugano, K.; Testa, B. Passive Lipoidal Diffusion and Carrier-Mediated Cell Uptake are Both Important Mechanisms of Membrane Permeation in Drug Disposition. *Mol. Pharm*. **2014**, 11, 1727-1738.

43. Bailey, B. R. 4-Alkyl and aryl semicarbazides as oxygen scavengers. US Patent 5 904 857, 1999.

44. Pham-Huy, L.A.; He, H.; Pham-Huy, C. Free Radicals and Antioxidants in Disease and Health. *Int. J. Biomed. Sci*. **2008**, 4(2)89-96.

45. Agrawal, K.C.; Booth, B.A.; DeNuzzo, S.M.; Sartorelli, A.C. Potential Antitumor Agents 14: 4-Substituted 2-Formylpyridine Thiosemicarbazones. *J. Med. Chem*. **1976**, 19(10) 1209-1214.

46. Lesniak, S.; Pieczonka, A.M.; Jarzynski, S.; Justyna, K.; Rachwalski, M. Synthesis and Evaluation of the Catalytic Properties of Semicarbazides Derived from *N*-triphenylmethyl-aziridine-2-carbohydrazides. *Tetrahedron:Asymmetry* **2013**, 24(20) 1341-1344.

47. Nguyen, L.A.; He, H.; Pham-Huy, C. Chiral Drugs: An Overview. *Int. J. Biomed. Sci*. **2006**, 2(2) 85-100.

48. Vasquez, J.; Albericio, F. A Convenient Semicarbazide Resin for the Solid-Phase Synthesis of Peptide Ketones and Aldehydes. *Tetrahedron Lett*. **2006** (47)1657-1661.

49. Friedlander, R.M. Apoptosis and Caspases in Neurodegenerative Diseases. *N. Engl. J. Med*. **2003**, 348: 1365-1375.

50. Philchenkov, A. Caspases: Potential Targets for Regulating Cell Death. *J. Cell. Mol. Med*. **2004**, 8(4) 432-44.

51. (a) Liu, Q.; Luedtke, N.W.; Tor, Y. A Simple Conversion of Amines into Monosubstituted Ureas in Organic and Aqueous Solvents. *Tetrahedron Lett*. **2001**, *42*, 1445-1447.; (b) Kreye, O.; Mutlu, H.; Meier, M.A.R. Sustainable Routes to Polyurethane Precursors. *Green Chem*. **2013**, *15*, 1431-1455.; (c) Zhang, L.; Xia, W.; Wang, B.; Luo, Y.; Lu, W. Convenient Synthesis of Sorafenib and Its Derivatives. *Synth. Commun.* **2011**, *41*, 3140-3146.; (d) Guo, X.; Shang, J.; Li, J.; Wang, L.; Ma, Y.; Shi, F.; Deng, Y. Green and Practical Synthesis of Carbamates from Ureas and Organic Carbonates. *Synth. Commun.* **2011**, *41*, 1102-1111.

52. (a) Ilieva, S.; Nalbantova, D.; Hadjieva, B.; Galabov, B. Aminolysis of Phenyl *N*-Phenylcarbamates via an Isocyanate Intermediate: Theory and Experiment. *J. Org. Chem*. **2013**, *78*, 6440-6449.; (b)Weber, H. W. Process for Preparing Alkyl Isocyanates. US Patent 4 123 450, 1978.

53. Brewer, A.D.; Minatelli, J.A. 5-Pyrimidinecarboxamides and Treatment of Leukemia and Tumors Therewith. US Patent 4634707, 1987.

54. Deweese, J.E.; Osheroff, M.A.; Osheroff, N. DNA Topology and Topoisomerases. *Biochem. Mol. Bio. Educ*. **2009** (37) 2-10.

55. Larsen, A.K.; Escargueil, A.E.; Skladanowski, A. Catalytic Topoisomerase II Inhibitors in Cancer Therapy. *Pharmacol. Ther*. **2003**, 90, 167-181.

56. Pommier, Y.; Leo, E.; Zhang, H.; Marchand, C. DNA Topoisomerases and Their Poisoning by Anticancer and Antibacterial Drugs. *Chem. Biol*. **2010** (17) 5, 421-433.

57. Thakur, D.S. Topoisomerase II Inhibitors in Cancer Treatment. *Int. J. Pharm. Sci. Nanotech*. **2011**, 3(4) 1173-1181.

58. Sorensen, B. S.; Sinding, J.; Andersen, A.H.; Alsner, J.; Jensen, P.B.; Westergaard, O. Mode of Action of Topoisomerase II-Targeting Agents at a Specific DNA Sequence: Uncoupling the DNA Binding, Cleavage and Religation Events. *J. Mol. Biol*. **1992**, 228 (3) 778-786.

59. Bojanowski, K.; Lelievre, S.; Markovits, J.; Couprie, J.; Jacquemin-Sablon, A.; Larsen, A.K. Suramin is an Inhibitor of DNA Topoisomerase II *In Vitro* and in Chinese Hamster Fibrosarcoma Cells. *Proc. Natl. Acad. Sci*. **1992**, 89, 3025-3029.

60. Fortune, J.M.; Osheroff, N. Merbarone Inhibits the Catalytic Activity of Human Topoisomerase IIα by Blocking DNA Cleavage. *J. Biol. Chem.* **1998**, 273, 17643- 17650.

61. Pastor, N.; Dominguez, I.; Orta, M.L.; Campanella, C.; Mateos, S.; Cortes, F. The DNA Topoisomerase II Catalytic Inhibitor Merbarone is Genotoxic and Induces Endoreduplication. *Mutat. Res. Fund. Mol. Mech*. **2012**, 738, 45-51.

62. Baviskar, A.T.; Amrutkar, S.M.; Trivedi, N.; Chaudhary, V.; Nayak, A.; Guchhait, S.K.; Banerjee, U.C.; Bharatam, P.V.; Kundu, C.N. Switch in Site of Inhibition: A Strategy for Structure-Based Discovery of Human Topoisomerase IIα Catalytic Inhibitors. *ACS Med. Chem. Lett*. **2015**, 6, 481-485.

63. Knolker, H.; Braxmeier, T. Isocyanates Part III: Synthesis of Carbamates by DMAP-Catalyzed Reaction of Amines with Di-*tert*-butyldicarbonate and Alcohols. *Tetrahedron Lett*. **1996**, 37 (33) 5861-5864.

64. Shimizu, M.; Sodeoka, M. A Convenient Method for the Preparation of Carbamates, Carbonates and Thiocarbonates. *Org. Lett*. **2007**, 9(25)5231-5234.

65. Uriz, P.; Queralt, M.S.; Salagre, P.; Castillion, S.; Claver, C.; Fernandez, E. A New and Efficient Catalytic Method for Synthesizing Isocyanates from Carbamates. *Tetrahedron Lett*. **2002**, 43, 1673-1676.

66. Laursen, J. S.; Engel-Andreasen, J.; Fristrup, P.; Harris, P.; Olsen, C.A. *Cis-Trans* Amide Bond Rotomers in β-Peptoids and Peptoids: Evaluation of Stereoelectronic Effects in Backbone and Side Chains. *J. Am. Chem. Soc*. **2013**, 135, 2835-2844.

67. Preusser, M.; de Ribaupierre, S.; Wohrer, A.; Erridge, S.C.; Hegi, M.; Weller, M.; Stupp, R. Current Concepts and Management of Glioblastoma. *Ann. Neurol*. **2011**, 70, 9-21.

68. Sathornsumetee, S.; Reardon, D.A.; Desjardins, A.; Quinn, J.A.; Vredenburgh, J.J.; Rich, J.N. Molecularly Targeted Therapy for Malignant Glioma. *Cancer* **2007**, 110, 13-24.

69. vanTellingen, O.; Yetkin-Arik, B.; de Gooijer, M.C.; Wesseling, P.; Wurdinger, T.; de Vries, H.E. Overcoming the Blood-Brain Tumor Barrier for Effective Glioblastoma Treatment. *Drug Resist. Updat.* **2015**, 19, 1-12.

70. Manallack, D.T. The pKa Distribution of Drugs: Application to Drug Discovery. *Perspect. Medicin. Chem*. **2007**, 1, 25-38.

71. Hitchcock S. A.; Pennington, L. D. Structure-Brain Exposure Relationships. *J. Med. Chem.* **2006**, 49, 7559-7583.

72. Hron, R.J.; Jursic, B.S.; Neumann, D.M. Synthesis of *N*-Aryl and *N*-Arylcarbamoylamino Derivatives of 1,3- Diazinane-5-Carboxamide and Their Activity Against Glioblastoma LN-229 Cell Line. *Bioorg. Med. Chem*. **2016**, 24:23, 6183-6193.

Experimental

All starting materials were reagent grade purchased from Sigma-Aldrich or Ark Pharm. ^{1}H-NMR and ^{13}C-NMR spectra were recorded on Varian Unity 400 MHz, Varian Inova 500 MHz, Varian Inova 600 MHz, Bruker 300 MHz, or Agilent 400 MHz NMRs in $CDCl_3$, DMSO-d_6, $CDCl_3$-TFA, DMSO-d_6-TFA, and in TFA with internal D_2O tube as NMR solvents using the solvent chemical shifts as an internal standard. Electrospray Mass Spectroscopy (EMS) was performed on MDS Sciex 3200 Qtrap LC/MS/MS system in positive or negative mode with methanol or acetonitrile as solvents.

Biological Testing

Testing against the CLlymphoma and B16 melanoma cell lines courtesy of Lee Roy Morgan. Testing against glioblastoma LN-229 cell line courtesy of Donna Neumann and LSUHSC. Biological testing on the LN-229 cell line was done via glioblastoma cultures (LN-229) which were grown in Dulbecco's modified Eagle's medium supplemented with 10% fetal bovine serum and incubated at a temperature of 37°C with 5% CO_2. Once the cells reached confluency, the media was replaced with serum-free media and treated with our compounds at 100μg/ml and 10μg/ml concentrations (in DMSO). After 24 hours, the media was removed and the cells were crosslinked with formalin before being stained with crystal violet for visualization.

Selected Examples for the Preparation of Chromenopyrimidinediones

Method A

Preparation of 2*H*-benzo[5,6]chromeno[2,3-*d*]pyrimidine-2 ,4 (3*H*)dione (CP10)

An ethanolic solution of salicylaldehyde (1.000 mmol) was added to an aqueous solution of barbituric acid (1.000 mmol) dropwise. The reaction mixture was allowed to stir overnight at room temperature, resulting in a precipitate. The precipitate was collected via vacuum filtration, washed with water (3 x 10.00 ml) and thoroughly dried in the oven at 110°C to give the coupled barbituric acid-salicaldehyde product. The coupled product was refluxed in a mixture of acetic anhydride (5.000 ml) and acetic acid (20.00 ml) for four hours before being cooled to room temperature and the resulting solid material vacuum filtered, washing with ethanol and placed in the oven to dry at 110°C to give the pure product (190.0 mg; 72%). ^{1}H-NMR (DMSO-d_6, Varian Mercury 300 MHz) δ11.2 (1H, s), 9.51 (1H, s), 8.82 (1H, d, *J*= 8.10 Hz), 8.48 (1H, d, *J*= 9.30 Hz), 8.14 (1H, d, *J*= 7.50 Hz), 7.82 (2H, m) and 7.71 (1H, m) ppm. EMS$^-$ (CH_3CN) m/z 265 (M+1) and 264 (M); MS2 (264) 264, 263, 221, 177, 166, 156, 152, 134, 111, 81 and 62.

Method B

Preparation of 5-(4-chlorophenyl)-3-methyl-1,5-dihydro-2*H*-benzo[5,6]chromeno[2,3-*d*]pyrimidine-2,4-dione (CP36)

A solution of phosphoric acid (5.000 ml) and acetic acid (25.00 ml) was added to a flask containing barbituric acid 128.0 mg; 1.000 mmol), 2-naphthol (144.0 mg;1.000 mmol) and 4-chlorobenzaldehyde (140.0 mg; 1.000 mmol) and refluxed for one hour or until the total reaction volume was reduced by approximately 2/3 of the original volume. The reaction mixture was allowed to cool to room temperature before water (20.00 ml) added. The resulting suspension was then vacuum filtered, washing well with water (3 x 10.00 ml) to remove all acid and dried at 110°C to give the pure product (152.0 mg; 39%).

^{1}H-NMR (DMSO-d_6, Varian Inova 500 MHz) δ 12.4 (1H, broad s), 7.40 (3H, m), 7.45 (3H, m), 7.32 (2H, d, *J*= 8.00 Hz), 7.22 (2H, d, *J*=8.00 Hz), 5.59 (1H, s) and 3.08 (3H, s) ppm.

^{13}C-NMR (DMSO-d_6, Varian Inova 500 MHz) δ 162.919, 152.825, 150.434, 147.266, 144.091, 131.925, 131.716, 130.940, 130.782, 130.577, 129.328, 128.834, 128.138, 126.043, 124.278, 117.382, 117.104, 89.534 and 35.348 ppm.

EMS^{-} (CH_3CN) m/z 390 (M), 389 (M-1); MS2 (390) m/z 390, 319, 278, 189, 167 and 80.

Preparation of 5-(2,4,6-trichlorophenyl)-2-sulfanylidene-1,2,3,5-tetrahydro-2*H*-benzo[5,6]chromeno [2,3-*d*]pyrimidin-4-one (CP50)

A solution of phosphoric acid (5.000 ml) and acetic acid (25.00 ml) was added to a flask containing thiobarbituric acid (144.0 mg; 1.000 mmol), 2-naphthol (144.0 mg; 1.000 mmol) and 2, 4, 6- trichlorobenzaldehyde (209.0 mg; 1.000 mmol) and refluxed for three hours. Acetic acid was evaporated from the reaction mixture until the total reaction volume was reduced by approximately 2/3 of the original volume. The reaction mixture was allowed to cool to room

temperature before water (20.00 ml) added. The resulting suspension was then vacuum filtered, washing well with water (3 x 10.00 ml) to remove all acid. The solid material was further purified by refluxing in ethanol (20.00 ml) for fifteen minutes and dried at 110°C to give the pure product (92.00 mg; 20%). ^{1}H-NMR (DMSO-d_6, Varian Mercury 300 MHz) δ 13.6 (1H, broad s), 12.5 (1H, s), 7.98 (3H, m), 7.68 (1H, s), 7.48 (2H, m), 7.42 (2H, d, *J*= 8.40 Hz), 7.18 (1H, d of d, J_1= 8.10 Hz and J_2= 8.10 Hz) and 5.67 (1H, s) ppm.EMS^{-} (CH_3CN) m/z 427(M) and 426 (M-1); MS2 (427) m/z 42, 60 and 58.

Selected Examples for the Preparation of Pyrimidinequinolinedione Compounds

General Procedure for the Preparation of Reduced Pyrimidinequinolinediones

Acetic acid (25.00 ml) was added to a flask containing barbituric acid (1.000 mmol), the substituted aromatic amine (1.000 mmol) and the aldehyde (1.000 mmol) and refluxed for one hour or until the total reaction volume was reduced by approximately 2/3 of the original volume. The reaction mixture was allowed to cool to room temperature before water (20.00 ml) added. The resulting suspension was then vacuum filtered, washing well with water (3 x 10.00 ml) to remove all acid and dried at 110°C to give the pure product.

Preparation of 5-(3-nitro-4-hydroxyphenyl)-12-methyl-5,12-dihydrobenzo[*f*]pyrimido[4,5-*b*]quinoline-2,4(1*H*, 3*H*) dione (AQ149)

Acetic acid (25.00 ml) was added to a flask containing barbituric acid (128.0 mg; 1.000 mmol), 2-*N*-methylnaphthylamine (157.0 mg; 1.000 mmol) and 4-hydroxy-3-nitrobenzaldehyde (167.0 mg; 1.000 mmol) and refluxed for one hour or until the total reaction volume was reduced by approximately 2/3 of the original volume. The reaction mixture was allowed to cool to room temperature before water (20.00 ml) added. The resulting suspension was then vacuum filtered, washing well with water (3 x 10.00 ml) to remove all acid and dried at 110°C to give the pure

product (358.0 mg; 86%). ^{1}H-NMR (DMSO-d_6, Varian Inova 500 MHz) δ 11.9 (1H, broad s), 10.8 (1H, s), 10.7 (1H, s), 7.96 (1H, d, *J*= 7.00 Hz), 7.91 (1H, d, *J*= 7.50 Hz), 7.87 (1H, d, *J*= 6.50 Hz), 7.57 (1H, d, *J*= 6.50 Hz), 7.45 (1H, t, *J*= 6.00 Hz), 7.36 (1H, t, *J*= 6.50 Hz), 7.12 (2H, d, *J*= 7.00 Hz), 7.02 (2H, d, *J*= 6.50 Hz), 5.74 (1H, s), and 3.53 (3H, s) ppm. EMS^{-}(CH_3CN) m/z 415 (M-1); MS2 (416) m/z 416, 401, 343, 328 and 133.

General Procedure for the Preparation of Oxidized Pyrimindinequinolinediones

Barbituric acid (1.000 mmol), the substituted aromatic amine (1.000 mmol) and the aldehyde (1.000 mmol) were combined and refluxed in acetic acid (25.00 ml) for one week. Acetic acid was evaporated and the resulting residue refluxed in ethanol (20.00 ml) for 15 minutes before being vacuum filtered, washing with ethanol and dried at 110°C to give the pure product.

Preparation of 5-phenyl-7-methoxy-10-methylpyrimido[4,5-*b*]quinoline-2,4(3*H*,10*H*)-dione (AQ14)

Barbituric acid (128.0 mg; 1.000 mmol), 4-methoxy-*N*-methylaniline (136.0 mg; 1.000 mmol) and benzaldehyde (106.0 mg; 1.000mmol) were combined and refluxed in acetic acid (25.00 ml) for one week. Acetic acid was evaporated and the resulting residue refluxed in ethanol (20.00 ml) for 15 minutes before being vacuum filtered, washing with ethanol and dried at 110°C to give the pure product (316.0 mg; 95%). ^{1}H-NMR (DMSO-d_6, Varian Mercury 300 MHz) δ 10.7 (1H, s), 7.95 (1H, d, *J*= 9.60 Hz), 7.60 (1H, d, *J*= 12.3 Hz), 7.48 (3H, m), 7.22 (2H, d, *J*= 7.50 Hz), 6.49 (1H, s), 4.10 (3H, s) and 3.58 (3H, s) ppm. EMS^{+} (CH_3CN) m/z 334 (M+1) and 333 (M); MS2 (334) 331, 332, 317, 291, 290, 275, 260 and 223.

Selected Examples for the Preparation of Semicarbazides

Preparation of ethyl pyridin-2-ylcarbamate

Ethyl chloroformate (2.200 g; 20.00mmol) was added dropwise into an ice-cooled solution of ethyl acetate (250.0 ml) 2-aminopyridine (1.840 g, 20.00 mmol). This reaction mixture was stirred on ice at 0°C for 30 minutes before being allowed to warm to ambient temperature. To this reaction mixture, a saturated sodium bicarbonate solution was added and stirred for five minutes before isolating the organic layer. Filtering the organic layer through a 1 inch silica gel column and evaporating it to dryness gives the pure product (3.050 g; 91%). ^{1}H-NMR (400 MHz, $CDCl_3$) δ 9.10 (1H, s), 8.31 (1H, d, *J* =5.20 Hz), 8.02 (1H, d, *J* = 8.40 Hz), 7.71 (1H, m), 6.98 (1H, m), 4.26 (2H, q, *J* = 7.20 Hz), and 1.35 (3H, t, *J* = 7.20 Hz) ppm. ^{13}C-NMR (400 MHz, $CDCl_3$) δ 153.8, 152.4, 147.7, 138.8, 118.8, 112.7, 61.6, and 17.8 ppm.

Preparation of *N*-(pyridin-2-yl)hydrazinecarboxamide

Ethyl 2-pyridinylcarbamate (1.660 g; 10.00 mmol) in 5.000 ml of hydrazine hydrate was warmed at 80°C for 12 hours. After 12 hours, the reaction mixture was cooled on ice for two hours. The formed precipitate was then isolated via vacuum filtration, washing with cold diethyl ether (3 x 5.000 ml) and dried to yield the desired pure product (1.200 g; ~80%). ^{1}H-NMR (400 MHz, DMSO-d_6) δ 9.10 (1H, s), 8.31 (1H, d, *J* =5.20 Hz), 8.02 (1H, d, *J* = 8.40 Hz), 7.71 (1H, s), 7.71 (1H, m), 6.98 (1H, m), and 4.41 (2H, s) ppm. ^{13}C-NMR (400 MHz, DMSO-d_6) δ 157.3, 153.1, 147.9, 138.8, 117.8, and 112.1 ppm

Selected Examples for the Preparation of Phenyl Carbamates

Preparation of phenyl (3,4,5-trimethoxyphenyl)carbamate

To an ice cooled solution of 3, 4, 5-trimethoxyaniline (1.830 g; 10.00 mmol), aqueous sodium bicarbonate (1.000 g; 12.00 mmol) and tetrahydrofuran (20.00 ml) a solution of phenyl chloroformate (1.640 g; 10.50 mmol) also in tetrahydrofuran (10.00 ml) was added dropwise. The resulting reaction mixture was then allowed to stir at ambient temperature for approximately

five minutes. After five minutes, ethyl acetate (200.0 ml) and water (50.00 ml) were added to the reaction mixture and the organic layer separated. The organic layer was then washed sequentially with water (3 x 50.00ml), 5% hydrochloric acid (3x 50.00 ml) and water (3 x 50.00 ml) before being dried over anhydrous sodium solvent and the evaporated to dryness to produce the desired pure product (2.880 g; 95%). ^{1}H-NMR (400 MHz, DMSO-d_6) δ 7.47 (1H, s), 7.37 (2H, t, *J* = 8.00 Hz), 7.22 (1H, t, *J* = 7.60 Hz), 7.15 (2H, t, *J* = 7.60 Hz), 6.74 (2H, s), 3.81 (3H, s) and 3.76 (6H, s) ppm. ^{13}C-NMR (400 MHz, $CDCl_3$) δ 153.6, 152.3, 150.7, 134.1, 129.7, 126.0, 121.9, 96.6, 92.9, 61.3 and 56.2 ppm.

General Procedure for the preparation of 4-arylsemicarbazides

Preparation of *N*-(2-methoxy-5-methylphenyl) hydrazinecarboxamide

To a solution of phenyl 2-methoxy-5-methylphenylcarbamate (514.0 mg; 2.000 mmol) in acetonitrile (50.00 ml) hydrazine hydrate (250.0 mg 5.000 mmol) was added. A few drops of water were added to the reaction mixture just until the reaction mixture becomes transparent. The resulting reaction mixture was sonicated for three hours at room temperature with stirring. After three hours, the solvent was removed and the resulting residue combined with diethyl ether (10.00 ml). Hexanes were added to this solution just until it became slightly cloudy. This mixture was then allowed to stay at room temperature for an hour before being cooled on ice for another hour. The formed precipitate was isolated via vacuum filtration, washing with hexane and dried to give the desired pure product (363.0 mg; 93%). ^{1}H-NMR (400 MHz, DMSO-d_6) δ 8.81 (1H, broad s), 7.99 (1H, s), 7.59 (1H, s), 6.82 (2H, d, *J* = 8.00 Hz), 6.66 (2H, d, *J* = 8.00 Hz), 4.49 (2H, broad s), 3.77 (3H, s) and 2.18 (3H, s) ppm. ^{13}C-NMR (400 MHz, DMSO-d_6) δ 157.6, 145.9, 129.8, 129.2, 121.9, 118.5, 110.9, 56.4 and 21.5 ppm.

General procedure for the preparation of 4-alkylsemicarbazides

Preparation of *N*-hexylhydrazinecarboxamide

Phenyl hexylcarbamate (2.210 g; 10.00 mmol) in hydrazine hydrate (2.500 g; 50.00 mmol) was sonicated at 60°C for twelve hours. After twelve hours, the reaction mixture was allowed to cool to room temperature before ethyl acetate (250.0 ml) and 50.00 ml of a saturated sodium bicarbonate solution were added. The resulting organic layer was then washed with saturated sodium bicarbonate (3 x 30.00 ml) before being dried over anhydrous sodium sulfate. Once the solvent was evaporated, cold hexanes (15.00 ml) were added to the formed residue. The suspension was then filtered via vacuum filtration, washed with hexanes (3 x 5.00 ml) and dried to give the pure product (1.460 g; 92%) ^{1}H-NMR (400 MHz, $CDCl_3$) δ6.97 (1H, s, H), 6.13 (1H, s), 3.75 (2H, broad s), 3.13 (2H, m), 1.43 (2H, m), 1.25 (6H, m) and 0.830 (3H, t, *J* = 6.70 Hz) ppm. ^{13}C-NMR (400 MHz, $CDCl_3$) δ 161.4, 39.9, 31.7, 30.4, 26.8, 22.8 and 14.2 ppm.

General procedure for the preparation of multi-substituted semicarbazides

Preparation of ethyl 4-(2-tosylhydrazinecarboxamido) benzoate

Ethyl 4-(phenoxycarbonylamino) benzoate (285.0 mg; 1.000 mmol) was sonicated with 4-methylbenzenesulfonohydrazide (186.0 mg; 1.000 mmol) and anhydrous potassium carbonate (138.0 mg; 1.000 mmol) in acetonitrile (50.00 ml) for three hours at room temperature. After three hours, acetonitrile was evaporated to yield a white solid, to which water was added (10.00 ml). The resulting suspension was separated by vacuum filtration, washing with water (3 x 5.000 ml) followed by diethyl ether (3 x 5.000 ml) and dried to yield the desired product (350.0 mg; 93%). ^{1}H-NMR (400 MHz, DMSO-d_6) δ 9.65 (1H, s), 8.96 (1H, s), 8.52 (1H, s), 7.81 (2H, d, *J* = 8.00 Hz), 7.73 (2H, d, *J* = 7. 60 Hz), 7.51 (2H, d, *J* = 8.40 Hz), 7.37 (2H, d, *J* = 8.00 Hz), 4.24 (2H, q, *J* = 7.20 Hz), 2.33 (3H, s) and 1.27 (3H, t, *J* = 6.80 Hz) ppm.^{13}C-NMR (400 MHz,

DMSO-d_6) δ 166.1, 155.1, 144.6, 144.2, 136.0, 130.8, 130.2, 128.5, 123.7, 118.5, 61.0, 21.7 and 14.9 ppm.

Alternative procedure for the preparation of multi-substituted semicarbazides

Preparation of cholesteryl 2-(4-(ethoxycarbonyl) phenylcarbamoyl) hydrazinecarboxylate

Ethyl 4-(phenoxycarbonylamino) benzoate (285.0 mg; 1.000 mmol) was added to a solution of cholesterylhydrazinecarboxylate (445.0 mg; 1.000 mmol) in acetonitrile (20.00 ml) and *N*-methylmorpholine (3.000 ml) and sonicated for three hours at 60°C. The white solid resulting after the evaporation of acetonitrile was then mixed with cold acetonitrile (15.00 ml), filtered, washing with cold acetonitrile (3 x 5.000 ml), and dried to give the product (570.0 mg; 90%). ^{1}H-NMR (400 MHz, $CDCl_3$) selected signals δ 8.36 (1H, broad s), 7.81 (3H, d, *J* = 8.00 Hz), 7.64 (2H, d, *J* = 8.40 Hz), 5.26 (1H, m), 4.47 (1H, m) and 4.30 (2H, q, *J* = 7.20 Hz) ppm. ^{13}C-NMR (400 MHz, $CDCl_3$) selected signals δ 166.4, 156.3, 142.7, 139.4, 130.8, 124.9, 123.2, 118.4, 77.0, 60.9, 56.9 and 56.4 ppm.

Preparation of cholesterylhydrazinecarboxylate

Cholesteryl chloroformate (22.50 g; 50.00 mmol) in dichloromethane (200.0 ml) was added slowly to a mixture of tetrahydrofuran-water (210.0 ml, 20:1) and hydrazine hydrate (50.00 g; 1.000 mol) and stirred at room temperature for two hours. After two hours, dichloromethane (200.0 ml) was added to the reaction mixture and the organic layer washed with water (3 x 200.0 ml), dried over sodium solvent and evaporated to dryness. Hexanes (100.0 ml) was added to the formed residue, suspension vacuum filtrated and dried to give the pure product (21.10 g; 95%). ^{1}H-NMR (400 MHz, $CDCl_3$) selected signals δ 6.26 (1H, s), 5.35 (1H, m), 4.15 (1H, m) and 3.75 (2H, s) ppm. ^{13}C-NMR (400 MHz, $CDCl_3$) selected signals δ 158.7, 139.8, 122.9, 75.4, 56.9, 56.4 and 50.2 ppm.

Selected Examples for the Preparation of Phenyl Arylcarbamates

Method I (ethyl acetate/THF/ aqueous Na_2CO_3)

Preparation of phenyl 4-carbamoylphenylcarbamate

Phenyl chloroformate (17.10 g; 110.0 mmol) was added dropwise into a solution of ethyl acetate (300.0 ml), tetrahydrofuran (100.0 ml), water (100.0 ml), sodium carbonate (6.400 g; 60.00 mmol) and 4-aminobenzamide (13.60 g; 100.0 mmol) on ice. The reaction mixture was stirred on ice at 0°C for one hour followed by one hour at ambient temperature. The organic layer was then isolated from the reaction mixture and washed with water (3 x 20.00 ml), 5% hydrochloric acid (3 x 20.00 ml) and water (3 x 20.00 ml) before being dried over anhydrous sodium sulfate and the solvent evaporated to give the pure product (22.10 g; 86%). If the product is not of sufficient purity, it may be easily purified by crystallization in a mixture of ethyl acetate and hexanes. ^{1}H-NMR (DMSO-d_6, Varian Unity 400 MHz) δ 10.5 (1H, s), 7.90 (1H, broad s), 7.85 (2H, d, *J* = 8.40 Hz), 7.56 (2H, d, *J* = 8.4 Hz), 7.41 (2H, t, *J* = 8.00 Hz), and 7.22 (4H multiplet = 1 broad s + 1t + 1d) ppm. ^{13}C-NMR (DMSO-d_6, Varian Unity 400 MHz) δ 152.4, 151.0, 142.1, 130.2, 129.3, 129.2, 126.3, 122.6 and 118.3 ppm. EMS- (CH_3OH) m/z 264.5 (M-1), 363.5 (M-2), EMS MS2 (265) 265.1, 178.2, 153.0, and 134.8.

Method II (ethyl acetate/triethylamine)

Preparation of phenyl 4-fluorophenylcarbamate

Phenyl chloroformate (1.700 g; 11.00 mmol) was added dropwise into a solution of ethyl acetate (50.00 ml), triethylamine (5.000 ml), 4-fluoroaniline (1.110 g; 10.00 mmol) on ice. The reaction mixture was stirred on ice at 0°C for one hour followed by two hours at ambient temperature. The ethyl acetate layer was washed with water (5 x 15.00 ml), 5% hydrochloric acid (5 x 15.00 ml), again with water (5 x 15.00 ml) before being dried over anhydrous sodium sulfate and the

solvent evaporated. The solid material was then combined with hexanes (15.00 ml), sonicated at room temperature for 30 minutes, filtered washing with hexanes (3 x 5.000 ml) and dried to give the product (1.900 g; 82%). ^{1}H-NMR (DMSO-d_6, Varian Unity 400 MHz) δ10.3 (1H, s) 7.55 (2H, d of d, J_1 = 6.40 Hz, J_2 = 3.20 Hz), 7.44 (2H, t, J = 6.40 Hz), 7.27 (1H, t, J = 6.40 Hz), 7.23 (2H, d, J =6.40 Hz), and 7.18 (2H, t, J = 6.40 Hz) ppm. ^{13}C-NMR (DMSO-d_6, Varian Inova 500 MHz) δ 158.7 (d, J = 952.5 Hz), 152.6, 151.2, 135.7, 130.1, 126.2, 122.6, 120.9, and 116.2 (d, J = 90 Hz) ppm.

Method III (tetrahydrofuran/pyridine)

For highly THF soluble anilines

Preparation of phenyl 2, 3-dichlorophenylcarbamate

Phenyl chloroformate (1.700 g; 11.00 mmol) was added dropwise into a solution of tetrahydrofuran (30.00 ml), 2, 3-dichloroaniline (1.620 g; 10.00 mmol) and pyridine (0.9000 ml; 0.9000 g; 11.00 mmol) on ice. The reaction mixture was stirred on ice at 0°C for 30 minutes followed by one hour at ambient temperature. Once the solvent was carefully evaporated, taking care that the temperature does not exceed 20 °C, the solid material was dissolved in dichloromethane (50.00 ml), washed with 3% hydrochloric acid (3 x 10.00 ml), water (3 x 10.00 ml) before being dried over anhydrous sodium sulfate and the drying agent removed by gravity filtration. The volume of the organic solution was reduced to 10.00 ml and 20.00 ml of hexanes was added, resulting in the formation of a precipitate. This precipitate was then vacuum filtrated, washing with hexanes and dried at room temperature to give the pure product (2.500 g; 88%). ^{1}H-NMR ($CDCl_3$, Varian Inova 600 MHz) δ 8.14 (1H, d, J = 6.60 Hz), 7.56 (1H, broad s), 7.40 (2H, t, J = 7.80 Hz), 7.26 (1H, t, J =7.80 Hz), 7.24 (1H, d, J = 6.60 Hz), and 7.21 (2H, t, J = 7.80 Hz) ppm. EMS^+ (CH_3CN) m/z 283 (M+1), 305 (M+Na).

Method IV (ethyl acetate/tetrahydrofuran/pyridine)

For poorly THF soluble and less reactive anilines

Preparation of phenyl 4-nitrophenylcarbamate

A suspension of 4-nitroaniline (1.380 g; 10.00 mmol) in pyridine (20.00 ml) and tetrahydrofuran (20.00 ml) was sonicated for one hour or until all nitroaniline was dissolved. One nitroaniline dissolved, ethyl acetate (200.0 ml) was added to the reaction mixture and the mixture cooled on ice. To this ice-cold solution, a solution of phenyl chloroformate (1.710 g; 11.00 mmol) in ethyl acetate (30.00 ml) was added dropwise. The reaction was then allowed to stir at 0°C for an hour and then room temperature overnight. After several hours, the reaction mixture was isolated by washing with water (3 x 50.00 ml), 5% hydrochloric acid (3 x 50.00 ml) and again with water (3 x 50.00 ml) and the organic layer dried over sodium sulfate before being evaporated to give the pure product (2.200 g; 85%). ^{1}H-NMR ($CDCl_3$, Varian Unity 400 MHz) δ 8.23 (2H, d, *J* = 9.20 Hz), 7.62 (2H, d, *J* = 9.20 Hz), 7.41 (2H, t, *J* = 7.60 Hz), 7.33 (1H, broad s), 7.28 (1H, t, *J* = 7.60 Hz), and 7.19 (2H, d, *J* = 7.60 Hz) ppm.

Method V (ethyl acetate/*N*-methylmorpholine)

For reactive arylamines

Preparation of phenyl 3, 4, 5-trimethoxyphenylcarbamate

Phenyl chloroformate (3.420 g; 22.00 mmol) in ethyl acetate (15.00 ml) was added dropwise to a solution of 3, 4, 5-trimethoxyaniline (3.660 g, 20.00 mmol), *N*-methylmorpholine (15.00 ml) and ethyl acetate (150.0 ml) at 0°C. After all reagents were added, the reaction mixture was allowed to warm to room temperature and continue stirring for one hour. After one hour, the organic layer was washed with water (3 x 50.00 ml), 5% hydrochloric acid (3 x 50.00 ml) and again with water (3 x 50.00 ml). The organic filtrate was dried over anhydrous sodium sulfate, and solvent

evaporated to give the pure product (2.600 g; 86%). ^{1}H-NMR ($CDCl_3$, Varian Inova 600 MHz) δ 7.39 (2H, t, *J* = 7.80 Hz), 7.34 (1H, t, *J* = 7.80 Hz), 7.17 (2H, d, *J* = 7.80 Hz), 6.92 (1H, broad s), 6.74 (2H, s), 3.83 (6H, s), and 3.81 (3H, s) ppm. EMS^+ (CH_3CN) m/z 304 (M+1), 326 (M+Na).

Selected Examples for the Preparation of N-arylhydrazinecarboxamides

Preparation of *N*-(4-hydroxy-3-nitrophenyl)hydrazinecarboxamide

The appropriate carbamate (here, *N*-(4-hydroxy-3-nitrophenyl)phenylcarbamate, 20.00 g; 73.00 mmol) was dissolved in 500.0 ml of ethanol with hydrazine monohydrate (20.00 g; 0.4000 mol) and refluxed for one hour. After the reaction was completed, the volume of the reaction mixture was reduced to 10.00 ml, forming a dark red suspension. To this suspension, 300.0 ml of water was added and the mixture cooled on ice for two hours. After two hours, the formed insoluble product was separated by vacuum filtration, washing with cold water (3 x 30.00 ml) before being dried at 110ºC to give the pure product (12.50 g; 81%). ^{1}H-NMR (DMSO-d_6, Varian Inova 600 MHz) δ 10.70 (1H, s), 9.99 (1H, s), 8.41 (1H, s, 1H, s), 7.46 (1H, s), 7.15 (1H, d, *J* = 10.8 Hz), and 4.61 (2H, broad s) ppm. ^{13}C-NMR (DMSO-d_6 Varian Inova 600 MHz) δ 157.6, 152.0, 137.0, 129.1, 124.6, 123.2, and 110.6 ppm.

Selected Examples for the Preparation of 2, 4, 6-trioxo-N-phenyl-1, 3-diazinane-5-carboxamide

Method A (Pyridine)

Preparation of *N*-(4-fluorophenyl)-2, 4, 6-trioxo-1, 3-diazinane-5-carboxamide

Barbituric acid (128.0 mg; 1.000 mmol) and phenyl 4-fluorophenylcarbamate (231.0 mg; 1.000 mmol) were refluxed in pyridine (5.000 ml) overnight. After the reaction was completed, the pyridine solvent was evaporated to yield a residue. To this residue, water (10.00 ml) and concentrated hydrochloric acid (5.000 ml) were added and the mixture sonicated at 60°C for 30

minutes. After 30 minutes, the insoluble crystalline material was removed by filtering the mixture, washing with water (3 x 5.000 ml) and dried at 110° C to yield the crude product. An ethanolic (15.00 ml) solution of the crude product was refluxed for 30 minutes and then allowed to cool to room temperature before being isolated via vacuum filtration, washing with cold ethanol to obtain the pure product (240.0 mg; 90%). ^{1}H-NMR (DMSO-d_6 Varian Inova 600 MHz) δ 12.1 (1H, broad s), 11.4 (1H, s), 11.3 (1H, broad s), 7.53 (2H, m, J_1 = 8.40 Hz, J_2 = 4.80 Hz), and 7.21 (2H, t, J = 8.40 Hz) ppm. EMS- (CH_3OH) m/z 264.5 (M-1), 363.5 (M-2), EMS MS2 (265) 265.1, 178.2, 153.0, and 134.8.

Method B (TEA/DMSO)

Preparation of *N*-(3, 4-dichlorophenyl)-2, 4, 6-trioxo-1, 3-diazinane-5-carboxamide

Barbituric acid (422.0 mg; 3.300 mmol) and phenyl 3, 4-dichlorophenylcarbamate (840.0 mg; 3.000 mmol) were refluxed for three hours in a dimethyl sulfoxide (3.000 ml)- triethylamine (3.000 ml) mixture. After three hours, the triethylamine was removed by evaporation under reduced pressure. Once triethylamine was removed, 5% hydrochloric acid (15.00 ml) was added to the resulting mixture and the suspension cooled on ice. This suspension was filtered, washed with water (5 x 5.000 ml) and dried at 110° C to give the crude product. This crude material was then sonicated followed by refluxing in ethanol (20.00 ml) for one hour and the solid material removed by vacuum filtration to yield the desired pure product (870.0 mg; 92%). ^{1}H-NMR (DMSO-d_6, Varian Inova 500 MHz) δ 11.8 (2H, broad s), 11.5 (1H, s), 7.90 (1H, d, J = 1.50 Hz), 7.59 (1H, d, J = 7.00 Hz), and 7.45 (1H, d of d, J_1 = 7.00 Hz, J_2 = 1.50 Hz) ppm. EMS^{-}(CH_3OH) m/z 315 (M-1).

Method C (NMM/DMSO)

Preparation of 4-(2, 4, 6-trioxo-1, 3-diazinane-5-amido) benzoic acid

Barbituric acid (128.0 mg; 1.000 mmol) and 4-(phenoxycarbonylamino) benzoic acid (257.0 mg; 1.000 mmol) were refluxed in a mixture of *N*-methylmorpholine (10.00 ml) and DMSO (5.000 ml) for five hours. After the requisite five hours, the reaction volume was reduced to 1/3 of the original volume, cooled to room temperature. To this resulting mixture 5% hydrochloric acid (20.00 ml) was added and allowed to stir at ambient temperature for a few hours. After several hours, the insoluble material was isolated by vacuum filtration, washing with water (5 x 10.00 ml) to give the crude product. This crude product may be purified by refluxing in 80% ethanol (15.00 ml) with 5 drops of concentrated hydrochloric acid for 30 minutes, before being cooled to room temperature followed by cooling on ice. The formed material was then separated by vacuum filtration, washing with water (3 x 10.00 ml) and dried at 110°C to yield the pure product (260.0 mg; 89%). ^{1}H-NMR (DMSO-d_6, Varian Inova 500 MHz) δ 12.8 (1H, s), 11.7 (1H, s), 11.6 (1H, broad s), 7.91 (2H, d, *J* = 7.00 Hz), and 7.73 (2H, d, *J* = 7.00 Hz) ppm. EMS^{-} (CH_3OH) m/z 290 (M-1). MS2 (291) m/z 291, 204, 153, 152, 136, 126, and 66.

Method D (Na_2CO_3/DMF)

Preparation of *N*-{[(4-hydroxy-3-nitrophenyl) carbamoyl] amino}-2, 4, 6-trioxo-1, 3-diazinane-5-carboxamide

Barbituric acid (256.0 mg 2.200 mmol) was sonicated with sodium bicarbonate (130.0 mg; 1.200 mmol), *N*, *N*-dimethylformamide (3.000 ml) for one hour at 60ºC. The appropriate phenyl carbamate (603.0 mg; 2.200 mmol) was added and the mixture sonicated for two hours at 60ºC and then heated via conventional heating for two hours at 130ºC. The reaction mixture was allowed to cool to room temperature before 30.00 ml of 5% hydrochloric acid was added and

continued to stir for one hour. After one hour, the solid material was separated by filtration, washing with water (3 x 30.00 ml) to give the crude product. This crude product was then refluxed in 15.00 ml of ethanol for 30 minutes, cooled to room temperature and filtered to produce the pure product (89%). ^{1}H-NMR (DMSO-d_6, Agilent 400 MHz) δ 11.2 (3H, broad s), 10.6 (1H, s), 9.42 (1H, broad s), 9.30 (1H, s), 7.87 (1H, d, J = 8.00 Hz), 7.36 (1H, d, J = 4.00 Hz), and 7.08 (1H, d of d, J_1 =8.00 Hz, J_2 = 4.00) ppm.

EMS$^-$ (CH_3OH) m/z 365 (M-1); M2 (366) m/z 366, 185 and 186.

Appendices

Appendix I: ^{1}H-NMR, ^{13}C-NMR and EMS Data for Selected Chromenopyrimidinediones

2*H*-[1]benzopyrano[2,3-*d*]pyrimidine-2,4(3*H*)-dione (CP1)

^{1}H-NMR (DMSO-d_6, Varian Mercury 300 MHz) δ11.5 (1H, s), 8.94 (1H, s), 8.07 (1H, d, J= 7.80 Hz), 7.90 (1H, t, J= 7.80 Hz), 7.71 (1H, d, J= 9.00 Hz) and 7.55 (1H, t, J= 7.50 Hz) ppm.

EMS$^-$ (CH_3CN) m/z 215 (M+1), 214 (M) and 213 (M-1); MS2 (214) 214, 213, 198, 186, 150, 135, 134, 133 and 58.

3-phenyl-2*H*-[1]benzopyrano[2,3-*d*]pyrimidine-2,4(3*H*)-dione (CP2)

^{1}H-NMR (DMSO-d_6, Varian Mercury 300 MHz) δ12.2 (1H, s), 7.44 (2H, m), 7.40 (1H, m), 7.35 (1H, d of d, J_1= 7.50 Hz and J_2= 7.50 Hz), 7.30 (1H, m), 7.25 (2H, d of d, J_1= 6.60 Hz and J_2= 7.20 Hz), 7.18 (1H, m), 7.10 (1H, d, J= 7.80 Hz) and 3.58 (2H, s) ppm.

EMS^{-} (CH_3CN) m/z 290 (M); MS2 (290) 290 and 170.

7-methoxy-2*H*-[1]benzopyrano[2,3-*d*]pyrimidine-2,4(3*H*)-dione (CP3)

^{1}H-NMR (DMSO-d_6, Varian Inova 500 MHz) δ 11.4 (1H, s), 8.89 (1H, s), 7.68 (2H, d of d, J_1= 9.00 Hz, J_2=9.00 Hz) and 7.52 (1H, d, J= 9.00 Hz) ppm.

EMS^{+} (CH_3CN) m/z 266 (M+ Na) and 244 (M); MS2 (244) m/z 245, 202, 174, 158 and 145.

7-methoxy-3-methyl-2*H*-[1]benzopyrano[2,3-*d*]pyrimidine-2,4(3*H*)-dione (CP4)

^{1}H-NMR ($CDCl_3$-TFA, Varian Inova 500 MHz) δ 9.44 (1H, s), 7.88 (1H, d, J= 9.00 Hz), 7.81 (1H, d, J= 3.00 Hz), 7.46 (1H, s), 4.03 (3H, s) and 3.53 (3H,s) ppm.

EMS^{+} (CH_3CN) m/z 258 (M); MS2 (258) m/z 257, 244, 234, 216, 202, 173, 154, 151 and 123.

9-methoxy-2*H*-[1]benzopyrano[2,3-*d*]pyrimidine-2,4(3*H*)-dione (CP5)

^{1}H-NMR (DMSO-d_6, Varian Inova500 MHz) δ 11.5 (1H, s), 8.93 (1H, s), 7.62 (1H, d of d, J_1= 11.0 Hz, J_2=12.0 Hz), 7.50 (1H, t, J =8.00 Hz) and 4.00 (3H, s) ppm.

EMS^{+} (CH_3CN) m/z 266 (M+Na) and 244 (M); MS2 (244) m/z 244 and 243.

9-methoxy-3-methyl-2*H*-[1]benzopyrano[2,3-*d*]pyrimidine-2,4(3*H*)-dione (CP6)

^{1}H-NMR ($CDCl_3$-TFA, Varian Inova 500 MHz) δ 9.25 (1H, s), 7.69 (1H, m), 7.61 (2H, m), 4.09 (3H, s) and 3.53 (3H, s) ppm.

EMS^{+} (CH_3CN) m/z 258 (M); MS2 (258) m/z 257, 154, 126 and 98.

8-methyl-2*H*-[1]benzopyrano[2,3-*d*]pyrimidine-2,4(3*H*)-dione (CP7)

^{1}H-NMR (DMSO-d_6, Varian Inova 500 MHz) δ 11.4 (1H, s), 8.92 (1H, s), 7.97 (1H, d, J= 8.00 Hz), 7.58 (1H, s) and 7.41 (1H, d, J= 8.50 Hz) ppm.

^{13}C-NMR (DMSO-d_6, Varian Inova 500 MHz) δ 168.249, 161.972, 157.201, 154.256, 149.155, 145.412, 131.602, 128.134, 117.872, 117.781, 113.438 and 22.486 ppm.

EMS^+ (CH_3CN) m/z 250 (M+ Na) and 228 (M); MS2 (228) m/z 227.

3,8-dimethyl-2*H*-[1]benzopyrano[2,3-*d*]pyrimidine-2,4(3*H*)-dione (CP8)

^{1}H-NMR ($CDCl_3$-TFA, Varian Inova 500 MHz) δ 9.399 (1H,s), 8.035 (1H, d, *J*=8.5 Hz), 7.740 (1H,s), 7.669 (1H, d, *J*= 8.0 Hz), 3.525 (3H,s) and 2.738 (3H, s) ppm.

EMS^+ (CH_3CN) m/z 242 (M); MS2 (242) m/z 242, 153, 128 and 88.

7-bromo-2*H*-[1]benzopyrano[2,3-*d*]pyrimidine-2,4(3*H*)-dione (CP9)

^{1}H-NMR (DMSO-d_6, Varian Inova 500 MHz) δ 11.5(1H, s), 8.87 (1H, s), 8.35 (1H, s), 8.06 (1H, d, *J*=9.00 Hz) and 7.71 (1H, d, *J*= 9.00 Hz) ppm.

EMS^- (CH_3CN) m/z 292 (M-1); MS2 (293) m/z 292, 96 and 81.

2*H*-benzo[5,6]chromeno[2,3-*d*]pyrimidine-2 ,4 (3*H*)dione (CP10)

^{1}H-NMR (DMSO-d_6, Varian Mercury 300 MHz) δ11.2 (1H, s), 9.51 (1H, s), 8.82 (1H, d, *J*= 8.10 Hz), 8.48 (1H, d, *J*= 9.30 Hz), 8.14 (1H, d, *J*= 7.50 Hz), 7.82 (2H, m) and 7.71 (1H, m) ppm.

EMS^- (CH_3CN) m/z 265 (M+1) and 264 (M); MS2 (264) 264, 263, 221, 177, 166, 156, 152, 134, 111, 81 and 62.

5,7-diphenyl-1,5-dihydro-2*H*-[1]benzopyrano[2,3-*d*]pyrimidine-2,4(3*H*)-dione (CP11)

^{1}H-NMR (DMSO-d_6, Varian Inova 500 MHz) δ 11.981 (1H, s), 10.983 (1H, s), 7.530 (4H, d, *J*= 3.0 Hz), 7.400 (2H, t, *J*=6.5 Hz), 7.304 (3H, m), 7.224 (3H, t, *J*= 7.5 Hz), 7.115 (1H, t, *J*= 6.0 Hz) and 5.072 (1H, s) ppm.

EMS^- (CH_3CN) m/z 368 (M) and 367 (M-1); MS2 (368) m/z 368, 325, 297 and 66.

5,7-diphenyl-2-sulfanylidene-1,2,3,5-tetrahydro-4*H*-[1]benzopyrano[2,3-*d*]pyrimidin-4-one (CP12)

^{1}H-NMR (DMSO-d_6, Varian Mercury 300 MHz) δ 12.40 (1H, s), 11.56 (1H, s), 7.55 (3H, m), 7.41 (2H, t, *J*= 6.90 Hz), 7.34 (2H, m), 7.25 (2H, m), 7.14 (1H, t, *J*= 5.70 Hz), 6.99 (1H, m) and 5.11 (1H, s) ppm.

EMS^{-} (CH_3CN) m/z 384 (M), 383 (M-1) and 382 (M-2); MS2 (384) m/z 384, 383, 325, 59 and 58.

5-phenyl-7-phenyl-1,5-dihydro-2*H*-[1]benzopyrano[2,3-*d*]pyrimidine-2,4(3*H*)-dione (CP13)

^{1}H-NMR (DMSO-d_6, Varian Mercury 300 MHz) δ 8.31 (1H, s), 8.02 (2H, d, *J*= 8.10 Hz), 7.54 (5H, m), 7.46 (3H, d, *J*= 9.00 Hz), 7.39 (3H, t, *J*= 8.40 Hz), 7.25 (1H, m), 6.83 (3H, d, *J*= 9.00 Hz), 3.22 (3H, s) and 3.16 (3H, s) ppm.

EMS^{+} (CH_3CN) m/z 493 (M+Na); MS2 (472) m/z 471, 452, 409, 377, 303, 262, 227, 133, 118, 102, 100 and 74.

5-(4-fluorophenyl)-7-phenyl-1,5-dihydro-2*H*-[1]benzopyrano[2,3-*d*]pyrimidine-2,4(3*H*)-dione (CP14)

^{1}H-NMR (DMSO-d_6, Varian Mercury 300 MHz) δ 9.027 (1H, s), 7.995 (1H, t, *J*= 6.0 Hz), 7.751 (2H, d of d, J_1= 3.0 Hz and J_2= 4.5 Hz), 7.314 (2H, m), 7.234 (1H, m) and 7.082 (2H, m) ppm.

EMS^{-} (CH_3CN) m/z 358 (M); MS2 (358) m/z 358, 316, 288, 264, 143, 67 and 66.

5-(4-fluorophenyl)-7-phenyl-2-sulfanylidene-1,2,3,5-tetrahydro-4*H*-[1]benzopyrano[2,3-*d*]pyrimidin-4-one (CP15)

^{1}H-NMR (DMSO-d_6, Varian Mercury 300 MHz) δ 13.3 (1H, broad s), 12.4 (1H, s), 7.54 (4H, m), 7.41 (3H, m), 7.35 (2H, m), 7.23 (1H, d, *J*= 8.10 Hz), 7.07 (1H, d, *J*= 8.70 Hz), 7.044 (1H, d, *J*= 9.00 Hz) and 5.14 (1H, s) ppm.

EMS$^-$ (CH_3CN) m/z 401 (M-1) and 400 (M-2); MS2 (402) m/z 402, 343, 58 and 56.

5-(2-chlorophenyl)-7-phenyl-1,5-dihydro-2*H*-[1]benzopyrano[2,3-*d*]pyrimidine-2,4(3*H*)-dione (CP16)

^{1}H-NMR (DMSO-d_6, Varian Mercury 300 MHz) δ 13.4 (1H, s), 12.4 (1H, s), 7.57 (1H, d of d, J_1= 8.10 Hz and J_2= 8.10 Hz), 7.46 (5H, m), 7.33 (1H, d, *J*= 7.20 Hz), 7.22 (2H, m) and 5.54(1H, s) ppm.

EMS$^-$ (CH_3CN) m/z 418 (M) and 416 (M-2); MS2 (418) m/z 418, 382, 359, 348, 58 and 57.

5-(2-bromophenyl)-3-methyl-7-phenyl-1,5-dihydro-2*H*-[1]benzopyrano[2,3-*d*]pyrimidine-2,4(3*H*)-dione (CP18)

^{1}H-NMR (DMSO-d_6, Varian Mercury 300 MHz) δ 13.5 (1H, broad s), 12.4 (1H, s), 7.57 (2H, d, *J*= 7.50 Hz), 7.45 (5H, m), 7.37 (2H, m), 7.29 (1H, m), 7.23 (1H, d, *J*= 8.70 Hz), 7.11 (1H, t, *J*= 8.70 Hz) and 5.56 (1H, s) ppm.

EMS$^-$ (CH_3CN) m/z 463 (M), 462 (M-1) and 461 (M-2); MS2 (463) m/z 463, 404, 381, 81, 60 and 58.

5-(3-bromophenyl)-7-phenyl-2-sulfanylidene-1,2,3,5-tetrahydro-4*H*-[1]benzopyrano[2,3-*d*]pyrimidin-4-one (CP19)

^{1}H-NMR (DMSO-d_6, Varian Mercury 300 MHz) δ 13.5 (1H, broad s), 12.4 (1H, s), 7.06 (1H, m), 7.55 (4H, m), 7.42 (3H, m), 7.33 (2H, m), 7.27 (1H, d, *J*= 8.70 Hz), 7.22 (1H, d, *J*= 7.50 Hz) and 5.13 (1H, s) ppm.

EMS$^-$ (CH_3CN) m/z 463 (M), 462 (M-1) and 461 (M-2); MS2 (463) m/z 463, 404, 60 and 58.

5-(2,3-dichlorophenyl)-1,3-dimethyl-7-phenyl-1,5-dihydro-2*H*-[1]benzopyrano[2,3-*d*]pyrimidine-2,4(3*H*)-dione (CP21)

^{1}H-NMR (DMSO-d_6, Varian Mercury 300 MHz) δ 8.31 (1H, s), 7.69 (1H, d, *J*= 8.70 Hz), 7.55 (3H, d, *J*= 8.10 Hz), 7.46 (3H, m), 7.39 (3H, t, *J*= 8.40 Hz), 7.25 (1H, m), 6.83 (2H, d of d, J_1= 3.00 Hz and J_2= 2.40 Hz), 3.23 (3H, s) and 3.09 (3H, s) ppm.

EMS^{+} (CH_3CN) m/z 488 (M+Na) and 466 (M+1); MS2 (465) m/z 465, 423, 408, 319, 262 and 74.

5-(2,3-dichlorophenyl)-1,3-dimethyl-7-phenyl-2-sulfanylidene-1,2,3,5-tetrahydro-4*H*-[1]benzopyrano[2,3-*d*]pyrimidin-4-one (CP22)

^{1}H-NMR (DMSO-d_6, Varian Mercury 300 MHz) δ 13.5 (1H, broad s), 12.4 (1H, s), 7.58 (1H, d of d, J_1= 9.00 Hz and J_2= 9.00 Hz), 7.48 (3H, m), 7.42 (3H, m), 7.33 (2H, m), 7.28 (1H, d, *J*= 7.50 Hz), 7.25 (1H, d, *J*= 9.00 Hz) and 5.62 (1H, s) ppm.

EMS^{-} (CH_3CN) m/z 453 (M), 452 (M-1) and 451 (M-2); MS2 (453) m/z 453, 417, 394, 356, 246, 60 and 58.

5-(2,4-dichlorophenyl)-1,3-dimethyl-7-phenyl-1,5-dihydro-2*H*-[1]benzopyrano[2,3-*d*]pyrimidine-2,4(3*H*)-dione (CP24)

^{1}H-NMR (DMSO-d_6, Varian Mercury 300 MHz) δ 8.28 (1H, s), 7.74 (1H, s), 7.68 (1H, d, *J*= 8.70 Hz), 7.55 (2H, d of d, J_1= 1.20 Hz and J_2= 1.00 Hz), 7.47 (3H, m), 7.36 (2H, t, *J*= 15.3 Hz), 7.28 (1H, m), 6.83 (2H, d of d, J_1= 1.80 Hz and J_2= 1.80 Hz), 3.32 (3H, s) and 3.11 (3H, s) ppm.

EMS^{+} (CH_3CN) m/z 467 (M+2) and 466 (M+1); MS2 (465) m/z 465, 423, 408, 319, 262, 235, 111 and 97.

5-(3,4-dichlorophenyl)-7-phenyl-2-sulfanylidene-1,2,3,5-tetrahydro-4*H*-[1]benzopyrano[2,3-*d*]pyrimidin-4-one (CP27)

^{1}H-NMR (DMSO-d_6, Varian Mercury 300 MHz) δ 13.3 (1H, broad s), 12.4 (1H, s), 7.71 (1H, s), 7.56 (5H, m), 7.48 (1H, s), 7.43 (2H, t, *J*= 8.70 Hz), 7.33 (2H, t, *J*= 9.30 Hz), 7.25 (1H, d, *J*= 8.40 Hz) and 5.17 (1H, s) ppm.

EMS^{-} (CH_3CN) m/z 453 (M), 452 (M-1) and 451 (M-2); MS2 (453) m/z 453, 394, 60 and 58.

5-(3-nitrophenyl)-7-phenyl-2-sulfanylidene-1,2,3,5-tetrahydro-4*H*-[1]benzopyrano[2,3-*d*]pyrimidin-4-one (CP28)

^{1}H-NMR (DMSO-d_6, Varian Mercury 300 MHz) δ 13.6 (1H, broad s), 12.4 (1H, s), 8.25 (1H, s), 8.02 (1H, d of d, J_1= 8.10 Hz and J_2= 5.10 Hz), 7.77 (1H, d, *J*= 8.10 Hz), 7.56 (5H, m), 7.42 (1H, d, *J*= 7.20 Hz), 7.40 (1H, d, *J*= 8.10 Hz), 7.33 (1H, d, *J*= 7.20 Hz), 7.28 (1H, d, *J*= 8.70 Hz) and 5.33 (1H, s) ppm.

EMS^{-} (CH_3CN) m/z 428 (M-1) and 427 (M-2); MS2 (429) m/z 429, 428, 370 and 58.

5-(4-nitrophenyl)-7-phenyl-2-sulfanylidene-1,2,3,5-tetrahydro-4*H*-[1]benzopyrano[2,3-*d*]pyrimidin-4-one (CP29)

^{1}H-NMR (DMSO-d_6, Varian Mercury 300 MHz) δ 13.3 (1H, broad s), 12.5 (1H, s), 8.11 (2H, d, *J*= 8.70 Hz), 7.66 (3H, d, *J*= 8.70 Hz), 7.54 (5H, m), 7.41 (3H, t, *J*= 7.80 Hz), 7.33 (1H, d, *J*= 7.20 Hz), 7.26 (1H, d, *J*= 7.20 Hz) and 5.31 (1H, s) ppm.

EMS^{-} (CH_3CN) m/z 429 (M), 428 (M-1) and 427 (M-2); MS2 (429) m/z 429, 370, 343, 169, 59 and 58.

5-(4-hydroxy-3-methoxyphenyl)-7-phenyl-2-sulfanylidene-1,2,3,5-tetrahydro-4*H*-[1]benzopyrano[2,3-*d*]pyrimidin-4-one (CP30)

^{1}H-NMR (DMSO-d_6, Varian Mercury 300 MHz) δ 13.3 (1H, broad s), 12.3 (1H, s), 9.63 (1H, s), 7.51 (2H, m), 7.39 (3H, m), 7.28 (2H, m), 7.01 (1H, m), 6.92 (1H, d, *J*= 8.10 Hz), 6.85 (1H, d, *J*= 7.50 Hz), 6.75 (1H, d, *J*= 8.40 Hz), 5.19 (1H, s) and 3.82 (3H, s) ppm.

EMS^{-} (CH_3CN) m/z 429 (M-1) and 428 (M-2); MS2 (430) m/z 430, 307, 261, 260, 169, 123 and 58.

5-(3,4,5-trimethoxyphenyl)-7-phenyl-2-sulfanylidene-1,2,3,5-tetrahydro-4*H*-[1]benzopyrano[2,3-*d*]pyrimidin-4-one (CP31)

^{1}H-NMR (DMSO-d_6, Varian Mercury 300 MHz) δ 13.4 (1H, broad s), 12.4 (1H, s), 7.64 (1H, s), 7.57 (3H, d, *J*= 7.50 Hz), 7.43 (2H, t, *J*= 6.90 Hz), 7.33 (1H, m), 7.23 (1H, d, *J*= 8.10 Hz), 6.60 (2H, s), 5.05 (1H, s), 3.70 (6H, s) and 3.56 (3H, s) ppm.

EMS^{-} (CH_3CN) m/z 474 (M), 473 (M-1) and 472 (M-2); MS2 (474) m/z 474, 459, 444, 58 and 57.

5-phenyl-1,5-dihydro-2*H*-benzo[5,6]chromeno[2,3-*d*]pyrimidine-2,4(3*H*)-dione (CP32)

^{1}H-NMR (DMSO-d_6, Varian Inova 500 MHz) δ 12.0 (1H, s), 11.0 (1H, s), 7.98 (1H, d, *J*= 7.00 Hz), 7.94 (1H, d, *J*= 7.50 Hz), 7.91 (1H, d, *J*= 7.00 Hz), 7.47 (1H, t, *J*= 6.00 Hz), 7.41 (2H, t, *J*= 4.00 Hz), 7.28 (2H, d, *J*=6.50 Hz), 7.16 (2H, d, *J*= 6.50 Hz), 7.05 (1H, t, *J*= 5.50 Hz) and 5.55 (1H, s) ppm.

EMS^{+} (CH_3CN) m/z 364 (M+Na) and 343 (M+1).

5-(4-fluorophenyl)-1,5-dihydro-2*H*-benzo[5,6]chromeno[2,3-*d*]pyrimidine-2,4(3*H*)-dione (CP33)

^{1}H-NMR (DMSO-d_6, Varian Mercury 300 MHz) δ 12.1 (1H, s), 11.1 (1H, s), 7.95 (3H, m), 7.47 (3H, m), 7.33 (2H, m), 7.01 (2H, m) and 6.00 (1H, s) ppm.

EMS^{-} (CH_3CN) m/z 360 (M) and 359 (M-1); MS2 (360) m/z 360, 359, 317, 316, 289, 261, 133, 113, 67 and 66.

5-(4-fluorophenyl)-2-sulfanylidene-1,2,3,5-tetrahydro-2*H*-benzo[5,6]chromeno [2,3-*d*]pyrimidin-4-one (CP34)

^{1}H-NMR (DMSO-d_6, Varian Mercury 300 MHz) δ 13.5 (1H, broad s), 12.4 (1H, s),7.96 (3H, m), 7.47 (3H, m), 7.35 (1H, d, *J*= 8.10 Hz), 7.32 (1H, d, *J*= 8.40 Hz), 7.01 (2H, t, *J*= 8.70 Hz) and 5.63 (1H, s) ppm.

EMS^{-} (CH_3CN) m/z 375 (M-1) and 374 (M-2); MS2 (376) m/z 376, 59 and 58.

5-(4-chlorophenyl)-1,5-dihydro-2*H*-benzo[5,6]chromeno[2,3-*d*]pyrimidine-2,4(3*H*)-dione (CP35)

^{1}H-NMR (DMSO-d_6, Varian Inova 500 MHz) δ 12.1 (1H, broad s), 11.1 (1H, s), 7.98 (3H, m), 7.49 (3H, m), 7.34 (2H, d, *J*= 8.50 Hz), 7.26 (2H, d, *J*= 8.50 Hz) and 5.62 (1H, s) ppm.

EMS^{-} (CH_3CN) m/z 376 (M), 374 (M-2); MS2 (376) m/z 376, 332 and 66.

5-(4-chlorophenyl)-3-methyl-1,5-dihydro-2*H*-benzo[5,6]chromeno[2,3-*d*]pyrimidine-2,4-dione (CP36)

^{1}H-NMR (DMSO-d_6, Varian Inova 500 MHz) δ 12.4 (1H, broad s), 7.40 (3H, m), 7.45 (3H, m), 7.32 (2H, d, *J*= 8.00 Hz), 7.22 (2H, d, *J*=8.00 Hz), 5.59 (1H, s) and 3.08 (3H, s) ppm.

^{13}C-NMR (DMSO-d_6, Varian Inova 500 MHz) δ 162.919, 152.825, 150.434, 147.266, 144.091, 131.925, 131.716, 130.940, 130.782, 130.577, 129.328, 128.834, 128.138, 126.043, 124.278, 117.382, 117.104, 89.534 and 35.348 ppm.

EMS^{-} (CH_3CN) m/z 390 (M), 389 (M-1); MS2 (390) m/z 390, 319, 278, 189, 167 and 80.

5-(4-chlorophenyl)-2-sulfanylidene-1,2,3,5-tetrahydro-2*H*-benzo[5,6]chromeno [2,3-*d*]pyrimidin-4-one (CP38)

^{1}H-NMR (DMSO-d_6, Varian Mercury 300 MHz) δ 13.6 (1H, broad s), 12.4 (1H, s), 7.97 (2H, t, *J*= 9.30 Hz), 7.94 (2H, d, *J*= 6.90 Hz), 7.49 (1H, m), 7.42 (1H, d, *J*= 9.00 Hz), 7.32 (2H, d, *J*= 9.00 Hz), 7.27 (2H, d, *J*= 9.00 Hz) and 5.62 (1H, s) ppm.

EMS^{-} (CH_3CN) m/z 392(M), 391 (M-1) and 390 (M-2); MS2 (392) m/z 392, 333, 58 and 57.

5-(2,3-dichlorophenyl)-1,5-dihydro-2*H*-benzo[5,6]chromeno[2,3-*d*]pyrimidine-2,4(3*H*)-dione (CP39)

^{1}H-NMR (DMSO-d_6, Varian Inova 500 MHz) δ 12.1 (1H, s), 11.0 (1H, s), 7.90 (4H, m), 7.47 (1H, t, *J*= 6.50 Hz), 7.41 (1H, t, *J*=6.00 Hz), 7.36 (3H, m), 7.16 (1H, s) and 5.86 (1H,s) ppm.

^{13}C-NMR (DMSO-d_6, Varian Inova 500 MHz) δ 163.524, 154.927, 150.202, 147.502, 132.846, 131.975, 131.266, 131.002, 131.000, 130.981, 129.691, 129.398, 129.321, 128.627, 128.244, 126.004, 125.984, 124.956, 124.872, 117.648 and 117.233 ppm.

EMS^{-} (CH_3CN) m/z 411 (M), 410 (M-1), 109 (M-2); MS2 (411) m/z 411, 332, 263, 220, 192, 147 and 66.

5-(2,3-dichlorophenyl)-3-methyl-1,5-dihydro-2*H*-benzo[5,6]chromeno[2,3-*d*]pyrimidine-2,4-dione (CP40)

^{1}H-NMR (DMSO-d_6, Varian Inova 500 MHz) δ 12.9 (1H, broad s), 7.95 (3H, m), 7.50 (1H, t, *J*= 6.00 Hz), 7.43 (1H, m), 7.37 (2H, t, *J*= 7.00 Hz), 7.16 (1H, t, *J*=6.00 Hz), 5.93 (1H, s) and 3.04 (3H,s) ppm.

EMS^{+} (CH_3CN) m/z 424 (M-1); MS2 (425) m/z 422 and 381.

5-(2,3-dichlorophenyl)-2-sulfanylidene-1,2,3,5-tetrahydro-2*H*-benzo[5,6]chromeno [2,3-*d*]pyrimidin-4-one (CP42)

^{1}H-NMR (DMSO-d_6, Varian Mercury 300 MHz) δ 13.6 (1H, broad s), 12.4 (1H, s), 7.97 (2H, t, *J*= 8.70 Hz), 7.96 (2H, d, *J*= 6.30 Hz), 7.52 (1H, t, *J*= 7.20 Hz), 7.46 (1H, d, *J*= 7.20 Hz), 7.41 (2H, t, *J*= 8.70 Hz), 7.19 (1H, t, *J*= 7.80 Hz) and 5.95 (1H, s) ppm.

EMS^{-} (CH_3CN) m/z 427(M) and 425 (M-2); MS2 (427) m/z 427, 391, 330, 60 and 58.

5-(2,4-dichlorophenyl)-1,5-dihydro-2*H*-benzo[5,6]chromeno[2,3-*d*]pyrimidine-2,4(3*H*)-dione (CP43)

^{1}H-NMR (DMSO-d_6, Varian Inova 500 MHz) δ 12.1 (1H, s), 11.0 (1H, s), 7.92 (3H, m), 7.47(1H, t, *J*= 6.50 Hz), 7.41 (2H, m), 7.35 (2H, d, *J*= 7.50 Hz), 7.22 (1H, d, *J*= 7.00 Hz) and 5.79 (1H, s) ppm.

EMS^{-} (CH_3CN) m/z 411 (M); MS2 (411) m/z 411, 375, 368, 332, 302, 263, 220, 192, 147 and 66.

5-(2,4-dichlorophenyl)-3-methyl-1,5-dihydro-2*H*-benzo[5,6]chromeno[2,3-*d*]pyrimidine-2,4-dione (CP44)

^{1}H-NMR (DMSO-d_6, Varian Inova 500 MHz) δ 12.3 (1H, broad s), 7.89 (3H, m), 7.42 (3H, m), 7.31 (2H, m), 7.18 (1H, d, *J*=7.00 Hz), 5.75 (1H, s) and 3.04 (1H, s) ppm.

EMS^{+} (CH_3CN) m/z 424 (M-1); MS2 (425) m/z 422, 386, 347, 329, 322, 300, 266, 238 and 232.

5-(2,4-dichlorophenyl)-2-sulfanylidene-1,2,3,5-tetrahydro-2*H*-benzo[5,6]chromeno [2,3-*d*]pyrimidin-4-one (CP45)

^{1}H-NMR (DMSO-d_6, Varian Mercury 300 MHz) δ 13.6 (1H, broad s), 12.4 (1H, s), 7.97 (3H, m), 7.48 (4H, m), 7.39 (1H, d of d, J_1= 8.70 Hz and J_2= 9.60 Hz), 7.26 (1H, d, *J*= 8.10 Hz) and 5.86 (1H, s) ppm.

EMS^{-} (CH_3CN) m/z 427(M) and 426 (M-1); MS2 (427) m/z 427, 391, 330, 60 and 58.

5-(3,4-dichlorophenyl)-1,5-dihydro-2*H*-benzo[5,6]chromeno[2,3-*d*]pyrimidine-2,4(3*H*)-dione (CP46)

^{1}H-NMR (DMSO-d_6, Varian Inova 500 MHz) δ 12.1 (1H, broad s), 11.1 (1H, s), 7.94 (3H, m), 7.63 (1H, s), 7.44 (4H, m), 7.14 (1H, d, *J*= 7.00Hz) and 5.62 (1H,s) ppm.

EMS$^-$ (CH_3CN) m/z 410 (M-1); MS2 (411) m/z 411, 368, 340, 264, 143 and 66.

5-(3,4-dichlorophenyl)-3-methyl-5-hydro-2*H*-benzo[5,6]chromeno[2,3-*d*]pyrimidine-2,4-dione (CP47)

^{1}H-NMR (DMSO-d_6, Varian Inova 500 MHz) δ 12.5 (1H, broad s), 7.93 (3H, m), 7.62 (1H, s), 7.47 (1H, t, *J*= 6.50 Hz), 7.40 (3H, m), 7.17 (1H, d, *J*=7.00 Hz), 5.62 (1H, s) and 3.07 (3H, s) ppm.

EMS$^+$ (CH_3CN) m/z 424 (M-1); MS2 (425) m/z 422 and 380.

5-(3,4-dichlorophenyl)-2-sulfanylidene-1,2,3,5-tetrahydro-2*H*-benzo[5,6]chromeno [2,3-*d*]pyrimidin-4-one (CP49)

^{1}H-NMR (DMSO-d_6, Varian Mercury 300 MHz) δ 13.6 (1H, broad s), 12.5 (1H, s), 7.98 (3H, m), 7.68 (1H, s), 7.48 (2H, m), 7.42 (2H, d, *J*= 8.40 Hz), 7.18 (1H, d of d, J_1= 8.10 Hz and J_2= 8.10 Hz) and 5.67 (1H, s) ppm.

EMS$^-$ (CH_3CN) m/z 427(M) and 426 (M-1); MS2 (427) m/z 42, 60 and 58.

5-(2,4,6-trichlorophenyl)-2-sulfanylidene-1,2,3,5-tetrahydro-2*H*-benzo[5,6]chromeno [2,3-*d*]pyrimidin-4-one (CP50)

^{1}H-NMR (DMSO-d_6, Varian Inova 500 MHz) δ 12.1 (1H,s), 11.0 (1H, s), 7.94 (2H, d of d, J_1= 7.00 Hz, J_2= 6.50 Hz), 7.80 (1H, d of d, J_1= 7.00 Hz, J_2= 7.00 Hz), 7.45 (3H, m), 7.29 (1H, t, *J*=8.00 Hz), 6.29 (1H, d of d, J_1= 4.50 Hz, J_2= 3.50 Hz) and 4.31 (1H, s) ppm.

^{13}C-NMR (DMSO-d_6, Varian Inova 500 MHz) δ 163.364, 155.162, 155.012, 150.163, 148.555, 148.453, 139.304, 135.767, 133.437, 131.811, 131.412, 131.258, 130.346, 129.702, 128.156, 125.853, 123.630, 123.542, 117.085, 113.907 and 86.215 ppm.

EMS$^-$ (CH_3CN) m/z 443 (M-2); MS2 (445) m/z 445, 409, 366, 263 and 181.

5-(2-bromophenyl)-2-sulfanylidene-1,2,3,5-tetrahydro-2*H*-benzo[5,6]chromeno [2,3-*d*]pyrimidin-4-one (CP51)

^{1}H-NMR (DMSO-d_6, Varian Mercury 300 MHz) δ 13.6 (1H, broad s), 12.4 (1H, s), 8.09 (1H, d, *J*= 7.50 Hz), 7.98 (1H, d, *J*= 8.70 Hz), 7.94 (1H, d, *J*= 8.70 Hz), 7.48 (3H, m), 7.39 (1H, d, *J*= 8.70 Hz), 7.29 (1H, broad s), 7.20 (1H, t, *J*= 7.20 Hz), 7.04 (1H, t, *J*= 8.00 Hz) and 5.84 (1H, s) ppm.

EMS$^-$ (CH_3CN) m/z 437(M), 436 (M-1) and 435 (M-2); MS2 (437) m/z 437, 355, 81, 79, 60 and 58.

5-(3-bromophenyl)-2-sulfanylidene-1,2,3,5-tetrahydro-2*H*-benzo[5,6]chromeno [2,3-*d*]pyrimidin-4-one (CP52)

^{1}H-NMR (DMSO-d_6, Varian Mercury 300 MHz) δ 13.6 (1H, broad s), 12.5 (1H, s), 7.98 (3H, m), 7.87 (1H, s), 7.84 (2H, m), 7.43 (1H, d, *J*= 8.70 Hz), 7.30 (1H, d, *J*= 9.30 Hz), 7.21 (1H, t, *J*= 7.50 Hz), 7.14 (1H, t, *J*= 8.40 Hz) and 5.64 (1H, s) ppm.

EMS$^-$ (CH_3CN) m/z 437 (M), 436 (M-1) and 435 (M-2); MS2 (437) m/z 437, 60 and 58.

5-(3-hydroxyphenyl)-2-sulfanylidene-1,2,3,5-tetrahydro-2*H*-benzo[5,6]chromeno [2,3-*d*]pyrimidin-4-one (CP53)

^{1}H-NMR (DMSO-d_6, Varian Mercury 300 MHz) δ 13.6 (1H, broad s), 12.4 (1H, s), 9.26 (1H, s), 7.96 (3H, m), 7.48 (2H, m), 7.42 (1H, d, *J*= 9.00 Hz), 6.98 (1H, t, *J*= 7.50 Hz), 6.75 (1H, d, *J*= 7.80 Hz), 6.63 (1H, s), 6.56 (1H, d of d, J_1= 7.50 Hz and J_2= 7.50 Hz) and 5.50 (1H, s) ppm.

EMS$^-$ (CH_3CN) m/z 374 (M), 373 (M-1) and 372 (M-2); MS2 (374) m/z 374, 58 and 57.

5-(3-nitrophenyl)-2-sulfanylidene-1,2,3,5-tetrahydro-2*H*-benzo[5,6]chromeno [2,3-*d*]pyrimidin-4-one (CP54)

^{1}H-NMR (DMSO-d_6, Varian Mercury 300 MHz) δ 13.6 (1H, broad s), 12.5 (1H, s), 8.18 (1H, s), 8.03 (1H, d, *J*= 8.70 Hz), 7.97 (3H, m), 7.75 (1H, d, *J*= 8.40 Hz), 7.46 (4H, m) and 5.83 (1H, s) ppm.

EMS$^-$ (CH_3CN) m/z 403 (M), 402 (M-1) and 401 (M-2); MS2 (403) m/z 403, 402, 344, 66, 59, 58 and 57.

5-(4-nitrophenyl)-2-sulfanylidene-1,2,3,5-tetrahydro-2*H*-benzo[5,6]chromeno [2,3-*d*]pyrimidin-4-one (CP55)

^{1}H-NMR (DMSO-d_6, Varian Mercury 300 MHz) δ 13.6 (1H, broad s), 12.5 (1H, s), 8.04 (3H, m), 7.96 (2H, m), 7.62 (2H, d, *J*= 8.40 Hz), 7.47 (3H, m) and 5.79 (1H, s) ppm.

EMS$^-$ (CH_3CN) m/z 403 (M), 402 (M-1) and 401 (M-2); MS2 (403) m/z 403, 344, 58 and 57.

5-(4-pyridinyl)-2-sulfanylidene-1,2,3,5-tetrahydro-2*H*-benzo[5,6]chromeno [2,3-*d*]pyrimidin-4-one (CP56)

^{1}H-NMR (DMSO-d_6, Varian Mercury 300 MHz) δ 13.5 (1H, broad s), 12.4 (1H, s), 8.02 (1H, d, *J*= 8.70 Hz), 7.96 (1H, d, *J*= 9.00 Hz), 7.92 (1H, d, *J*= 8.40 Hz), 7.47 (2H, m), 7.31 (1H, d of d, J_1= 7.50 Hz and J_2= 7.50 Hz), 7.15 (2H, m) and 5.84 (1H, s) ppm.

EMS$^+$ (CH_3CN) m/z 359 (M); MS2 (359) m/z 359, 281, 235, 149, 118 and 102.

5-(3-methoxy-5-bromophenyl)-2-sulfanylidene-1,2,3,5-tetrahydro-2*H*-benzo[5,6]chromeno [2,3-*d*]pyrimidin-4-one (CP57)

^{1}H-NMR (DMSO-d_6, Varian Mercury 300 MHz) δ 13.5 (1H, broad s), 12.4 (1H, s), 8.09 (1H, d, *J*= 9.00 Hz), 7.93 (1H, d, *J*= 8.70 Hz), 7.91 (1H, d, *J*= 8.10 Hz), 7.54 (1H, s), 7.51 (2H, m), 7.36 (1H, d, *J*= 9.30 Hz), 7.27 (1H, d of d, J_1= 8.70 Hz and J_2= 8.70 Hz), 6.86 (1H, d, *J*= 8.70 Hz), 5.72 (1H, s) and 3.69 (3H, s) ppm.

EMS$^-$ (CH_3CN) m/z 467 (M), 466 (M-1) and 465 (M-2); MS2 (467) m/z 467, 408, 60 and 58.

5-(3, 4, 5-trimethoxyphenyl)-2-sulfanylidene-1,2,3,5-tetrahydro-2*H*-benzo[5,6]chromeno [2,3-*d*]pyrimidin-4-one (CP58)

^{1}H-NMR (DMSO-d_6, Varian Mercury 300 MHz) δ 13.3 (1H, broad s), 12.4 (1H, s), 7.64 (1H, s), 7.57(3H, d, *J*= 7.50 Hz), 7.43 (2H, t, *J*= 6.90 Hz), 7.33 (1H, m), 7.23 (1H, d, *J*= 8.10 Hz), 6.60 (2H, s), 5.05 (1H, s), 3.70 (6H, s) and 3.56 (3H, s) ppm.

EMS$^-$ (CH_3CN) m/z 474 (M), 472 (M-2); MS2 (474) m/z 474, 459, 444, 58 and 57.

Appendix II: ^{1}H-NMR and EMS Data for Selected *N*-Alkylated Pyrimidinequinolinediones

7,10-dimethylpyrimido[4,5-*b*]quinoline-2,4(3*H*,10*H*)-dione (AQ1)

^{1}H-NMR (DMSO-d_6, Varian Mercury 300 MHz) δ 11.0 (1H, s), 8.94 (1H, s), 7.89 (1H, d, *J*= 9.30 Hz), 7.73 (1H, s), 7.60 (1H, d, *J*= 9.30 Hz), 4.03 (3H, s) and 3.87 (3H, s) ppm.

EMS$^-$(CH_3CN) m/z 278 (M+Na) and 278 (M+K) and 263 (M+Na); MS2 (241) m/z 241, 223, 209, 197, 153, 154, 98, 97, 83, 81, 79, 69 and 59.

7,8,10-trimethylpyrimido[4,5-*b*]quinoline-2,4(3*H*,10*H*)-dione (AQ2)

^{1}H-NMR (DMSO-d_6, Varian Mercury 300 MHz) δ 11.0 (1H, s), 8.85 (1H, s), 7.90 (1H, s), 7.77 (1H, s), 4.03 (3H, s), 3.19 (3H, s) and 2.35 (3H, s) ppm.

EMS$^+$(CH_3CN) m/z 278 (M+Na) and 255 (M); MS2(256) 256, 213, 212, 185, 170 and 156.

7-chloro-10-methylpyrimido[4,5-*b*]quinoline-2,4(3*H*,10*H*)-dione (AQ3)

^{1}H-NMR (DMSO-d_6, Varian Mercury 300 MHz) δ 11.1 (1H, s), 8.96 (1H, s), 8.31 (1H, s), 7.96 (1H, s), 7.95 (1H, s) and 4.01 (3H, s) ppm.

EMS$^+$(CH_3CN) m/z 284 (M+Na) and 262 (M); MS2(262) 262, 261, 244, 237, 219, 218, 191, 176, 164 and 156.

7-bromo-10-methylpyrimido[4,5-*b*]quinoline-2,4(3*H*,10*H*)-dione (AQ4)

^{1}H-NMR (DMSO-d_6, Varian Mercury 300 MHz) δ 11.1 (1H, s), 9.93 (1H, s), 8.44 (1H, s), 8.05 (1H, d of d, J_1= 8.70 Hz and J_2= 8.70 Hz), 7.86 (1H, d, J= 9.30 Hz) and 3.99 (3H, s) ppm.

EMS$^+$(CH_3CN) m/z 307 (M+1) and 306 (M); MS2(307) 306, 263, 262, 250, 235, 221, 220, 208, 206, 180 and 156.

12-methylbenzo[*f*]pyrimido[4,5-*b*]quinoline-2,4(3*H*) dione (AQ5)

^{1}H-NMR (DMSO-d_6, Varian Mercury 300 MHz) δ 11.1 (1H, s), 9.60 (1H, s), 8.82 (1H, d, J= 7.80 Hz), 8.48 (1H, d, J= 9.90 Hz), 8.12 (2H, t, J= 8.40 Hz), 7.82 (1H, m), 7.73 (1H, m) and 4.18 (3H, s) ppm.

EMS$^+$(CH_3CN) m/z 278 (M+1) and 277 (M); MS2(278) 278, 277, 276, 262, 191 and 139.

12-butylbenzo[*f*]pyrimido[4,5-*b*]quinoline-2,4(3*H*) dione (AQ6)

^{1}H-NMR (DMSO-d_6, Varian Mercury 300 MHz) δ 11.1 (1H, s), 9.60 (1H, s), 8.83 (1H, d, *J*= 8.70 Hz), 8.46 (1H, d, *J*= 9.60 Hz), 8.11 (2H, t, *J*= 9.90 Hz), 7.82 (1H, t, *J*= 7.50 Hz), 7.71 (1H, t, *J*= 6.90 Hz), 4.82 (2H, broad s), 1.75 (2H, m), 1.49 (2H, m) and 0.973 (3H, m) ppm.

EMS^{+} (CH_3CN) m/z 321 (M+2) and 319 (M); MS2 (320) 319, 291, 277, 263, 134, 124 and 68.

5-(3-hydroxyphenyl)-7-methoxy-10-methylpyrimido[4,5-*b*]quinoline-2,4(3*H*,10*H*)-dione (AQ7)

^{1}H-NMR (DMSO-d_6, Varian Mercury 300 MHz) δ 10.7 (1H, s), 9.57 (1H, s), 7.96 (1H, d, *J*= 10.2 Hz), 7.62 (1H, d of d, J_1= 9.60 Hz and J_2= 9.30 Hz), 7.29 (1H, t, *J*= 8.10 Hz), 6.61 (3H, m), 4.10 (3H, s), and 3.63 (3H, s) ppm.

EMS^{+} (CH_3CN) m/z 350 (M+1) and 349 (M); MS2 (350) 349, 348, 332, 319, 306, 305, 291, 278, 268 and 258.

5-(3-methoxy-4-hydroxyphenyl)-7-methoxy-10-methylpyrimido[4,5-*b*]quinoline-2,4(3*H*,10*H*)-dione (AQ8)

^{1}H-NMR (DMSO-d_6, Varian Mercury 300 MHz) δ 10.7 (1H, s), 9.22 (1H, s), 7.92 (1H, d, *J*= 9.60 Hz), 7.58 (1H, d, *J*=9.30 Hz), 6.87 (1H, d, *J*= 8.10 Hz), 6.80 (1H, s), 6.72 (1H, s), 6.61 (1H, d, *J*= 9.20 Hz), 4.07 (3H, s), 3.69 (3H, s) and 3.6 (3H, s) ppm.

EMS^{+} (CH_3CN) m/z 379 (M); MS2 (380) 379.

5-(3,4-dimethoxyphenyl)-7-methoxy-10-methylpyrimido[4,5-*b*]quinoline-2,4(3*H*,10*H*)-dione (AQ9)

^{1}H-NMR (DMSO-d_6, Varian Mercury 300 MHz) δ 10.7 (1H, s), 7.94 (1H, d, *J*= 9.30 Hz), 7.11 (1H, d of d, J_1= 9.30 Hz and J_2= 9.30 Hz), 6.60 (2H, d, *J*= 8.10 Hz), 6.38 (2H, s), 4.09 (3H, s), 3.73 (6H, s) and 3.64 (3H, s) ppm.

EMS^{+} (CH_3CN) m/z 394 (M+1) and 393 (M); MS2 (393) 393, 347 and 332.

5-(4-methoxyphenyl)-7-methoxy-10-methylpyrimido[4,5-*b*]quinoline-2,4(3*H*,10*H*)-dione (AQ10)

^{1}H-NMR (DMSO-d_6, Varian Mercury 300 MHz) δ 10.7 (1H, s), 7.94 (1H, d, *J*= 9.30 Hz), 7.60 (1H, d of d, J_1= 9.30 Hz and J_2= 9.30 Hz), 7.15 (2H, d, *J*= 8.70 Hz), 7.04 (2H, d, *J*= 9.00 Hz), 6.63 (1H, s), 4.09 (3H, s), 3.83 (3H, s) and 3.62 (3H, s) ppm.

EMS^+ (CH_3CN) m/z 364 (M+1) and 363 (M); MS2 (364) 363, 362, 348, 319 and 305.

5-(4-methylphenyl)-7-methoxy-10-methylpyrimido[4,5-*b*]quinoline-2,4(3*H*,10*H*)-dione (AQ11)

^{1}H-NMR (DMSO-d_6, Varian Mercury 300 MHz) δ 10.7 (1H, s), 7.97 (1H, d, *J*= 9.30 Hz), 7.62 (1H, d, *J*= 9.90 Hz), 7.31 (2H, d, *J*= 8.10 Hz), 7.12 (2H, d, *J*= 8.40 Hz), 6.58 (1H, s), 4.11 (3H, s), 3.63 (3H, s) and 2.43 (3H, s) ppm.

EMS^+ (CH_3CN) m/z 385 (M+Na); MS2 (364) 363, 333, 320 and 317.

5-(1-naphthyl)-7-methoxy-10-methylpyrimido[4,5-*b*]quinoline-2,4(3*H*,10*H*)-dione (AQ12)

^{1}H-NMR (DMSO-d_6, Varian Mercury 300 MHz) δ 10.7 (1H, s), 8.02 (3H, m), 7.59 (2H, m), 7.48 (1H, m), 7.31 (3H, m), 7.23 (1H, s), 4.16 (3H, s) and 3.43 (3H, s) ppm.

EMS^+ (CH_3CN) m/z 384 (M+1) and 383 (M); MS2 (384) 383, 382 and 367.

5-(4-biphenyl)-7-methoxy-10-methylpyrimido[4,5-*b*]quinoline-2,4(3*H*,10*H*)-dione (AQ13)

^{1}H-NMR (DMSO-d_6, Varian Mercury 300 MHz) δ 10.76 (1H, s), 7.97 (1H, d, *J*= 9.3 Hz), 7.80 (4H, m), 7.64 (1H, d of d, J_1= 6.00 Hz and J_2= 6.00 Hz), 7.50 (2H, t, *J*= 6.90 Hz), 7.40 (1H, d, *J*= 7.50 Hz), 7.32 (2H, d, *J*= 8.10 Hz), 6.60 (1H, s), 4.11 (3H, s) and 3.61 (3H, s) ppm.

EMS^+ (CH_3CN) m/z 410 (M+1) and 409 (M); MS2 (410) 409, 408, 394, 367, 365, 332, 86 and 67.

5-phenyl-7-methoxy-10-methylpyrimido[4,5-*b*]quinoline-2,4(3*H*,10*H*)-dione (AQ14)

^{1}H-NMR (DMSO-d_6, Varian Mercury 300 MHz) δ 10.7 (1H, s), 7.95 (1H, d, *J*= 9.60 Hz), 7.60 (1H, d, *J*= 12.3 Hz), 7.48 (3H, m), 7.22 (2H, d, *J*= 7.50 Hz), 6.49 (1H, s), 4.10 (3H, s) and 3.58 (3H, s) ppm.

EMS^+ (CH_3CN) m/z 334 (M+1) and 333 (M); MS2 (334) 331, 332, 317, 291, 290, 275, 260 and 223.

5-(2-pyridinyl)-7-methoxy-10-methylpyrimido[4,5-*b*]quinoline-2,4(3*H*,10*H*)-dione (AQ15)

^{1}H-NMR (DMSO-d_6, Varian Mercury 300 MHz) δ 10.8 (1H, s), 8.70 (1H, m), 7.80 (1H, d, *J*= 9.60 Hz), 7.93 (1H, t, *J*= 7.80 Hz), 7.64 (1H, d of d, J_1= 9.30 Hz and J_2= 9.30 Hz), 7.43 (1H, d, *J*= 7.50 Hz), 6.35 (1H, s), 4.13 (3H, s) and 3.62 (3H, s) ppm.

EMS^+ (CH_3CN) m/z 335 (M+1) and 334 (M); MS2 (335) 334, 319, 302, 291, 289, 275, 252 and 69.

5-(3-pyridinyl)-7-methoxy-10-methylpyrimido[4,5-*b*]quinoline-2,4(3*H*,10*H*)-dione (AQ16)

^{1}H-NMR (DMSO-d_6, Varian Mercury 300 MHz) δ 10.8 (1H, s), 8.70 (1H, m), 8.46 (1H, s), 8.01 (1H, d, *J*= 9.30 Hz), 7.74 (1H, d, *J*= 7.50 Hz), 7.66 (1H, d, *J*= 9.30 Hz), 7.56 (2H, m), 7.49 (1H, s), 4.14 (3H, s) and 3.66 (3H, s) ppm.

EMS^+ (CH_3CN) m/z 334 (M); MS2 (334) 334, 304, 276 and 179.

5-(4-pyridinyl)-7-methoxy-10-methylpyrimido[4,5-*b*]quinoline-2,4(3*H*,10*H*)-dione (AQ17)

^{1}H-NMR (DMSO-d_6, Varian Mercury 300 MHz) δ 10.7 (1H, s), 8.72 (2H, d, *J*= 6.00 Hz), 8.01 (1H, d, *J*= 9.90 Hz), 7.65 (d of d, J_1= 9.30 Hz and J_2= 9.30 Hz), 7.32 (2H, d, *J*= 5.70 Hz), 6.42 (1H, s), 4.13 (3H, s) and 3.62 (3H, s) ppm.

EMS^+ (CH_3CN) m/z 335 (M+1) and 334 (M); MS2 (335) 334, 319, 291 and 71.

5-(4-bromophenyl)-7-methoxy-10-methylpyrimido[4,5-*b*]quinoline-2,4(3*H*,10*H*)-dione (AQ18)

^{1}H-NMR (DMSO-d_6, Varian Mercury 300 MHz) δ 10.8 (1H, s), 7.97 (1H, d, *J*= 9.30 Hz), 7.64 (1H, d of d, J_1= 9.60 Hz and J_2= 9.30 Hz), 7.20 (2H, d, *J*= 8.70 Hz), 6.50 (1H, s), 4.10 (3H, s) and 3.63 (3H, s) ppm.

EMS$^+$ (CH_3CN) m/z 414 (M+2) and 411 (M-1); MS2 (412) 412, 369, 368, 324, 290 and 275.

5-(2,3-dichlorophenyl)-7-methoxy-10-methylpyrimido[4,5-*b*]quinoline-2,4(3*H*,10*H*)-dione (AQ19)

^{1}H-NMR (DMSO-d_6, Varian Mercury 300 MHz) δ 10.9 (1H, s), 8.01 (1H, d, *J*= 9.30 Hz), 7.77 (1H, d, *J*= 8.10 Hz), 7.66 (1H, d of d, J_1= 9.60 Hz and J_2= 9.30 Hz), 7.50 (1H, t, *J*= 7.50 Hz), 6.39 (1H, s), 4.12 (3H, s) and 3.64 (3H, s) ppm.

EMS$^+$ (CH_3CN) m/z 439 (M+K), 423 (M+Na) and 402 (M); MS2 (403) 402, 366, 359, 324, 309 and 296.

5-(3,4-dichlorophenyl)-7-methoxy-10-methylpyrimido[4,5-*b*]quinoline-2,4(3*H*,10*H*)-dione (AQ20)

^{1}H-NMR (DMSO-d_6, Varian Mercury 300 MHz) δ 10.8 (1H, s), 7.98 (1H, d, *J*= 9.30 Hz), 7.76 (1H, d, *J*= 8.40 Hz), 7.62 (2H, m), 7.26 (1H, d of d, J_1= 8.10 Hz and J_2= 8.40 Hz), 6.52 (1H, s), 4.10 (3H, s) and 3.65 (3H, s) ppm.

EMS$^+$ (CH_3CN) m/z 439 (M+K), 423 (M+Na) and 403 (M+1); MS2 (403) 402, 366, 359, 358, 324, 316, 309 and 296.

5-(4-chlorophenyl)-7-methoxy-10-methylpyrimido[4,5-*b*]quinoline-2,4(3*H*,10*H*)-dione (AQ21)

^{1}H-NMR (DMSO-d_6, Varian Mercury 300 MHz) δ 10.8 (1H, s), 7.96 (1H, d, *J*= 9.60 Hz), 7.61 (1H, d of d, J_1= 9.30 Hz and J_2= 9.30 Hz), 7.55 (2H, d of d, J_1= 6.30 Hz and J_2= 6.60 Hz), 7.26 (2H, d of d, J_1= 6.30 Hz and J_2= 6.30 Hz), 6.49 (1H, s), 4.09 (3H, s) and 3.62 (3H, s) ppm.

EMS^+ (CH_3CN) m/z 369 (M+2) and 367 (M); MS2 (367) 367.

5-(4-methylthiophenyl)-7-methoxy-10-methylpyrimido[4,5-*b*]quinoline-2,4(3*H*,10*H*)-dione (AQ22)

^{1}H-NMR (DMSO-d_6, Varian Mercury 300 MHz) δ 10.8 (1H, s), 7.97 (1H, d, *J*= 9.30 Hz), 7.63 (1H, d of d, J_1= 9.30 Hz and J_2= 10.2 Hz), 7.37 (2H, d of d, J_1= 6.60 Hz and J_2= 6.60 Hz), 7.19 (2H, d of d, J_1= 6.30 Hz and J_2= 6.30 Hz), 6.61 (1H, s), 4.11 (3H, s) and 3.65 (3H, s) ppm.

EMS^+ (CH_3CN) m/z 380 (M+1) and 379 (M); MS2 (380) 379, 378, 348, 336, 333, 332, 290 and 289.

5-(4-trifluoromethylphenyl)-7-methoxy-10-methylpyrimido[4,5-*b*]quinoline-2,4(3*H*,10*H*)-dione (AQ23)

^{1}H-NMR (DMSO-d_6, Varian Mercury 300 MHz) δ 10.83 (1H, s), 8.01 (1H, d, *J*= 9.30 Hz), 7.88 (2H, d, *J*= 8.40 Hz), 7.66 (1H, d of d, J_1= 9.30 Hz and J_2= 9.30 Hz), 6.41 (1H, s), 4.13 (3H, s) and 3.63 (3H, s) ppm.

EMS^+ (CH_3CN) m/z 402 (M+1) and 401 (M); MS2 (402) 401 and 400.

5-(3-nitrophenyl)-7-methoxy-10-methylpyrimido[4,5-*b*]quinoline-2,4(3*H*,10*H*)-dione (AQ24)

^{1}H-NMR (DMSO-d_6, Varian Mercury 300 MHz) δ 10.9 (1H, s), 8.37 (1H, d, *J*= 9.90 Hz), 8.02 (1H, d, *J*= 9.30 Hz), 7.82 (1H, t, *J*= 7.80 Hz), 7.73 (1H, d, *J*= 8.10 Hz), 7.66 (1H, d, *J*= 9.30 Hz), 6.46 (1H, s), 4.14 (3H, s) and 3.64 (3H, s) ppm.

EMS^+ (CH_3CN) m/z 379 (M), 377 (M-1) and 376 (M-2); MS2 (379) 378, 347, 333, 332, 331, 317, 316, 303, 301 and 289.

5-(4-nitrophenyl)-7-methoxy-10-methylpyrimido[4,5-*b*]quinoline-2,4(3*H*,10*H*)-dione (AQ25)

^{1}H-NMR (DMSO-d_6, Varian Mercury 300 MHz) δ 10.9 (1H, s), 8.36 (2H, d, *J*= 6.60 Hz), 7.99 (1H, d, *J*= 9.60 Hz), 7.65 (1H, d, *J*= 6.30 Hz), 7.55 (2H, d of d, J_1= 6.90 Hz and J_2= 6.60 Hz), 6.39 (1H, s), 4.11 (3H, s) and 3.61 (3H, s) ppm.

EMS^+ (CH_3CN) m/z 401 (M+Na) and 378 (M); MS2 (379) 378 and 332.

5-(3-methoxy-4-hydroxy-5-nitrophenyl)-7-methoxy-10-methylpyrimido[4,5-*b*]quinoline-2,4(3*H*,10*H*)-dione (AQ26)

^{1}H-NMR (DMSO-d_6, Varian Mercury 300 MHz) δ 10.8 (1H, s), 7.73 (1H, d, *J*= 9.60 Hz), 7.62 (1H, d of d, J_1= 9.60 Hz and J_2= 9.30 Hz), 7.34 (1H, s), 7.09 (1H, s), 6.80 (1H, s), 4.10 (3H, s), 3.77 (3H, s) and 3.68 (3H, s) ppm.

EMS^+ (CH_3CN) m/z 423 (M-1); MS2 (424) 424, 409, 85, 83 and 81.

5-(2-hydroxy-5-nitrophenyl)-7-methoxy-10-methylpyrimido[4,5-*b*]quinoline-2,4(3*H*,10*H*)-dione (AQ27)

^{1}H-NMR (DMSO-d_6, Varian Mercury 300 MHz) δ 11.2 (1H, s), 10.8 (1H, s), 8.28 (1H, d of d, J_1= 9.30 Hz and J_2= 9.30 Hz), 8.02 (2H, m), 7.66 (1H, d of d, J_1= 9.60 Hz and J_2= 9.30 Hz), 7.13 (1H, d, *J*= 9.00 Hz), 6.62 (1H, s), 4.14 (3H, s) and 3.67 (3H, s) ppm.

EMS^+ (CH_3CN) m/z 394 (M); MS2 (395) 394 and 353.

5-(4-hydroxy-3-methoxyphenyl)-7,8,10-trimethylpyrimido[4,5-*b*]quinoline-2,4(3*H*,10*H*)-dione (AQ28)

^{1}H-NMR (DMSO-d_6, Varian Inova 500 MHz) δ 10.6 (1H, s), 9.20 (1H, s), 7.80 (1H, s), 7.09 (1H, s), 6.87 (1H, d, *J*= 6.50 Hz), 6.78 (1H, s), 6.58 (1H, d, *J*= 6.50 Hz), 4.09 (3H, s), 3.70 (3H, s), 2.47 (3H, s) and 2.21 (3H, s) ppm.

EMS$^+$(CH_3CN) m/z 399 (M+Na) and 377(M); MS2 (377) m/z 376, 333, 120 and 118.

5-(3,4-dimethoxyphenyl)-7,8,10-trimethylpyrimido[4,5-*b*]quinoline-2,4(3*H*,10*H*)-dione (AQ29)

^{1}H-NMR (DMSO-d_6, Varian Inova 500 MHz) δ 10.9 (1H, s), 7.82 (1H, s), 7.01 (1H, s), 6.60 (1H, s), 6.54 (2H, s), 4.09 (3H, s), 3.75 (6H, s), 2.47 (3H, s) and 2.20 (3H, s) ppm.

EMS$^+$(CH_3CN) m/z 430 (M+K), 413 (M+Na) and 391(M); MS2 (391) m/z 390, 372, 325, 237, 187, 162, 141, 136, 118, 76, 71 and 59.

5-(4-methoxyphenyl)-7,8,10-trimethylpyrimido[4,5-*b*]quinoline-2,4(3*H*,10*H*)-dione (AQ30)

^{1}H-NMR (DMSO-d_6, Varian Inova 500 MHz) δ 10.6 (1H, s), 7.80 (1H, s), 7.12 (2H, d, *J*= 7.00 Hz), 7.04 (2H, d, *J*= 7.00 Hz), 7.00 (2H, s), 4.08 (3H, s) and 3.85 (3H, s) ppm.

EMS$^+$(CH_3CN) m/z 399 (M+K), 383 (M+Na) and 361(M); MS2 (361) m/z 361 and 118.

5-(4-methylphenyl)-7,8,10-trimethylpyrimido[4,5-*b*]quinoline-2,4(3*H*,10*H*)-dione (AQ31)

^{1}H-NMR (DMSO-d_6, Varian Inova 500 MHz) δ 10.7 (1H, s), 7.82 (1H, s), 7.29 (2H, d, *J*= 6.00 Hz), 7.08 (2H, d, *J*= 6.50 Hz), 6.93 (1H, s), 4.09 (3H, s), 2.50 (3H, s), 2.43 (3H, s) and 2.17 (3H, s) ppm.

EMS$^+$(CH_3CN) m/z 368 (M+Na) and 345(M); MS2 (345) m/z 344, 154 and 118.

5-(4-biphenyl)-7,8,10-trimethylpyrimido[4,5-*b*]quinoline-2,4(3*H*,10*H*)-dione (AQ32)

^{1}H-NMR (DMSO-d_6, Varian Inova 500 MHz) δ 10.7 (1H, s), 7.85 (1H, s), 7.82 (4H, d, *J*= 6.50 Hz), 7.53 (2H, t, *J*= 6.50 Hz), 7.43 (1H, t, *J*= 6.50 Hz), 7.31 (2H, d, *J*= 6.50 Hz), 6.99 (1H, s), 4.11 (3H, s) and 2.48 (3H, s) ppm.

EMS$^+$(CH_3CN) m/z 446 (M+K), 429 (M+Na) and 407(M); MS2 (407) m/z 406, 401, 87 and 67.

5-phenyl-7,8,10-trimethylpyrimido[4,5-*b*]quinoline-2,4(3*H*,10*H*)-dione (AQ33)

^{1}H-NMR (DMSO-d_6, Varian Mercury 300 MHz) δ 10.7 (1H, s), 7.81(1H, s), 7.47 (3H, m), 7.19 (2H, m), 6.86 (1H, s), 4.08 (3H, s), 2.45 (3H, s) and 2.14 (3H, s) ppm.

EMS$^+$ (CH_3CN) m/z 370 (M+K), 353 (M+Na) and 331(M); MS2 (331) m/z 331.

5-(2-pyridinyl)-7,8,10-trimethylpyrimido[4,5-*b*]quinoline-2,4(3*H*,10*H*)-dione (AQ34)

^{1}H-NMR (DMSO-d_6, Varian Mercury 300 MHz) δ 10.8 (1H, s), 8.66 (1H, d, *J*= 6.00 Hz), 7.90 (1H, t, *J*= 6.90 Hz), 7.83 (1H, s), 7.48 (1H, m), 6.73 (1H, s), 4.09 (3H, s), 2.46 (3H, s) and 2.15 (3H, s) ppm.

EMS$^+$ (CH_3CN) m/z 333 (M+1) and 332 (M); MS2 (333) 332, 289, 288, 261 and 246.

5-(3-pyridinyl)-7,8,10-trimethylpyrimido[4,5-*b*]quinoline-2,4(3*H*,10*H*)-dione (AQ35)

^{1}H-NMR (DMSO-d_6, Varian Mercury 300 MHz) δ 10.8 (1H, s), 8.62 (1H, d, *J*= 1.80 Hz), 8.40 (1H, s), 7.85 (1H, s), 7.68 (1H, d, *J*= 7.50 Hz), 7.53 (1H, m), 6.88 (1H, s), 4.10 (3H, s), 3.40 (3H, s) and 2.18 (3H, s) ppm.

EMS$^+$ (CH_3CN) m/z 333 (M+1) and 332 (M); MS2 (333) 332, 314, 289, 288, 273, 261, 246, 245 and 232.

5-(4-pyridinyl)-7,8,10-trimethylpyrimido[4,5-*b*]quinoline-2,4(3*H*,10*H*)-dione (AQ36)

^{1}H-NMR (DMSO-d_6, Varian Mercury 300 MHz) δ 10.8 (1H, s), 8.68 (2H, d, *J*= 5.70 Hz), 7.85 (1H, s), 7.27 (2H, d of d, J_1= 3.90 Hz and J_2= 4.50 Hz), 6.81 (1H, s), 4.09 (3H, s), 2.46 (3H, s) and 2.17 (3H, s) ppm.

EMS^+ (CH_3CN) m/z 333 (M+1) and 332 (M); MS2 (333) 332, 314, 289, 288, 274, 261, 246 and 232.

5-(4-bromophenyl)-7,8,10-trimethylpyrimido[4,5-*b*]quinoline-2,4(3*H*,10*H*)-dione (AQ37)

^{1}H-NMR (DMSO-d_6, Varian Inova 500 MHz) δ 10.7 (1H, s), 7.83 (1H, s), 7.64 (2H, d of d, J_1= 11.0 Hz and J_2= 12.0 Hz), 7.17 (2H, d of d, J_1= 11.0 Hz and J_2= 11.0 Hz), 6.90 (1H, s), 4.00 (3H, s), 2.46 (3H, s) and 2.18 (3H, s) ppm.

EMS^+(CH_3CN) m/z 433 (M+Na) and 410(M); MS2 (410) m/z 409, 367, 365, 337, 328, 288 and 118.

5-(4-chlorophenyl)-7,8,10-trimethylpyrimido[4,5-*b*]quinoline-2,4(3*H*,10*H*)-dione (AQ38)

^{1}H-NMR (DMSO-d_6, Varian Inova 500 MHz) δ 10.7 (1H, s), 7.84 (1H, s), 7.55 (2H, d, *J*= 6.50 Hz), 7.25 (2H, d, *J*= 6.50 Hz), 6.91 (1H, s), 4.10 (3H, s), 2.47 (3H, s) and 2.20 (3H, s) ppm.

EMS^+(CH_3CN) m/z 387 (M+Na) and 365(M); MS2 (365) m/z 364.

5-(2,3-dichlorophenyl)-7,8,10-trimethylpyrimido[4,5-*b*]quinoline-2,4(3*H*,10*H*)-dione (AQ39)

^{1}H-NMR (DMSO-d_6, Varian Inova 500 MHz) δ 10.9 (1H, s), 7.88 (1H, s), 7.77 (1H, d, *J*= 6.50 Hz), 7.50 (1H, t, *J*= 6.50 Hz), 7.24 (1H, d, *J*= 6.50 Hz), 6.85 (1H, s) 4.12 (3H, s), 2.48 (3H, s) and 2.21 (3H, s) ppm.

EMS^+(CH_3CN) m/z 439 (M+K), 423 (M+Na) and 400(M); MS2 (400) m/z 398, 381, 295 and 274.

5-(3,4-dichlorophenyl)-7,8,10-trimethylpyrimido[4,5-*b*]quinoline-2,4(3*H*,10*H*)-dione (AQ40)

^{1}H-NMR (DMSO-d_6, Varian Mercury 300 MHz) δ 10.8 (1H, s), 7.84 (1H, s), 7.74 (1H, d, *J*= 8.40 Hz), 7.55 (1H, s), 7.22 (1H, d of d, J_1= 8.70 Hz and J_2= 8.10 Hz), 6.95 (1H, s), 4.09 (3H, s), 2.48 (3H, s) and 2.21 (3H, s) ppm.

EMS$^+$(CH_3CN) m/z 402 (M+2), 401 (M+1) and 399 (M-1); MS2 (400) m/z 400, 357, 322 and 314.

5-(4-methylthiophenyl)-7,8,10-trimethylpyrimido[4,5-*b*]quinoline-2,4(3*H*,10*H*)-dione (AQ41)

^{1}H-NMR (DMSO-d_6, Varian Inova 500 MHz) δ 10.7 (1H, s), 7.82 (1H, s), 7.35 (2H, d, *J*= 6.00 Hz), 7.15 (2H, d, *J*= 6.00 Hz), 6.97 (1H, s), 4.09 (3H, s), 2.56 (3H, s), 2.47 (3H, s) and 2.19(3H, s) ppm.

EMS$^+$(CH_3CN) m/z 399 (M+Na) and 377(M); MS2 (377) m/z 376 and 361.

5-(4-trifluoromethylphenyl)-7,8,10-trimethylpyrimido[4,5-*b*]quinoline-2,4(3*H*,10*H*)-dione (AQ42)

^{1}H-NMR (DMSO-d_6, Varian Inova 500 MHz) δ 10.8 (1H, s), 7.86 (3H, m), 7.46 (2H, d, *J*= 6.50 Hz), 6.82 (1H, s), 4.11 (3H, s), 2.48(3H, s) and 2.18 (3H, s) ppm.

EMS$^+$(CH_3CN) m/z 437(M+K), 421 (M+Na) and 399(M); MS2 (399) m/z 398 and 118.

5-(3-nitrophenyl)-7,8,10-trimethylpyrimido[4,5-*b*]quinoline-2,4(3*H*,10*H*)-dione (AQ43)

^{1}H-NMR (DMSO-d_6, Varian Mercury 300 MHz) δ 10.78 (1H, s), 8.35 (1H, d of d, J_1= 8.10 Hz and J_2= 8.10 Hz), 8.13 (1H, s), 7.85 (1H, s), 7.79 (1H, t, *J*= 7.80 Hz), 7.69 (1H, d, *J*= 6.30 Hz), 6.88 (1H, s), 4.10 (3H, s), 2.46 (3H, s) and 2.17 (3H, s) ppm.

$EMS^+(CH_3CN)$ m/z 376 (M); MS2 (376) m/z 375, 329, 315 and 119.

5-(4-nitrophenyl)-7,8,10-trimethylpyrimido[4,5-*b*]quinoline-2,4(3*H*,10*H*)-dione (AQ44)

^{1}H-NMR (DMSO-d_6, Varian Inova 500 MHz) δ 10.8 (1H, s), 7.86 (3H, m), 7.46 (2H, d, J= 6.50 Hz), 6.82 (1H, s), 4.11 (3H, s), 2.48 (3H, s) and 2.18 (3H, s) ppm.

$EMS^+(CH_3CN)$ m/z 399 (M+Na) and 376 (M); MS2 (376) m/z 375, 368, 358, 258, 218, 188, 137, 123, 118, 73 and 65.

5-(3-methoxy-4-hydroxy-5-nitrophenyl)-7,8,10-trimethylpyrimido[4,5-*b*]quinoline-2,4(3*H*,10*H*)-dione (AQ45)

^{1}H-NMR (DMSO-d_6, Varian Mercury 300 MHz) δ 10.7 (1H, s), 10.5 (1H, broad s), 7.82 (1H, s), 7.32 (1H, s), 7.19 (1H, s), 7.11 (1H, s), 4.10 (3H, s), 3.80 (3H, s), 2.46 (3H, s) and 2.22 (3H, s) ppm.

$EMS^-(CH_3CN)$ m/z 422(M); MS2 (422) m/z 422 and 407.

5-(2-hydroxy-5-bromophenyl)-7,8,10-trimethylpyrimido[4,5-*b*]quinoline-2,4(3*H*,10*H*)-dione (AQ46)

^{1}H-NMR (DMSO-d_6, Varian Mercury 300 MHz) δ 10.7 (1H, s), 9.68 (1H, s), 7.81 (1H, s), 7.43 (1H, d of d, J_1= 8.70 Hz and J_2= 8.40 Hz), 7.15 (1H, s), 6.98 (1H, s), 6.87 (1H, d, J= 9.00 Hz), 4.08 (3H, s), 2.46 (3H, s) and 2.20 (3H, s) ppm.

EMS^+ (CH_3CN) m/z 427 (M+1); MS2 (427) 426, 409, 408, 383, 382, 368, 366, 353, 338, 324, 304, 276, 259, 234 and 171.

5-(2-hydroxy-5-chlorophenyl)-7,8,10-trimethylpyrimido[4,5-*b*]quinoline-2,4(3*H*,10*H*)-dione (AQ47)

^{1}H-NMR (DMSO-d_6, Varian Mercury 300 MHz) δ 10.7 (1H, s), 9.65 (1H, s), 7.81 (1H, s), 7.31 (1H, d of d, J_1= 8.70 Hz and J_2= 8.70 Hz), 7.04 (1H, s), 6.89 (1H, s), 6.92 (1H, d, *J*= 9.00 Hz), 4.08 (3H, s), 2.46 (3H, s) and 2.20 (3H, s) ppm.

EMS^+ (CH_3CN) m/z 382 (M+1); MS2 (382) 382, 338, 321, 283 and 252.

5-(3-hydroxyphenyl)-7,10-dimethylpyrimido[4,5-*b*]quinoline-2,4(3*H*,10*H*)-dione (AQ49)

^{1}H-NMR (DMSO-d_6, Varian Mercury 300 MHz) δ 10.7 (1H, s), 9.54 (1H, s), 7.88 (1H, d, *J*= 9.00 Hz), 7.76 (1H, d, *J*= 8.70 Hz), 7.26 (1H, t, *J*= 8.10 Hz), 6.99 (1H, s), 6.84 (1H, d, *J*= 10.50 Hz), 6.58 (2H, m), 4.07 (3H, s) and 2.25 (3H, s) ppm.

EMS^+ (CH_3CN) m/z 335 (M+2) and 334 (M+1); MS2 (334) 333, 316, 291, 288, 276 and 263.

5-(3-methoxy-4-hydroxyphenyl)-7,10-dimethylpyrimido[4,5-*b*]quinoline-2,4(3*H*,10*H*)-dione (AQ50)

^{1}H-NMR (DMSO-d_6, Varian Mercury 300 MHz) δ 10.7 (1H, s), 8.61 (1H, s), 7.88 (1H, d, *J*= 9.00 Hz), 7.74 (1H, d, *J*= 9.00 Hz), 7.04 (2H, m), 6.87 (1H, t, *J*= 8.10 Hz), 6.56 (1H, d, *J*= 7.50 Hz), 4.08 (3H, s), 3.85 (3H, s) and 2.27 (3H, s) ppm.

EMS^+ (CH_3CN) m/z 366 (M+3), 364 (M+1) and 363 (M); MS2 (363) 363, 348 and 331.

5-(3,4-dimethoxyphenyl)-7,10-dimethylpyrimido[4,5-*b*]quinoline-2,4(3*H*,10*H*)-dione (AQ51)

^{1}H-NMR (DMSO-d_6, Varian Mercury 300 MHz) δ 10.7 (1H, s), 7.88 (1H, d, *J*= 8.70 Hz), 7.77 (1H, d, *J*= 6.00 Hz), 7.04 (1H, s), 6.59 (1H, m), 6.36 (2H, m), 4.08 (3H, s), 3.74 (6H, s) and 2.29 (3H, s) ppm.

EMS^+ (CH_3CN) m/z 378 (M+1) and 377 (M); MS2 (378) 377, 361, 347, 345 and 331.

5-(4-methoxyphenyl)-7,10-dimethylpyrimido[4,5-*b*]quinoline-2,4(3*H*,10*H*)-dione (AQ52)

^{1}H-NMR (DMSO-d_6, Varian Mercury 300 MHz) δ 10.7 (1H, s), 7.88 (1H, d, *J*= 9.00 Hz), 7.75 (1H, d, *J*= 9.00 Hz), 7.13 (2H, d, *J*= 9.00 Hz), 7.03 (3H, m), 4.08 (3H, s), 3.84 (3H, s) and 2.28 (3H, s) ppm.

EMS^{+} (CH_3CN) m/z 348 (M+1) and 347 (M); MS2 (348) 347 and 306.

5-(1-naphthyl)-7,10-dimethylpyrimido[4,5-*b*]quinoline-2,4(3*H*,10*H*)-dione (AQ53)

^{1}H-NMR (DMSO-d_6, Varian Mercury 300 MHz) δ 10.7 (1H, s), 8.02 (2H, m), 7.95 (1H, d, *J*= 8.70 Hz), 7.74 (1H, d, *J*= 8.70 Hz), 7.62 (1H, t, *J*= 7.20 Hz), 7.50 (1H, m), 7.29 (3H, m), 6.68 (1H, s), 4.15 (3H, s) and 2.12 (3H, s) ppm.

EMS^{+} (CH_3CN) m/z 368 (M+1) and 367 (M); MS2 (368) 367, 366, 238, 161 and 135.

5-(4-biphenyl)-7,10-dimethylpyrimido[4,5-*b*]quinoline-2,4(3*H*,10*H*)-dione (AQ54)

^{1}H-NMR (DMSO-d_6, Varian Mercury 300 MHz) δ 10.8 (1H, s), 7.91 (1H, d, *J*= 9.00 Hz), 7.80 (5H, m), 7.51 (2H, t, *J*= 8.70 Hz), 7.41 (1H, d, *J*= 7.80 Hz), 7.31 (2H, d of d, J_1= 6.30 Hz and J_2= 6.30 Hz), 7.02(1H, s), 4.10 (3H, s) and 2.27 (3H, s) ppm.

EMS^{+} (CH_3CN) m/z 415 (M+Na), 395 (M+2) and 394 (M+1); MS2 (395) 394, 376, 351, 350, 336, 323, 308 and 294.

5-phenyl-7,10-dimethylpyrimido[4,5-*b*]quinoline-2,4(3*H*,10*H*)-dione (AQ55)

^{1}H-NMR (DMSO-d_6, Varian Mercury 300 MHz) δ 10.7 (1H, s), 7.90 (1H, d, *J*= 8.70 Hz), 7.76 (1H, d of d, J_1= 9.30 Hz and J_2= 9.00 Hz), 7.48 (3H, m), 7.200 (2H, m), 6.91 (1H, s), 4.09 (3H, s) and 2.25 (3H, s) ppm.

EMS^{+} (CH_3CN) m/z 340 (M+Na), 318 (M+1) and 317 (M); MS2 (317) 317.

5-(2-pyridinyl)-7,10-dimethylpyrimido[4,5-*b*]quinoline-2,4(3*H*,10*H*)-dione (AQ56)

^{1}H-NMR (DMSO-d_6, Varian Mercury 300 MHz) δ 10.8 (1H, s), 8.67 (1H, d of d, J_1= 3.60 Hz and J_2= 4.20 Hz), 7.90 (2H, m), 7.77 (1H, d of d, J_1= 8.70 Hz and J_2= 8.70 Hz), 7.49 (1H, m), 7.39 (1H, d, J= 8.10 Hz), 6.78 (1H, s), 4.10 (3H, s) and 2.26 (3H, s) ppm.

EMS^{+} (CH_3CN) m/z 320 (M+2) and 318 (M); MS2 (319) 318, 312, 303, 290, 275, 274, 273, 261, 247, 246, 233, 232, 219, 210, 186, 130, 125, 111, 88, 69 and 62.

5-(3-pyridinyl)-7,10-dimethylpyrimido[4,5-*b*]quinoline-2,4(3*H*,10*H*)-dione (AQ57)

^{1}H-NMR (DMSO-d_6, Varian Mercury 300 MHz) δ 10.8 (1H, s), 8.67 (1H, d of d, J_1= 5.40 Hz and J_2= 4.80 Hz), 8.41 (1H, s), 7.93 (1H, d, J= 8.70 Hz), 7.80 (1H, d, J= 6.00 Hz), 7.67 (1H, m), 6.92 (1H, s), 4.10 (3H, s) and 2.28 (3H, s) ppm.

EMS^{+} (CH_3CN) m/z 320 (M+2) and 318 (M); MS2 (318) 319, 318, 303, 301, 286, 275, 261, 248, 246, 232, 220, 219, 210, 199, 189 and 155.

5-(4-pyridinyl)-7,10-dimethylpyrimido[4,5-*b*]quinoline-2,4(3*H*,10*H*)-dione (AQ58)

^{1}H-NMR (DMSO-d_6, Varian Mercury 300 MHz) δ 10.9 (1H, s), 8.69 (2H, d of d, J_1= 3.90 Hz and J_2= 4.50 Hz), 7.93 (1H, d, J= 9.30 Hz), 7.79 (1H, d of d, J_1= 9.00 Hz and J_2= 7.20 Hz), 7.29 (2H, d of d, J_1= 4.20 Hz and J_2= 4.80 Hz), 6.86 (1H, s), 4.10 (3H, s) and 2.27 (3H, s) ppm.

EMS^{+} (CH_3CN) m/z 320 (M+2) and 318 (M); MS2 (319) 320, 318, 303, 301, 275, 256, 247, 226, 220, 217, 206, 195, 179, 174, 165, 144, 133 and 102.

5-(4-bromophenyl)-7,10-dimethylpyrimido[4,5-*b*]quinoline-2,4(3*H*,10*H*)-dione (AQ59)

^{1}H-NMR (DMSO-d_6, Varian Mercury 300 MHz) δ 10.8 (1H, s), 7.91 (1H, d, J= 8.70 Hz), 7.77 (1H, d, J= 8.70 Hz), 7.68 (2H, d of d, J_1= 6.30 Hz and J_2= 6.30 Hz), 7.19 (2H, d of d, J_1= 6.30 Hz and J_2= 6.30 Hz), 6.94 (1H, s), 4.09 (3H, s) and 2.29 (3H, s) ppm.

EMS^{+} (CH_3CN) m/z 398 (M+2) and 395 (M-1); MS2 (397) 396, 368, 353, 352, 274, 273, 259, 256 and 231.

5-(4-chlorophenyl)-7,10-dimethylpyrimido[4,5-*b*]quinoline-2,4(3*H*,10*H*)-dione (AQ60)

^{1}H-NMR (DMSO-d_6, Varian Mercury 300 MHz) δ 10.8 (1H, s), 7.90 (1H, d, *J*= 8.70 Hz), 7.77 (1H, d of d, J_1= 8.70 Hz and J_2= 9.30 Hz), 7.54 (2H, d of d, J_1= 6.60 Hz and J_2= 7.20 Hz), 7.25 (2H, d of d, J_1= 9.60 Hz and J_2= 9.00 Hz), 6.94 (1H, s), 4.09 (3H, s) and 2.28 (3H, s) ppm.

EMS$^+$ (CH_3CN) m/z 389 (M+K), 373 (M+Na), 354 (M+3), 352 (M+1) and 351 (M); MS2 (351) 350, 345, 329, 316, 311, 310, 297, 278, 268, 240, 236, 216, 204, 198, 185, 167, 148, 146, 114, 94, 77, 76, 61 and 58.

5-(2,3-dichlorophenyl)-7,10-dimethylpyrimido[4,5-*b*]quinoline-2,4(3*H*,10*H*)-dione (AQ61)

^{1}H-NMR (DMSO-d_6, Varian Mercury 300 MHz) δ 10.92 (1H, s), 7.95 (1H, d, *J*= 8.10 Hz), 7.79 (2H, t, *J*= 8.10 Hz), 7.50 (1H, t, *J*= 8.10 Hz), 7.25 (1H, d, *J*= 7.80 Hz), 6.89 (1H, s), 4.12 (3H, s) and 2.30 (3H, s) ppm.

EMS$^+$ (CH_3CN) m/z 386 (M); MS2 (387) 386, 368, 350, 343, 308, 307 and 280.

5-(3,4-dichlorophenyl)-7,10-dimethylpyrimido[4,5-*b*]quinoline-2,4(3*H*,10*H*)-dione (AQ62)

^{1}H-NMR (DMSO-d_6, Varian Mercury 300 MHz) δ 10.9 (1H, s), 7.92 (1H, d, *J*= 9.00 Hz), 7.77 (2H, m), 7.57 (1H, s), 7.24 (1H, d of d, J_1= 8.10 Hz and J_2= 8.10 Hz), 6.99(1H, s), 4.09 (3H, s) and 2.31 (3H, s) ppm.

EMS$^+$ (CH_3CN) m/z 385 (M-1); MS2 (387) 386, 350, 343, 308 and 280.

5-(4-methylthiophenyl)-7,10-dimethylpyrimido[4,5-*b*]quinoline-2,4(3*H*,10*H*)-dione (AQ63)

^{1}H-NMR (DMSO-d_6, Varian Mercury 300 MHz) δ 10.7 (1H, s), 7.89 (1H, d, *J*= 8.70 Hz), 7.76 (1H, d of d, J_1= 8.70 Hz and J_2= 9.00 Hz), 7.34 (2H, d, *J*= 8.40 Hz), 7.16 (2H, m), 6.70 (1H, s), 4.08 (3H, s), 2.55 (3H, s) and 2.28 (3H, s) ppm.

EMS$^+$ (CH_3CN) m/z 402 (M+K), 364 (M+1) and 363 (M); MS2 (364) 363, 348, 346, 320, 318, 232, 219, 201, 195, 125, 91 and 96.

5-(3-nitrophenyl)-7,10-dimethylpyrimido[4,5-*b*]quinoline-2,4(3*H*,10*H*)-dione (AQ64)

^{1}H-NMR (DMSO-d_6, Varian Mercury 300 MHz) δ 10.8 (1H, s), 8.35 (1H, d, *J*= 6.00 Hz), 8.15 (1H, s), 7.93 (1H, d, *J*= 8.70 Hz), 7.79 (2H, m), 7.71 (1H, m), 6.99 (1H, s), 4.11 (3H, s) and 2.27 (3H, s) ppm.

EMS^{+} (CH_3CN) m/z 363 (M+1) and 362 (M); MS2 (363) 363, 316, 259 and 105.

5-(4-nitrophenyl)-7,10-dimethylpyrimido[4,5-*b*]quinoline-2,4(3*H*,10*H*)-dione (AQ65)

^{1}H-NMR (DMSO-d_6, Varian Mercury 300 MHz) δ 10.9 (1H, s), 8.35 (2H, d, *J*=8.10 Hz), 7.93 (1H, d, *J*= 8.70 Hz), 7.79 (1H, d, *J*= 6.00 Hz), 7.53 (2H, d, *J*= 8.70 Hz), 6.87 (1H, s), 4.10 (3H, s) and 2.27 (3H, s) ppm.

EMS^{+} (CH_3CN) m/z 363 (M+1) and 362 (M); MS2 (363) 362, 345 and 316.

5-(3-methoxy-4-hydroxy-5-nitrophenyl)-7,10-dimethylpyrimido[4,5-*b*]quinoline-2,4(3*H*,10*H*)-dione (AQ66)

^{1}H-NMR (DMSO-d_6, Varian Mercury 300 MHz) δ 10.8 (1H, s), 7.94 (1H, d, *J*= 8.70 Hz), 7.79 (1H, d, *J*= 6.00 Hz), 7.34 (1H, s), 7.18 (2H, d, *J*= 10.2 Hz), 4.10 (3H, s), 3.80 (3H, s) and 2.32 (3H, s) ppm.

EMS^{+} (CH_3CN) m/z 430 (M+Na) and 408 (M); MS2 (409) 408, 390, 372, 355, 362, 336, 332, 324, 318, 316, 286, 280, 271, 264, 242, 167, 146, 135 and 115.

5-(2-hydroxy-5-nitrophenyl)-7,10-dimethylpyrimido[4,5-*b*]quinoline-2,4(3*H*,10*H*)-dione (AQ69)

^{1}H-NMR (DMSO-d_6, Varian Mercury 300 MHz) δ 11.1 (1H, s), 10.8 (1H, s), 8.26 (1H, d of d, J_1= 8.70 Hz and J_2= 9.00 Hz), 7.98 (1H, s), 7.92 (1H, d, *J*= 9.00 Hz), 7.79 (1H, d, *J*= 6.00 Hz), 7.09 (2H, d, *J*= 8.70 Hz), 4.11 (3H, s) and 2.30 (3H, s) ppm.

EMS$^-$ (CH_3CN) m/z 377 (M-1); MS2 (378) 378, 350, 335, 334 and 306.

7-bromo-5-(3-hydroxyphenyl)-10-methylpyrimido[4,5-*b*]quinoline-2,4(3*H*,10*H*)-dione (AQ70)

^{1}H-NMR (DMSO-d_6, Varian Inova 500 MHz) δ 10.9 (1H, s), 9.63 (1H, s), 8.06 (1H, d, *J*= 8.00 Hz), 7.93 (1H, d, *J*= 8.00 Hz), 7.31 (1H, t, *J*= 6.50 Hz), 7.24 (1H, s), 6.88 (1H, d, *J*= 6.50 Hz), 6.63 (1H, d, *J*= 6.00 Hz), 6.61 (1H, s) and 4.07 (3H, s) ppm.

EMS$^+$(CH_3CN) m/z 420 (M+Na) and 399 (M+1); MS2 (398) m/z 398, 355, 327 and 312.

7-bromo-5-(4-methoxyphenyl)-10-methylpyrimido[4,5-*b*]quinoline-2,4(3*H*,10*H*)-dione (AQ73)

^{1}H-NMR (DMSO-d_6, Varian Inova 500 MHz) δ 10.806 (1H, s), 8.02 (1H, d, *J*= 7.50 Hz), 7.90 (1H, d, *J*= 7.50 Hz), 7.25 (1H, s), 7.14 (2H, d, *J*= 5.50 Hz), 7.04 (2H, d, *J*= 6.50 Hz), 4.04 (3H, s) and 3.83 (3H, s) ppm.

EMS$^+$(CH_3CN) m/z 435 (M+Na) and 412 (M); MS2 (412) m/z 412 and 369.

7-bromo-5-(4-methylphenyl)-10-methylpyrimido[4,5-*b*]quinoline-2,4(3*H*,10*H*)-dione (AQ74)

^{1}H-NMR (DMSO-d_6, Varian Inova 500 MHz) δ 10.9 (1H, s), 8.05 (1H, d of d, J_1= 8.00 Hz, J_2= 7.50 Hz), 7.94 (1H, d, *J*= 7.50 Hz), 7.33 (2H, d, *J*= 6.50 Hz), 7.21 (1H, s), 7.13 (2H, d, *J*= 6.50 Hz), 4.08 (3H, s) and 2.44 (3H, s) ppm.

EMS$^+$(CH_3CN) m/z 435 (M+K), 417 (M+Na) and 398 (M); MS2 (398) m/z 394 and 118.

7-bromo-5-(2-naphthyl)-10-methylpyrimido[4,5-*b*]quinoline-2,4(3*H*,10*H*)-dione (AQ75)

^{1}H-NMR (DMSO-d_6, Varian Inova 500 MHz) δ 10.9 (1H, s), 8.05 (3H, m), 7.93 (2H, m), 7.76 (1H, s), 7.58 (2H, q, J_1= 6.50 Hz, J_2= 6.50 Hz), 7.37 (1H, d, J= 6.50 Hz), 7.15 (1H, s) and 4.09 (3H, s) ppm.

EMS^{+}(CH_3CN) m/z 471 (M+K) and 454 (M+Na); MS2 (432) m/z 432, 389, 374 and 309.

7-bromo-5-(4-biphenyl)-10-methylpyrimido[4,5-*b*]quinoline-2,4(3*H*,10*H*)-dione (AQ76)

^{1}H-NMR (DMSO-d_6, Varian Inova 500 MHz) δ 10.9 (1H, s), 8.04 (1H, s), 7.94 (1H, m), 7.80 (5H, m), 7.50 (2H, m), 7.39 (1H, s), 7.32 (2H, m), 7.24 (1H, s) and 4.07 (3H, s) ppm.

EMS^{+}(CH_3CN) m/z 497 (M+K) and 458 (M); MS2 (458) m/z 458, 415 and 370.

7-bromo-5-phenyl-10-methylpyrimido[4,5-*b*]quinoline-2,4(3*H*,10*H*)-dione (AQ77)

^{1}H-NMR (DMSO-d_6, Varian Inova 500 MHz) δ 10.8 (1H, s), 8.03 (1H, d of d, J_1= 8.00 Hz, J_2= 7.50 Hz), 7.92 (1H, d, J= 7.50 Hz), 7.48 (3H, m), 7.21 (2H, d, J= 6.00 Hz), 7.12 (1H, s), and 4.06 (3H, s) ppm.

EMS^{+}(CH_3CN) m/z 405 (M+Na) and 382 (M); MS2 (382) m/z 404 and 154.

7-bromo-5-(2-pyridinyl)-10-methylpyrimido[4,5-*b*]quinoline-2,4(3*H*,10*H*)-dione (AQ78)

^{1}H-NMR (DMSO-d_6, Varian Inova 500 MHz) δ 10.9 (1H, s), 8.72 (1H, s), 8.06 (1H, d, J= 6.50 Hz), 7.96 (2H, m), 7.53 (1H, m), 7.45 (1H, d, J= 6.00 Hz), 7.04 (1H, s) and 4.10 (3H, s) ppm.

EMS^{+}(CH_3CN) m/z 422 (M+K), 404 (M+Na) and 383 (M); MS2 (383) m/z 383, 340, 312, 297 and 273.

7-bromo-5-(3-pyridinyl)-10-methylpyrimido[4,5-*b*]quinoline-2,4(3*H*,10*H*)-dione (AQ79)

^{1}H-NMR (DMSO-d_6, Varian Inova 500 MHz) δ 10.9 (1H, s), 8.71 (1H, s), 8.46 (1H, s), 8.10 (1H, d, *J*= 7.00 Hz), 7.98 (1H, d, *J*= 7.50 Hz), 7.74 (1H, d, *J*= 6.50 Hz), 7.58 (1H, m), 7.17 (1H, s) and 4.10 (3H, s) ppm.

$EMS^{+}(CH_3CN)$ m/z 406 (M+Na), 384 (M+2) and 383 (M); MS2 (383) m/z 381, 335, 293, 207 and 113.

7-bromo-5-(4-pyridinyl)-10-methylpyrimido[4,5-*b*]quinoline-2,4(3*H*,10*H*)-dione (AQ80)

^{1}H-NMR (DMSO-d_6, Varian Inova 500 MHz) δ 10.9 (1H, s), 8.73 (2H, broad s), 8.09 (1H, d, *J*= 7.50 Hz), 7.98 (1H, d, *J*= 7.50 Hz), 7.33 (2H, broad s), 7.10 (1H, s) and 4.10 (3H, s) ppm.

$EMS^{+}(CH_3CN)$ m/z 406 (M+Na), and 383 (M); MS2 (383) m/z 381, 333, 295, 276, 266, 207, 104 and 118.

7-bromo-5-(4-chlorophenyl)-10-methylpyrimido[4,5-*b*]quinoline-2,4(3*H*,10*H*)-dione (AQ81)

^{1}H-NMR (DMSO-d_6, Varian Inova 500 MHz) δ 10.9 (1H, s), 8.04 (1H, d, *J*= 7.50 Hz), 7.92 (1H, d, *J*= 7.50 Hz), 7.56 (2H, d, *J*= 6.50 Hz), 7.26 (2H, d, *J*= 6.50 Hz), 7.15 (1H, s) and 4.05 (3H, s) ppm.

$EMS^{+}(CH_3CN)$ m/z 439 (M+Na) and 416 (M); MS2 (439) m/z 438 and 312.

7-bromo-5-(3,4-dichlorophenyl)-10-methylpyrimido[4,5-*b*]quinoline-2,4(3*H*,10*H*)-dione (AQ82)

^{1}H-NMR (DMSO-d_6, Varian Inova 500 MHz) δ 10.9 (1H, s), 8.06 (1H, d, *J*= 7.50 Hz), 7.93 (1H, d, *J*= 8.00 Hz), 7.76 (1H, d, *J*= 7.00 Hz), 7.58(1H, s), 7.25 (1H, d, *J*= 7.00 Hz), 7.21 (1H, s) and 4.06 (3H, s) ppm.

$EMS^{-}(CH_3CN)$ m/z 451 (M) and 449 (M-2); MS2 (451) m/z 451, 408, 381, 304 and 77.

7-bromo-5-(3-trifluoromethylphenyl)-10-methylpyrimido[4,5-*b*]quinoline-2,4(3*H*,10*H*)-dione (AQ83)

^{1}H-NMR (DMSO-d_6, Varian Inova 500 MHz) δ 11.0 (1H, s), 8.09 (1H, d, *J*= 8.00 Hz), 7.98 (1H, d, *J*= 7.50 Hz), 7.90 (2H, d, *J*= 7.00 Hz), 7.51 (2H, d, *J*= 7.00 Hz), 7.09 (1H, s) and 4.10 (3H, s) ppm.

EMS^{+}(CH_3CN) m/z 489 (M+K), 472 (M+Na) and 451 (M+1); MS2 (450) m/z 450, 407 and 362.

7-bromo-5-(4-nitrophenyl)-10-methylpyrimido[4,5-*b*]quinoline-2,4(3*H*,10*H*)-dione (AQ84)

^{1}H-NMR (DMSO-d_6, Varian Inova 500 MHz) δ 11.0 (1H, s), 8.35 (2H, d, *J*= 7.00 Hz), 8.06 (1H, m), 7.95 (1H, d, *J*= 7.50 Hz), 7.54 (2H, d, *J*= 7.00 Hz), 7.10 (1H, s) and 4.07 (3H, s) ppm.

EMS^{+}(CH_3CN) m/z 466 (M+K), 449 (M+Na) and 428 (M+1); MS2 (449) m/z 449.

7-bromo-5-(3-methoxy-4-hydroxy-5-nitrophenyl)-10-methylpyrimido[4,5-*b*]quinoline-2,4(3*H*,10*H*)-dione (AQ85)

^{1}H-NMR (DMSO-d_6, Varian Inova 500 MHz) δ 10.9 (1H, s), 10.8 (1H, broad s), 8.05 (1H, d, *J*= 7.50 Hz), 7.92 (1H, d, *J*= 7.50 Hz), 7.40 (1H, s), 7.35 (1H, s), 7.16 (1H, s), 4.06 (3H, s) and 3.78 (3H, s) ppm.

EMS^{-}(CH_3CN) m/z 473 (M); MS2 (473) m/z 473, 459, 430, 168 and 153.

7-chloro-5-(3-hydroxyphenyl)-10-methylpyrimido[4,5-b]quinoline-2,4(3H,10H)-dione (AQ88)

^{1}H-NMR (DMSO-d_6, Varian Inova 500 MHz) δ 10.8 (1H, s), 9.57 (1H, s), 7.96 (1H, d, *J*= 6.50 Hz), 7.92 (1H, d, *J*= 6.00 Hz), 7.27 (1H, t, *J*= 6.50 Hz), 7.07 (1H, s), 6.85 (1H, d, *J*= 6.50 Hz), 6.59 (2H, m) and 4.05 (3H, s) ppm.

EMS^{+}(CH_3CN) m/z 376 (M+Na) and 353 (M); MS2 (353) m/z 352 and 309.

7-chloro-5-(4-methylphenyl)-10-methylpyrimido[4,5-*b*]quinoline-2,4(3*H*,10*H*)-dione (AQ90)

^{1}H-NMR (DMSO-d_6, Varian Inova 500 MHz) δ 10.8 (1H, s), 7.98 (1H, d, *J*= 7.50 Hz), 7.92 (1H, d, *J*= 7.50 Hz), 7.30 (2H, d, *J*= 6.00 Hz), 7.10 (2H, d, *J*= 6.50 Hz), 7.03 (1H, s), 4.06 (3H, s) and 2.40 (3H, s) ppm.

$EMS^{+}(CH_3CN)$ m/z 389 (M+K), 373 (M+Na) and 351 (M); MS2 (351) m/z 351.

7-chloro-5-(1-naphthyl)-10-methylpyrimido[4,5-*b*]quinoline-2,4(3*H*,10*H*)-dione (AQ91)

^{1}H-NMR (DMSO-d_6, Varian Inova 500 MHz) δ 10.8 (1H, s), 8.03 (2H, d, *J*= 8.00 Hz), 8.01 (1H, d, *J*= 7.00 Hz), 7.90 (1H, m), 7.61 (1H, t, *J*= 6.50 Hz), 7.50 (1H, m), 7.31 (2H, d, *J*= 7.00 Hz), 7.29 (2H, d, *J*= 6.00 Hz), 6.73 (1H, s) and 4.12 (3H, s) ppm.

$EMS^{+}(CH_3CN)$ m/z 409 (M+Na) and 387 (M); MS2 (387) m/z 386.

7-chloro-5-(2-naphthyl)-10-methylpyrimido[4,5-*b*]quinoline-2,4(3*H*,10*H*)-dione (AQ92)

^{1}H-NMR (DMSO-d_6, Varian Inova 500 MHz) δ 10.9 (1H, s), 8.02 (4H, m), 7.93 (2H, t, *J*= 8.00 Hz), 7.76 (1H, s), 7.58 (2H, m), 7.37 (1H, d, *J*= 7.00 Hz), 7.02 (1H, s) and 4.10 (3H, s) ppm.

$EMS^{-}(CH_3CN)$ m/z 375 (M); MS2 (375) m/z 375, 295, 267, 188 and 69.

7-chloro-5-(4-biphenyl)-10-methylpyrimido[4,5-*b*]quinoline-2,4(3*H*,10*H*)-dione (AQ93)

^{1}H-NMR (DMSO-d_6, Varian Inova 500 MHz) δ 10.9 (1H, s), 8.01 (1H, d, *J*= 8.00 Hz), 7.95 (1H, d, *J*= 8.00 Hz), 7.81 (5H, m), 7.50 (2H, t, *J*= 6.00 Hz), 7.39 (1H, t, *J*= 6.00 Hz), 7.32 (2H, d, *J*= 6.50 Hz), 7.10(1H, s) and 4.08 (3H, s) ppm.

$EMS^{+}(CH_3CN)$ m/z 425 (M+Na).

7-chloro-5-(2-pyridinyl)-10-methylpyrimido[4,5-*b*]quinoline-2,4(3*H*,10*H*)-dione (AQ94)

^{1}H-NMR (DMSO-d_6, Varian Inova 500 MHz) δ 10.9 (1H, s), 8.68 (1H, s), 7.99 (1H, d, *J*= 6.50 Hz), 7.92 (2H, m), 7.49 (1H, m), 7.42 (1H, d, *J*= 6.00 Hz), 6.88 (1H, s) and 4.07 (3H, s) ppm.

$EMS^{+}(CH_3CN)$ m/z 360 (M+Na) and 338 (M); MS2 (338) m/z 337.

7-chloro-5-(3-pyridinyl)-10-methylpyrimido[4,5-*b*]quinoline-2,4(3*H*,10*H*)-dione (AQ95)

^{1}H-NMR (DMSO-d_6, Varian Inova 500 MHz) δ 10.9 (1H, s), 8.86 (1H, m), 8.43 (1H, s), 8.02 (1H, d, *J*= 7.50 Hz), 7.96 (1H, d, *J*= 7.00 Hz), 7.71 (1H, d, *J*= 6.50 Hz), 7.45 (1H, m), 7.01 (1H, s) and 4.08 (3H, s) ppm.

$EMS^{+}(CH_3CN)$ m/z 360 (M+Na), 340 (M+2) and 338 (M); MS2 (338) m/z 337.

7-chloro-5-(4-pyridinyl)-10-methylpyrimido[4,5-*b*]quinoline-2,4(3*H*,10*H*)-dione (AQ96)

^{1}H-NMR (DMSO-d_6, Varian Inova 500 MHz) δ 10.9 (1H, s), 8.70 (2H, m), 8.02 (1H, d, *J*= 8.00 Hz), 7.96 (1H, d, *J*= 7.50 Hz), 7.29 (2H, m), 6.94 (1H, s) and 4.07 (3H, s) ppm.

$EMS^{+}(CH_3CN)$ m/z 360 (M+Na) and 338 (M); MS2 (338) m/z 359, 271, 209 and 105.

7-chloro-5-(4-bromophenyl)-10-methylpyrimido[4,5-*b*]quinoline-2,4(3*H*,10*H*)-dione (AQ97)

^{1}H-NMR (DMSO-d_6, Varian Inova 500 MHz) δ 10.9 (1H, s), 8.00 (1H, d, *J*= 7.50 Hz), 7.94 (1H, d, *J*= 7.50 Hz), 7.69 (2H, d, *J*= 7.00 Hz), 7.20 (2H, d, *J*= 6.50 Hz), 7.01(1H, s) and 4.06 (3H, s) ppm.

$EMS^{+}(CH_3CN)$ m/z 455 (M+K), 439 (M+Na) and 417 (M+1); MS2 (416) m/z 416, 373, 294, 266 and 118.

7-chloro-5-(3,4-dichlorophenyl)-10-methylpyrimido[4,5-*b*]quinoline-2,4(3*H*,10*H*)-dione (AQ99)

^{1}H-NMR (DMSO-d_6, Varian Inova 500 MHz) δ 10.9 (1H, s), 8.01 (1H, d, *J*= 8.00 Hz), 7.70 (1H, d, *J*= 8.00 Hz), 7.76 (1H, d, *J*= 6.50 Hz), 7.58 (1H, s), 7.25 (1H, d, *J*= 6.50 Hz), 7.10 (1H, s) and 4.07 (3H, s) ppm.

$EMS^{+}(CH_3CN)$ m/z 405 (M-1); MS2 (406) m/z 406, 363 and 328.

7-chloro-5-(4-methylthiophenyl)-10-methylpyrimido[4,5-*b*]quinoline-2,4(3*H*,10*H*)-dione (AQ100)

^{1}H-NMR (DMSO-d_6, Varian Inova 500 MHz) δ 10.8 (1H, s), 7.99 (1H, d, *J*= 7.50 Hz), 7.94 (1H, d, *J*= 7.00 Hz), 7.35 (2H, d, *J*= 6.50 Hz), 7.16 (2H, d, *J*= 7.00 Hz), 7.07 (1H, s) and 4.06 (3H, s) ppm.

$EMS^{+}(CH_3CN)$ m/z 405 (M+Na); MS2 (383) m/z 381 and 118.

7-chloro-5-(4-nitrophenyl)-10-methylpyrimido[4,5-*b*]quinoline-2,4(3*H*,10*H*)-dione (AQ101)

^{1}H-NMR (DMSO-d_6, Varian Inova 500 MHz) δ 11.0 (1H, s), 8.35 (2H, d, *J*= 7.00Hz), 8.03 (1H, d, *J*= 8.00 Hz), 7.97 (1H, d, *J*= 8.00 Hz), 7.54 (2H, d, *J*= 7.00 Hz), 6.98 (1H, s) and 4.08 (3H, s) ppm.

$EMS^{+}(CH_3CN)$ m/z 405 (M+Na) and 382 (M); MS2 (382) m/z 381 and 118.

7-chloro-5-(3-methoxy-4-hydroxy-5-nitro-phenyl)-10-methylpyrimido[4,5-*b*]quinoline-2,4(3*H*,10*H*)-dione (AQ102)

^{1}H-NMR (DMSO-d_6, Varian Inova 500 MHz) δ 10.9 (1H, s), 10.67 (1H, s), 8.00 (1H, d, *J*= 7.50 Hz), 7.95 (1H, d, *J*= 8.00 Hz), 7.35 (1H, s), 7.27 (1H, s), 7.20 (1H, s), 4.08 (3H, s) and 3.79 (3H, s) ppm.

$EMS^{+}(CH_3CN)$ m/z 450 (M+Na) and 428 (M); MS2 (428) m/z 428.

7-chloro-5-(2-hydroxy-5-nitrophenyl)-10-methylpyrimido[4,5-*b*]quinoline-2,4(3*H*,10*H*)-dione (AQ103)

^{1}H-NMR (DMSO-d_6, Varian Inova 500 MHz) δ 11.1 (1H, s), 8.93 (1H, s), 8.30 (1H, s), 7.92 (2H, m) and 3.99 (3H, s) ppm.

$EMS^{-}(CH_3CN)$ m/z 398(M) and 396 (M-2); MS2 (398) m/z 398, 397, 212, 141, 126 and 97.

7-(2-benzoxazolyl)-5-(3-methoxy-4-hydroxyphenyl)-10-methylpyrimido[4,5-*b*]quinoline-2,4(3*H*,10*H*)-dione (AQ104)

^{1}H-NMR (DMSO-d_6, Varian Mercury 300 MHz) δ 10.8 (1H, s), 9.36 (1H, s), 8.52 (1H, d, *J*= 8.70 Hz), 8.12 (2H, m), 7.75 (2H, m), 7.35 (2H, m), 6.95 (1H, d, *J*= 8.10 Hz), 6.88 (1H, s), 6.67 (1H, d, *J*= 8.10 Hz), 4.11 (3H, s) and 3.72 (1H, s) ppm.

EMS^{+} (CH_3CN) m/z 488 (M+Na) and 466 (M); MS2 (467) 466, 465, 433, 404, 394, 376, 354, 343, 324, 319, 303, 279, 275, 242, 243, 215, 177, 149, 135, 100 and 69.

7-(2-benzoxazolyl)-5-(4-pyridinyl)-10-methylpyrimido[4,5-*b*]quinoline-2,4(3*H*,10*H*)-dione (AQ106)

^{1}H-NMR (DMSO-d_6, Varian Mercury 300 MHz) δ 11.0 (1H, s), 8.79 (2H, d, *J*= 6.00 Hz), 8.61 (1H, d, *J*= 9.00 Hz), 8.21(1H, d, *J*= 9.60 Hz), 7.88 (1H, s), 7.76 (2H, t, *J*= 6.60 Hz), 7.38 (4H, m) and 4.15 (3H, s) ppm.

EMS^{+} (CH_3CN) m/z 443 (M+Na) and 421 (M); MS2 (422) 421, 321 and 147.

5-(1-naphthyl)-7,8,10-trimethyl-5,10-dihydropyrimido[4,5-*b*]quinoline-2,4(1*H*,3*H*)-dione (AQ108)

^{1}H-NMR (DMSO-d_6, Varian Mercury 300 MHz) δ 13.5 (1H, broad s), 12.4 (1H, s), 8.07 (1H, d, *J*= 8.10 Hz), 7.96 (2H, t, *J*= 9.30 Hz), 7.48 (3H, m), 6.56 (2H, s) and 5.58 (1H, s) ppm.

EMS^{-} (CH_3CN) m/z 448 (M) and 446 (M-2); MS2 (448) m/z 448, 433, 418 and 58.

7-bromo-5-(2,3-dichlorophenyl)-10-methyl-5,10-dihydropyrimido[4,5-*b*]quinoline-2,4(1*H*,3*H*)-dione (AQ110)

^{1}H-NMR (DMSO-d_6, Varian Inova 500 MHz) δ 10.9 (1H, s), 10.8 (1H, s), 7.39 (3H, m), 7.25 (1H, d, *J*= 7.50 Hz), 7.19 (1H, t, *J*= 6.00 Hz), 7.11 (2H, d, *J*= 7.50 Hz), 5.64 (1H, s) and 3.39 (3H, s) ppm.

EMS^{-}(CH_3CN) m/z 451 (M-2); MS2 (453) m/z 452, 425, 304 and 79.

7-(2-benzoxazolyl)-5-(3,4-dimethoxyphenyl)-10-methyl-5,10-dihydropyrimido[4,5-*b*]quinoline-2,4(1*H*,3*H*)-dione (AQ112)

^{1}H-NMR (DMSO-d_6, Varian Mercury 300 MHz) δ 10.9 (1H, s), 10.8 (1H, s), 8.10 (1H, s), 8.04 (1H, d of d, J_1= 9.00 Hz and J_2= 8.40 Hz), 7.74 (2H, m), 7.38 (4H, m), 6.38 (1H, m), 6.28 (1H, m), 5.16 (1H, s), 3.65 (6H, s) and 3.48 (3H, s) ppm.

EMS$^+$ (CH_3CN) m/z 504 (M+Na); MS2 (483) 481, 438, 397 and 118.

7-(2-benzoxazolyl)-5-(4-bromophenyl)-10-methyl-5,10-dihydropyrimido[4,5-*b*]quinoline-2,4(1*H*,3*H*)-dione (AQ118)

^{1}H-NMR (DMSO-d_6, Varian Mercury 300 MHz) δ 10.9 (1H, s), 10.9 (1H, s), 8.07 (2H, m), 7.75 (2H, m), 7.39 (5H, m), 7.24 (2H, d, *J*= 8.70 Hz), 5.25 (1H, s) and 3.47 (3H, s) ppm.

EMS$^+$ (CH_3CN) m/z 522 (M+Na) and 500 (M-1); MS2 (502) 501.

7-(2-benzoxazolyl)-5-(4-nitrophenyl)-10-methyl-5,10-dihydropyrimido[4,5-*b*]quinoline-2,4(1*H*,3*H*)-dione (AQ124)

^{1}H-NMR (DMSO-d_6, Varian Mercury 300 MHz) δ 11.0 (1H, s), 10.9 (1H, s), 8.16 (1H, s), 8.08 (3H, m), 7.74 (2H, m), 7.59 (2H, d, *J*= 9.00 Hz), 7.40 (3H, m), 5.46 (1H, s) and 3.49 (3H, s) ppm.

EMS$^-$ (CH_3CN) m/z 466 (M-1).

5-(3-hydroxyphenyl)-12-methyl-5,12-dihydrobenzo[*f*]pyrimido[4,5-*b*]quinoline-2,4(1*H*, 3*H*) dione (AQ126)

^{1}H-NMR (DMSO-d_6, Varian Inova 500 MHz) δ 10.8 (1H, s), 10.7 (1H, s), 9.10 (1H, s), 7.95 (1H, d, *J*= 7.50 Hz), 7.91 (1H, d, *J*= 7.50 Hz), 7.87 (1H, d, *J*= 7.00 Hz), 7.57 (1H, d, *J*= 7.50 Hz), 7.47 (1H, t, *J*= 6.50 Hz), 7.37 (1H, t, *J*= 6.50 Hz), 6.90 (1H, t, *J*= 6.50 Hz), 6.61 (1H, d, *J*= 6.00 Hz), 6.58 (1H, s), 6.42 (1H, d, *J*= 6.50 Hz), 5.70 (1H, s) and 3.53 (3H, s) ppm.

EMS$^-$(CH_3CN) m/z 371 (M), 370 (M-1) and 369 (M-2); MS2 (371) m/z 371, 328, 301, 278, 234 and 93.

5-(3-methoxy-4-hydroxyphenyl)-12-methyl-5,12-dihydrobenzo[*f*]pyrimido[4,5-*b*]quinoline-2,4(1*H*, 3*H*) dione (AQ127)

^{1}H-NMR (DMSO-d_6, Varian Inova 500 MHz) δ 10.8 (1H, s), 10.7 (1H, s), 8.63 (1H, s), 8.00 (1H, d, *J*= 7.00 Hz), 7.89 (1H, d, *J*= 8.00 Hz), 7.86 (1H, d, *J*= 6.50 Hz), 7.55 (1H, d, *J*= 7.50 Hz), 7.46 (1H, t, *J*= 6.00 Hz), 7.36 (1H, t, *J*= 6.50 Hz), 6.87 (1H, s), 6.48 (1H, d, *J*= 6.50 Hz), 6.40 (1H, d of d, J_1= 6.50 Hz, J_2= 6.50 Hz), 3.61 (3H, s) and 3.53 (3H, s) ppm.

EMS$^-$ (CH_3CN) m/z 400 (M–1) and 399 (M-2); MS2 (401) m/z 403, 113 and 69.

5-(3,4-dimethoxyphenyl)-12-methyl-5,12-dihydrobenzo[*f*]pyrimido[4,5-*b*]quinoline-2,4(1*H*, 3*H*) dione (AQ128)

^{1}H-NMR (DMSO-d_6, Varian Inova 500 MHz) δ 10.8 (1H, s), 10.7 (1H, s), 7.97(1H, d, *J*= 7.00 Hz), 7.92 (1H, d, *J*= 7.50 Hz), 7.88 (1H, d, *J*= 6.50 Hz), 7.56 (1H, d, *J*=7.50 Hz), 7.47 (1H, t, *J*= 6.00 Hz), 7.38 (1H, t, *J*= 6.00 Hz), 6.29 (2H, s), 6.20 (1H, s), 5.73 (1H, s), 3.57 (6H, s) and 3.53 (3H, s) ppm.

EMS$^+$ (CH_3CN) m/z 415 (M); MS2 (415) m/z 414, 370, 355 and 118.

5-(4-methoxyphenyl)-12-methyl-5,12-dihydrobenzo[*f*]pyrimido[4,5-*b*]quinoline-2,4(1*H*, 3*H*) dione (AQ129)

^{1}H-NMR (DMSO-d_6, Varian Inova 500 MHz) δ 10.8 (1H, s), 10.7 (1H, s), 7.97 (1H, d, *J*= 7.00 Hz), 7.90 (1H, d, *J*= 7.50 Hz), 7.86 (1H, d, *J*= 7.00 Hz), 7.56 (1H, d, *J*= 8.00 Hz), 7.45 (1H, t, *J*= 6.00 Hz), 7.36 (1H, t, *J*= 6.50 Hz), 7.08 (2H, d, *J*= 7.00 Hz), 6.68 (2H, d, *J*= 7.50 Hz), 5.72 (1H, s), 3.59 (3H, s) and 3.53 (3H, s) ppm.

EMS$^-$ (CH_3CN) m/z 384 (M – 1) and 383 (M – 2); MS2 (385) m/z 386, 371, 356 and 278.

5-(4-methylphenyl)-12-methyl-5,12-dihydrobenzo[*f*]pyrimido[4,5-*b*]quinoline-2,4(1*H*, 3*H*) dione (AQ130)

^{1}H-NMR (DMSO-d_6, Varian Inova 500 MHz) δ 10.8 (1H, s), 10.7 (1H, s), 7.96 (1H, d, *J*= 7.00 Hz), 7.90 (1H, d, *J*= 7.50 Hz), 7.86 (1H, d, *J*= 6.50 Hz), 7.56 (1H, d, *J*= 7.50 Hz), 7.45 (1H, t, *J*= 6.00 Hz), 7.36 (1H, t, *J*= 6.00 Hz), 7.05(2H, d, *J*= 6.50 Hz), 6.91 (2H, d, *J*= 6.50 Hz), 5.73 (1H, s) and 3.53 (3H, s) ppm.

EMS^{-}(CH_3CN) m/z 369 (M) and 367 (M-2); MS2 (369) m/z 369 and 263.

5-(1-naphthyl)-12-methyl-5,12-dihydrobenzo[*f*]pyrimido[4,5-*b*]quinoline-2,4(1*H*, 3*H*) dione (AQ131)

^{1}H-NMR (DMSO-d_6, Varian Inova 500 MHz) δ 10.9 (1H, s), 10.7 (1H, s), 9.26 (1H, d, *J*= 7.00 Hz), 7.91 (1H, d, *J*= 8.00 Hz), 7.81 (3H, m), 7.65 (3H, m), 7.50 (1H, t, *J*= 6.00 Hz), 7.26 (2H, m), 7.20 (1H, t, *J*= 6.50 Hz), 7.09 (1H, d, *J*= 6.50 Hz), 6.53 (1H, s) and 3.65 (3H, s) ppm.

EMS^{+}(CH_3CN) m/z 445 (M+K) and 405 (M); MS2 (405) m/z 404, 360 and 345.

5-(2-naphthyl)-12-methyl-5,12-dihydrobenzo[*f*]pyrimido[4,5-*b*]quinoline-2,4(1*H*, 3*H*) dione (AQ132)

^{1}H-NMR (DMSO-d_6, Varian Inova 500 MHz) δ 10.9 (1H, s), 10.8 (1H, s), 8.07 (1H, d, *J*=7.00 Hz), 7.94 (1H, d, *J*= 7.50 Hz), 7.86 (1H, d, *J*= 6.50 Hz), 7.72 (2H, t, *J*= 5.00 Hz), 7.67 (2H, m), 7.62 (1H, d, *J*=8.00 Hz), 7.39 (5H, m) and 3.59(3H, s) ppm.

EMS^{+}(CH_3CN) m/z 444 (M+K), 427 (M + Na) and 403 (M-2); MS2 (405) m/z 404 and 360.

5-(4-biphenyl)-12-methyl-5,12-dihydrobenzo[*f*]pyrimido[4,5-*b*]quinoline-2,4(1*H*, 3*H*) dione (AQ133)

^{1}H-NMR (DMSO-d_6, Varian Inova 500 MHz) δ 10.9 (1H, s), 10.8 (1H, s), 8.02 (1H, d, *J*= 7.00 Hz), 7.93 (1H, d, *J*= 7.50 Hz), 7.88 (1H, d, *J*= 6.50 Hz), 7.59 (1H, d, *J*= 8.00 Hz), 7.48 (3H, m),

7.41 (2H, d, *J*= 7.00 Hz), 7.36 (4H, q, J_1= 7.50 Hz, J_2= 6.50 Hz), 7.26 (3H, m), 5.84 (1H, s) and 3.56 (3H, s) ppm.

$EMS^+(CH_3CN)$ m/z 453 (M + Na) and 431 (M); MS2 (431) m/z 430 and 386.

5-phenyl-12-methyl-5,12-dihydrobenzo[*f*]pyrimido[4,5-*b*]quinoline-2,4(1*H*, 3*H*) dione (AQ134)

^{1}H-NMR (DMSO-d_6, Varian Inova 500 MHz) δ 10.9 (1H, s), 10.8 (1H, s), 7.98 (1H, d, *J*= 7.00 Hz), 7.91 (1H, d, *J*= 8.00 Hz), 7.86 (1H, d, *J*= 6.50 Hz), 7.57 (1H, d, *J*= 7.50 Hz), 7.45 (1H, t, *J*= 6.00 Hz) 7.36 (1H, t, *J*= 6.00 Hz), 7.19 (2H, d, *J*= 6.00 Hz), 7.12 (2H, t, *J*= 6.00 Hz), 7.03 (1H, t, *J*= 6.50 Hz), 5.78 (1H, s) and 3.54 (3H, s) ppm.

^{13}C-NMR (DMSO-d_6, Varian Inova 500 MHz) δ163.292, 151.328, 147.797, 146.156, 138.004, 131.042, 130.808, 129.024, 128.993, 127.863, 126.823, 125.029, 123.352, 119.821, 116.595 and 89.714 ppm.

EMS^- (CH_3CN) m/z 354 (M-1) and 353 (M-2); MS2 (355) m/z 355, 325, 263 and 113.

5-(3-pyridinyl)-12-methyl-5,12-dihydrobenzo[*f*]pyrimido[4,5-*b*]quinoline-2,4(1*H*, 3*H*) dione (AQ135)

^{1}H-NMR (DMSO-d_6, Varian Inova 500 MHz) δ 10.9 (1H, s), 10.8 (1H, s), 8.49 (1H, s), 8.25 (1H, d, *J*= 3.50 Hz), 7.99 (1H, d, *J*= 7.00 Hz), 7.94 (1H, d, *J*= 7.50 Hz), 7.88 (1H, d, *J*= 6.50 Hz), 7.59 (1H, d, *J*= 7.50 Hz), 7.51 (1H, d, *J*= 7.00 Hz), 7.46 (1H, t, *J*= 6.50 Hz), 7.37 (1H, t, *J*= 6.50 Hz), 7.16 (1H, d of d, J_1= 6.50 Hz, J_2= 6.50 Hz), 5.81 (1H, s) and 3.55 (3H, s) ppm.

$EMS^-(CH_3CN)$ m/z 356 (M), 355 (M-1) and 354 (M-2); MS2 (356) m/z 356, 277 and 263.

5-(4-pyridinyl)-12-methyl-5,12-dihydrobenzo[*f*]pyrimido[4,5-*b*]quinoline-2,4(1*H*, 3*H*) dione (AQ136)

^{1}H-NMR (DMSO-d_6, Varian Inova 500 MHz) δ 10.9 (1H, s), 10.8 (1H, s), 8.31 (2H, d, *J*= 4.50 Hz), 7.95 (2H, d, *J*= 7.50 Hz), 7.89 (1H, d, *J*= 7.00 Hz), 7.59 (1H, d, *J*= 7.50 Hz), 7.47 (1H, t, *J*= 6.00 Hz), 7.38 (1H, t, *J*= 6.50 Hz), 7.17 (2H, d, *J*= 4.50 Hz), 5.81 (1H, s) and 3.54 (3H, s) ppm.

EMS^{-}(CH_3CN) m/z 356 (M), 355 (M-1) and 354 (M-2); MS2 (356) m/z 356, 277 and 263.

5-(4-bromophenyl)-12-methyl-5,12-dihydrobenzo[*f*]pyrimido[4,5-*b*]quinoline-2,4(1*H*, 3*H*) dione (AQ137)

^{1}H-NMR (DMSO-d_6, Varian Inova 500 MHz) δ 10.9 (1H, s), 10.8 (1H, s), 7.93 (2H, t, *J*= 5.50 Hz), 7.87 (1H, d, *J*=6.50), 7.58 (1H, d, *J*= 7.50), 7.46 (1H, t, *J*= 6.00 Hz), 7.37 (1H, t, *J*= 6.00 Hz), 7.31 (2H, d, *J*= 7.00 Hz), 7.14 (2H, d, *J*= 7.50 Hz), 5.77 (1H, s) and 3.53 (3H, s) ppm.

EMS^{+}(CH_3CN) m/z 433 (M – 1); MS2 (434) m/z 431.

5-(4-chlorophenyl)-12-methyl-5,12-dihydrobenzo[*f*]pyrimido[4,5-*b*]quinoline-2,4(1*H*, 3*H*) dione (AQ138)

^{1}H-NMR (DMSO-d_6, Varian Inova 500 MHz) δ 10.9 (1H, s), 10.8 (1H, s), 7.93 (2H, t, *J*= 6.50 Hz), 7.87 (1H, d, *J*= 6.50 Hz), 7.57 (1H, d, *J*= 8.00 Hz), 7.46 (1H, t, *J*= 6.00 Hz), 7.37 (1H, t, *J*= 6.50 Hz), 7.18 (4H, m) and 3.53 (1H, s) ppm.

^{13}C-NMR (DMSO-d_6, Varian Inova 500 MHz) δ 163.271, 151.279, 149.213, 146.414, 138.012, 131.482, 130.958, 130.755, 129.992, 129.313, 129.250, 128.961, 128.001, 127.992, 125.275, 125.044, 123.398, 123.359, 119.156, 117.751, 117.603 and 89.990 ppm.

EMS^{+}(CH_3CN) m/z 389 (M); MS2 (389) m/z 388, 344, 309 and 282.

5-(2,3-dichlorophenyl)-12-methyl-5,12-dihydrobenzo[*f*]pyrimido[4,5-*b*]quinoline-2,4(1*H*, 3*H*) dione (AQ139)

^{1}H-NMR (DMSO-d_6, Varian Inova 500 MHz) δ 10.9 (1H, s), 10.7 (1H, s), 8.11 (1H, d, *J*=7.00 Hz), 7.91 (1H, d, *J*= 8.00 Hz), 7.86 (1H, d, *J*=6.50 Hz), 7.56 (1H, d, *J*= 7.50 Hz), 7.49 (1H, t, *J*=

6.50 Hz), 7.37 (1H, t, *J*= 6.50 Hz), 7.34 (1H, t, *J*= 6.50 Hz), 7.28 (1H, d, *J*=7.00 Hz), 7.11 (1H, t, *J*= 6.50 Hz), 6.12 (1H, s) and 3.59 (3H, s) ppm.

EMS^- (CH_3CN) m/z 422 (M-2); MS2 (424) m/z 425, 277 and 148.

5-(3,4-dichlorophenyl)-12-methyl-5,12-dihydrobenzo[*f*]pyrimido[4,5-*b*]quinoline-2,4(1*H*, 3*H*) dione (AQ140)

^{1}H-NMR (DMSO-d_6, Varian Inova 500 MHz) δ 10.9 (1H, s), 10.8 (1H, s), 7.95 (2H, d, *J*= 7.50 Hz), 7.88 (1H, d, *J*= 6.50 Hz), 7.59 (1H, d, *J*= 7.50 Hz), 7.48 (2H, m), 7.38 (2H, m), 7.05 (1H, d, *J*= 7.00 Hz), 5.83 (1H, s) and 3.54 (3H, s) ppm.

EMS^+ (CH_3CN) m/z 422 (M – 2); MS2 (424) m/z 421 and 379.

5-(3-nitrophenyl)-12-methyl-5,12-dihydrobenzo[*f*]pyrimido[4,5-*b*]quinoline-2,4(1*H*, 3*H*) dione (AQ141)

^{1}H-NMR (DMSO-d_6, Varian Inova 500 MHz) δ 10.9 (1H, s), 10.8 (1H, s), 8.07 (1H, s), 7.97 (2H, d, *J*= 7.50 Hz), 7.91 (2H, m), 7.63 (1H, d, *J*= 6.50 Hz), 7.56 (1H, d, *J*= 6.50 Hz), 7.45 (2H, m), 7.38 (1H, t, *J*= 6.50 Hz), 5.96 (1H, s) and 3.56 (3H, s) ppm.

EMS^-(CH_3CN) m/z 400 (M), 399 (M-1) and 398 (M-2); MS2 (400) m/z 401, 314, 278, 193, 160 and 136.

5-(4-nitrophenyl)-12-methyl-5,12-dihydrobenzo[*f*]pyrimido[4,5-*b*]quinoline-2,4(1*H*, 3*H*) dione (AQ142)

^{1}H-NMR (DMSO-d_6, Varian Inova 500 MHz) δ 10.9 (1H, s), 10.8 (1H, s), 8.01 (2H, d, *J*= 7.50 Hz), 7.95 (2H, t, *J*= 7.50 Hz), 7.89 (1H, d, *J*=7.00 Hz), 7.61 (1H, d, J= 8.00 Hz), 7.46 (3H, m), 7.37 (1H, t, *J*= 6.00 Hz), 5.93 (1H, s) and 3.56 (3H, s) ppm.

EMS$^-$ (CH_3CN) m/z 400 (M), 399 (M-1) and 398 (M–2); MS2 (400) m/z 401 and 277.

5-(4-methylthiophenyl)-12-methyl-5,12-dihydrobenzo[*f*]pyrimido[4,5-*b*]quinoline-2,4(1*H*, 3*H*) dione (AQ143)

^{1}H-NMR (DMSO-d_6, Varian Inova 500 MHz) δ 10.9 (1H, s), 10.8 (1H, s), 7.81 (2H, m), 7.88 (1H, d, *J*= 6.50 Hz), 7.69 (1H, s), 7.59 (1H, d, *J*= 7.50 Hz), 7.47 (1H, t, *J*= 6.50 Hz), 7.38 (1H, t, *J*= 6.50 Hz), 7.29 (1H, d, *J*= 7.50 Hz), 6.90 (1H, d, *J*= 7.50 Hz), 5.79 (1H, s) and 3.53 (3H, s) ppm.

EMS$^-$(CH_3CN) m/z 401 (M); MS2 (401) m/z 401, 262, 138 and 108.

5-(4-trifluoromethylphenyl)-12-methyl-5,12-dihydrobenzo[*f*]pyrimido[4,5-*b*]quinoline-2,4(1*H*, 3*H*) dione (AQ144)

^{1}H-NMR (DMSO-d_6, Varian Inova 500 MHz) δ 10.9 (1H, s), 10.8 (1H, s), 7.95 (2H, d, *J*= 7.50 Hz), 7.60 (1H, d, *J*= 7.50 Hz), 7.50 (2H, d, *J*= 6.50 Hz), 7.46 (1H, t, *J*= 6.00 Hz), 7.41 (2H, d, *J*= 7.00 Hz), 7.37 (1H, t, *J*= 6.50 Hz), 5.89 (1H, s) and 3.55 (3H, s) ppm.

EMS$^+$(CH_3CN) m/z 443 (M+Na) and 421(M-2); MS2 (423) m/z 420, 402, 376, 334, 251, 168 and 141.

5-(2-hydroxy-5-bromophenyl)-12-methyl-5,12-dihydrobenzo[*f*]pyrimido[4,5-*b*]quinoline-2,4(1*H*, 3*H*) dione (AQ145)

^{1}H-NMR (DMSO-d_6, Varian Inova 500 MHz) δ 10.8 (1H, s), 10.6 (1H, s), 8.14 (1H, d, *J*= 7.00 Hz), 7.85 (1H, d, *J*= 7.50 Hz), 7.82 (1H, d, *J*= 6.50 Hz), 7.51 (1H, d, *J*= 7.50 Hz), 7.46 (1H, t, *J*= 6.00 Hz), 7.34 (2H, m), 7.19 (1H, d of d, J_1= 7.00 Hz, J_2= 7.00 Hz), 6.84 (1H, d, *J*= 7.00 Hz), 5.94 (1H, s), 3.74 (1H, s) and 3.58 (1H, s) ppm.

EMS^{-}(CH_3CN) m/z 449 (M-1); MS2 (450) m/z 450, 262, 187, 157 and 81.

5-(3-methoxy-4-hydroxy-5-nitrophenyl)-12-methyl-5,12-dihydrobenzo[*f*]pyrimido[4,5-*b*] quinoline-2,4(1*H*, 3*H*) dione (AQ148)

^{1}H-NMR (DMSO-d_6, Varian Inova 500 MHz) δ 10.9 (1H, s), 10.8 (1H, s),10.1 (1H, s), 8.01(1H, d, *J*= 7.00 Hz), 7.95 (1H, d, *J*= 7.50), 7.89 (1H, d, *J*= 7.00 Hz), 7.59 (1H, d, *J*= 8.00 Hz), 7.48 (1H, t, *J*= 6.00 Hz), 7.39 (1H, t, *J*= 6.00 Hz), 7.21 (1H, s), 7.02 (1H, s), 5.81 (1H, s), 3.72 (3H, s) and 3.54 (3H, s) ppm.

EMS^{-} (CH_3CN) m/z 445 (M-1); MS2 (446) 446, 167 and 153.

5-(3-nitro-4-hydroxyphenyl)-12-methyl-5,12-dihydrobenzo[*f*]pyrimido[4,5-*b*]quinoline-2,4(1*H*, 3*H*) dione (AQ149)

^{1}H-NMR (DMSO-d_6, Varian Inova 500 MHz) δ 11.9 (1H, broad s), 10.8 (1H, s), 10.7 (1H, s), 7.96 (1H, d, *J*= 7.00 Hz), 7.91 (1H, d, *J*= 7.50 Hz), 7.87 (1H, d, *J*= 6.50 Hz), 7.57 (1H, d, *J*= 6.50 Hz), 7.45 (1H, t, *J*= 6.00 Hz), 7.36 (1H, t, *J*= 6.50 Hz), 7.12 (2H, d, *J*= 7.00 Hz), 7.02 (2H, d, *J*= 6.50 Hz), 5.74 (1H, s), and 3.53 (3H, s) ppm.

EMS^{-}(CH_3CN) m/z 415 (M-1); MS2 (416) m/z 416, 401, 343, 328 and 133.

5-(2-hydroxy-5-nitrophenyl)-12-methyl-5,12-dihydrobenzo[*f*]pyrimido[4,5-*b*]quinoline-2,4(1*H*, 3*H*) dione (AQ150)

^{1}H-NMR (DMSO-d_6, Varian Inova 500 MHz) δ 11.6 (1H, s), 11.1 (1H, s), 11.0 (1H, s), 7.95 (1H, d, *J*= 7.50 Hz), 7.91 (1H, d, *J*= 7.00 Hz), 7.87 (1H, d, *J*= 6.50 Hz), 7.83 (1H, d of d, J_1= 7.00 Hz, J_2= 7.50 Hz), 7.63 (2H, m), 7.46 (1H, t, *J*= 6.00 Hz), 7.37 (1H, t, *J*= 6.00 Hz), 6.91 (1H, d, *J*= 7.50 Hz), 5.99 (1H, s) and 3.60 (3H, s) ppm.

EMS^{+}(CH_3CN) m/z 454 (M+K) and 414 (M-2); MS2 (416) m/z 415, 372, 325 and 118.

5-(3-hydroxyphenyl)-12-butyl-5,12-dihydrobenzo[*f*]pyrimido[4,5-*b*]quinoline-2,4(1*H*, 3*H*) dione (AQ151)

^{1}H-NMR (DMSO-d_6, Varian Mercury 300 MHz) δ 10.9 (1H, s), 10.8 (1H, s), 9.13 (1H, s), 7.79 (3H, m), 7.67 (1H, d, *J*= 9.60 Hz), 7.46 (1H, m), 7.39 (1H, m), 6.90 (1H, t, *J*= 8.10 Hz), 6.56 (2H, m), 6.43 (1H, d of d, J_1= 8.70 Hz and J_2= 8.10 Hz), 5.76 (1H, s), 4.11 (2H, m), 1.49 (2H, m), 1.24 (2H, q, J_1= 7.50 Hz and J_2= 6.90 Hz) and 0.814 (3H, m) ppm.

EMS^{-} (CH_3CN) m/z 412 (M-1); MS2 (413) 413, 370, 357, 352, 343, 327, 314, 285, 262, 219, 127 and 93.

5-(3,4-dimethoxyphenyl)-12-butyl-5,12-dihydrobenzo[*f*]pyrimido[4,5-*b*]quinoline-2,4(1*H*, 3*H*) dione (AQ152)

^{1}H-NMR (DMSO-d_6, Varian Mercury 300 MHz) δ 10.9 (1H, s), 10.8 (1H, s), 7.91 (3H, m), 7.67 (1H, d, *J*= 8.70 Hz), 7.43 (2H, m), 6.29 (2H, m), 5.79 (1H, s), 4.14 (2H, m), 3.57 (6H, s), 1.50 (2H, m), 1.26 (2H, m) and 0.812 (3H, m) ppm.

EMS^{-} (CH_3CN) m/z 456 (M-1); MS2 (457) 457, 442, 401, 400, 385, 319, 263 and 122.

5-(4-biphenyl)-12-butyl-5,12-dihydrobenzo[*f*]pyrimido[4,5-*b*]quinoline-2,4(1*H*, 3*H*) dione (AQ155)

^{1}H-NMR (DMSO-d_6, Varian Mercury 300 MHz) δ 10.9 (2H, s), 7.91 (3H, m), 7.707 (1H, d, *J*= 9.30 Hz), 7.50 (3H, m), 7.41 (3H, m), 7.32 (3H, m), 7.24 (2H, m), 5.89 (1H, s), 4.15(2H, m), 1.53 (2H, m), 1.25 (2H, m) and 0.828 (3H, m) ppm.

EMS^{+} (CH_3CN) m/z 495 (M+Na); MS2 (474) 473 and 472.

5-phenyl-12-butyl-5,12-dihydrobenzo[*f*]pyrimido[4,5-*b*]quinoline-2,4(1*H*, 3*H*) dione

(AQ156)

^{1}H-NMR (DMSO-d_6, Varian Inova 500 MHz) δ 10.8 (1H, s), 7.9 (2H, m), 7.86 (1H, d, *J*= 7.00 Hz), 7.65 (1H, d, *J*= 7.50 Hz), 7.44 (1H, t, *J*= 6.50 Hz), 7.37 (1H, t, *J*= 6.00 Hz), 7.12 (4H, m), 7.03 (1H, t, *J*= 5.50 Hz), 5.83 (1H, s), 4.13 (2H, m), 1.64 (1H, m), 1.50 (1H, m), 1.23 (2H, m) and 0.809 (3H, m) ppm.

EMS^{+}(CH_3CN) m/z 436 (M+K) and 395 (M-2); MS2 (397) m/z 397, 340, 323, 297, 118 and 57.

5-(2-pyridinyl)-12-butyl-5,12-dihydrobenzo[*f*]pyrimido[4,5-*b*]quinoline-2,4(1*H*, 3*H*) dione (AQ157)

^{1}H-NMR (DMSO-d_6, Varian Mercury 300 MHz) δ 10.9 (1H, s), 10.8 (1H, s), 8.23 (1H, s), 8.18 (1H, d, *J*= 8.70 Hz), 7.85 (2H, d, *J*= 9.30 Hz), 7.59 (2H, m), 7.47 (2H, m), 7.37 (1H, m), 7.05 (1H, m), 5.91 (1H, s), 4.14 (2H, m), 1.58 (2H, m), 1.33 (2H, m) and 0.840 (3H, m) ppm.

EMS^{+} (CH_3CN) m/z 400 (M+2), 399 (M+1) and 398 (M); MS2 (399) 398, 356, 343, 342, 327, 319, 300, 294 and 130.

5-(3-pyridinyl)-12-butyl-5,12-dihydrobenzo[*f*]pyrimido[4,5-*b*]quinoline-2,4(1*H*, 3*H*) dione (AQ158)

^{1}H-NMR (DMSO-d_6, Varian Mercury 300 MHz) δ 10.9 (2H, s), 8.44 (1H, s), 8.26 (1H, s), 7.92 (3H, m), 7.69 (1H, d, *J*= 9.30 Hz), 7.45 (3H, m), 7.26 (1H, m), 5.87 (1H, s), 4.15 (2H, m), 1.51 (2H, m), 1.28 (2H, m) and 0.838 (3H, m) ppm.

EMS^{+} (CH_3CN) m/z 400 (M+2), 399 (M+1) and 398 (M); MS2 (399) 398, 342, 319, 300, 118 and 70.

5-(4-pyridinyl)-12-butyl-5,12-dihydrobenzo[*f*]pyrimido[4,5-*b*]quinoline-2,4(1*H*, 3*H*) dione (AQ159)

^{1}H-NMR (DMSO-d_6, Varian Mercury 300 MHz) δ 10.9 (2H, s), 8.34 (2H, m), 7.93 (4H, m), 7.69 (1H, d, *J*= 9.30 Hz), 7.44 (3H, m), 7.11 (2H, m), 5.87 (1H, s), 4.14 (2H, m), 1.40 (2H, m), 1.20 (2H, m) and 0.805 (3H, m) ppm.

EMS^{+} (CH_3CN) m/z 398 (M); MS2 (399) 398, 355, 342, 341, 324, 319, 300, 299, 298, 296, 271, 255, 157 and 57.

5-(4-bromophenyl)-12-butyl-5,12-dihydrobenzo[*f*]pyrimido[4,5-*b*]quinoline-2,4(1*H*, 3*H*) dione (AQ160)

^{1}H-NMR (DMSO-d_6, Varian Mercury 300 MHz) δ 10.9 (1H, s), 7.91 (3H, m), 7.67 (1H, d, *J*= 8.70 Hz), 7.40 (2H, m), 7.20 (2H, m), 7.08 (2H, d of d, J_1= 6.60 Hz and J_2= 6.60 Hz), 5.83 (1H, s), 4.13 (2H, m), 1.15 (2H, m), 1.22 (2H, m) and 0.816 (3H, m) ppm.

EMS^{+} (CH_3CN) m/z 497 (M+Na); MS2 (477) 476, 475,420, 321, 320, 296, 264, 233 and 151.

5-(4-chlorophenyl)-12-butyl-5,12-dihydrobenzo[*f*]pyrimido[4,5-*b*]quinoline-2,4(1*H*, 3*H*) dione (AQ161)

^{1}H-NMR (DMSO-d_6, Varian Mercury 300 MHz) δ 10.9 (2H, s), 7.91 (3H, m), 7.67 (1H, d, *J*= 9.30 Hz), 7.44 (2H, m), 7.24 (4H, m), 5.85 (1H, s), 4.13 (2H, m), 1.48 (2H, m), 1.23 (2H, m) and 0.812 (3H, m) ppm.

EMS^{-} (CH_3CN) m/z 431 (M) and 429 (M-2); MS2 (431) 431, 395, 375, 374, 332, 319, 289, 271, 263, 262, 219, 168, 153, 138, 123 and 62.

5-(2,3-dichlorophenyl)-12-butyl-5,12-dihydrobenzo[*f*]pyrimido[4,5-*b*]quinoline-2,4(1*H*, 3*H*) dione (AQ162)

^{1}H-NMR (DMSO-d_6, Varian Mercury 300 MHz) δ 10.8 (1H, s), 10.7 (1H, s), 8.12 (1H, d, *J*= 8.70 Hz), 7.92 (1H, d, *J*= 9.60 Hz), 7.86 (1H, d, *J*= 8.10 Hz), 7.64 (1H, d, *J*= 9.30 Hz), 7.48 (1H, t, *J*= 7.50 Hz), 7.34 (2H, m), 7.24(1H, m), 7.12 (1H, m), 6.13 (1H, s), 4.17 (2H, m), 1.63 (2H, m), 1.48 (2H, m) and 0.976 (3H, m) ppm.

EMS^{-} (CH_3CN) m/z 466 (M) and 464 (M-2); MS2 (466) 466, 430, 387, 371, 320, 318, 275, 262, 232 and 147.

5-(3,4-dichlorophenyl)-12-butyl-5,12-dihydrobenzo[*f*]pyrimido[4,5-*b*]quinoline-2,4(1*H*, 3*H*) dione (AQ163)

^{1}H-NMR (DMSO-d_6, Varian Mercury 300 MHz) δ 10.9 (1H, s), 7.93 (3H, m), 7.70 (1H, d, *J*= 8.70 Hz), 7.43 (3H, m), 7.31 (1H, s), 7.10 (1H, d of d, J_1= 8.70 Hz and J_2= 10.5 Hz), 5.87 (1H, s), 4.15 (2H, m), 1.49 (2H, m), 1.24 (2H, m) and 0.822 (3H, m) ppm.

EMS^{-} (CH_3CN) m/z 465 (M-1).

5-(3-nitrophenyl)-12-butyl-5,12-dihydrobenzo[*f*]pyrimido[4,5-*b*]quinoline-2,4(1*H*, 3*H*) dione (AQ164)

^{1}H-NMR (DMSO-d_6, Varian Mercury 300 MHz) δ 11.0 (1H, s), 10.9 (1H, s), 7.95 (5H, m), 7.75 (1H, d, *J*= 9.60 Hz), 7.68 (1H, d, *J*= 7.50 Hz), 7.45 (3H, m), 6.00 (1H, s), 4.18 (2H, m), 1.45 (2H, m), 1.04 (2H, m) and 0.816 (3H, m) ppm.

EMS^{-} (CH_3CN) m/z 442 (M) and 440 (M-2); MS2 (442) 442, 441, 386, 319, 262 and 122.

5-(4-nitrophpenyl)-12-butyl-5,12-dihydrobenzo[*f*]pyrimido[4,5-*b*]quinoline-2,4(1*H*, 3*H*) dione (AQ165)

^{1}H-NMR (DMSO-d_6, Varian Mercury 300 MHz) δ 10.9 (2H, s), 8.05 (1H, d of d, J_1= 4.50 Hz and J_2= 6.60 Hz), 7.99 (2H, d, *J*= 9.60 Hz), 7.71 (1H, d, *J*= 9.00 Hz), 7.43 (4H, m), 5.98 (1H, s), 4.14 (2H, m), 1.15 (2H, m), 1.34 (2H, m) and 0.830 (3H, m) ppm.

EMS^{-} (CH_3CN) m/z 440 (M-1); MS2 (442) 442, 440, 386, 385, 372, 342, 319, 262 and 122.

5-(2-hydroxy-5-bromophenyl)-12-butyl-5,12-dihydrobenzo[*f*]pyrimido[4,5-*b*]quinoline-2,4(1*H*, 3*H*) dione (AQ166)

^{1}H-NMR (DMSO-d_6, Varian Mercury 300 MHz) δ 11.3 (1H, s), 11.2 (1H, s), 10.6 (1H, s), 7.96 (1H, d, *J*= 9.60 Hz), 7.89 (1H, d, *J*= 7.50 Hz), 7.72 (1H, m), 7.43 (3H, m), 7.09 (1H, d of d, J_1= 8.70 Hz and J_2= 9.00 Hz), 6.78 (1H, d, *J*= 9.80 Hz), 6.60 (1H, s), 5.90 (1H, s), 4.24 (2H, m), 1.61 (2H, m), 1.40 (2H, m) and 0.930 (3H, m) ppm.

EMS^{-} (CH_3CN) m/z 492 (M) and 490 (M-2); MS2 (493) 493, 319, 201, 174, 173 and 171.

5-(3-methoxy-4-hydroxy-5-nitrophenyl)-12-butyl-5,12-dihydrobenzo[*f*]pyrimido[4,5-*b*]quinoline-2,4(1*H*, 3*H*) dione (AQ167)

^{1}H-NMR (DMSO-d_6, Varian Mercury 300 MHz) δ 10.9 (1H, s), 10.1 (1H, broad s), 7.93 (3H, m), 7.72 (1H, d, *J*= 9.30 Hz), 7.44 (3H, m), 6.88 (1H, s), 5.85 (1H, s), 4.14 (2H, m), 3.77 (3H, s), 1.50 (2H, m), 1.25 (2H, m) and 0.801 (3H, m) ppm.

EMS^{-} (CH_3CN) m/z 488 (M) and 487 (M-1); MS2 (488) 488, 456, 445, 441, 432, 373, 319, 262, 168, 154 and 153.

Vita

Rebecca Hron was born in New Orleans, Louisiana. She graduated from Tulane University in 2011 with a Bachelor of Science in cell and molecular biology and a minor in classical studies. In the spring of 2012, she became a graduate student at the University of New Orleans in the Department of Chemistry. She joined the research group of Professor Branko Jursic in the fall of 2012 and in December of 2014, she obtained a Master's degree in Organic Chemistry